Ventilation for optimisation of energy efficiency and indoor environments in Danish homes

Christopher Just Johnston

PhD Thesis

Department of Civil Engineering
2019

DTU Civil Engineering Report 395

DTU Civil Engineering
Department of Civil Engineering

Ventilation for optimisation of energy efficiency and indoor environments in Danish homes

PhD Thesis by
Christopher Just Johnston

Section for Energy and Services
Department of Civil Engineering
Technical University of Denmark

February 2019

Title: Ventilation for optimisation of energy efficiency and indoor environments in Danish homes

Period: 1st September 2013 – 11th February 2019

Institute: Section for Energy and Services, Department of Civil Engineering, Technical University of Denmark

Ph.D. student: Christopher Just Johnston

Place of employment: NIRAS A/S

Main supervisor: Associate Professor and Head of Section Toke Rammer Nielsen, PhD

Supervisor: Professor Jørn Toftum, PhD

Supervisor: Competence Director Peter Noyé, MSc

Funding: The NIRAS Group and the Innovation Fund Denmark

Cover illustrations: Dall & Lindhardtsen A/S, Architect

This PhD thesis is based on the following publications. Parts of these publications have been used directly or indirectly.

Paper 1: Johnston, C. J., Birck Laustsen, J., Toftum, J., Rammer Nielsen, T. Comparing relative performance of supply air windows with conventional and heat recovery ventilation systems in a temperate climate. **Submitted to Energy and Buildings on 9th February 2019.**

Paper 2: Johnston, C. J., Rammer Nielsen, T., Toftum, J. Comparing predictions by existing emission models to real world observations of formaldehyde emissions from solid materials. **Submitted to Building Simulation on 10th February 2019.**

Paper 3: Johnston, C. J., Korsholm Andersen, R., Toftum, J., Rammer Nielsen, T. Effect of formaldehyde on ventilation rate and energy demand in Danish homes: Development of emission models and building performance simulation. **Submitted to Building Simulation on 10th February 2019.**

Report 1. Birck Laustsen, J., Johnston, C. J., Raffnsøe, L.M. ProVent; Projekteringsviden om ventilationsvinduer. Published May 2014.

Preface

The work presented in this thesis has been carried out in a collaboration between the NIRAS Group, the Section for Energy and Services and the Section for Indoor Environment, Department of Civil Engineering (BYG), Technical University of Denmark (DTU) within the period 1st September 2013 – 11th February 2019. This thesis has been written as part of an Industrial PhD programme funded by the NIRAS Group and the Innovation Fund Denmark.

The process of writing a PhD thesis, I suppose, is individual and dependent on your field of research, who you are as a researcher and who you are as a person. For me, it has been an opportunity not only to reflect on and surmise my work, but also give pause and look back at the past five and a half years. So much has happened. I have been allowed to dig deep into what I find most interesting. I have been down dead-end roads and experienced eureka moments. I have been invited into Chinese culture with open arms. I have met inspirational and truly clever people. I have made friends. I have built a home for my family. But chief among all, my brilliant girlfriend has gifted me with two rowdy, noisy and so incredibly wonderful children.

Admittedly, it has not always been fun or easy. I have worked hard. Often at the expense of my family and friends. I have been frustrated. I have been tired. And so has my family and friends. However, now, the feeling I am left with is gratitude. I am grateful to a lot of people; I am grateful for their never-wavering support and apparent never-ending reserve of patience.

I would like to extend a heart-felt thank you to my advisors Associate Professor Toke Rammer Nielsen, Professor Jørn Toftum and Competence Director Peter Noyé for patiently steering me off paths leading to nowhere and always competently showing me how to best improve my work – all the while somehow finding a way to let me have a say and be heard. I appreciate that it has not always been easy. Thank you.

It would not have been possible for me to do this project if it had not been for the support of my colleagues and employers at the NIRAS Group. I want to

thank the NIRAS Group for taking a chance on me. I hope that you find me worth the gamble. However, support has gone well beyond funding. I would like to thank my colleagues and employers for taking an earnest interest in me and my project, for invaluable professional sparring and for always lending me support when I needed it.

I thank everybody at the Section for Energy and Services and the Section for Indoor Environment at the Technical University of Denmark for a stimulating, supportive environment and for always listening to me – even when it should have been clear to me that you had more important things to do (e.g. work).

I thank everybody at the Institute of Built Environment at Tsinghua University. You truly made me feel welcome. A special thanks goes to Professor Yinping Zhang for making my visit possible and your earnest and successful effort to ensure that my stay was a pleasant one.

As I have already mentioned, I have had the good fortune to meet some truly clever and inspiring people. In no particular order, I would like to thank Jacob Birck Laustsen, Lau Markussen Raffnsøe, Carsten Rode, Gabriel Bekö, Søren Peter Bjarløv, Morten Hjorslev Hansen, Ruut Hannele Peuhkuri, Casper Pold, Rune Korsholm Andersen, Charles J. Weschler, Philip Hopke, Tunga Salthammer and Jianyin Xiong. You have all, each in your own way, helped me along my merry way.

Also, I would like to thank Brynhildur Eggertsdottír Lindergård, architect, for somehow always being able to find or produce just the right illustrations.

My biggest thanks of all goes out to my family and friends. I am simply amazed at your capacity for patience. I cannot imagine how incredibly boring it must have been for you, my friends, to listen to me drone on about the virtues of good indoor air quality. But that must pale in comparison to the labours of my family: You have had to live with me. Truth be told, I have not been on my best behaviour the past few years. I am aware of it. I apologise for all the weekends that I have been working and all the holidays that I have missed.

Emilie, without you, this would not have been possible. Without you, it would not have been a worthwhile journey. Then again, without you, nothing would.

Copenhagen, Denmark, February 2019

Christopher Just Johnston

Abstract

We use ventilation to ensure that people are healthy and comfortable in their homes and workplaces. However, ventilation comes at a cost. In terms of energy, indoor environments are expensive to condition. In a time where the production of energy still has a negative impact on the environment and global demand is growing, it is in everybody's best interest that ventilation is done correctly. When designing ventilation systems the focus – in prioritised order – has to be on health, comfort and energy efficiency.

At present, many Scandinavian homes have air change rates that are lower than the currently recommended 0.5 h^{-1}. This means that many Scandinavians risk long term exposure to hazardous chemicals present in the indoor environment. Raising ventilation rates to the currently recommended level will help protect occupants from poor indoor air quality negatively impacting their health.

The work presented in this thesis has shown that it is possible to design ventilation systems that can ensure healthy and comfortable indoor environments at no extra cost in terms of energy.

Predictions of published physics-based models for the emission of pollutants – volatile organic compounds – from building materials were compared to measurements of formaldehyde emissions done in practice. The comparison revealed that the physics-based models fail to accurately predict emissions in real world settings.

Data-driven emission models present an alternative to physics-based models. Regression analysis on data gathered in newer detached and semi-detached single-family homes in rural and suburban Denmark yielded two emission models for formaldehyde. One for 'normal' emission levels and one for 'high' emission levels. Data on formaldehyde emission in Danish homes were scarce. The scarcity of data has imposed limitations on the use of the derived models. Still, the derived emission models were accurate to a level that allowed them to be used for analysis in building performance simulation. The derived emission models were successfully implemented in a validated building performance

simulation tool. Simulations were performed in order to estimate the impact of building generated pollution on ventilation airflow rates, indoor air quality and energy demand under Danish climatic conditions.

The results show that designers of ventilation systems should consider some form of heat recovery on exhaust air, because this is the single most effective measure to reduce the energy demand of ventilation systems under Danish climatic conditions. When using heat recovery, the performance of constant air volume (CAV) ventilation and of demand controlled ventilation (DCV) are comparable in terms of energy. In terms of indoor air quality and thermal comfort, DCV delivers better results than CAV. Compared to CAV, DCV can deliver improvements in indoor air quality and thermal without a negative impact on energy demand.

Before DCV can be allowed to lower ventilation rates below the current recommendation for minimum ventilation rates, more research and development is needed. The three main issues that need resolving are: (i) it is unclear which pollutants are dominant and can be used to reliably represent pollution from building materials and furniture, (ii) the needed sensor technology is not mature enough to meet the demands of the industry and (iii) the necessary legislative framework is not in place. Until the two first issues have been resolved, it is recommended to continue the practice of prescribing base ventilation rates.

Due to the nature of the work presented in this thesis, all of the above results and conclusions are only valid in the context of the Danish weather and climate. Also, all considerations and conclusions on how DCV and CAV ventilation compare to each other are based on comparisons where both use heat recovery to reduce the energy demand.

Resumé

Vi bruger ventilation til at sikre, at folk er raske og veltilpas i deres hjem og på deres arbejdspladser. Men ventilation er ikke gratis. Det koster energi at opretholde et godt indeklima. I en tid hvor energiproduktionen stadigvæk skader miljøet, og den globale efterspørgsel på energi vokser, er det i alles bedste interesse, at ventilationssystemer designes og installeres korrekt. Ved design af ventilationssystemer skal fokus – i prioriteret rækkefølge – være på sundhed, komfort og energieffektivitet.

I dag har mange skandinaviske hjem et luftskifte, der er lavere end de anbefalede 0,5 h^{-1}. Det betyder, at mange skandinavere risikerer at blive udsat for skadelige kemikalier i indeklimaet igennem længere tid. Hæves ventilationsrater til det anbefalede niveau, så kan det hjælpe til med at beskytte beboere mod de negative helbredseffekter, der kan komme som følge af et dårligt indeklima.

I denne afhandling er det blevet demonstreret, at det er muligt at designe ventilationssystemer, der kan sikre skandinaviske hjem et sundt og behageligt indeklima uden at øge energibehovet.

Forudsigelser af emissionsmodeller for forurening fra bygningsmaterialer – her repræsenteret af flygtige organiske forbindelser – baseret på teoretisk-fysiske modeller for massetransport blev sammenlignet med målinger af formaldehydemissioner i bygninger og praktiske forsøg. Sammenligningen viste, at de teoretisk-fysiske modeller ikke kunne forudsige emissionsrater under virkelige forhold.

Datadrevne emissionsmodeller er et alternativ til teoretisk-fysiske emissionsmodeller. Regressionsanalyse af data indsamlet i nyere danske række- og fritliggende huse ledte til to emissionsmodeller for formaldehyd. En for 'normale' og en for 'høje' emissionsniveauer. Der findes ikke meget data om formaldehydkoncentrationer i danske boliger. Manglen på data har gjort, at det er begrænset, hvad de udviklede emissionsmodeller kan bruges til. Alligevel var de udviklede emissionsmodeller nøjagtige nok til, at de kunne bruges til analyse. Resultater fra simuleringer kørt i et valideret bygningssimuleringsprogram blev

brugt til at analysere, hvilken indflydelse forurening fra bygningsmaterialer og møbler har på ventilationsrater, luftkvalitet og energibehov i danske enfamiliehuse.

Resultaterne viste, at ventilationssystemer altid bør inkludere en form for varmegenvinding på afkastluften, fordi det isoleret set er det mest effektive tiltag til at reducere ventilationssystemers energibehov under danske klimaforhold. Bruges varmegenvinding, så er energibehovet ved ventilation med konstant volumenstrøm (CAV) og ved behovsstyret ventilation (DCV) sammenligneligt. Sammenlignes DCV med CAV ved samme energibehov, så kan DCV både levere en højere indendørs luftkvalitet og en højere termisk komfort.

Inden DCV kan blive tilladt at ventilere med rater, der er lavere end det i dag foreskrevne niveau, er der brug for mere forskning. De tre største udfordringer, der skal overkommes, er: (i) at det er uklart, hvilke stoffer der er de dominerende, og hvilke der bedst egner sig til brug som indikatorer for niveauet af forurening fra bygningsmaterialer og møbler, (ii) at den sensorteknologi, der er nødvendig for at kunne måle forurening i luften, endnu ikke er moden, og (iii) at de lovgivningsmæssige rammer, der skal definere de funktionskrav, DCV skal fungere under, endnu ikke på plads. Indtil de to første problemer er blevet løst, er anbefalingen at fortsætte den nuværende praksis med at foreskrive laveste tilladte ventilationsrater.

Arbejdet, der er præsenteret i denne afhandling, har haft fokus på danske forhold. Alle overvejelser og konklusioner er derfor kun gyldige for danske vejr- og klimaforhold. På samme måde gælder det for de præsenterede sammenligninger af CAV og DCV, at alle overvejelser og konklusioner er gjort under antagelse af, at ventilation er udført med varmegenvinding.

Table of Contents

Nomenclature

A	Floor area of the room	[m^2]
A_g	Glazed area of the supply air window	[m^2]
A_m	Emitting surface area of the sample material	[m^2]
AH	Absolute humidity	[g/m^3]
Bi_m	Biot number for mass transfer	[-]
$c_{p,a}$	Specific heat capacity of air	[$J/(kg \cdot K)$]
C_0	Initial emittable concentration	[kg/m^3]
C_{1-3}	Coefficients determined in climate chambers	[-]
C_a	Concentration in the chamber or room air	[kg/m^3]
C_{as}	Concentration in air near the surface of material	[kg/m^3]
C_m	Concentration in the sample material	[kg/m^3]
C_s	Concentration in the supply air	[kg/m^3]
D_{1-2}	Coefficients determined in climate chambers	[-]
D_m	Diffusion coefficient for mass transfer	[m^2/s]
E	Emission rate estimated by models derived from regression analysis	[$mg/(s \cdot m^2)$]
Fo_m	Fourier number for mass transfer	[-]
G_a	Volume flow rate of air	[m^3/s]
$G_{a,max}$	Maximum volume flow rate for the DCV system	[m^3/s]
h_m	Convective mass transfer coefficient	[m/s]
I_s	Solar irradiance	[W/m^2]
K_{1-2}	Coefficients determined in climate chambers	[-]

K_{ma}	Material to air partition coefficient	[-]
n	Air exchange rate	[s^{-1}]
N	Air change rate per hour	[h^{-1}]
PLR	Part load of the flow [0,1]	[-]
$Q_{a,in}$	Energy entrained in the supply air	[W]
$Q_{a,out}$	Ventilation loss	[W]
Q_{diff}	Term correcting the energy balance in IESVE	[W]
$Q_{g,win}$	Heat loss from the glazed part of a basic window	[W]
Q_{heat}	Heating demand/heat loss	[W]
Q_{Ueff}	Effective heat loss through supply air windows	[W]
R	Emission rate	[$kg/(s \cdot m^2)$]
SFP_{Frac}	Fraction of the SFP a DCV is running [0,1]	[-]
t	Time	[s]
T	Absolute temperature	[K]
U_{eff}	Effective U-value	[$W/(m^2 \cdot K)$]
U_g	(simulated) centre pane U-value of the window	[$W/(m^2 \cdot K)$]
V	Volume of the room	[m^3]
x	Distance (between surfaces of emitting material)	[m]

Greek symbols

α	Dimensionless air exchange rate	[-]
β	Ratio of building material volume to room volume	[-]
δ	Material thickness	[m]
θ_a	Supply(/inlet) air temperature	[°C]

θ_e	Outdoor temperature	[°C]
θ_i	Indoor temperature	[°C]
$\theta_{a,Is=0}$	Supply air temperature w/o solar radiation	[°C]
ϱ_a	Density of air	[kg/m^3]

Acronyms

ACH	Air change per hour
AH	Absolute humidity (mass of water per unit volume of air)
BPS	Building performance simulation
BR18	The Danish Building Regulations of 2018
CAV	Constant air volume
CO_2	Carbon dioxide
DCV	Demand controlled ventilation
DK2004	VOC emission model by Deng and Kim, 2004
HCHO	Formaldehyde
HH2002	VOC emission model by Huang and Haghighat, 2002
HR	Heat recovery
HVAC	Heating, ventilation and air conditioning
IAQ	Indoor air quality
IDA ICE	Building performance simulation tool
IESVE	Building performance simulation tool
·OH	Hydroxyl radical
NMF	Neutral model format
NO_x	Nitrogen oxides

NO_2	Nitrogen dioxide
O_2	Oxygen
O_3	Ozone
PM	Particulate matter
Qa2007	VOC emission model by Qian et al., 2007
RH	Relative humidity
SHGC	Solar heat gain coefficient
SVOC	Semi-volatile organic compound
SFP	Specific fan power
TC	Thermal comfort
VAV	Variable air volume
VOC	Volatile organic compound
WHO	World Health Organization
WIS	Windows Information System
XZ2003	VOC emission model by Xu and Zhang, 2003

1 Introduction

In the industrialized part of the world, buildings are responsible for approximately 40 % of the total energy consumption [1,2]. Here, the energy demand has been at this level for decades [3]. Meanwhile, due to increases in the building stock in developing countries, the global energy demand of buildings is expected to increase. Compared to 2013 levels, the global energy demand of buildings is projected to increase by a further 30 % by 2035 [4]. This projected development is in direct conflict with the need for an overall reduction in the global energy demand if climate changes are to be avoided [5]. Now, incentivised by the threat of climate change and continuously stricter energy requirements in national standards, the construction industry is working towards low-energy buildings [6].

Westerners spend 60-70 % of their lives in their homes [7–9]. With this exposure duration we are vulnerable to pollutants in our home environments. Since the first Global Burden of Disease Study in 1990, household air pollution has consistently ranked as one of the 20 leading risks for a life in poor health and premature death [10]. Energy conservation measures include general increases in insulation levels and an overall increase of the airtightness of the building envelope. If means of ventilation are not considered, increased airtightness can lead to a lower air change rate (ACH), result in poorer indoor air quality (IAQ) and ultimately have a negative impact on occupants' health [11–14].

One of the challenges of low energy status is developing methods that can ensure healthy and comfortable indoor environments at low costs in terms of energy. Currently there is an industry wide concerted effort to determine ventilation standards [15] and update building performance simulation (BPS) tools with the capability to determine the indoor environmental quality to a level that ensures that building designs deliver on both health and comfort at low energy demands [16].

The official goal of the Danish government is to make Denmark independent of fossil fuels by 2050. In order to reach this goal, it has been estimated that the energy demand for heating must be reduced by 40 % [17]. As energy renovations are crucial to efforts to become independent of fossil fuels, a surge in energy renovations could be imminent. A study of 500 Danish children's bedrooms found that 68 % had average carbon dioxide (CO_2) concentrations above 1000 ppm [18]. This indicates that Danish homes are already insufficiently ventilated. In order to achieve both necessary reductions in energy demand and healthy and comfortable indoor environments, it is vital that the most efficient means of ventilation are identified before such a surge.

The performance of a given ventilation system, in terms of energy and supply air temperature, is dependent on the local weather and climate. Previous studies that have researched the potential of various forms of ventilation under Danish climatic conditions have not established if any approach to ventilation holds clear advantage over others [19]. This thesis was written in an attempt to further the understanding of how ventilation is best used to keep energy demand low while maintaining an indoor environment that is safe and comfortable under Danish climatic conditions.

1.1 Scope and main results

The main topics of the work presented in this thesis are building energy and IAQ. The thesis covers work done in three different but related fields: heat transfer, mass transfer and BPS. The focus of the work was on identifying what characteristics that made ventilation efficient in terms of energy and arrive at an estimate of the minimum ventilation rates necessary to meet criteria for health and comfort. Due to the nature of the work, all results and conclusions are only valid in the context of the Danish weather and climate.

The work was planned in three steps. The first step was to find the most energy efficient forms of ventilation for the Danish climate. To do this, a study was designed to compare the relative performances of representative ventilation systems. The comparison included both mechanical and natural ventilation systems. Special attention was given to supply air windows, incorporated into the study as an example of highly efficient natural ventilation. The main conclusion was that, in connection with an energy renovation, heat recovery (HR) on the exhaust air is the single most efficient energy conservation measure under Danish climatic conditions.

The second step was to research how best to represent the influence that pollution from building materials and furniture has on ventilation control, airflow rates and energy demand in a BPS context. One fundamental hypothesis was that accurate emission models for pollution from building materials and furniture existed in published literature, or that it would be possible to derive such models from data collected in existing buildings. During the course of the project, it became apparent that such models did in fact not exist and that data on emission was scarce. In order to move forward, it was chosen to derive data-driven emission models from available data, even though data were scarce. Formaldehyde (HCHO), a pollutant found in both building materials and furniture, was chosen as a proxy for pollution from building materials and furniture.

Regression analysis yielded two emission models for HCHO. One for 'normal' emission levels and one for 'high' emission levels. The models were based on data gathered in newer detached and semi-detached single-family homes in rural and suburban Denmark. The models, therefore, are limited to use for indoor climates and conditions present in such types of homes. Moreover, the scarcity of data influenced what could reasonably be inferred from the regression analysis and derived emission models. Though potential predictor variables were selected based on a documented ability to influence emission rates and all correlations between dependent and predictor variables were statistically significant, the models suffer from being overfitted and predict behaviour that is inconsistent with laboratory observations. Meanwhile, predicted emission rates are in good agreement with the underlying observations and the emission models do appear to capture at least part of the dynamic behaviour exhibited by HCHO emissions in real world settings. Ultimately, in spite of their flaws, the emission models were concluded to have value in the context of BPS and the present research project.

The third step was to implement pollution emission models into a BPS model. The BPS model was used to run a parameter variation. The purpose of the exercise was twofold: (i) to examine how considerations of building generated pollution would affect ventilation control systems and energy demand and (ii) to estimate the minimum ventilation rates necessary to keep occupants healthy and comfortable. The study was subject to the limitations that the HCHO emission models imposed on the BPS model. Still, after evaluating the method, it was concluded that it was possible to come to some general conclusions valid for Danish single-family homes. The study concluded that building generated pollution may still present a problem and that demand controlled ventilation (DCV) with HR, compared to the performance of constant air volume (CAV) ventilation with HR, can help improve both IAQ and thermal comfort (TC). For now, based on considerations of the current level of technology and pricing, it was recommended to continue the current practice of prescribing base ventilation rates.

The framework for the research project was the Danish Industrial Ph.D. Programme. As such, the motivation was inherently commercial and one prerequisite was that research output has commercial value. The commercial goal of this project was to give the host company, the NIRAS Group, an advantage in the competitive construction sector. The research conducted under the framework of this project was organised to meet that commercial goal. As a consequence, in order to succeed, pragmatic compromises have been made during the course of the project. One example of such a pragmatic compromise is the derived data-driven HCHO emission models. Here, the pragmatic compromise was to choose a small data pool over no immediate solution.

1.2 Objectives

The aim of the work presented in this thesis was to determine what general form of ventilation best helps in the efforts to develop low-energy homes with high quality indoor environments in Denmark.

The first objective of this thesis was to compare the performance – in terms of energy demand and supply air temperature – of natural and mechanical ventilation under Danish climatic conditions and quantify the magnitude of the difference in terms of energy.

The second objective of this thesis was to develop a method to estimate the impact that building generated pollution has on IAQ, the energy demand and ventilation rates under Danish climatic conditions and to use this method to evaluate the minimum requirements for ventilation rates as prescribed by the Danish Building Regulations of 2018 (BR18) [20].

1.3 Hypotheses

The hypotheses of the thesis are that

1. air change rates in Danish dwellings are often insufficient in relation to national and international recommendations for a healthy indoor environment,
2. ventilation with heat recovery (HR) is the best choice in terms of energy needs when a building is to be energy renovated,
3. indoor concentration of pollution from building materials and furniture can reach levels that can cause discomfort and negatively impact occupants' health,
4. accurate emission models for pollution from building materials and furniture exist – or that it is possible to derive such models from data collected from existing buildings and
5. demand controlled ventilation (DCV) can control indoor concentration of pollution from building materials and furniture better than constant air volume (CAV) ventilation and do so without a negative impact on the energy demand.

Existing published peer-reviewed literature supports the first and third hypothesis. While there are many examples of models for emission of pollution from building materials and furniture in published peer-reviewed literature, a closer examination found that they fail to estimate emissions in real world settings. Meanwhile, it was found that it is convenient to derive models for emission of pollution from building materials and furniture by regression analysis of data collected in buildings. The derived emission models were accurate to a level that allowed them to be used for analysis in BPS. This, in part, substantiated the second half of the fourth hypothesis. The second and fifth hypotheses were substantiated by results from dynamic simulations performed with validated BPS tools.

1.4 Outline of the thesis

The thesis contains findings from published peer-reviewed literature, regression analysis of pollutant emissions and results from dynamic simulations performed with validated BPS tools.

The thesis is structured as follows. After this introductory chapter, Chapter 2 summarises the state of the art of research fields related to the work presented in the thesis. The chapter gives introductions to the fields of ventilation, emission modelling and BPS.

Chapters 3, 4 and 5 present results from the studies this thesis is founded on. Each chapter also serves to account for the applied method and discuss findings and results. The chapters are presented in the order that the respective studies were executed. This way, the order of the chapters also map out the progression of the work the thesis is based on.

Chapter 3 presents a study comparing the relative performance of ventilation systems under Danish climatic conditions. Chapter 3 is based on Paper 1 and Report 1. Chapter 4 presents findings from a comparison of physics-based emission models with observations made in practice. The chapter also presents the results of a regression analysis performed in order to derive HCHO emission models. Chapter 4 is based on Paper 2 and Paper 3. Chapter 5 presents results from a parameter variation performed in a BPS tool. The purpose of the parameter variation was to learn about the influence that building generated pollution has on energy demand and ventilation rates. Building generated pollution was simulated using models derived in Chapter 4. Chapter 5 is based on Paper 3.

Chapters 6 and 7 contain sections on discussions, conclusions and perspectives.

2 Background

This chapter introduces the research fields related to the work presented in the thesis. The chapter consists of five sections. The first section gives an introduction to the concept of ventilation and how it can be brought about. The second section summarises the main categories of ventilation control. The third and fourth sections cover pollutants in the indoor air and theory on pollution emission modelling relevant to the work presented in this thesis. The fifth and final section is on BPS, BPS tools and a review of the prerequisites that BPS tools must meet in order to allow implementation of pollution emission models.

2.1 Ventilation

ASHRAE defines ventilation as the "intentional introduction of air from the outside into a building" [21]. Overall, there are two forms of ventilation; natural and mechanical ventilation, see Figure 2.1. Ventilation strategies that employ both natural and mechanical elements are called hybrids.

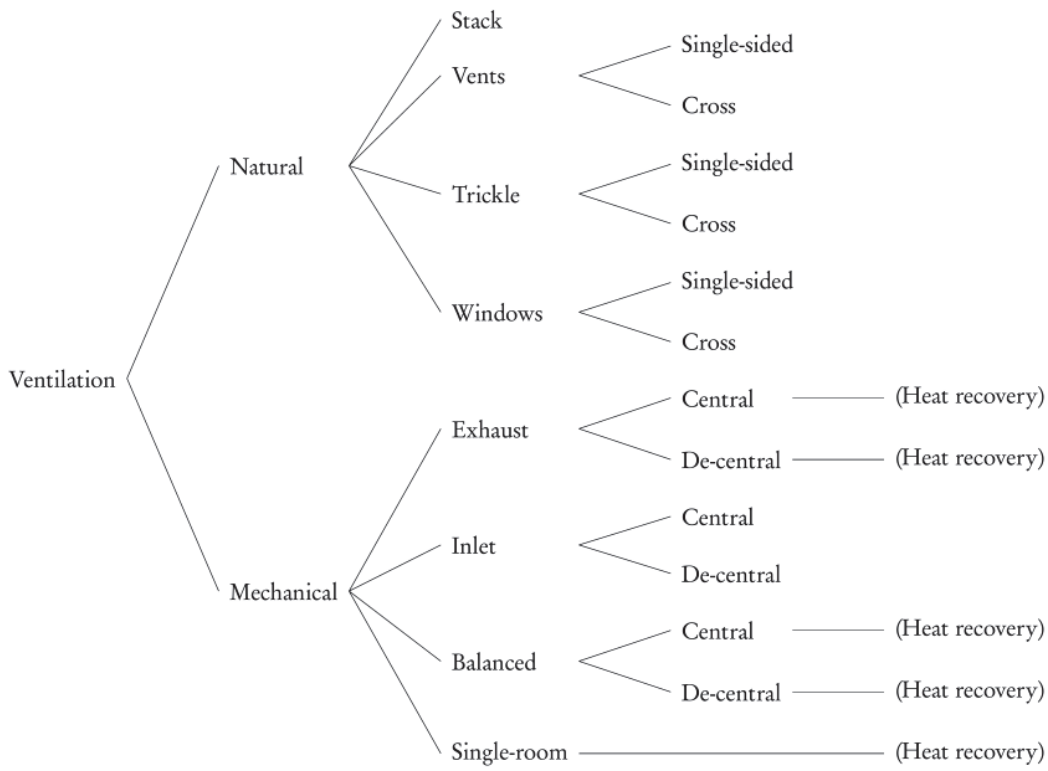

Figure 2.1: Categories of ventilation

All ventilation is driven by pressure differences; air naturally moves from zones with high pressure to zones with lower pressures. The magnitude of a given air flow is a function of the pressure difference between zones and the total resistance offered by the path the air flow follows while moving from high to the low pressures. The magnitude of an air flow increases with increasing pressure differences and decreases with increasing flow resistances. Natural ventilation is driven by pressure differences that occur naturally in and around buildings. The total driving pressure depends on the wind speed and direction, the temperature difference between zones (e.g. the interior and exterior) and the difference in height between inlets and outlets. Mechanical ventilation relies on fans to create local high pressures to drive ventilation.

2.1.1 Natural ventilation

Natural ventilation is driven by the pressure differences that occur naturally over a building. When wind moves air over and around a building, it increases pressures on the windward side and lowers pressures on the leeward side. When indoor and outdoor temperatures are different, the warmer air becomes buoyant relative to the colder air resulting in an upward movement of the warmer air. The pressure difference that drives natural ventilation is a result of the combined effects of wind speed and direction and the temperature difference between the indoors and outdoors. Natural ventilation can be facilitated and controlled through strategically placed and shaped openings in a building envelope [22,23]. Figure 2.1 gives four examples of such openings.

The first of the four examples is a stack. In the context of natural ventilation, a stack serves as an example of an opening located at a height above a ventilated room. Due to differences in the density of warm and cold air, warm air is buoyant relative to cold air. When indoor air is warmer than outdoor air, the natural buoyancy of the indoor air can drive it up through a stack. The process driving the ventilation is known as the stack effect. In order for a stack to be efficient, it needs openings at the room level. Stacks are an efficient form of natural ventilation and air flow rates can be controlled by changing the height difference between inlets and outlets and their cross-sectional areas.

If a building design does not allow for the use of the stack effect, it is possible to ventilate at the room level by controlling openings in the building façade. Figure 2.1 gives three examples of such openings. Here vents are examples of simple openings in the façade. As with a stack, it is possible to control the air flow rates by adjusting the cross-sectional area of a vent by shutters, dampers or similar mechanisms.

Trickle vents are similar to ordinary vents in that they are simple openings to the exterior. However, they are smaller than ordinary vents and allow only small flow rates of air to pass through them at any given time. Where trickle vents do not allow for the same level of control as larger vents, they can be used to establish a base ventilation rate without occupants having to continuously adjust the cross-sectional area. Trickle vents are usually placed in window frames.

Of the three examples given in Figure 2.1, windows can supply the largest air volumes. Ventilation can be controlled by adjusting the size of the cross-sectional area by either opening or closing the window.

Disregarding stack, natural ventilation at the room level can be achieved either by using openings in a single wall or by using openings in two opposing walls. If a room is ventilated by openings in a single wall, the form of natural ventilation is called single-sided. If a room is ventilated by openings in two opposing walls that both face the exterior, the form of natural ventilation is called cross ventilation. Of the two forms, cross ventilation is the most efficient. When wind passes over or round a building, it creates pressure differences across the building; the windward side has a higher pressure than the leeward. Cross ventilation makes use of this pressure difference to drive air flows across a room or building.

2.1.1.1 Pros and cons

A well designed natural ventilation system is passive and efficient in supplying un-conditioned exterior air. Being passive, a natural ventilation system has no need for maintenance and uses no energy to drive ventilation.

Since the driving potential is dependent on the exterior conditions, natural ventilation can be difficult to control [22]. The supply air is un-conditioned and this can at times affect thermal comfort (TC) and indoor air quality (IAQ). In periods with cold outdoor temperatures, occupants may experience low indoor temperatures and draught. Denmark is not a big country and geographical variations in the climate are small. The Danish coast (which constitutes the majority of the land mass) has a temperate oceanic climate while the inland has a warm-summer humid continental climate (with Köppen climate classifications Cfb and Dfb, respectively). For 28 % of the full year and 90 % of summer, outdoor temperatures allow outdoor air to be used unconditioned [24,25]. With outdoor temperatures averaging a little above 1 °C, Denmark also has mild winters [26]. Consequently, Denmark has had a long tradition for natural ventilation in homes. This tradition continued up until 2010 when the Danish building regulations were updated to include requirements for preheated supply air and a minimum heat recovery (HR) rate on exhaust air of 80 % for multi-family housing [27]. With driving pressures being low and unstable, it is not possible to implement filters or heat exchangers into a natural ventilation system [28]. Therefore, if exterior air is polluted, supply air volumes will bring this pollution indoors [29–31]. However, as the outdoor air is relatively clean, this is generally not a problem in Denmark [32].

It is possible to improve control by adding a control system and fitting actuators to shutters, dampers and windows. However, the system will then no longer be passive or entirely maintenance-free. Arguably, a system fitted with active controls and actuators should be classified as a hybrid system. Still, this may be worthwhile as hybrid systems have been shown to be able to combine the benefits of natural and mechanical ventilation resulting in lower energy demands [22,24].

A natural ventilation system is a part of the fundamental design of a building. To make use of the stack effect, there must be a stack. To make use of cross ventilation, air flowing from one side of a building to another must be unobstructed. Densely occupied rooms – such as meeting rooms and class rooms – and rooms with a large production of heat – such as server rooms – constitute particularly difficult cases. Therefore, it is not always possible to implement a new, efficient natural ventilation system in connection with an energy renovation; the design of the building that is to be renovated may simply not allow it.

2.1.1.2 Supply air windows

A common supply air window design will take outdoor air in trough a valve at the bottom. From here it will lead the air up through a cavity between window panes before directing it into the conditioned interior via a valve at the top of the window. For any temperature difference across a window, energy moves from high to low temperatures. In a supply air window, heat is entrained in the supply air as it passes up through the ventilated cavity between window panes. If not entrained in the supply air, this heat would otherwise have been be lost to the exterior. This way, supply air windows can both lower the heat loss through a window and preheat supply air. Figure 2.2 shows a sketch outlining the principles governing heat exchange in and around a supply air window.

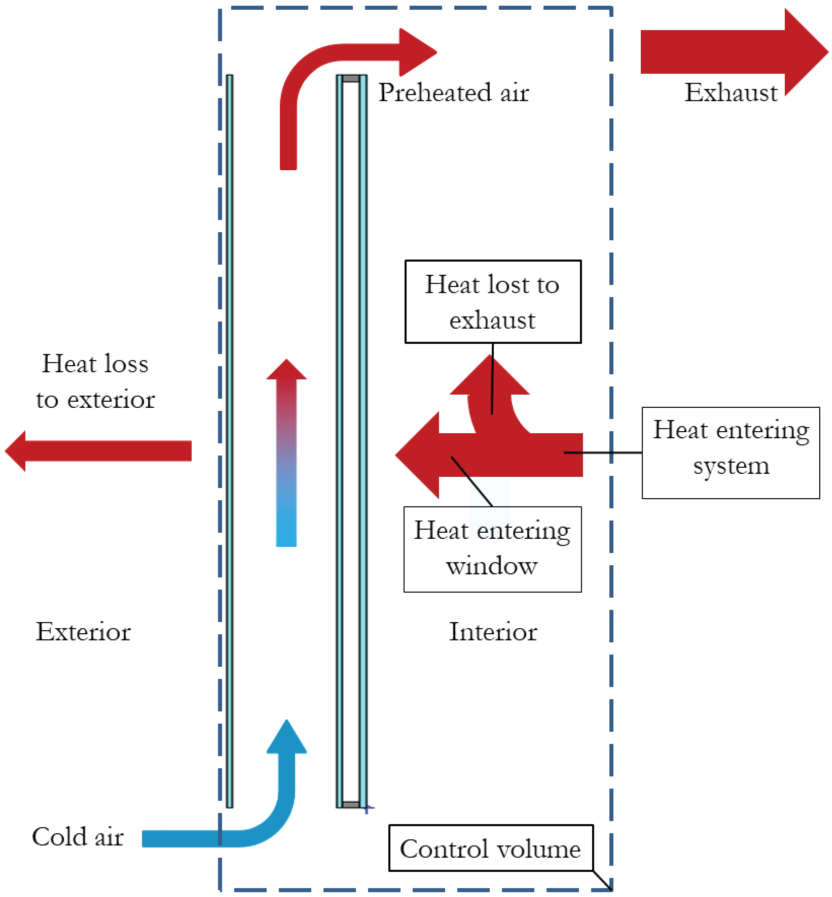

Figure 2.2: Sketch showing the principles of the supply air window

Published literature (project reports and peer-reviewed journal articles) contains several studies of supply air windows [33–39]. The studies cover many different window designs and mathematical models – both white and grey box – have been created to examine the effects of design variations [40–45]. Consensus seems to be that the supply air window has significant advantages when compared to classical natural ventilation where outdoor air is delivered through fresh air valves. When compared to conventional natural ventilation, studies estimate that for ACHs between 0.4 h^{-1} and 0.64 h^{-1} supply air windows can help reduce energy demand for ventilation by 11-24 % [33,34,38].

There are two mechanisms that facilitate preheating of the supply air in supply air windows. One, and by far the most important, makes use of the heat loss inherent to all window designs. Heat driven by a temperature difference over the window is entrained in the supply air stream. In this way a well-designed supply air window can have a very low effective U-value (the effective U-value being defined as heat leaving the system by the outermost pane normalised by area and the temperature difference between the interior and exterior). Increasing supply airflows have the effect of lowering the effective U-value.

The second way to preheat supply air is by solar energy. Incident solar irradiation that is not reflected from or transmitted directly through the window, is absorbed in the panes. The window panes can release the absorbed energy to the supply air by convection. Increasing the supply airflow will increase the solar heat gain coefficient (SHGC) and the g-value (here defined as the total solar heat gain divided by the incident solar radiation) as the fraction of energy that is transferred to the supply air grows while the fraction reemitted to the exterior diminishes. While using solar energy to preheat supply air is efficient, its usefulness is subject to availability. A window's orientation, shadows cast by nearby objects and structures and the amount of incident solar radiation in occupied hours – especially during dark northern winters – are all factors that can have a negative impact on the usefulness of solar energy as a way to preheat the supply air.

2.1.2 Mechanical ventilation

There are three categories of mechanical ventilation: supply, exhaust and balanced, see Figure 2.1. With the exception of de-centralised, self-contained ventilation units [46], all types of mechanical ventilation transport ventilation air via ducting. Air is transported from the exterior, through the ventilation unit and into the interior. Supply ventilation is facilitated by an increase in the indoor static pressure, where room air is transferred to the exterior through vents or by leaking through the building envelope. Exhaust ventilation removes room air to the exterior. Facilitated by a decrease in the indoor static pressure, outdoor air is drawn in through vents or by leaking through the building envelope. Since both supply and exhaust ventilation need ventilation air to pass through the building envelope, they do not work well in buildings that are airtight. Since balanced ventilation transports both supply and exhaust air through ducts, it can be used even if a building is airtight.

Mechanical ventilation takes up space. The design process involves consideration on where to locate the ventilation unit. A suitable location allows a ventilation unit access to outdoor air while minimising the risk of exhausted air being re-entrained in the supply air. A chosen location will often be away from otherwise useful space, be hidden from sight, allow for noise insulation and be accessible for maintenance. In single-storey housing, ventilation units are often located in attics. In multi-storey housing, ventilation units are often located in attics, on roofs or in basements.

A single ventilation unit can be used to service a single room, a home or an entire block of apartments. A system consisting of one ventilation unit servicing multiple homes is called a centralised system. A system where every single apartment has its own ventilation unit is called a de-centralised system. A system where (small) ventilation units are located in the single room they service is called a single-room system.

An aspect that can influence the choice between central, de-central and single-room systems is the available options for ducting. It has only recently become mandatory to include considerations of mechanical ventilation as part of a new development in Denmark [27]. The majority of the existing building stock was built before mechanical ventilation was even an option [47]. New developments will use installation shafts and suspended ceilings to allow ducting to go where it is needed. Most of the existing building stock does not have installation shafts and it may not be possible to suspend the ceilings. Usually, this is not a problem for single-storey housing as it is often possible to place ventilation units in attics. However, it can cause difficulties when designing systems for multi-storey housing.

Ducting invariably leads to inlets and outlets. Inlets are used to supply fresh air and outlets to exhaust room air. The shape and position of inlets and outlets can influence both TC and how effective a ventilation system is at removing polluted air [23,48–51]. For example, if an inlet is located close to an outlet, there is a risk that the supply air will not reach the polluted zones but move directly from the inlet to the outlet. This is known as a short circuit. Conversely, if an outlet is placed close to a source of pollution, it may exhaust polluted air before pollution diffuses into the main body of air. For these reasons a common strategy is to place inlets in the occupied zones – e.g. in living rooms and bedrooms – and to place outlets far from inlets but close to sources of pollution – e.g. in kitchens and bathrooms.

2.1.2.1 Pros and cons

A well designed mechanical ventilation system allows for appropriate control of TC and IAQ [23]. Mechanical ventilation units can be fitted with filters and heat exchangers that can help increase comfort and health and reduce heat losses [52,53].

Being mechanical, a mechanical ventilation system takes up space and needs energy and maintenance in order to ensure continuous performance. Also, mechanical ventilation systems can be expensive to design and set up. Historically, there have been issues with maintenance and quality of installations and design that – justifiably – have given mechanical ventilation a bad reputation with home owners and building operators [54–56].

2.1.2.2 Heat recovery

Mechanical exhaust ventilation allows for heat recovery (HR) by using a heat exchanger. Heat recovered from exhausted air can be transferred to a heat storage, e.g. a hot water storage tank. Balanced mechanical ventilation systems allow heat (or cold) recovered by heat exchangers to be transferred to the supply air.

The Danish Building Regulations of 2018 (BR18) [20] prescribes that multi-family housing must use a heat exchanger with a minimum efficiency of 80 %. Fixed plate and rotary wheel heat exchangers can achieve this efficiency [57]. The nominal HR efficiency of a contemporary heat exchanger can be rated higher than 90 % at peak performance (e.g. Genvex [58], Nilan [59] and InVentilate [60]). Though it is possible for a carefully constructed ventilation system to meet the nominal HR efficiency [61], there is a risk that systems will not perform as well as planned. Ventilation systems with HR are vulnerable to leaks and studies have found that systems with nominal HR rates between 70-80 % often do not recover more than 50-70 % [62,63]. The HR rate of large systems, such as centralised ventilation systems in multi-storey housing, can also be negatively affected by temperature changes in ducting.

HR ventilation has the potential to lower ventilation losses – and by extension the energy demand – for climates as they are in the Scandinavian region [19]. Two independent Swedish studies, both assuming a constant heat exchanger efficiency of 80 %, have estimated that HR ventilation can reduce energy demand by 22 % [64,65]. Similar to the Swedish studies, a Danish study identified scenarios where the purchase and implementation of HR ventilation in connection with a renovation was net profitable over a period of 30 years [66].

2.1.3 Ventilation in homes

The current base minimum air flow rate prescribed by BR18 is 0.3 $l/(s \cdot m^2)$. This is comparable to an ACH of 0.5 h^{-1}, which is the current standard for minimum ACHs of most European countries [67]. Before 1982, Danish building regulations did not prescribe a base ventilation rate. Instead, ventilation was ensured by prescribing minimum sizes for vents in kitchens and bathrooms and stating that living rooms and bedrooms needed windows or other similar openings to the exterior [27]. Criteria for the overall airtightness of homes were included in the Danish building regulations in 2005 [27]. Up until then, natural ventilation was the standard form for ventilation. 2010 saw the implementation of criteria for supply air and HR for multi-storey housing [27]. Between 2005 and 2010, exhaust ventilation was the standard form for ventilation for multi-storey housing.

Of the total Danish housing stock in 2018, 91 % was constructed before 2005 and 96 % was constructed before 2010 [47]. In other words, 91 % of the Danish housing stock was designed with natural ventilation, 5 % was designed airtight with exhaust ventilation and up till 4 % have been designed airtight with balanced ventilation and HR (single-family homes are exempt from the rule of balanced ventilation with HR).

As stated, most European standards prescribe a minimum ACH of 0.5 h^{-1}. This ACH has been put in place to protect occupants from indoor air pollution and to protect buildings from being harmed by elevated moisture levels. Studies have found that a significant proportion (> 50 %) of Scandinavian homes have ACHs below 0.5 h^{-1} [18,67,68]. The studies measured ventilation rates either by calculating them from results of real-time measurements of occupant generated CO_2 or by estimating average ACHs from deposits of (passive) tracer gas collected in tubes. A recent study compared results from these methods to measurements done with an active tracer gas. The study concluded that the used methods may well overestimate ACHs by a factor of 2-3 [69]. This indicates that average ventilation rates in Scandinavia may be lower than what studies have shown.

2.2 Ventilation control

In order to keep occupants healthy and comfortable, ventilation is used to dilute and exhaust polluted air and assist in the control of indoor temperatures. International guidelines [13,14,70–72] and national standards [20,73,74] suggest and prescribe maximum concentration levels for pollutants, acceptable intervals for temperature and maximum air speeds. Historically, when designing ventilation systems for homes, focus has been CO_2, relative humidity (RH) and temperature. In the context of ventilation, CO_2 is used as a proxy for the total load of bioeffluents emitted by occupants. Prolonged periods with moisture levels in excess of 75 % RH can damage building materials [75] and therefore RH in buildings is sought kept below this level. In the context of ventilation of homes, compliance with prescribed temperature ranges (operative or air) is accepted as sufficient evidence that a building design will deliver an acceptable level of TC.

Being passive and dependent on external conditions, natural ventilation offers little in the way of active control [22]. Criteria are sought met by compliance with prescribed minimum air flow rates. Mechanical ventilation systems can be controlled by adjusting fan speeds in the ventilation unit and adjusting dampers in ducting, inlets and outlets. The level of control depends on the system. A simple system can use a constant air volume (CAV) to keep IAQ and TC at the desired level. CAV ventilation can be used when the dimensioning load is well known and stable over time. If loads vary over time, as system can use a variable air volume (VAV) to adjust air flow rates according to the demand. VAV ventilation systems are more sophisticated than CAV systems. As a general rule, VAV systems will need to be able to control dampers throughout the system. Depending on the design of a VAV system, air flow rates may be adjusted in real time as a response to a change in the indoor environment or simply follow a set schedule. Demand controlled ventilation (DCV) is a special case of VAV ventilation. Where VAV ventilation is any system that can vary air flows (usually controlled by temperature), DCV is designed to relate air flow rates to the conditions in the environment it services (e.g. RH and CO_2). A sophisticated DCV system can respond to changes in the indoor environment in real time. In order to do this, a DCV system needs sensors to measure conditions and a control system that can interpret changes in the indoor environment and correspond accordingly.

2.2.1 Impact on energy demand

All well designed ventilation systems can deliver high quality indoor environments with good IAQ. However, the choice of ventilation control principle can influence system performance in terms of energy. Results from studies of European residences suggest that it may be possible to reduce ventilation volumes below prescribed levels for 30-60 % of the time without compromising IAQ [76,77]. This, in turn, suggests that VAV ventilation can deliver IAQ at levels equal to CAV ventilation at lower costs in terms of energy. Specifically, when compared to CAV ventilation, DCV has been found to be able to reduce the energy demand for ventilation by as much as 40-60 % [78–81]. Another way to reduce the energy demand for ventilation is by using HR. When the performance of DCV is compared to CAV – both using HR – reported reductions in energy demand are significantly smaller [81]. Meanwhile, though DCV has been in use in commercial buildings for many years, smart ventilation is still an emerging technology and the application of demand controlled ventilation in residences is limited [77,82,83].

The level of control a given balanced ventilation system has over IAQ and energy demand is related to the airtightness of the building envelope; a leak between an inlet and an outlet may prevent conditioned and polluted air from being exhausted. Such a leak can result in a higher concentration of pollution in the indoor air and a lower global HR rate [23]. Lowering the infiltration rate is known to improve performance of balanced mechanical ventilation systems with HR [23,65,84]. Dependent of type of housing, un-renovated Danish housing stock (prior to 2006) has average infiltration rates ranging from 0.22-0.28 $l/(m^2 \cdot s)$ [85]. The current maximum infiltration rate air allowed by BR18 is 0.13 $l/(s \cdot m^2)$. Studies have found that renovations can reduce infiltration rates by 70-80 % in single-family housing [84,86]. Reducing the average infiltration rate by 70 % would lower it to 0.06-0.08 $l/(s \cdot m^2)$.

In 1979, in response to the second oil crisis, Danish building regulations were updated with stricter demands to insulation levels in buildings [27]. Before this time, demands to insulation levels were low. With 76 % of the current day Danish housing stock built before 1979 [47] and 91 % designed with natural ventilation (see Section 2.1.3), there is a large potential for reducing energy demand by renovating housing stock and implementing smart ventilation systems. Also, energy renovations may be cost efficient for home owners. A Danish study concluded that implementing balanced ventilation with HR in connection with an energy renovation can be net profitable in multi-family residential housing [66]. Similarly, based on a life cycle cost analysis, a Swedish study identified balanced mechanical VAV ventilation with HR as the most cost efficient ventilation system for multi-family residential housing [87].

2.3 Pollutants in indoor air

Pollution in indoor air comes from a large range of sources. Sources can be divided into two overall categories: outdoor and indoor sources. Outdoor sources can be anthropogenic or non-anthropogenic. Examples of non-anthropogenic sources are particulate matter (PM) from wind erosion, evaporation of organic compounds and pollen from trees and grasses. Examples of anthropogenic sources are flue gases from the transport sector, heavy industries and power production. Flue gases contain pollutants such as nitrogen oxides (NO and NO_x), volatile organic compounds (VOCs) and PM. The hydroxyl radical (·OH) can come from both anthropogenic and non-anthropogenic sources [88,89]. In the presence of sunlight, photocatalytic reactions between oxygen (O_2) and nitrogen dioxide (NO_2) produce ozone (O_3). VOCs, PM, ·OH and O_3 are all considered important pollutants in indoor air. In high doses, they can cause discomfort in occupants. In case of longer term exposure, they can have a negative impact on health [71,90]. Pollutants originating from outdoor air enter the indoor air entrained in the supply or via infiltration through the building envelope [29–31].

Indoor sources can be divided into two main groups: sources stemming from occupancy and sources stemming from building materials. Occupants pollute in two ways. Humans themselves are a source of pollution. Bioeffluents are emitted through the skin and via exhaled breath [91,92]. Occupants' activities are also a source of pollution. Cooking can be a source of flue gases, bathing a source of moisture and cleaning a source of VOCs (from cleaning products) [29,93–95]. Building materials and furniture contain chemicals – VOCs and semi-volatile organic compounds (SVOCs) – that are emitted over time [96,97].

It is useful to consider the sources of indoor pollution as separate as each category of source impacts the IAQ differently. Risks of outdoor pollution affecting the IAQ can be mitigated using filtering technology [52,53]. Sources stemming from occupancy follow a daily schedule and only adds to the pollution when people are home. Building materials and furniture can be cleaned, sealed or exchanged with less polluting alternatives.

2.3.1 Formaldehyde as a proxy for building generated pollution

While many chemical processes in the indoor air are now known, there is no consensus on what type of emission that can be used as a proxy for building generated pollution [82]. The reason is that the chemistry of the indoor air is complex and driven by many processes in the air and on interior surfaces [98–100]. There are daily cycles driven by factors such as the presence of daylight and ambient pollution (e.g. O_3 and NO_2) [101]. Here VOCs can react with ozone and form potentially harmful reactive oxygen species [90]. Adding to the complexity is that chemical components in our cleaning products, personal care products, furniture and building materials change over time [96]. Also, legislation regulating the use of chemicals in our indoor environment varies from country to country. Despite the complex nature of indoor air chemistry, researchers have suggested that a carefully selected proxy will allow a BPS tool to estimate the energy demand and overall IAQ without a detailed chemical model [82].

A suitable proxy for building generated pollution may consider two main categories of pollutants: VOCs and SVOCs. SVOCs are different from VOCs in that they readily condense on surfaces in the indoor environment [102]. Once introduced, SVOCs migrate throughout the indoor environment sticking to surfaces and dust. This has two immediate consequences. The first is that modelling SVOC behaviour is a lot more complex. The other is that SVOCs cannot be handled by ventilation alone. In addition to ventilation, SVOCs have to be managed by source control, cleaning and potentially also by sealing or removal.

Since SVOCs cannot be handled by ventilation alone, VOCs are the better option in cases where focus is on how ventilation affects the IAQ. Choosing

VOCs over SVOCs means that it is necessary to assume that it is possible to disregard the impact SVOCs have on the IAQ. In cases where the aim is to study the impact that building generated pollution has on the energy demand and ventilation control, this is a reasonable assumption. However, for the assumption to hold true, it is necessary to identify a VOC whose emission rate (to the indoor air) exceeds those of the SVOCs found in the examined indoor environment.

Several researchers have suggested that, in the absence of a consensus, it is possible to use formaldehyde (HCHO) as a proxy for building generated pollution [82,103]. There are several reasons for this suggestion. Since HCHO is used in resins used to bond fibreboards and plywood, it is prevalent in both construction materials and furniture [104]. Being ubiquitous in our environment and a known carcinogen [13], HCHO has been the subject of investigation for decades and has been used as the foundation for several VOC emission models [97]. As a result, the behaviour and prevalence of HCHO is well documented. The World Health Organization's (WHO) guideline for HCHO is a maximum concentration of 0.1 mg/m^3 (30-minute average concentration) [13]. Independent reviews have concluded that the WHO guideline concentration for HCHO is well assessed and justified [105,106].

HCHO emission rates have been found to be dependent on the loading ratio (the ratio of the surface area of the emitting material to the room/chamber volume) [107,108] and changes in temperature [109–112], humidity level [110,111,113,114] and ACH [115–118]. Also, although well understood and heavily regulated, HCHO still poses a problem in indoor environments. Based on a study of emission rates of different chemicals from building materials, Wei et al. concluded that out of the examined building materials it was medium density fibreboard containing HCHO that required the highest ventilation rate to meet criteria for concentration levels [103]. A real world example of the impact that HCHO can have on the IAQ can be found in a study of HCHO concentrations in Danish homes by Logadóttir and Gunnarsen [119] where they document indoor levels in excess of the WHO guidelines of 0.1 mg/m^3 (30-minute average concentration) [13].

2.4 VOC emission models

Pollutant emission patterns are unique to given materials and products. Little et al. suggested that it might be possible to predict volatile organic compound (VOC) emissions based on knowledge of the physical properties of an emitting material [120]. Specifically, it was suggested that it might be possible to make predictions based on knowledge on the initial emittable concentration (C_0), the mass diffusion coefficient (D_m) and the material to air partition coefficient (K_{ma}). The proposed theory gained popularity and forms the theoretical foundation for a long line of emission models; a list including 20 of the most important models and model developments is given by Zhang et al. in their exhaustive review article from 2016 [97]. More recent efforts have resulted in the development of experimental procedures that allow rapid determination of the relevant physical properties of an emitting material [121–123]. Classically, emission models such as those developed by Andersen, Lundqvist and Mølhave [107] and Hoetjer and Koerts [108] have been semi-empirical. One important result of Little's work is that it has allowed researchers to develop fully analytical solutions for emissions.

Besides the properties of an emitting material itself, VOC concentration levels are influenced by the parameters listed below. The effect changes in the listed parameters are specific to a given VOC. Some VOCs may not be affected by all the listed parameters. However, HCHO emissions are influenced by all listed parameters.

1. Loading ratio (the ratio of the surface area of the emitting material to the room/chamber volume) [107,108].
2. Temperature [109–112].
3. Humidity level [110,111,113,114].
4. Air change rates [115–118].

In order to be useful in the context of dynamic building simulations, a candidate model must consider the influence of all these parameters. Also, the performance of a candidate model has to be well documented. In his review published in 2002 Guo presents a comprehensive list of emission models published up till that point in time [124]. In 2016 Zhang et al. published an equally comprehensive review that mapped out recent advances in the field of mass transfer theory. Their combined work offers an exhaustive overview of the published emission models and their respective strengths and weaknesses. Most recent models have analytical solutions, however models are often complicated and potentially computationally expensive. Preferably, a candidate model should have a form that allows for easy implementation into a BPS tool. Qian et al. has published a model that complies with all the above requirements [125].

2.5 Building performance simulations

BPSs are an industry standard and are used to design buildings and to document compliance with building codes and regulations (e.g. EN 15251 [72] and ASHRAE 90.1 [126]). They include considerations on local climate, details on constructions and installations, purpose of use and occupancy and operation. Over time, the programmes have become more sophisticated. Most early BPS tools were relatively simple numerical algorithms designed to solve heat balances. Later versions have included mass balances to handle moisture and air transportation processes [127]. Now, commercially available simulation environments such as IES VE, IDA ICE and OpenStudio have highly developed user interfaces that allow direct import of building models from CAD programmes [128]. However, in most programmes, IAQ models are still limited to considerations on moisture and CO_2.

At their core, BPS tools are either data-driven or physics-based. Data-driven BPS tools are based on statistical models derived from measured data. When properly calibrated to a given building design, data-driven models can make accurate predictions on performance [129]. Physics-based BPS tools are based on systems of equations that describe the physical behaviour of the individual parts that constitute a building. Often, there is a discrepancy between predictions by physics-based BPS tools and the observed performance of actual buildings [130–133]. Buildings are complex and the number of variables that influence performance is far greater than the number of measureable performance criteria. Due to the high ratio of input to output variables, it has proven difficult to calibrate physics-based models in a systematic manner [129,133]. The predictive power of a model built in a physics-based BPS tool depends on the quality of the input and therefore also on the experience of the developers of the model [134,135]. The immediate advantage that physics-based BPS tools have over their data-driven counterparts is their ability to "predict system behaviour given previously unobserved conditions" [129]. This ability allows designers to estimate how changes in building design impact performance and to compare performances of different designs [136,137].

Currently there is an industry wide concerted effort to update BPS tools with the capability to determine the IAQ accurately to a level that ensures that building designs deliver on both health and comfort at low energy demands [16]. In order for BPS tools to accurately predict the IAQ of a design, BPS tools need to consider how indoor air chemistry affects the IAQ. The first step in the process of updating BPS tools is to identify or build a model that can determine the concentrations of relevant (representative) pollutants in the indoor air. The second step is to identify or build a BPS tool that allows such a chemical model to be implemented. A suitable BPS tool would have to be able to respond to the calculated concentration levels. Considering the limitations of data-driven driven models, a suitable model must be physics-based. An example of a BPS tool that meets these requirement is the commercially available open-source BPS tool IDA ICE [138].

3 Relative performance of ventilation designs

This chapter presents the findings of a study designed to identify what defining characteristics or means of ventilation that are the most energy efficient under Danish climatic conditions. The chapter also includes a discussion of the results and a description of the method used in the study. The study gave special consideration to highly efficient natural ventilation, here represented by supply air windows. Prior to this study, such an analysis had not been done for Danish climatic conditions. The main conclusion of the study was that in regards to ventilation, adding HR on the exhaust air was the single most efficient energy conservation measure.

The first objective of this thesis was to compare natural and mechanical ventilation and quantify the difference in performance under Danish climatic conditions. The successful conclusion of this work fulfils the first objective of this thesis. The chapter is based on the work presented in Paper 1 and Report 1. The original material can be found in the appendix, see list on page 112.

3.1 Introduction

Previous studies comparing performance of ventilation designs in temperate climates fall into one of two groups: real world case studies [139,140] and simulated scenarios [19,64–66,78,141]. Meanwhile, these studies often do not compare the different ventilation systems on an equal basis [23]. In many ways, this is understandable: Regulations and traditions vary from country to country and use and design vary from scenario to scenario; drawing general conclusions from a comparison of a large centralised ventilation system supplying landscape offices with a de-centralised system in semi-detached housing may not be feasible or meaningful. This may explain why findings from existing literature appear contradictory at times. One UK case study that compared performance of ventilation systems in two office buildings found that, in terms of energy, a hybrid ventilation system without HR performed better than a fully mechanical system with HR [139]. Meanwhile, another UK case study comparing performance of ventilation systems in social housing found naturally ventilated homes to have a total energy demand that was nearly twice as high as mechanically ventilated homes using HR [140]. With such inconsistent and diverging conclusions, results are not clear [19].

Conclusions presented in existing literature suggest that HR ventilation may be the most energy efficient for Danish homes [19,64–66]. Two independent Swedish studies, both assuming that ventilation systems are upgraded with HR with an efficiency of 80 %, estimate the potential to be a 22 % reduction of energy demand [64,65]. However, studies of supply air windows conducted in northern Europe estimate a comparable achievable reduction in energy demand. When upgrading ventilation systems to include supply air windows, studies estimate that for ACHs between 0.4 h^{-1} and 0.64 h^{-1} reductions in energy demand can be on the order of 11-24 % [33,34,38]. With comparable estimates of achievable reduction in energy demand, existing literature did not allow for a definite conclusion as to which ventilation technology that is best in terms of energy efficiency in a temperate climate such as the Danish.

3.2 Method

The study was designed to allow for direct comparison of the performance of natural ventilation, ventilation using supply air windows and mechanical ventilation using HR. The study used supply air temperature and energy demand as performance indicators. As primary energy factors have been found to be inaccurate predictors of actual primary energy demand and are subject change over time [142–144], they were disregarded in the study. Instead, the total energy demand was used. As the total energy demand under Danish climatic conditions is almost entirely dependent on the heat loss, the uncertainty this introduced was negligible. The respective performances were calculated relative to a reference scenario simulated with mechanical exhaust ventilation without HR (scenario 1).

3.2.1 Supply air window

The supply air window used in this study consisted of three panes of 4 mm float glass. The two inner panes were separated by a 15 mm argon filled gap and the supply air was passed through an 84 mm gap between the middle and outermost panes. The innermost pane had a soft coating facing the argon filled gap and the middle plane a hard coating facing the ventilated air gap. The window measured

1.48 x 1.23 m² and had a solid pine frame with a width of 82 mm, yielding a glazing fraction of 0.76. The glazing had a U-value of 0.80 W/(m²K) and a g-value of 0.56. Estimates of performance of supply air window when unventilated was calculated in Windows Information System (WIS) [145], a programme based on ISO 15099:2003 [146]. The unventilated window had a U-value of 1.07 W/(m²K) and a g-value of 0.43. Figure 3.1 shows the principle of the supply air window.

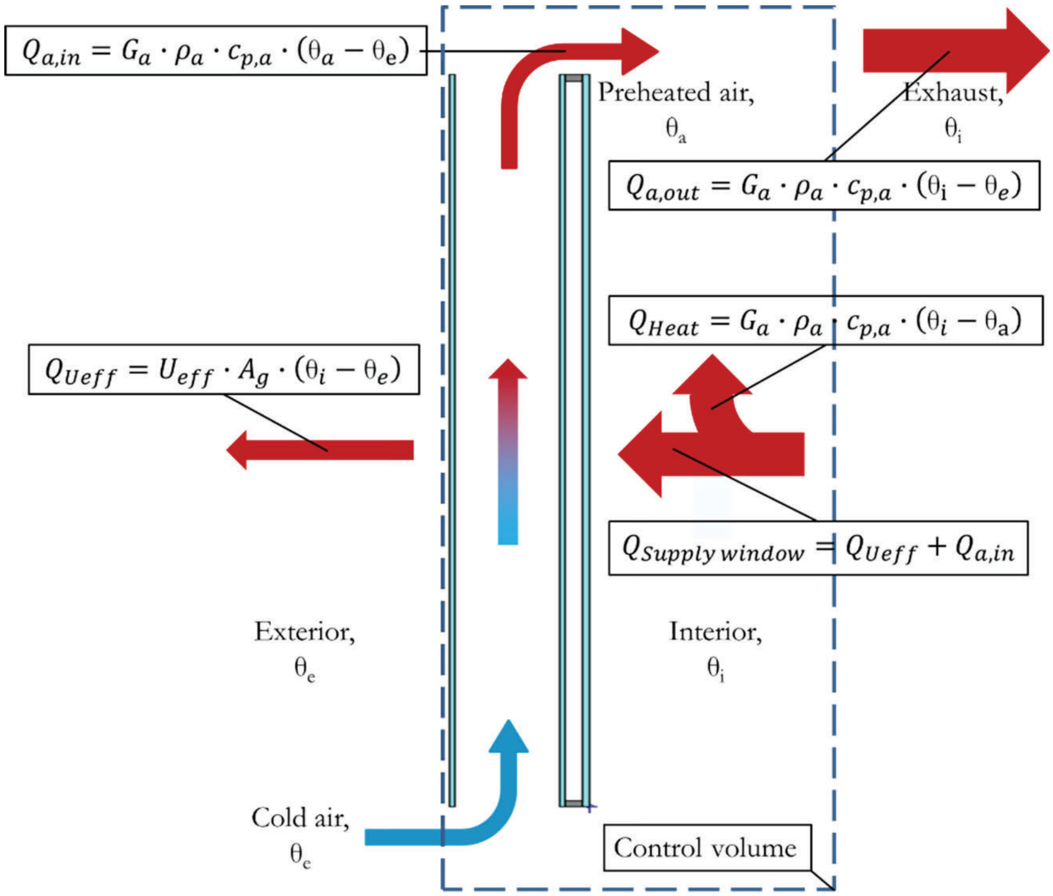

Figure 3.1 – Sketch showing the principles of the supply air window along with expressions for heat losses and gains

The heat balance for the system shown in Figure 3.1 can be written as seen below.

$$Q_{heat} = Q_{Ueff} + Q_{a,out} \qquad \text{Eq. 1}$$

Where	Q_{heat} is the heating demand/heat loss	[W]
	Q_{Ueff} is the effective heat loss through the supply air windows	[W]

$Q_{a,out}$ is the ventilation loss [W]

The different parts of the energy balance can be written as

$$Q_{Ueff} = U_{eff} \cdot A_g \cdot (\theta_i - \theta_e)$$
$$Q_{a,out} = G_a \cdot \rho_a \cdot c_{p,a} \cdot (\theta_\mathrm{i} - \theta_e) \quad \text{Eq. 2}$$

Where U_{eff} is the effective U-value [W/(m²·K)]

A_g is the glazed area of the supply air window [m²]

θ_i is the indoor temperature [°C]

θ_e is the outdoor temperature [°C]

G_a is the volume flow rate [m³/s]

ρ_a is the density of air [kg/m³]

$c_{p,a}$ is the specific heat capacity of air [J/(kg·K)]

Supply air temperature and effective U-value (defined as heat leaving the system by the outermost pane normalised by area and the temperature difference between the interior and exterior) can be calculated by Eq. 3 and Eq. 4 respectively. The expressions were derived by regression analysis on 660 data sets derived from a parameter variation run in the WinVent algorithm (suggested by Raffnsøe [40] and validated by Laustsen et al. [39]). The parameter variation covered outdoor temperatures in the interval -10 to 16 °C, supply air flow rates in the interval 2 to 10 l/s and solar irradiance on the vertical plane in the interval 0 to 1000 W/m². As the chosen BPS tool (ISEVE, see Section 3.2.2) could not handle expressions containing more than 156 characters [147], the regression analysis was designed to keep relationships within this range. The expressions can be used for extrapolation outside the given intervals for outdoor temperatures.

$$\begin{aligned}\theta_a = {} & 5.7431 + 0.775930_e - 0.54042G_a + 3.3757 \cdot 10^{-2} I_s \\ & +1.5829 \cdot 10^{-2} G_a^2 - 1.5359 \cdot 10^{-6} I_s^2 \\ & +1.1067 \cdot 10^{-2} \theta_e \cdot G_a - 1.7066 \cdot 10^{-5} \theta_e \cdot I_s - 1.392 \cdot 10^{-3} G_a \cdot I_s\end{aligned} \quad \text{Eq. 3}$$

$$\begin{aligned}U_{eff} = {} & 0.84749 - 6.0054 \cdot 10^{-3} \theta_e - 0.1846 G_a \\ & -6.4186 \cdot 10^{-5} \theta_e^2 + 1.8095 \cdot 10^{-2} G_a^2 - 6.553 \cdot 10^{-4} G_a^3 \\ & +9.6559 \cdot 10^{-4} \theta_e \cdot G_a + 1.6195 \cdot 10^{-5} \theta_e^2 \cdot G_a - 3.6015 \cdot 10^{-5} \theta_e \cdot G_a^2\end{aligned} \quad \text{Eq. 4}$$

Where θ_a is the supply(/inlet) air temperature [°C]

I_s is the solar irradiance (on the supply air window) [W/m²]

3.2.2 Building performance simulation

Physics-based BPS tools can predict the performance of a given building design under variable climatic conditions [129]. Using this ability to perform parametric analysis allows designers to estimate how changes in building design impact performance and to compare performances of different designs [136,137].

For this study, a BPS tool would have to allow a supply air window to impact both heat balance and supply air temperature. IESVE [147] is a validated and commercially available BPS tool. IESVE allows users to modify models by expressing variables (e.g. the supply air temperature) with customisable expressions (e.g. Eq. 3). As such, IESVE met the criteria for this study.

3.2.2.1 Building performance simulation model

The BPS model was kept simple with generic construction parts complying with criteria given in the BR18. Complex design features were avoided in order to ensure that identified trends were indeed generic and uninfluenced by specificities like overly intricate occupancy patterns or mass transport between zones in a complicated geometry. The model constituted a single unoccupied room that was representative of the general Danish contemporary building stock fulfilling current minimum requirements for new constructions.

The model had a floor area of 104 m^2 (nett) (16.0 x 6.5 m) and a ceiling height of 2.50 m (nett). The outer insulated cavity walls had a U-value of 0.30 $W/(m^2 \cdot K)$, the floor slab a value of 0.20 $W/(m^2 \cdot K)$, and the roofing construction a value of 0.20 $W/(m^2 \cdot K)$. The U-values equal the prescribed minimum requirement in BR18.

The ACH was kept constant at 0.5 h^{-1}. This ACH is a little higher than the prescribed minimum requirement in BR18 of 0.3 $l/(m^2 \cdot s)$ (ACH = 0,432 h^{-1} for a room height of 2.5 m).

The temperature set point was kept constant at 20 °C. Heating was simulated using a traditional heating system with radiators. Besides the constant ventilation, the model did not use any form for cooling.

Operating hours were set to a full year (8760 hours) and the ventilation was simulated as active during all hours of the year. Values for specific fan power (SFP) for exhaust and balanced mechanical ventilation were 800 J/m^3 and 1800 J/m^3 respectively. These SFP values are the highest allowed by BR18 and so constituted a worst case scenario for energy demand for mechanical ventilation systems.

Scenarios with balanced mechanical ventilation were simulated with and without infiltration. In scenarios with infiltration, the rate was set to 0.13 $l(m^2 \cdot s)$. The value for infiltration was the highest allowed by BR18 and so constituted a worst case scenario.

Eight windows were fitted into the 16 m long south-facing façade of the model. The windows measured 1.48 x 1.23 m^2 and had a solid pine frame with a width of 82 mm, yielding a glazing fraction of 0.76. The basic window had a U-value of 1.07 $W/(m^2K)$ and a g-value of 0.43. The basic window was engineered to emulate the supply air window in the unventilated state.

With eight supply air windows ensuring an ACH of 0.5 h^{-1}, each supply air window had to supply air at a fixed rate of 4.57 l/s. For an outdoor temperature of 0 °C, an indoor temperature of 20 °C and no solar radiation, the supply air windows had an effective U-value of 0.33 $W/(m^2 \cdot K)$ and delivered supply air at a temperature of 3.5 °C. Each supply air window supplied fresh air to a floor area of 13 m^2.

3.2.2.2 Implementation of supply air window in BPS model

IESVE could not handle supply air windows natively. Instead, the model used "basic" windows alongside a contribution, Q_{diff} (Eq. 5), that corrected the energy balance while considering that the supply air temperature was calculated separately using Eq. 3 (expression derived from regression analysis, see Section 3.2.1 of main text).

In Eq. 5, $Q_{g,win}$ represents the heat loss from the glazed part of a basic window. Conversely, the sum of Q_{Ueff} and $Q_{a,in}$ represents the amount of heat entering a supply air window. This way, Q_{diff} represents the difference between energy entering a supply air window and leaving a basic window. When the exterior is colder than the interior, the amount of heat entering a supply air window is greater than the amount of heat leaving a basic window. Therefore Q_{diff} is usually negative. So, usually, Q_{diff} corrects the heat balance by increasing the total heat loss of the building. Meanwhile, this increase in heat loss is offset by the positive contribution of the increase in supply air temperature. Here, $Q_{a,in}$ represents the energy that is transferred to the supply air. This way the overall contribution of the supply air window ends up positive for outdoor temperatures colder than indoor temperatures.

$$Q_{diff} = Q_{g,win} - \left(Q_{Ueff} + Q_{a,in}\right) \Leftrightarrow$$
$$Q_{diff} = U_g \cdot A_g \cdot (\theta_i - \theta_e) - \left(U_{eff} \cdot A_g \cdot (\theta_i - \theta_e) + G_a \cdot \rho_a \cdot c_{p,a} \cdot \left(\theta_{a,I_s=0} - \theta_e\right)\right) \quad \text{Eq. 5}$$

Where	Q_{diff} is the term correcting the energy balance in IESVE	[W]
	$Q_{g,win}$ is the heat loss from the glazed part of a basic window	[W]
	Q_{Ueff} is the effective heat loss through the supply air windows (energy leaving the outer pane)	[W]
	$Q_{a,in}$ is the amount of energy entrained in the supply air	[W]
	U_g is the (simulated) centre pane U-value of the window	[W/(m²·K)]
	U_{eff} is the effective U-value of the supply air window (for A_g)	[W/(m²·K)]
	A_g is the glazed area of the supply air window	[m²]
	θ_i is the indoor temperature	[°C]
	θ_e is the outdoor temperature	[°C]
	θ_a is the supply(/inlet) air temperature	[°C]
	$\theta_{a,Is=0}$ is the supply air temperature w/o solar radiation	[°C]
	G_a is the volume flow rate	[m³/s]
	ρ_a is the density of air	[kg/m³]
	$c_{p,a}$ is the specific heat capacity of air	[J/(kg·K)]

Expanding Eq. 5, it can be seen that there were only two unknown variables: the effective U-value of the supply air window, U_{eff}, and the supply air temperature calculated without contribution from solar radiation, $\theta_{a,Is=0}$. With the volume flow rate fixed at 4.57 l/s and the indoor temperature kept at a minimum of 20 °C, $\theta_{a,Is=0}$ is a function of the outdoor temperature (Eq. 6). Eq. 6 was determined by regression analysis. As IESVE did not allow expressions with more than 156 characters and Eq. 6 was to be substituted into Eq. 5, Eq. 6 was kept short. A short expression for U_{eff}, Eq. 7, was also determined by regression analysis.

$$\theta_{\mathrm{a,I_s=0}} = 3.5487 + 0.81724 \cdot \theta_e \qquad \text{Eq. 6}$$

$$U_{eff} = 0.31958 - 0.0023482 \cdot \theta_e \qquad \text{Eq. 7}$$

Substituting Eq. 6, Eq. 7, the given values for U_g, A_g and G_a and representative values for ϱ_a and $c_{p,a}$ into Eq. 5 gave an expression for Q_{diff} (Eq. 8) that could be entered into IESVE. As Eq. 8 contains contributions from all of the eight supply air windows at a flow rate of 4.57 l/s, it is only valid for this specific BPS model.

$$\begin{aligned} \mathrm{Q_{diff}} &= 5.3038 \cdot \theta_\mathrm{i} + 2.9615 \cdot \theta_\mathrm{e} - 160.49 \\ &\quad + 0.0259 \cdot \theta_\mathrm{i} \cdot \theta_\mathrm{e} - 0.0259 \cdot \theta_\mathrm{e}^2 \end{aligned} \qquad \text{Eq. 8}$$

As solar energy is transferred to supply air, g-values (here defined as the fraction of incident solar radiation transmitted through the glazed part of the window) drop about 2 % when increasing solar irradiance on the supply window from 100 W/m^2 to 1000 W/m^2. By not adjusting g-values, this contribution is counted twice in the heat balance. Meanwhile, as cooling was not a concern of this study and periods with high solar irradiation are relatively uncommon, the effect on the overall heat balance of the BPS model was assumed negligible. As a consequence, g-values were assumed constant.

The temperature increase that happens in the frame of a supply air window has not been included. For a temperature difference of 20 °C and an airflow rate of 4.57 l/s, the temperature increase in the bottom frame of the used window is about 1 °C. In a similar fashion, infiltrating air is preheated when it passes through the building envelope. The effect of this preheating was not included either. The preheating in a supply air window frame and the preheating across a building envelope are approximately equivalent in size and therefore the omission of these effects should not affect the results or conclusions.

3.2.3 Examined scenarios

The BPS model was used to examine eight scenarios.

1. Basic windows (1+2 window panes) equivalent to the supply air window used in this investigation (without ventilation) with mechanical exhaust
2. Basic windows (1+2 window panes) equivalent to the supply air window used in this investigation (without ventilation) without mechanical exhaust
3. Supply air windows with mechanical exhaust
4. Supply air windows without mechanical exhaust
5. Basic windows (1+2 window panes) equivalent to the supply air window used in this investigation (without ventilation) and balanced mechanical ventilation with an HR of 75 % without infiltration
6. Traditional new three-layer low-emission windows (U-value = 0.79 $W/(m^2 \cdot K)$, g-value = 0.38) and balanced mechanical ventilation with an HR of 80 % without infiltration
7. Basic windows (1+2 windows) equivalent to the supply air window used in this investigation (without ventilation) and balanced mechanical ventilation with an HR rate of 75 % and an infiltration rate of 0.13 $l/(m^2 \cdot s)$
8. Traditional new three-layer low-emission windows (U-value = 0.79 $W/(m^2 \cdot K)$, g-value = 0.38) and balanced mechanical ventilation with an HR rate of 80 % and an infiltration rate of 0.13 $l/(m^2 \cdot s)$

Table 3.1 gives an overview of the input in the eight scenarios.

Table 3.1 – Overview of input in the eight simulated scenarios

Scenario	Short description	SFP [J/m³]	Inf. [l/(s·m²)]	HR [%]	U_{win} [W/(m²·K)]	g_{win} [-]
1	Basic windows w/ exhaust	800	-	-	U = 0.43	0.43
2	Basic windows w/o exhaust	-	-	-	U = 0.43	0.43
3	Supply air windows w/ exhaust	800	-	-	U_{eff}[1] = 0.43	0.43
4	Supply air windows w/o exhaust	-	-	-	U_{eff}[1] = 0.43	0.43
5	Basic windows w/ 75 % HR w/o infiltration	1800	-	75	U = 0.43	0.43
6	Efficient windows w/ 80 % HR w/o infiltration	1800	-	80	U = 0.38	0.38
7	Basic windows w/ 75 % HR w/ infiltration	1800	0.13	75	U = 0.43	0.43
8	Efficient windows w/ 80 % HR w/ infiltration	1800	0.13	80	U = 0.38	0.38

[1]Technically the window was implemented in the IESVE model as having a U-value of 1.07 and had the energy balance corrected by the variable Q_{diff} as defined by Eq. 5 (see appendix).

Table 3.2 – Energy demand by ventilation designs in IESVE model

Scenario	Short description	Heat loss [kWh/m²]	Fan [kWh/m²]	Total [kWh/m²]	Savings [%]
1	Basic windows w/ exhaust	87.1	2.0	89.2	0
2	Basic windows w/o exhaust	87.1	-	87.1	2
3	Supply air windows w/ exhaust	79.9	2.0	82.0	8
4	Supply air windows w/o exhaust	79.9	-	79.9	10
5	Basic windows w/ 75 % HR w/o infiltration	60.5	4.6	65.0	27
6	Efficient windows w/ 80 % HR w/o infiltration	57.6	4.6	62.2	30
7	Basic windows w/ 75 % HR w/ infiltration	75.8	4.6	80.4	10
8	Efficient windows w/ 80 % HR w/ infiltration	73.1	4.6	77.7	13

3.3 Results

3.3.1 Energy demand

Table 3.2 shows energy demand by different ventilation designs simulated in IESVE.

Scenario 1 is the reference scenario with basic windows and mechanical exhaust ensuring the required ACH. Scenario 2 represents a home ventilated purely by natural ventilation. Comparing results from Scenarios 1 and 2 show that the relative cost of mechanical exhaust (SFP 800 J/m^3) was negligible. In cases of exhaust ventilation with fresh air valves and supply air windows, fan power accounted for 2 % of the total yearly energy demand for heating and ventilation. For balanced mechanical ventilation (SFP 1800 J/m^3) with basic windows, an HR rate of 75 % and infiltration (scenario 7), fan power constituted 6 %. In the corresponding scenario without infiltration (scenario 5), fan power constituted 8 %.

Exchanging basic windows and fresh air valves for supply air windows resulted in savings of 8 % in terms of energy.

Infiltration significantly impacted the energy savings obtained by using balanced mechanical ventilation. The effect of keeping basic windows but exchanging natural ventilation for balanced mechanical with HR of 75 % was savings of 27 % when disregarding the effects of infiltration. Using efficient triple glazed windows and an HR rate of 80 % reduced the energy demand by 30 % when comparing to the reference case. Including the effect of infiltration, these savings were reduced to 10 % and 13 % respectively.

Comparing scenario 7 to scenario 4 showed equal levels of performance in terms of energy. That is, supply air windows driven by natural ventilation performed on par with a balanced mechanical ventilation system with an HR rate of 75 % and SFP of 1800 J/m^3 when the model with mechanical ventilation included an infiltration rate of 0.13 l/(m^2·s). Balanced mechanical ventilation with HR outperformed supply air windows in all remaining scenarios.

Implementing a system with efficient triple glazed windows and balanced mechanical ventilation with an HR rate of 80 % instead of a system with basic windows and an HR rate of 75 % resulted in savings of 3 % when including the effect of infiltration. When disregarding infiltration the savings were 4 %.

3.3.2 Supply air temperature

Figure 3.2 shows monthly averages of the supply air temperatures for a representative selection of simulated ventilation designs. The curve for fresh air valves shows the supply air temperatures for the scenarios with basic windows (scenarios 1-2). As air supplied by fresh air valves is unconditioned, the supply air temperature is equal to the outdoor temperature. The curve for supply air windows shows supply air temperatures for scenarios 3-4, the curve for an HR rate of 75 % shows the inlet temperatures of the scenarios 5 and 7 and the curve for an HR rate of 80 % shows the inlet temperatures of the scenarios 6 and 8.

On average, the supply air temperature was raised by 3.8 °C in the ventilated cavity between panes in the supply air window. The temperature increase was higher during the cold months of the year. The average supply air temperature was closely related to the outdoor temperature and averages 4.4 °C in the months from December to February.

The supply air temperatures from ventilation systems with HR were higher than the ones delivered by the supply air windows. In the months from December to

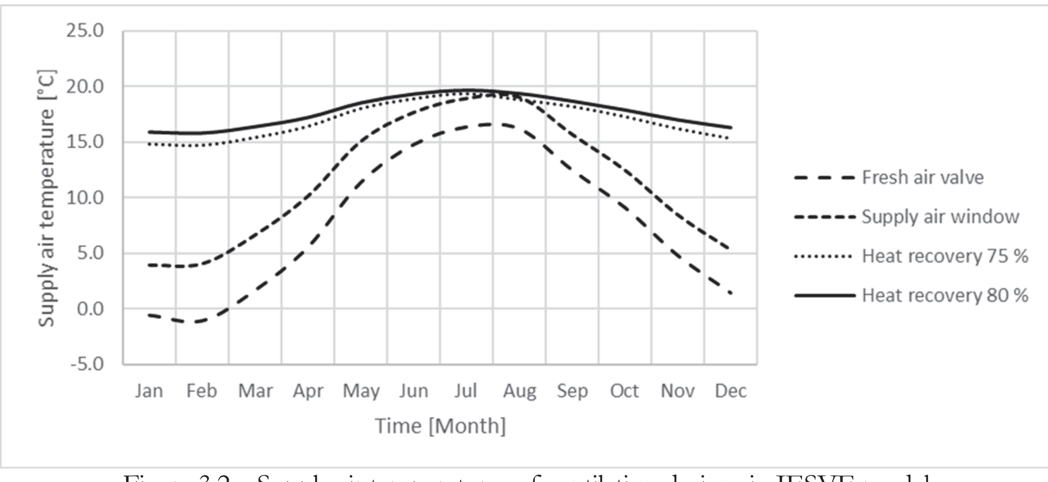

Figure 3.2 – Supply air temperatures of ventilation designs in IESVE model

February systems with an HR rate of 75 % averaged a supply air temperature of 15 °C. In the same period outdoor temperatures averaged 0 °C.

3.4 Discussion and conclusions

3.4.1 Energy demand

Balanced mechanical ventilation with HR outperformed natural ventilation in terms of energy in all instances but one. When comparing supply air windows driven by natural ventilation (scenario 4) with balanced mechanical ventilation with an HR rate of 75 %, a SFP of 1800 J/m^3 and an infiltration rate of 0.13 l/(m^2·s) (scenario 7) their performance in terms of energy was about equal. That the two scenarios were equal was largely due to the relatively high level of infiltration included in the scenario with balanced mechanical ventilation.

Lowering the infiltration rate is known to improve performance of balanced mechanical ventilation systems with HR [23,65,84]. When comparing the equivalent scenarios without infiltration (scenarios 4 and 5), the relative performance gap in terms of energy grew from about 0 % to 19 %. The reduction in energy demand is comparable with what is reported in the literature [84]. Dependent of type of housing, un-renovated Danish housing stock (prior to 2006) has average infiltration rates ranging from 0.22-0.28 l/(m^2·s) [85]. In order to ensure optimal performance, a home must be tightened to the exterior before employing a balanced mechanical ventilation system with HR. Studies have found that it is possible to reduce infiltration rates by 70-80 % in single-family housing [84,86]. This level of reduction in infiltration is enough to make balanced mechanical ventilation with HR net profitable [66]. Alternatively, if tightening the building envelope is either not possible or not wanted, a balanced mechanical ventilation system can minimise harmful exfiltration by setting the exhaust rate higher than the inlet rate.

Results show that fan power is negligible when compared to the reduction in energy demand for heating. For exhaust ventilation, fan power accounts for only 2 % of the combined energy demand for heating and ventilation. For balanced mechanical ventilation with HR, fan power constitutes between 6 % and 8 %. Choosing a ventilation system with energy efficient fans can lower the ratio further. Modern ventilation systems have nominal SFP values between 550 J/m^3 and 1450 J/m^3 [148]. Meanwhile, in practice, due to high pressure losses or malfunctions, actual SFP values can be higher than their nominal counterparts [62]. One study found that centralised ventilation systems in single- and multi-family housing, with nominal SFP values between 1050 J/m^3 and 1450 J/m^3, averaged a SFP value of 1730 J/m^3 [148]. Still, the potential for reduction in energy demand outweighs the possible consequences of implementing a ventilation system with higher than nominal SFP values.

The nominal HR efficiency of a contemporary heat exchanger can be rated higher than 90 % at peak performance (e.g. Genvex [58], Nilan [59] and InVentilate [60]). Though it is possible for a carefully constructed ventilation system to meet the nominal HR efficiency [61], there is a risk that systems will not perform as well as planned. Ventilation systems with HR are vulnerable to leaks and studies have found that systems with nominal HR rates between 70-80 % often do not recover more than 50-70 % [62,63]. In the above simulations, exchanging basic windows with efficient windows and improving the HR rate from 75 % to 80 % in scenarios without infiltration (scenarios 5 and 6) improved relative performance in terms of energy by 4 %. Considering the extent of renovations, the return on investment in form of reduction in energy demand was marginal. Still, the results show that even relatively modest HR rates can significantly reduce energy demand in Danish homes.

3.4.2 Supply air temperature

Balanced mechanical ventilation with HR outperform natural ventilation systems in terms of supply air temperature. On average, the supply air window raised the supply air temperature by 3.8 °C. In the cold months from December to February the supply air temperature averaged 4.4 °C. In the same period, when outdoor temperatures averaged 0 °C, the ventilation system with an HR rate of 75 % delivered supply air temperatures averaging 15 °C.

3.4.3 Supply air windows in system design

Supply air windows do not recover heat as such. The way supply air windows help reduce energy demand is by reducing the heat loss through the glazed part of the window. For a temperature difference of 20 °C and flow rate of 4.57 l/s, the effective U-value of the glazed part of the supply air window in this study was 0.33 W/(m^2·K). In recent years, windows have become much better. Today, a tripled layered low-E window with krypton gas filling can have a centre of glass U-value of 0.5 W/(m^2·K). In terms of energy, the difference is now marginal and supply air windows have lost some of their competitive edge.

Estimates in published literature were that, when compared to natural ventilation, HR with an efficiency of 80 % and supply air windows would reduce energy demand by 22 % [64,65] and 11-24 % respectively [33,34,38]. Where estimates for ventilation with HR were accurate, supply air windows only reduced energy demand by 8 %. Still, it is worth noting how close supply air windows and generic balanced mechanical ventilation with HR ventilation were in performance in terms of energy. It is possible that the Danish climate constitutes a form of critical point: it is highly conceivable that supply air windows can outperform HR ventilation in countries with warmer winters. Conversely, colder winters will probably exacerbate the performance gap that was observed in this study and favour HR ventilation.

The above does not mean that natural ventilation does not have a place in modern buildings in Denmark. Certainly supply air windows can be successfully implemented in energy efficient hybrid designs. For example, supply air windows are good at reducing ambient noise and can be used to facilitate natural ventilation in areas with high outdoor sound pressure levels [149,150]. Also, there are supply air window designs that are different from the one used in this study. In terms of energy, various different designs will probably perform on par with each other (per unit area), but there are designs that are better at increasing the supply air temperature [38,45]. It is possible to increase the supply air temperature by increasing the time supply air spends in the ventilated cavity (larger area or longer pathway) and by reducing the number of panes separating the conditioned interior from the ventilated cavity. Such a supply air window would work well in a ventilation system where heat recovered from exhaust air is transferred to a reservoir, such as a domestic hot water storage tank, instead of the supply air.

Considering the above, it is concluded that the primary lesson learned from this study is that designers aspiring to design an energy efficient ventilation system in a climate like the Danish should consider some form of HR on the exhaust air.

This work has not considered the carbon foot printing of a given ventilation system. Presumably a natural ventilation system will have lower production costs in terms of materials and energy. Also maintenance and reparations will play a role here. For example, supply air windows probably have a longer life span than a mechanical aggregate. It is wholly conceivable that a life cycle analysis of a building – or more specifically the ventilation systems in a building – can show that supply air windows are more cost effective in primary energy over the useful lifetime of the building than a mechanical ventilation system, despite the energy saving capability of air-to-air HR. This, however, is a question to be answered by future research.

4 Estimate of emission rate of pollution from building materials

This chapter consists of three subsections. The first subsection serves as a brief introduction to the theory behind contemporary physics-based VOC emission models. The following subsection examines how patterns and emission rates predicted by models based on mass transfer theory compare to observations made in practice. The comparison was done using HCHO as an example of a VOC and material properties that are representative for building materials known to contain and emit HCHO. The comparison revealed that the examined emission models overestimate emission rates and underestimate the time it takes to deplete the content of HCHO in building materials.

The second objective of this thesis was to develop a method to estimate the impact building generated pollution has on IAQ, the energy demand and ventilation rates. In order to achieve this, first it was necessary to identify emission models that give accurate estimates of emission rates of pollution. Since the attempts at identifying a suitable emission model in the existing literature failed, it was decided to develop VOC emission models by regression analysis of data collected in buildings in practice.

The regression analysis yielded two emission models for HCHO. One for 'normal' emission levels and one for 'high' emission levels. The models were based on data gathered in newer detached and semi-detached single-family homes in rural and suburban Denmark. However, data was scarce. This has imposed several limitations on the use of the derived emission models. The third and final subsection of this chapter contains a thorough description of the respective emission models, how they were derived and what their limitations are.

The chapter is based on work presented in Paper 2 and Paper 3. The original material can be found in the appendix, see list on page 112.

4.1 Formaldehyde emission models

VOC emission models from dry building materials can be classified as being either multi-phase or one-phase models. Multi-phase models consider the effect pores have on mass transfer within a given material. As such, multi-phase models consider VOCs in both the solid and the gas phase. One-phase models lump the solid and gas phases into to one and assume that a given material acts as if homogenous. This assumption has been found to hold true for values for a material to air partition coefficient, K_{ma}, that are 10 times greater than the porosity, ε [151]. Since K_{ma} for VOCs are often in the thousands while ε is always smaller than one, it is rarely necessary to use a multi-phase model. Therefore this study focused on one-phase models.

One-phase models have been developed for a large variety of scenarios: for VOCs and SVOCs, for one or multiple layers and for combinations where some layers act as sources while others act as sinks. As HCHO has a saturation pressure of about 5 atm at 23.8 °C [152] and 10^{-3} atm is a common demarcation between VOCs and SVOCs (with SVOCs having saturation pressures equal to or lower than 10^{-4} atm) [153], HCHO is considered a VOC. Also considering that most building and furniture materials are single-layered (albeit often coated), the focus of this study was on one-phase models for VOC emissions from single-layered, solid materials with a single emitting surface.

The model Little et al. published in 1994 [120] was the first to allow researchers to simulate how VOCs diffuse from a homogenous, solid material into ambient air. Eq. 9 forms the basis of all one-phase models. The equation, also known as Fick's second law of diffusion, describes how a VOC – under the assumption of one-dimensional flow – diffuses through a homogenous solid.

$$\frac{\partial C_m(x,t)}{\partial t} = D_m \frac{\partial^2 C_m(x,t)}{\partial x^2} \qquad \text{Eq. 9}$$

Where	C_m is the VOC concentration in the sample material	[kg/m^3]
	D_m is the diffusion coefficient for mass transfer	[m^2/s]
	x is the distance (between surfaces of emitting material)	[m]
	t is time	[s]

In order to obtain an analytical solution, Little et al. simplified the problem. They made the following seven assumptions:

(1) That the concentration of the compound of interest was uniformly distributed throughout the sample material at the beginning of a test.

$$C_m(x,t)|_{t=0} = C_0 \; for \; 0 \leq x \leq \delta \qquad \text{Eq. 10}$$

Where	C_0 is the initial emittable concentration	[kg/m³]
	δ is the material thickness	[m]

(2) That only one surface emits the compound of interest (as with a carpet on a floor) (emission at surface where x = δ).

$$\left.\frac{\partial C_m(x,t)}{\partial t}\right|_{x=0} = 0 \; for \; t > 0 \qquad \text{Eq. 11}$$

(3) That the convective mass transfer coefficient, h_m, is infinite (so that convective mass transfer from the emitting surface can be ignored) and (4) that the concentration of the compound of interest at the surface layer of the sample material is always in equilibrium with the concentration in the chamber or room air.

$$C_m(x,t)|_{x=\delta} = K_{ma}C_a \; for \; t > 0 \qquad \text{Eq. 12}$$

Where	K_{ma} is the material to air partition coefficient	[-]
	C_a is the concentration in the chamber or room air	[kg/m³]

(5) That the concentration in the inlet air and the initial concentration in the chamber or room air are both zero so that the mass balance reduces to Eq. 14.

$$C_a = 0 \; for \; t = 0, \qquad \text{Eq. 13}$$

$$V\frac{\partial C_a(t)}{\partial t} = -D_m A_m \left.\frac{\partial C_m(x,t)}{\partial t}\right|_{x=\delta} - C_a G_a \; for \; t > 0 \qquad \text{Eq. 14}$$

Where	V is the volume of the room	[m³]
	A_m is the emitting surface area of the sample material	[m²]
	G_a is the volume flowrate of air in and out the chamber or room	[m³/s]

(6) That both the diffusion coefficient for mass transfer, D_m, and the material to air partition coefficient, K_{ma}, are constants and, finally, (7) that the chamber or room air is well mixed.

The series of assumptions allowed Little et al. to arrive at a fully analytical solution that enabled them to calculate the concentration distribution in the sample material over time, $C_m(x,t)$, and the concentration in the chamber or room air, $C_a(t)$. The model was validated against data from an experiment conducted in a 20 m^3 environmental chamber where the temperature (23 °C), relative humidity (RH) (50 %) and air exchange rate (1 h^{-1}) were kept constant and a fan was used to ensure that the chamber air was well mixed [120]. A weakness of this model was the assumption that the convective mass transfer, h_m, was infinite. The assumption leads the model to overestimate the emission rate [154]. This particular problem was fixed within a decade; Huang and Haghighat published a fully analytical solution in 2002 (HH2002) [154], Xu and Zhang published their solution in 2003 (XZ2003) [155] and Deng and Kim published their solution in 2004 (DK2004) [156].

The new solutions were found by exchanging Eq. 12 with Eq. 15.

$$C_m(x,t)|_{x=\delta} = K_{ma}C_{as}(t)\ for\ t > 0 \qquad \text{Eq. 15}$$

Where	C_{as} is the concentration in the air near the surface (boundary layer) of the sample material	[kg/m^3]

And adding Eq. 16.

$$R(t) = -D_m \frac{\partial C_m(x,t)}{\partial t}\bigg|_{x=\delta} = h_m\big(C_{as}(t) - C_a(t)\big) \qquad \text{Eq. 16}$$

Where	R is the emission rate	[kg/(s·m^2)]
	h_m is the convective mass transfer coefficient	[m/s]

Models HH2002, XZ2003 and DK2002 have all been validated against experimental data published by Yang et al. [157]. The data used for validation was obtained from a series of experiments conducted for different VOCs (TVOC, hexanal and α-pinene) performed in a small test chamber (0.05 m^3) at constant temperature (23 °C), RH (50 %) and air exchange rate (1 h^{-1}) using a fan to ensure that the chamber air was well mixed.

Despite constituting a fairly specific subset of emission models, these three models share the fundamental basics of all other one-phase models and, so, can in this context be considered representative of emission models that are based on the tradition founded by Little et al.

4.1.1 Emission model with regressed coefficients

While the focus of this study was on how the emission models by Huang and Haghighat [154], Xu and Zhang [155] and Deng and Kim [156] perform when compared to real world observations of HCHO emission rates, it is worth mentioning a fourth model published by Qian et al. in 2007 (Qa2007) [125]. The model is based on the same system of assumptions and equations as the other models and has been validated against the same experimental data [157] and model DK2002. However, the model is different in two ways that makes it useful as a case study: The model is constructed using dimensionless parameters such as the Biot number for mass transfer, Bi_m, and the Fourier number for mass transfer, Fo_m, and coefficients have been regressed to the included dimensionless parameters. This means that the model is readily interpretable. The dimensionless parameters each represent a physical quality or aspect of the model and the regressed coefficients are the weight that each respective dimensionless parameter has in the model. Being a statistical model with coefficients fitted to real, physical parameters, it is what is known as a grey-box model.

Besides the value as an easily accessible example, the model has other qualities that are desirable in the context of BPS. The model would be the easiest of the four representative models to implement into a BPS environment and may be the least expensive in terms of computational power (note that the model is not continuous – it has three discrete parts – and that this may make the model incompatible with a BPS tool that uses time steps of variable length).

Using the model fitted for Fourier numbers lower than or equal to 0.2 and higher than 0.01 (not at steady state), the grey-box model can be written as shown in Eq. 17.

$$R(t) = 0.469\frac{D_m C_0}{\delta}\alpha^{0.022}(\beta K)^{-0.021}\left(\frac{Bi_m}{K}\right)^{0.021} Fo_m^{-0.48} \quad \text{Eq. 17}$$

Where α is the dimensionless air exchange rate [-]

β is the ratio of building material volume to room volume [-]

Bi_m is the Biot number for mass transfer [-]

Fo_m is the Fourier number for mass transfer [-]

The dimensionless parameters are defined as shown in Eq. 18.

$$\begin{aligned}
\alpha &= \frac{n\delta^2}{D_m}, 60 \leq \alpha \leq 36200 \\
\beta &= \frac{A\delta}{V}, 0.4 \leq \beta \cdot K \leq 150 \\
Bi_m &= \frac{h_m\delta}{D_m}, 20 \leq \frac{Bi_m}{K} \leq 700 \\
Fo_m &= \frac{D_m t}{\delta^2}, Fo_m \geq 0
\end{aligned} \quad \text{Eq. 18}$$

Where n is the air exchange rate [s^{-1}]

Qian et al. introduces two new dimensionless parameters in their model from 2007 [125]. The first is the dimensionless air exchange rate, α, which is the ratio between the actual air exchange rate and the mass diffusivity. According to model Qa2007, an increase in the actual air exchange rate seen relative to the mass diffusivity will result in an increase in the emission rate. The second dimensionless parameter is the ratio of the volume of building material to the volume of room or chamber air, β, which is directly related and proportional to the loading ratio (the ratio of the surface area of an emitting material to the volume of the surrounding air). According to model Qa2007, an increase in the material volume seen relative to the air volume ratio will result in a decrease in the emission rate.

The two other dimensionless parameters identified in the model are the Biot number for mass transfer, Bi_m, and the Fourier number for mass transfer, Fo_m. The Biot number for mass transfer describes the ratio between the mass transfer resistance at the surface of the material and the mass transfer resistance in the material itself. Here, decreasing the mass transfer resistance at the surface of the material – which, conceptually, is equivalent to increasing the convective mass transfer coefficient, h_m – will result in an increase in the emission rate and the Biot number for mass transfer.

Conceptually, the Fourier number for mass transport can be understood as the ratio of the rate of mass transport by diffusion to the rate of mass storage in a given material. Fo_m is dependent on time and increases as time passes. As such, Fo_m can be understood as dimensionless time and can under stable conditions be used as an indicator for proximity to steady state conditions. According to model Qa2007, an increase in the Fourier number for mass transport brought about by the progress of time will result in a decrease in the emission rate.

The patterns observed for model Qa2007 should all hold true for the other three models. That is, changes in α, β, Bi_m and Fo_m should affect emission rates estimated by models HH2002, XZ2003 and DK2002 in the same way as they affect the emission rate estimated by model Qa2007. This knowledge is useful to have when working with the other models as they are much less intuitive.

4.1.2 Expected pattern

The following is a description of the development of emission rates and concentration levels as expected in chamber tests [110].

1. Material emission rates in an environmental chamber decrease continuously.
2. In an environmental chamber, the highest emission rates usually occur at the beginning when materials are introduced.
3. When materials are tested in an environmental chamber, a "steady state" can be achieved with prolonged emission time.

Figure 4.1 shows how the four representative models predict the development of the VOC concentration in the air in small test chambers (e.g. 10-100 l [122]) over time. The input parameters were representative for fibreboards and the ACH was 1 h^{-1}. All four models can be seen to follow the expected development and are in good agreement with one another. Despite some variation in the timing and level of peak concentration, all four models can be seen to converge to the same level and pattern.

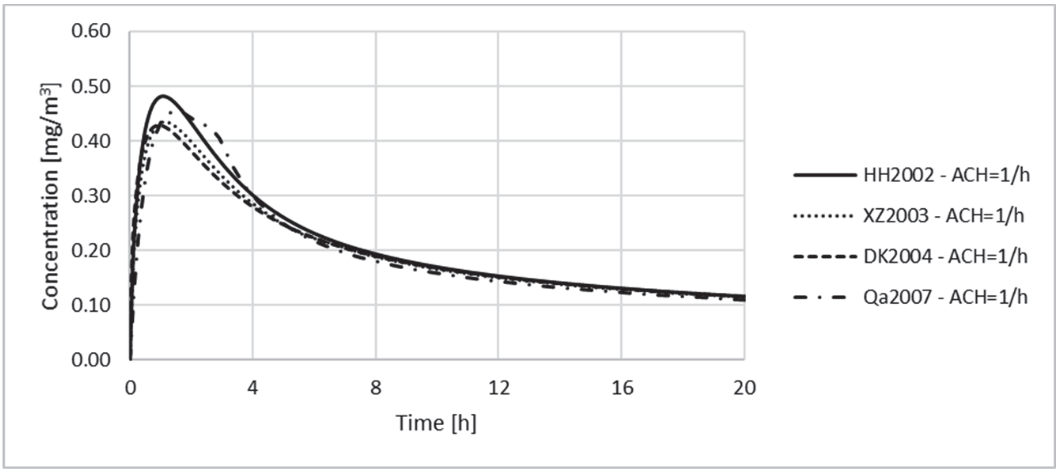

Figure 4.1 – Development in HCHO concentration level in small test chamber predicted by the four representative methods [125,154–156]

4.1.3 Influencing parameters

The initial emittable concentration, C_0, diffusion coefficient for mass transfer, D_m, and material to air partition coefficient, K_{ma}, are material properties and must be determined by tests in climate chambers using methods such as the C-History Method [121] or the Ventilated Chamber C-History Method [122]. The material properties are variable and influenced by the ambient environment. Eq. 19–Eq. 21 show how the material properties relate to the ambient environment [111–113].

$$C_0 = (1 + C_1 \cdot RH) C_2 T^{-0.5} \exp\left(-\frac{C_3}{T}\right) \qquad \text{Eq. 19}$$

$$D_m = D_1 T^{1.25} \exp\left(-\frac{D_2}{T}\right) \qquad \text{Eq. 20}$$

$$\ln(K_{ma}) = K_1 \cdot AH + K_2 \qquad \text{Eq. 21}$$

Where	$C_{1\text{-}3}$ are coefficients determined by tests in climate chambers	[-]
	$D_{1\text{-}2}$ are coefficients determined by tests in climate chambers	[-]
	$K_{1\text{-}2}$ are coefficients determined by tests in climate chambers	[-]
	T is the absolute temperature	[K]
	AH is the absolute humidity	[g/m^3]

Besides the properties of an emitting material itself, previous studies have established that HCHO concentration levels are influenced by the following parameters.

1. Loading ratio [107,108].
2. Temperature [109–112].
3. Humidity level [110,111,113,114].
4. Air change rate [115–118].

4.1.4 Mathematical limitations

The VOC emission models based on mass transfer theory are mathematical solutions to a mass balance equal or similar to Eq. 14. The mass balance can be recognised as an ordinary differential equation of the form shown in Eq. 22.

$$\frac{dO(t)}{dt} = -\lambda O(t), \lambda > 0, O(0) = O_0 \qquad \text{Eq. 22}$$

For an initial condition (or quantity) O_0 and (decay) constant λ, Eq. 22 has the following solution:

$$O(t) = O_0 e^{-\lambda t} \qquad \text{Eq. 23}$$

For the VOC emission models based on mass transfer theory, the initial condition and constant are, respectively, the initial emittable concentration, C_0, and the diffusion coefficient for mass transfer, D_m.

In order to derive fully analytical solutions, researchers have assumed that material properties (C_0, D_m and K_{ma}) and testing conditions (θ, AH and ACH) are constant. This imposes technical limitations on how the VOC emission models can be used. For example, should C_0 be simulated as variable in time (e.g. by using Eq. 19), it will not be possible to adhere to the principle of conservation of mass (that is, the calculated total emitted mass at $t = \infty$ will not sum to the total mass of VOC at $t = 0$).

Therefore, it can be seen that VOC emission models do not allow dynamic modelling, at least not from a strictly mathematical point the view. However, since indoor environments are fairly stable over time, VOC emission models may work in practice.

4.2 Comparing predictions to observations

The VOC emission models HH2002 [154] and XZ2003 [155] (the dimensionless version) have both decoupled the VOC emission rate R from ACH; presumably this is an artefact stemming from the assumptions that the ACH is constant (Eq. 14) and decoupled from h_m. Meanwhile, the VOC emission models DK2004 [156] and Qa2007 [125] both include ACH in their modelling of R.

As studies have found indications that changes in ACH can impact HCHO emission rates [115–118], there may be a discrepancy between theory and practice. The remainder of this section focuses on this observed possible difference between theory and practice. As such, this section does not include analyses of whether changes in temperature or humidity influence predictions by VOC emission models differently than they do in practice.

4.2.1 Predictions by models based on results from small test chambers

Figure 4.2 shows how concentration levels in a small test chamber change over time. Figure 4.3 shows how the emission rate in a small test chamber changes over time (including the effect of ACH on R). The figures show the development for ACHs of 1 h^{-1} and 5 h^{-1}. The graphs have been calculated using model DK2004. The input parameters were representative for fibreboards and test conditions used to validate emission models: $C_0 = 10^7$ µg/m³, $D_m = 1 \cdot 10^{-10}$ m²/s, K = 3000, δ = 0.01 m, V = 30 l, A_m = 45 cm² and h_m = 0.0025 m/s. The figures show that while changes in the ACH significantly impact concentration levels, they only have little influence on the emission rates. In this instance the concentration in the chamber air drops by approximately 85 % within 80 hours. Based on this the half-life of the air concentration can be calculated to be 27 h.

Figure 4.4 shows how emission rates predicted by Qa2007 change with ACH ($0.01 \leq Fo_m \leq 0.2$). In this particular model the dimensionless air exchange rate, α, is the term considering the ACH. With α raised to the power of 0.022 (Eq. 17) any change to the ACH will have little effect on the predicted emission rate. A fivefold increase in the ACH from 0.25 to 1.25 increases the emission rate by 3.6 %.

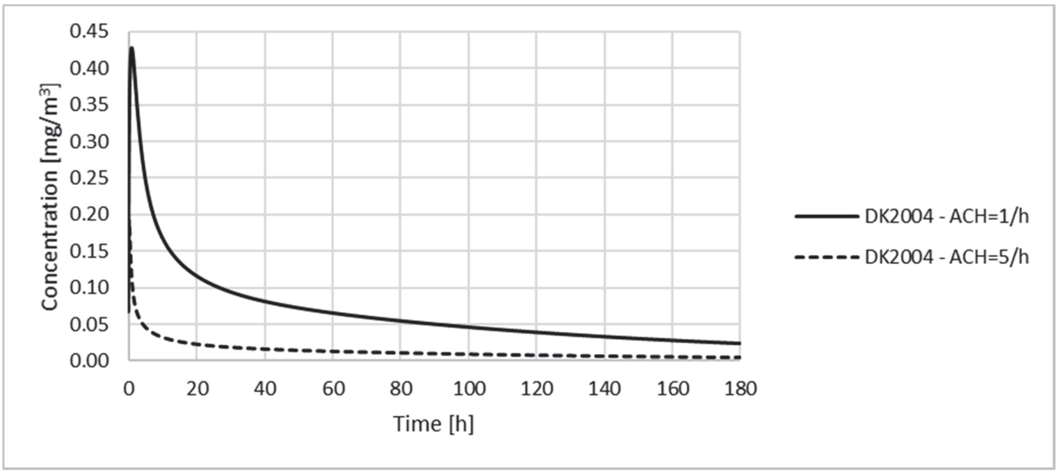

Figure 4.2 – Development in HCHO concentration level in small test chamber calculated using DK2004 [156]

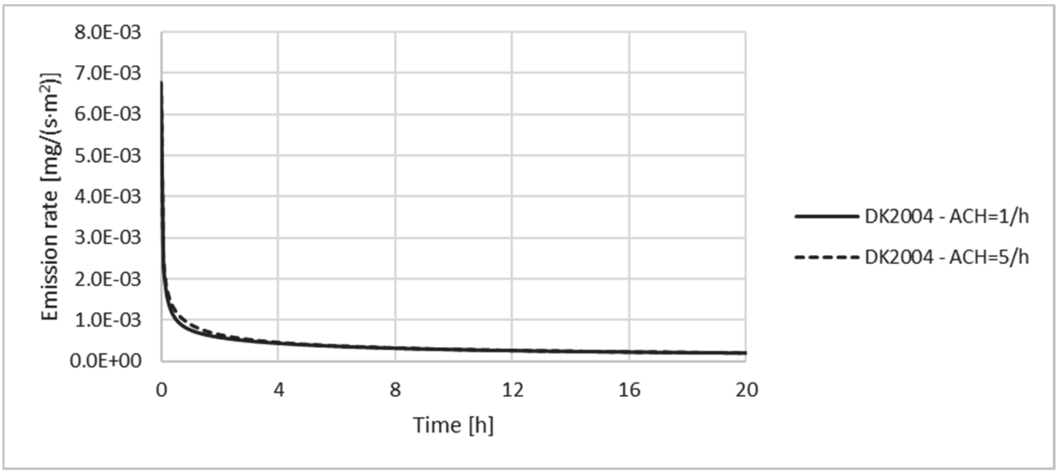

Figure 4.3 – Development in HCHO emission rate in small test chamber calculated using DK2004 [156]

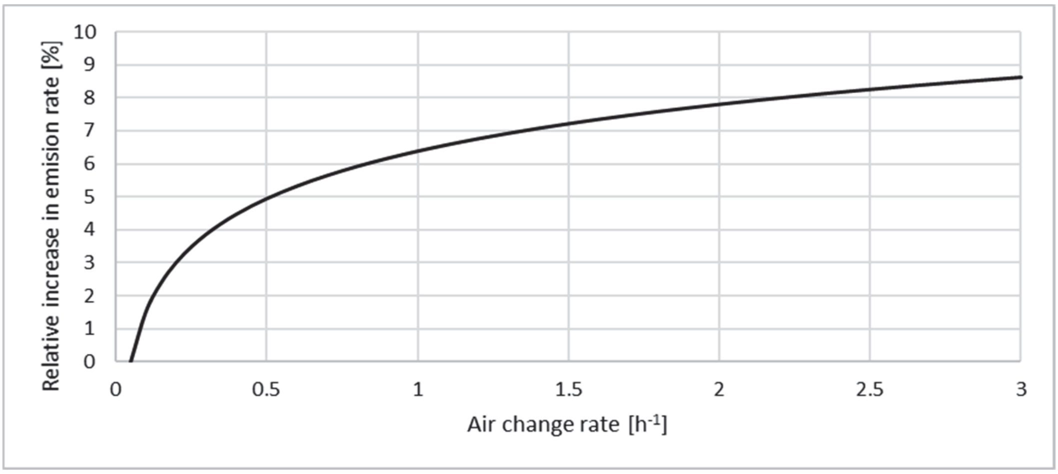

Figure 4.4 – Predicted relative increase in HCHO emission rates by model based on results from small test chamber using Qa2007 [125]

4.2.2 Observations from real world studies

Generally, studies that observe VOC emission rates in buildings do not include enough data on construction materials to allow for a simulation to be run for comparison. Instead, in order to compare predictions and observations, it is necessary to examine general trends. Existing literature contains information on how changes in ACH affect HCHO emission rates and how HCHO emission rates change over time. The four examined VOC emission models all predict that ACH has little or no influence on emission rates, that emission rates decrease continuously and that the half-life of the air concentration is of the order of days. If the emission models are to be used to simulate real world emission patterns, these patterns must be reflected in real world observations.

4.2.2.1 Influence of ACH on observed HCHO emission rates

Tests performed by Lehmann in a large-scale test chamber (55.4 m^3) found that a fivefold increase in the ACH (an ACH to loading ratio from 0.25 to 1.25 for an initial concentration of 0.6 ppm) would about halve the concentration of HCHO [116]. The fivefold increase in ACH resulted in a 170 % rise in the emission rate. An investigation of data gathered by Logadóttir and Gunnarsen, shown in Figure 4.5, shows a comparable trend [119]. Here a fivefold increase in ACH from 0.25 to 1.25 resulted in a roughly estimated 270 % rise in the emission rate. Similarly, a study of HCHO exposure in US residences conducted by Hult et al. found that, at a reference ACH of 0.35 h^{-1}, increasing ventilation was up to 60 % less effective

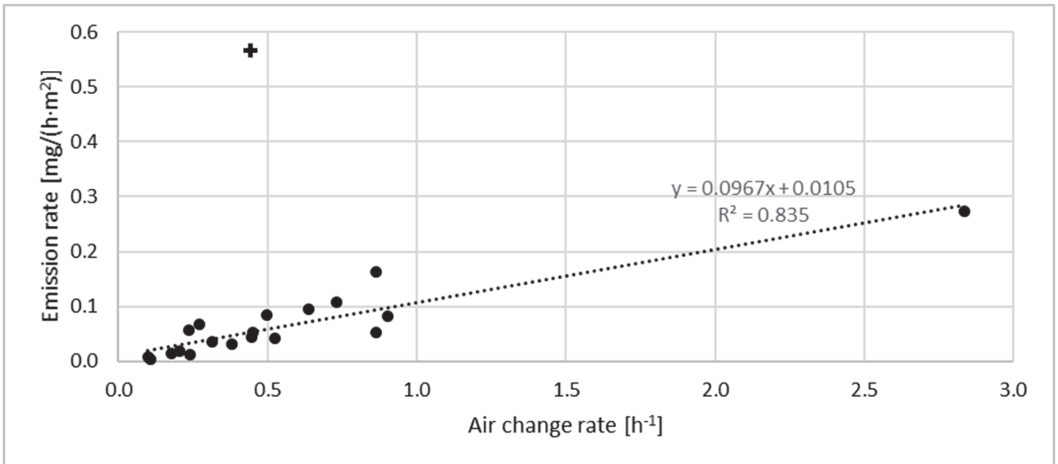

Figure 4.5 – HCHO emission rates derived from measured concentrations plotted over ACH [119] – outlier marked with a cross

than would be predicted if the HCHO emission rate was constant [117]. Hult et al. noted that this indicates that HCHO emission rates increase as air concentrations decrease.

Results from a study of VOC emissions from materials in vehicles by Xiong et al. suggest that change in the ACH might also influence emission rates for VOCs different from HCHO [158]. Xiong et al. reported a general relationship between the VOC concentration levels and the volume flow rate in the examined vehicles. Here a fivefold increase in ACH from 0.25 to 1.25 resulted in a 34 % drop in concentration levels and a 229 % increase in emission rates.

4.2.2.2 Influence of time on observed emission rates

Myers and Nagaoka tested emissions at low ACHs (an ACH to loading ratio of 0.060 m/h). They found that the amount of HCHO lost by some particleboard samples only amounted to a very small fraction of the potentially available amount. After 10 weeks of dynamic experiments, the loss was approximately 0.2 % of the total original content of HCHO [115]. Zinn et al. reported the findings of a long-term study of emissions from 16 particleboard products. They

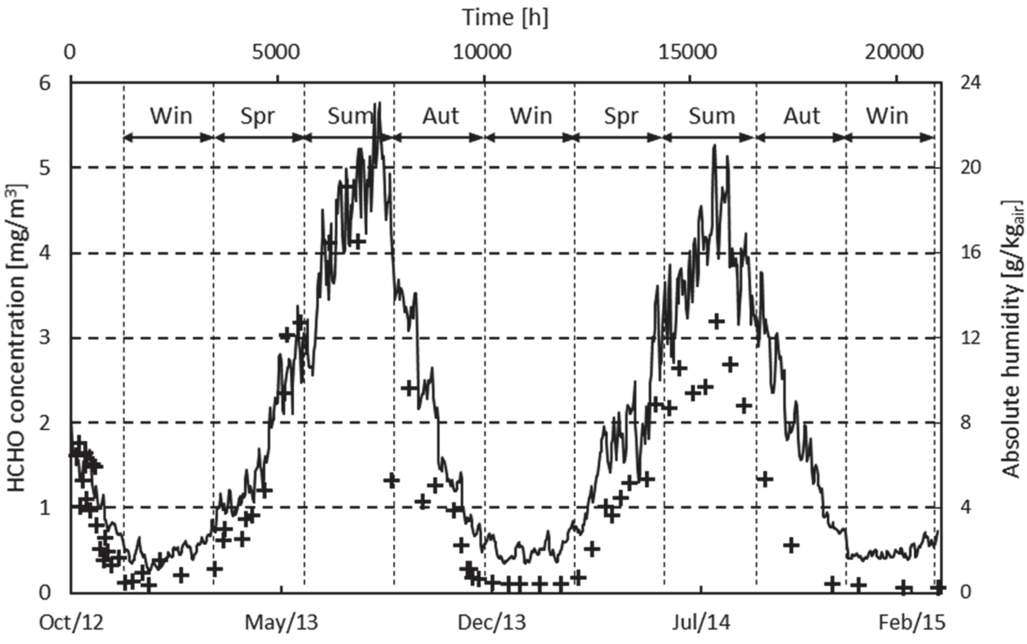

Figure 4.6 – Variation in HCHO concentration levels over the seasons in full-scale experiment seen in relation to AH [110] – the line traces the humidity level and the crosses mark the HCHO concentration

reported the half-life time of HCHO content in the particleboards to be 216 days [159]. Figure 4.6 shows excerpts from the results of a study by Liang et al. where a full-scale experiment followed a naturally ventilated building fitted with a loading of 0.5 m^2/m^3 raw MDF sheets for 29 months. The figure shows how the HCHO concentration varied over the seasons in relation to AH. The study found that the HCHO concentration decreased 20−65 % in corresponding months of the second year [110]. This corresponds well with the half-life time of 216 days as reported by Zinn et al. [159].

4.2.3 Discussion

The comparison found that emission rates predicted by the examined models based on mass transfer theory and validated against results from experiments performed in small test chambers do not correspond well with observations from homes, large test chambers and full scale experiments. Specifically, the emission models appear to underestimate the influence of changes in the ACH and forecasted drops in emission rates and concentration levels occur much later than predicted. Also, analysis of the mathematics behind the emission models found that such models have not been designed in a way that allows them to capture the dynamic behaviour of a system with varying temperature and RH.

The findings from the comparison and analysis show that the examined emission models are not suitable for use in connection with BPS. Moreover, the findings suggest that the examined models may lack or fail to properly appreciate aspects important to the emission process. This indicates that more research is needed in two areas: methods that will allow BPS to include considerations of building generated pollution and general mass transfer theory models for VOC emissions that can handle dynamic conditions. These two areas may well overlap. The latter of the two research areas include identification of why the examined models fail to emulate patterns observed in real world cases.

4.2.3.1 Influence of surface conditions on emission dynamics

It is possible that part of the reason for the observed discrepancy between predictions and observations is to be found in the physical test environment present in small test chambers using fans to ensure ideal mixing in the small test chambers. Myers and Nagaoka discuss the influence of air velocity on the emission pattern of HCHO [115]. They hypothesise that a high air velocity will lead to the depletion of the readily emittable (un-bound HCHO) concentration in a test specimen and that a low air velocity will not. They argue that, as a result, the problems are inherently different.

Hoetjer and Koerts describe several experiments to determine the emission characteristics of test specimens [108]. While Hoetjer and Koerts do not mention rate limitation as such, they do address the influence of ideal mixing. They state that experiments performed at low air velocities will not reach a steady state condition that allows for inference about HCHO levels in a test specimen. They also state that tests performed at low air velocities will yield results similar to those that would be found in a real world setting. They continue by stating that HCHO concentrations will be lower in tests with low air velocities and illustrate this by presenting results from their experiments. They explain the difference in concentrations by pointing out that still air presents a considerable resistance to mass transfer. This is directly analogous to the hypothesis presented by Myers and Nagaoka [115].

Surface conditions in test chambers are very different from what we observe in the real world. As mentioned, air velocities will be much higher at the emitting surface in small test chambers than in practice. Also, emitting materials such as particleboard are generally covered by upholstery or laminate. This positively affects the mass transfer resistance (lowers the effective mass transfer coefficient and Biot number for mass transfer) and may create a bottleneck that changes the emission dynamics.

4.2.3.2 Influence of HCHO generation in emitting material on emission dynamics

From the presented results it can be seen that while emissions in real world settings do decrease with time, the time it takes to deplete an original content of HCHO is on the order of years (with a half-life of 216 days it will take about 2.5 years for 95 % of the original content to diffuse out of the emitting material). Chamber tests reach steady state conditions – that is deplete the original content of HCHO – within a few weeks.

Figure 4.6 shows that emission rates change over time and that emission rates under the right conditions (higher temperature and humidity levels) can exceed those observed when test specimens are new. This departure from the behaviour predicted by models based on results from tests in small climate chambers (shown on Figure 4.3 and Figure 4.4) cannot be explained by a change in the surface mass transfer resistance alone.

Particleboards, fibreboards and plywood are all bonded by resins that contain urea-formaldehyde (UF) [104]. Unfortunately, UF resins have the undesirable trait that they react with water. The presence of free water results in hydrolysis that releases un-bound HCHO molecules from the building materials [104,110]. The strong correlation between AH and HCHO concentration levels shown on Figure 4.6 suggests that reactions between water and UF could be a significant source of HCHO. This implies that models may have to include considerations of the rate of generation of HCHO – e.g. as a result of hydrolysis – in order to accurately predict emission rates over time.

4.2.3.3 Perspectives

While there are a few mass transfer models that consider mass (e.g. HCHO) generation in emitting materials [160,161], not much is known about reaction rates (secondary sources) [160]. Judging from the conclusions of more recent reviews [97,162,163], it is apparent that more research into how environmental factors, such as temperature, RH and ventilation affect the emission dynamics is needed. Recent studies have shown and explained how temperature and humidity affect the initial emittable concentration, C_0, of HCHO [109,111–113]. However, dynamic effects, such as the reaction/generation rate and how the ambient environment affects this rate, still need to determined.

Liu, Ye and Little [162] describe Wang and Zhang's model [161] as the "most general" analytical solution. Like the models used for the above comparison, this model is also a one-phase exponential decay model that has been validated against the data published by Yang et al. [157]. As such, it shares some of the problems described in the discussion (i.e. unknown mass generation rate, unknown mass transfer resistance at emitting surface and material properties are assumed constant). As this is also one of the most – if not the most – recent of the VOC emission models, it can be concluded that more development is needed before models based on mass transfer theory can be used to estimate development in VOC emissions under real world conditions.

Since models based on mass transfer theory still cannot accurately predict VOC emissions under real world conditions, an alternative is needed. Recent work by Rackes and Waring [118] suggest that data driven (statistical) models may be such an alternative.

4.2.4 Conclusion

Comparing predictions from emission models for VOC based on mass transfer theory validated against results from small test chambers using fans to ensure ideal mixing to practical observations from homes, large test chambers and full scale experiments reveal that such emission models overestimate emission rates and underestimate the time it takes to deplete the original content of un-bound HCHO.

A part of the reason for the observed discrepancy might be that a test environment with high air velocity increases convective mass transfer rates to a level that is not observed outside such a test environment. Therefore scenarios in test chambers should be considered a subset of all emission scenarios and, as such, cannot be seen as representative of all emission scenarios.

The emission models included in this comparison were all based on the assumption that change in the concentration in an emitting material is determined by diffusion alone. It is implicit to this assumption that generation is negligible. Results of the comparison between predictions and observations indicate that models may have to include considerations of VOC generation in emitting materials in order to accurately predict emission rates over time.

It was concluded that models validated against experiments made in test chambers using a fan for ideal mixing are not suitable for estimating development in emissions under real world conditions.

4.3 Development of formaldehyde emission models

4.3.1 Data sample

HCHO emissions were estimated based on data on concentration levels gathered by Logadóttir and Gunnarsen [119]. The data set included observations from 20 newer Danish homes. The measurements were conducted in 2008 and the average age of the homes was 2.75 years.

Logadóttir and Gunnarsen measured HCHO concentration levels, ACH, temperature, RH and room geometry. Their study included notes on whether occupants smoked indoors and the type of ventilation system. Where the study did not include information on background HCHO levels or mention the type of outdoor environment (urban, suburban or rural) it did report that homes were either detached or semi-detached. This allowed the assumption that measurements were done in a suburban or rural environment which, in turn, allowed the assumption that HCHO background levels were 0.001 mg/m^3 [164].

HCHO emission rates were calculated using Eq. 25. The relationship was derived from Eq. 24 under the assumption that the ACH, supply air concentration and indoor air concentration were constant during measurements.

$$\frac{dC_a(t)}{dt} = \frac{R(t)A}{V} + C_s(t)n(t) - C_a(t)n(t) \qquad \text{Eq. 24}$$

Where	C_a is the concentration in the room air	[kg/m^3]
	C_s is the concentration in the supply air	[kg/m^3]
	R is the emission rate	[kg/(s·m^2)]
	n is the air exchange rate	[s^{-1}]
	t is the time	[s]
	V is the room volume	[m^3]
	A is the floor area of the room	[m^2]

$$R = \frac{V(C_a n - C_s n)}{A} \qquad \text{Eq. 25}$$

Logadóttir and Gunnarsen did not include estimations of the loading ratio in their report. Assuming a constant room height, the floor area was used as a proxy for the loading ratio. To allow comparison between different room sizes, the derived emission rates were normalised by the floor area. After also normalising the derived emission rates by ACH it became possible to describe the distribution with a log-normal distribution function. The test for log-normality identified a single outlier. Figure 4.7 shows the distribution of the emission rates normalised by area and ACH as it is without the outlier. Table 4.1 shows the descriptive statistics of the log-normal distribution.

Table 4.1 – Descriptive statistics of the log-normal distribution of the normalised emission rates

Statistic	[mg·h/(h·m²)]
Mean	0.181
Mode	0.0825
Median	0.105
StdDev	0.0615

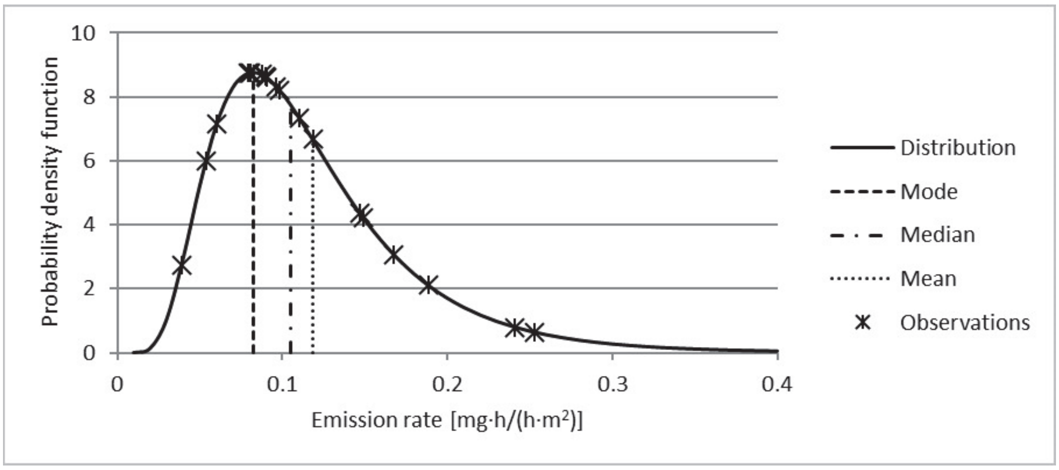

Figure 4.7 – Log-normal distribution describing normalised emission rates and observations

The emission rates normalised by area and ACH were divided into three groups; low, normal and high. Low emissions were found in the first quartile (up till 25 %) (≤ 0.0753 mg·h/(h·m²)), normal in the second quartile (from 25 % to 75 %) (0.0753 mg·h/(h·m²) < R < 0.146 mg·h/(h·m²)) and high in the third quartile (from 75 % and up) (≥ 0.146 mg·h/(h·m²)). Three observations were classified as being low emission rates, 10 as normal and 7 as high. The outlier (ID F15 in Table 4.2) was found among the high emission rates.

Table 4.2 – Data collected by Logadóttir and Gunnarsen [119] and derived normalised HCHO emission rates – outlier marked in bold

Level	ID	ACH	Temp.	RH	Conc.	Emission rate	
		[h^{-1}]	[°C]	[%]	[mg/m^3]	[$mg/(h·m^2)$]	[$mg·h/(h·m^2)$]
Low	F16	0.11	21.0	51	0.018	4.26E-03	3.91E-02
	F12	0.24	22.3	66	0.024	1.30E-02	5.39E-02
	F5	0.86	18.8	53	0.029	5.23E-02	6.05E-02
Normal	F8	0.52	20.0	58	0.034	4.15E-02	7.91E-02
	F4	0.38	20.6	54	0.035	3.06E-02	8.03E-02
	F17	0.18	22.8	43	0.033	1.45E-02	8.06E-02
	F20	0.20	22.0	49	0.030	1.78E-02	8.74E-02
	F6	0.90	22.0	37	0.031	8.13E-02	9.00E-02
	F9	0.10	27.0	51	0.036	8.99E-03	9.08E-02
	F10	2.84	24.2	59	0.042	2.73E-01	9.64E-02
	F18	0.45	24.0	55	0.040	4.40E-02	9.86E-02
	F14	0.31	23.4	58	0.050	3.46E-02	1.10E-01
	F11	0.45	22.4	53	0.050	5.32E-02	1.18E-01
High	F1	0.73	23.7	41	0.050	1.07E-01	1.47E-01
	F19	0.64	26.4	44	0.064	9.50E-02	1.49E-01
	F2	0.50	17.6	56	0.069	8.35E-02	1.67E-01
	F3	0.86	19.6	51	0.081	1.63E-01	1.89E-01
	F13	0.23	26.2	43	0.104	5.65E-02	2.41E-01
	F7	0.27	22.0	44	0.110	6.82E-02	2.53E-01
	F15	**0.44**	**22.4**	**55**	**0.550**	**5.67E-01**	**1.28E+00**

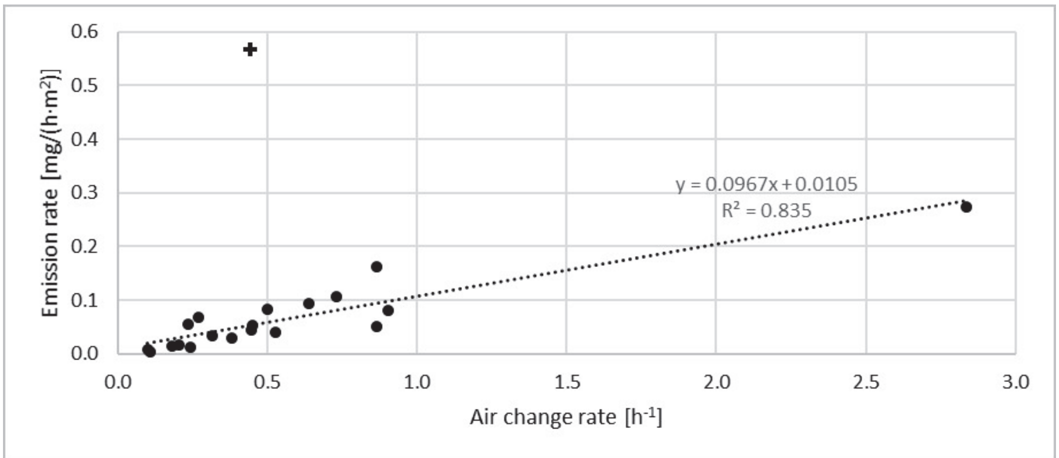

Figure 4.8 – HCHO emission rates derived from measured concentrations plotted over ACH – outlier marked with a cross

Figure 4.8 shows the emission rates normalised by area only plotted over ACH. The cross on Figure 4.8 marks the outlier. Table 4.2 contains a selection of the data collected by Logadóttir and Gunnarsen [119]. The second to last column contains HCHO emission rates normalised by area only. The last column contains HCHO emission rates normalised by both area and ACH.

4.3.2 Regression analysis

4.3.2.1 Independent variables

Temperature, RH, absolute humidity (AH) and ACH were included in the analysis as possible predictor variables. While both humidity and temperature are associated with ACH, this association was assumed negligible. Each possible predictor may affect emission in its own way [104]. ACH may work as a proxy for the driving potential for mass transport from material to air; increasing the ACH increases the concentration difference and therefore may increase the emission rate. Temperature may work as a proxy for kinetic energy in the HCHO molecules; increasing the temperature increases kinetic energy which helps molecules break their chemical bonds and therefore may increase the emission rate. Humidity may work as a proxy for production rate of HCHO; increasing the humidity level may increase the rate with which HCHO is being released from resin by hydrolysis and thereby increase the emission rate.

4.3.2.2 Zero-emission assumptions

Acknowledging the significance of the low number of observations in the respective bins and the narrow bands of the predictor variables, analyses in some instances also included assumptions for scenarios with zero-emission. It was assumed that emissions would go towards zero-as temperatures neared -19 °C, which is the boiling point of HCHO. Crossing this temperature, un-bound formaldehyde will undergo a phase change from a gaseous to a liquid state. While emissions can still continue by evaporation, it was assumed that this effect was negligible.

It was assumed that net emissions would go towards zero as the ACH neared zero. With no influx of clean air to dilute concentration levels, an equilibrium will be reached. At this equilibrium the flux of desorbed HCHO will be equal to the adsorbed totalling a net emission of zero. Of course, net positive emissions will continue in the time before a steady state is reached. However, it was judged that the assumption of zero-emissions at zero ACH was reasonable in the context of the regression analysis.

It was assumed that net emissions would go towards zero as the humidity levels neared zero. In the absence of un-bound HCHO molecules the rate of HCHO emission depends on urea−formaldehyde depolymerisation and hydrolysis, which needs water [110]. In the absence of water, HCHO emissions would continue until the time that stores of un-bound HCHO are depleted. However, it was judged that the assumption of zero-emissions at zero RH and AH was reasonable in the context of the regression analysis.

The assumptions were included in the regression analysis by adding fabricated "observations" to the pool of data. Since assumptions for zero-emission were included in the pool of data they did not constitute actual boundary conditions. Emission models were trained on the expanded data pool but were not forced to zero-emissions. A total of 12 fabricated data sets were added to the pool; 4 data sets per assumption. The fabricated data sets each contained a unique combination of values for the predictor variables. Table 4.3 shows the combinations of predictor variables used to train the regression model using the assumption of zero-emission.

Table 4.3 – Fabricated "observations" added to data pool to train model with assumptions of zero-emission

Predictor		Temperature				Humidity				ACH			
Θ	[°C]	-19	-19	-19	-19	10	30	10	30	10	30	10	30
RH	[%]	40	80	40	80	0.1	0.1	0.1	0.1	40	40	80	80
ACH	[h^{-1}]	0.2	0.2	0.4	0.4	0.2	0.2	0.4	0.4	0.01	0.01	0.01	0.01

4.3.2.3 Regression technique

The regression analysis was performed in Matlab. Emission models were developed in two steps. The first step was to identify potential models. This was done using the Matlab function for stepwise linear regression to construct models and the Akaike information criterion to estimate the relative quality of the constructed models. The next step was to test potential models by leave-one-out cross-validation. The models with the lowest cross-validation root-mean-square error were chosen. Using cross-validation allowed models to be trained on the complete data set (for each given bin) and ensured that the selected models were among the best to predict values in the held-out test sets. All included terms were statistically significant ($p < 0.05$).

4.3.3 Data-driven emission models

Regression analyses were done for normal level and high level emission rates. There were not enough observations to perform the analysis for low level emission rates. The regression analyses resulted in the development of three separate models for HCHO emissions normalised by area.

$$E_{extended} = -1.123 \cdot 10^{-5} N + 3.425 \cdot 10^{-6} n \cdot AH + 2.985 \cdot 10^{-5} N^2 - 2.478 \cdot 10^{-5} N^2 \cdot AH \qquad \text{Eq. 26}$$

$$E_{normal} = -1.340 \cdot 10^{-2} + 2.627 \cdot 10^{-5} N + 9.019 \cdot 10^{-5} T + 3.498 \cdot 10^{-7} AH - 1.518 \cdot 10^{-7} T^2 \qquad \text{Eq. 27}$$

$$E_{high} = 1.377 \cdot 10^{-5} + 3.723 \cdot 10^{-5} N^2 \qquad \text{Eq. 28}$$

Where	E is the emission rate estimated by models derived from regression analysis	[mg/(s·m^2)]
	N is the ACH	[h^{-1}]
	AH is the absolute humidity	[g/m^3]
	T is the absolute temperature	[K]

The first model is a general model for normal level emission rates (Eq. 26). The data pool consisted of 22 observations including 12 sets of data from the added assumptions for zero-emission. The model uses ACH and AH as predictor variables. The regression analysis found that neither temperature nor RH added to the predictive power of the model. The model has an adjusted R^2 of 1 and a root-mean-square error of $1.08 \cdot 10^{-6}$ mg/(s·m^2).

The second model (Eq. 27) is also for normal level emission rates but is based on data not including assumptions for zero-emission. As a possible outlier (F14) was excluded from the data, the model was based on 9 observations. The model uses ACH, AH and temperature as predictor variables. The regression analysis found that RH did not add to the predictive power of the model. The model has an adjusted R^2 of 1 and a root-mean-square error of $4.2 \cdot 10^{-7}$ mg/(s·m^2).

The high adjusted R^2 values for the two models for normal emission rates are not reliable measures of the goodness of fit. Rather, the high adjusted R^2 values are due to the high ratio of predictor variables to observations. As such, the adjusted R^2 values overestimate the variance that is explained by the independent variables. Here, the emission models for normal emission rate are overfitted.

The third model (Eq. 28) is for high level emission rates and is based on data not including assumptions for zero-emission. As a possible outlier (F21) was excluded from the data, the model was based on 6 observations. The model only uses ACH as a predictor variable. The regression analysis found that AH, RH and temperature did not add to the predictive power of the model. The model has an adjusted R^2 of 0.9 and a root-mean-square error of $3.31 \cdot 10^{-6}$ mg/(s·m^2).

4.3.3.1 Residual analysis

Analyses of normal probability plots found that residuals, on the whole, appear to follow a normal distribution. Still, there were indications of deviation from normality on the plots for the first and second model. On the plot for the first model (Eq. 26) (Figure 4.9), there was one data set at the end of the right hand tail did not follow the normal distribution. The value was identified as the highest measured emission rate in the bin for normal level HCHO emissions (ID F11 in Table 4.2). The residuals from the second model (Eq. 27) (Figure 4.10) follow a gentle s-shaped curve. Such a curve can indicate that a distribution may be short-tailed, meaning that it displays less variance than expected. This could be due to the low number of observations included in the analysis.

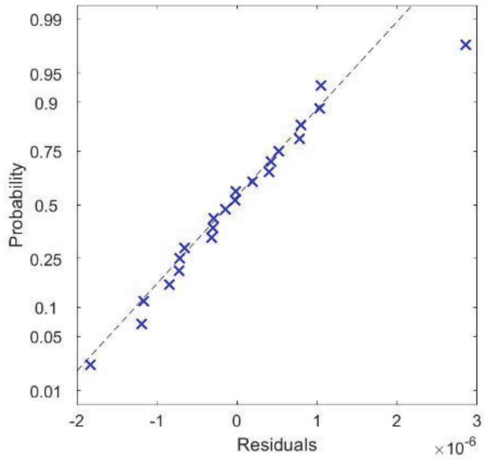

Figure 4.9 – Normal probability plot of residuals for normal level emission model from data including zero-emission assumptions

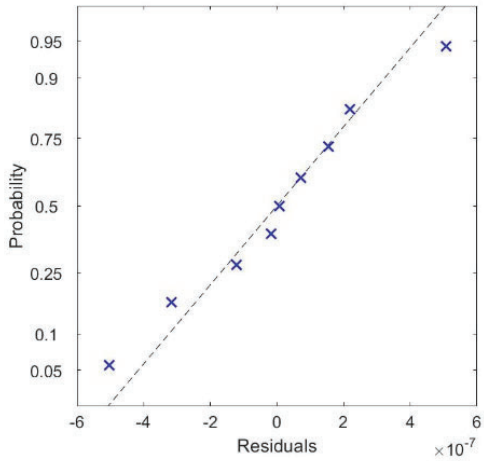

Figure 4.10 – Normal probability plot of residuals for normal level emission model from data without zero-emission assumptions

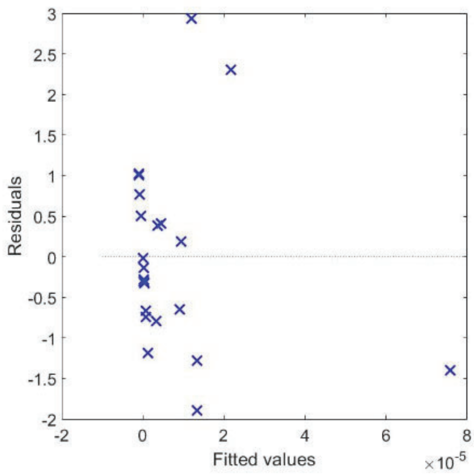

Figure 4.11 – Plot of standardised residuals for normal level emission model from data including zero-emission assumptions

Analysis of standardised residuals identified two possible outliers (standardised residual > 1.96) for the first model (Eq. 26) (Figure 4.11). This is a little higher than what would be expected as 95 % of standardised residuals were expected to be within a band of ±1.96 ($\alpha = 0.05$). The possible outliers were identified as F11 and F6. No outliers were identified for either of the second or third models. Analysis of standardised residuals found no indication of heteroscedasticity in either of the three models. However, the low number of observations and the limited variation in the ranges of the predictor variables make it impossible to come to a definite conclusion as to whether the data is heteroscedastic or not.

4.3.3.2 Evaluation of models

The above analysis found that the normal level HCHO emission model trained on data including zero-emission assumptions (Eq. 26) provide inaccurate predictions for emission rates higher than the median. Dividing the normal level emission rate group into bins for emissions below and above the median of the distribution (0.105 mg·h/(h·m^2)) shows that the lower bin contains 8 observations while the higher bin contains 2. The inability to accurately predict higher emission rates may be explained by the low number of observations of emission rates higher than the median.

Figure 4.12 shows how temperature affects the predicted normal level HCHO emission rate (Eq. 27). The effect is inconsistent with findings from earlier studies that suggest a continuous increase in emission rates with increasing temperatures. This limits the use of the model; the model cannot be used to estimate emission rates at temperatures higher than those included in the observations (F9 was measured at 27 °C). Possible explanations for the observed inconsistency are that the model may describe random error or noise instead of the underlying relationship and that the model is trained on a data set that does not contain observations above 27 °C. However, the effects are statistically significant (for both terms including temperature $p < 0.009$).

While it was found that the elements of the second model (Eq. 27) do not have a direct physical interpretation (and misinterprets the effect of temperature on emission), the predictive power for conditions found in the indoor environment is higher than that of the first model (Eq. 26). So, despite its flaws, it was found that the model for normal emission rates based on data without including assumptions of zero-emission (Eq. 27) has value in the framework of the study.

Besides being based on a very small sample of observations, no issues were identified during analysis of the residuals from the emission model for high level emission rates (Eq. 28).

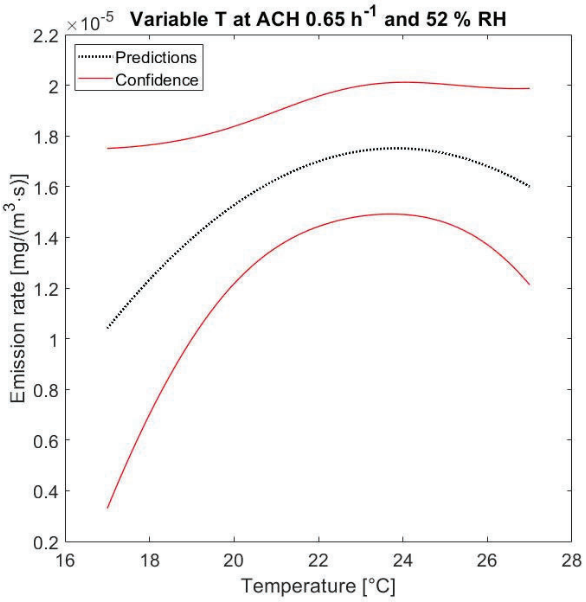

Figure 4.12 – Influence of temperature on model for normal level emission from data without zero-emission assumptions

4.3.3.3 Limitations on use of models

While the quality of the data used for the regression analysis was good, the number of observations was low. Also, due to the nature of conditioned indoor environments, all measurements were done within a narrow band of temperature, RH and ACH. Therefore, the use of the expressions for normal emission rates based on data not including assumptions for zero-emission (Eq. 27) is limited to temperatures ranging from 17 °C to 27 °C, RHs ranging from 30 % to 80 % and ACHs ranging from 0.05 h^{-1} to 3 h^{-1}. The use of the expression for high emission rates based on data not including assumptions for zero-emission (Eq. 28) is limited to ACHs ranging from 0.1 h^{-1} to 1.5 h^{-1}.

The measurements used to develop the models were made in detached and semi-detached Danish homes. Presumably in a sub-urban and/or rural environment. The models can be used to estimate emission rates only in such homes.

4.3.4 Discussion

The regression analysis was performed on the basis of a very small data set. Still, correlations between predictor variables and the dependent variable were all statistically significant. It was possible to identify two trends: ACH was a predictor in all models, RH in none. Temperature and AH were significantly correlated with the dependent variable in some models.

It is clear that the findings of this study support the findings of previous studies that have identified ACH as a powerful predictor variable [118,165]. The roles of the other possible predictor variables are less clear. To the best of our knowledge, there are no studies that have shown a statistically significant correlation between HCHO emission rates and temperature and humidity. Based solely on the presented regression analysis, it is not possible to conclude whether changes in temperature or humidity influence dynamics in HCHO emissions. However, there is still reason to believe that at least one of these may.

As explained, each possible predictor variable may influence the chemistry in a given material. Though inconclusive, the regression analysis may indicate that humidity does influence the rate of emission: Seen relative to RH, AH appears to be a much better predictor. If humidity did not influence the emission rate, the stepwise linear regression algorithm should be as likely to pick RH as it should AH. There may also be a physical explanation as to why AH would be a better predictor than RH. AH is a direct measure of the amount of water present in the air. RH is dependent on both temperature and AH. So, if the humidity level does influence the rate of production (or release by hydrolysis), it stands to reason that the AH would be the better indicator of the potential.

Temperature was only significantly correlated to the dependent variable in one model. In laboratory tests [109,111], changes in temperature have been shown to increase the initial emittable concentration. It has been hypothesised that increasing the temperature increases the rate of emission because the increase in kinetic energy helps HCHO molecules break the bonds that keep them adsorbed to the surfaces in porous materials. This then may have no effect on the rate of production. Since the initial emittable concentration has been seen to be depleted within weeks in laboratory experiments, it is possible that subsequent HCHO emissions are limited by the rate of production – and therefore not significantly influenced by changes in temperature. Either way, more research is needed before it can be concluded whether temperature influences the dynamics of emission rates in the long term.

The performed regression analysis is comparatively simple. Qian et al. have published an emission model where coefficients have been regressed to the (dimensionless) parameters [125]. As their model is non-linear (with power terms that are non-integers), it is wholly conceivable that stepwise linear regression does not allow the identification of the correct expression for an emission model. Nevertheless, the derived models for normal and high level emissions (Eq. 27 and Eq. 28) both give good predictions for HCHO emission rates within the stated boundaries and – being simple and easily implementable – therefore has value in the context of BPS.

4.3.5 Conclusion

Emission models developed by regression analysis represent an alternative to emission modelling based on mass transfer theory. With information on the baseline level of emission in a given indoor environment, this type of model can estimate emission rates for indoor environments under varying conditions. Since it is possible to express this type of emission model by simple equations, they can easily be implemented in BPS tools. Based on this, it was concluded that emission models developed by regression analysis can be used in BPS to estimate the effect building generated pollution has on IAQ and energy demand.

The findings of the regression analysis support the findings of previous studies that have identified ACH as a powerful predictor variable for HCHO emissions. The roles of temperature and humidity as possible predictor variables are less clear. Based solely on the presented regression analysis, it was not possible to conclude whether changes in temperature or humidity influence dynamics in HCHO emissions.

5 Estimate of effect of formaldehyde on ventilation rate and energy demand

This chapter presents the findings of a study designed to (i) examine how considerations of building generated pollution would affect ventilation control systems and energy demand and to (ii) estimate the minimum ventilation rates necessary to keep occupants healthy and comfortable. In accordance with the scope of the thesis, the study was conducted under Danish climatic conditions.

The main findings from the preceding studies, presented in the previous two chapters, were implemented into the study. To ensure that ventilation systems were as energy efficient as possible under Danish climatic conditions, all simulated ventilation systems used HR. To ensure that emissions of building generated pollution was estimated as accurately as possible, the derived data-driven HCHO emission models were implemented into the BPS models used for simulations. Multiple simulations were executed, each with a unique ventilation control system capable of controlling ventilation rates based on measurements of temperature, RH, CO_2 and HCHO.

The main conclusions of the study were that building generated pollution may still present a problem and that DCV with HR, compared to the performance of CAV ventilation with HR, can help improve both IAQ and TC at no extra costs in terms of energy. Based on considerations of the current level of technology and pricing, it was recommended to continue the current practice of prescribing base ventilation rates. It was noted that future advances in research and technology and lower prices could change the recommendation to allow DCV go below current recommended base ventilation rates.

The second objective of this thesis was to develop a method to estimate the impact that building generated pollution has on IAQ, the energy demand and ventilation rates under Danish climatic conditions and to use this method to evaluate the minimum requirements for ventilation rates as prescribed by BR18. The successful conclusion of this work fulfils the second objective of this thesis. The chapter is based on the work presented in Paper 3. The original material can be found in the appendix, see list on page 112.

5.1 Method

The purpose of the BPS was to study the impact that building generated pollution has on the energy demand and ventilation rates in a building fitted with a balanced mechanical ventilation system using HR. In order to do so, it was necessary to perform a parameter variation. Therefore, both BPS tool and model design needed to allow this. Furthermore, the chosen BPS tool also had to allow ventilation to react in response to the dynamic emissions of the HCHO emission models developed by regression analysis.

IDA ICE [138] is a validated open source BPS tool that has a built-in function that facilitates a parameter variation. Users can extend IDA ICE's functionality by importing blocks coded in either neutral model format (NMF) or Modelica. As such, IDA ICE was a well suited tool. The HCHO emission models were coded in NMF.

The BPS model was kept simple with generic construction parts and occupancy profile. Complex design features were avoided in order to ensure that identified trends were indeed generic and uninfluenced by specificities like overly intricate occupancy patterns or mass transport between zones in a complicated geometry. The model constituted a single room occupied by a single person that showered in the morning, left during office hours and cooked in the evening. In this way, the model could be said to be reminiscent of a small studio apartment.

The focus of the study was on energy demand and ventilation control. In order to ensure that ventilation rates were determined by need and not capacity, the main ventilation system had a larger than standard capacity. The pseudo-random influence of wind and stack driven infiltration can make trends harder to identify. Therefore, infiltration was disabled in the model. Also, the model ignored transient moisture effects; the only moisture that was considered was that which was present in the included air volumes.

5.1.1 Building performance simulation model

The model was subjected to Danish weather conditions (with Köppen climate classifications Cfb and Dfb, respectively corresponding to a temperate oceanic climate and a warm-summer humid continental climate).

The model consisted of a single rectangular room with a floor area of 20 m^2 (4 m x 5 m) and a room height of 2.6 m. The outer walls had a U-value of 0.30 W/($m^2 \cdot K$), the floor slab a value of 0.20 W/($m^2 \cdot K$), and the roofing construction a value of 0.20 W/($m^2 \cdot K$). The U-values are consistent with the minimum requirements given in BR18.

The building had two windows on the 4 m long north-facing façade of the model. The dimensions of the windows were 1.23 x 1.48 m. The windows had a U-value of 1.67 W/(m^2K) and a g-value of 0.68. The windows were placed in the northern façade to minimise the impact of solar radiation on the indoor temperatures.

Thermal bridges along the perimeter of the windows and the ground slab were included. Thermal bridges around the windows were simulated as 0.6 W/($m \cdot K$) and the thermal bridge around the ground slab was simulated as 0.4 W/($m \cdot K$). The values given for the thermal bridges are consistent with the minimum requirements given in BR18.

Operating hours were set to a full year (8760 hours) with occupancy following the profile shown in Table 5.1. Occupancy was simulated as a single person with an activity level of 1 Met. Simulations included moisture production from showers and cooking. Showers lasted 15 minutes from 6:45-7:00 and emitted water at a rate of $7.22 \cdot 10^{-4}$ kg/s [93]. Cooking lasted 30 minutes from 17:30-18:00 and emitted water at a rate of $1.33 \cdot 10^{-4}$ kg/s [93].

Table 5.1 – Occupancy profile

Weekday	Time interval	Occupancy
Mon-Fri:	08:00-15:00	0.0
	15:00-17:00	0.5
	17:00-08:00	1.0
Sat-Sun:	00:00-24:00	1.0

Heating was simulated using an ideal heater with a set-point temperature of 21 °C. Heating was simulated as being active all year round. The model did not include mechanical cooling. All cooling was done by ventilation with air at outdoor temperatures.

5.1.1.1 Ventilation control

The ventilation rate was controlled based on temperature, RH, CO_2 and HCHO. The control included a scheduling function that was used to select which of the control variables that would be included in a given simulation. Separate PI controllers were used to determine the ventilation volume flow rate based on the levels of the control variables. In scenarios including multiple control variables, the ventilation rate was determined by the variable requiring the highest ventilation rate. A schematic of the ventilation control system is shown in Figure 5.1. Set-points for ventilation control are shown in Table 5.2.

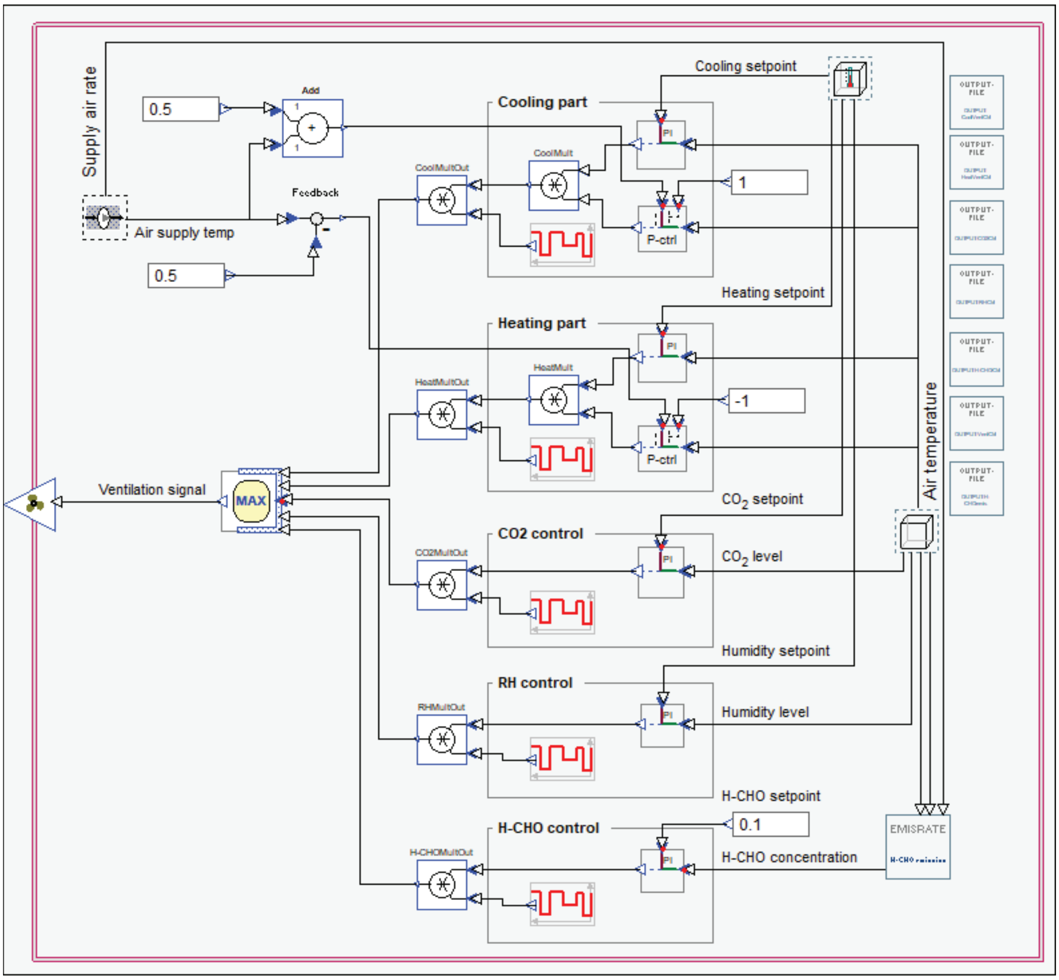

Figure 5.1 – Schematic of the ventilation control system in IDA ICE

Table 5.2 – Set-points for ventilation control

Variable	θ	RH	CO_2	HCHO
Unit	[°C]	[%]	[ppm]	[mg/m^3]
Min	21	20	700	0.0
Max	25	80	1100	0.1

Background levels for CO_2 and HCHO were 400 ppm and 0.001 mg/m^3, respectively [164]. Minimum and maximum ventilation rates depended on the examined scenario.

Five different ventilation systems were simulated (ventilation rates are normalised by unit floor area):

A. CAV at 0.3 l/(s·m^2)
B. DCV with a base ventilation rate of 0.3 l/(s·m^2)
C. DCV without a base ventilation rate (allowing a ventilation rate of 0 l/(s·m^2))
D. DCV with exhaust and a base ventilation rate of 0.3 l/(s·m^2)
E. DCV with exhaust without a base ventilation rate (allowing a ventilation rate of 0 l/(s·m^2))

Table 5.3 – Volume flow rates for the five different ventilation systems

ID	Ventilation [l/(s·m2)]		Exhaust [l/s]	
	Min	Max	Cooking	Shower
A	0.3	0.3	0	0
B	0.3	7	0	0
C	0	7	0	0
D	0.3	7	20	15
E	0	7	20	15

Table 5.3 shows the volume flow rates associated with the different ventilation systems listed above. The ventilation rate for CAV and base ventilation rate for the DCV systems correspond to the minimum rate stated in BR18. The maximum rate of 7 l/(s·m^2) was chosen to enable DCV to meet set-points for all control variables (disregarding problems that could arise from draught). When included, exhaust was simulated as 0.45 l/(s·m^2) during showers and 0.7 l/(s·m^2)

during cooking. Added to the base ventilation rate, the total ventilation rate was 15 l/s and 20 l/s during showers and cooking respectively. These ventilation rates correspond to the minimum criteria for exhaust as stated in BR18. Infiltration was not included in the calculations.

While designing the ventilation control system (Figure 5.1) it became apparent that it was not possible to solve the mass balance for HCHO (Eq. 24) using the total ACH; it was only possible to link the mass balance to one air flow (as opposed to the sum of all air flows). The mass balance was connected to the supply airflow of the main ventilation system. Therefore, the extra exhaust in systems D and E did not affect HCHO levels in the model. With infiltration set to zero, the only source of error was the extra exhaust. As the extra exhaust was only activated for a total of 45 minutes a day, it was assumed that the long term influence on the HCHO concentration was negligible. The extra exhaust did influence RH and CO_2 levels.

SFP values for the CAV and DCV system were both set to 1800 J/m^3 which is the highest allowed by BR18 for CAV (the allowed value for VAV/DCV is 2100 J/m^3). Fans had an efficiency of 60 %.

The ventilation systems all used HR with an effectiveness of 80 %. Exhaust ventilation did not use HR and the make-up air volumes were therefore all delivered at outdoor temperatures.

5.1.1.2 Parameter variation/scenarios

The model built in IDA ICE was used to simulate scenarios for different ventilation systems with varying control settings.

Simulations were run for normal and high levels of HCHO emission. The column labelled Emis shows which scenarios have normal (N) and high (H) emission levels. Also, simulations were run with controls set to be active during all hours and with controls set to be active during the occupied hours only. The base ventilation rate was active throughout all hours even if other controls were not active. The column labelled Occu shows which scenarios have controls active during all hours (A) and which scenarios only have controls active during the occupied hours (O). The combinations of control variables are shown on the right-hand side of Table 5.4. Here, an X marks an included control variable. In total, 161 scenarios were simulated.

Table 5.4 – Combinations of control variables used in simulations for the four DCV systems

Emis	Occu
N	O
N	A
H	O
H	A

→

θ	CO_2	RH	HCHO
X	-	-	-
-	X	-	-
-	-	X	-
-	-	-	X
X	X	-	-
X	-	X	-
-	X	X	-
-	-	X	X
X	X	X	-
X	X	X	X

The energy demand for every scenario was calculated for two different levels of SFP; constant and variable. Comparing energy demands calculated with a constant SFP is the equivalent of comparing the summed ventilation volumes for the full year. Comparing the variable SFP of the DCV to the constant of the CAV allows incorporating an estimate of the energy savings that comes from using DCV. IDA ICE uses the method described in ASHRAE's standard 90.1:2007 [166] Appendix G to estimate a generic performance curve for a VAV aggregate. The method uses a polynomial to estimate the fraction of the max SFP a DCV system is running under given conditions. Eq. 29 shows the polynomial used by IDA ICE.

$$SFP_{Frac} = 0.0013 + (0.147 \cdot (0.9506 - 0.0998 \cdot \mathrm{PLR}) \cdot \mathrm{PLR}) \cdot \frac{G_a}{\mathrm{G_{a,max}}}, \quad PLR = \min\left(\frac{G_a}{\mathrm{G_{a,max}}}, 1\right) \qquad \text{Eq. 29}$$

Where SFP_{Frac} is the fraction of the SFP a DCV is running [0,1] [-]

PLR is the part load of the flow [0,1] [-]

G_a is the volume flow rate at a given time [m^3/s]

$G_{a,max}$ is the maximum volume flow rate for the DCV system [m^3/s]

5.2 Results

Results focused on IAQ, TC and energy demand. TC refers to temperature levels only. IAQ refers to the levels of HCHO, CO_2 and RH. Here HCHO was a proxy for building generated pollution while CO_2 was a proxy for pollution from occupants. RH levels were a result of occupancy, activities (cooking and showering) and outdoor conditions and were primarily considered as a pollutant that could harm the building itself (e.g. cause mould infestation and rot in wood).

The results were scored for TC and IAQ as either A, B or C. The scenarios received an A if they had less than 25 hours above the values in Table 5.5, a B if they had between 25 and 100 hours and a C if they had above 100 hours. The value used to evaluate temperature corresponded to the upper limit for summer of category 1 in EN 15251 [72]. The value used to evaluate CO_2 (700 ppm above outdoor levels) was in compliance with the guidelines given by the Danish Working Environment Authority [167] (< 1500 ppm) and corresponded to category 3 in EN 15251. The value used to evaluate RH corresponded to category 4 in EN 15251. The value used to evaluate HCHO corresponded to the guidelines set by WHO [13] and BR18.

Table 5.5 – Evaluation criteria for simulated scenarios

	Limit
θ	25.5 °C
CO_2	1100 ppm
RH	80 %
HCHO	0.1 mg/m^3

The energy demand was simulated in part as a heating demand and in part as the auxiliary energy used for driving the ventilation systems. Due to the simplicity of the model, the calculated energy demands were not expected to relate to any real world energy demand. Therefore, the energy demand calculated in the simulations only had value when seen relative to each other. The energy demands are presented relative to the CAV reference scenario. To allow for easy interpretation, the energy demand for the reference scenario was defined as zero. This means that positive values for energy demand indicated a higher energy demand than the CAV scenario.

The below text contains an interpretation of the obtained results. For a full view of all obtained results readers are referred to the table of results shown on page 1 in the appendix. Table 5.6 contains a suite of selected results that are representative of the trends found in the simulation results. The scores for temperature, CO_2 and HCHO are for the fully occupied hours (Mon-Fri 17:00-08:00 and Sat-Sun 00:00-24:00, see Table 5.1). The presented scores for RH are for all hours of the year.

The energy demands for constant and variable SFPs are for the full year and are given in relative terms. Energy demands calculated for a constant SFP are in the column labelled conSFP. Energy demands calculated for a variable SFP are in the column labelled varSFP. Columns conSFP and varSFP contain intervals for energy demand. The intervals comprise of results from simulations with varying HCHO emission levels and with ventilation controls turned on and off outside the occupied hours (see left-hand side of Table 5.4) (8 results per interval). The intervals show the lowest and highest calculated changes in energy demand relative to the reference CAV scenario.

An X in the column labelled B03 indicates that the scenarios have a base ventilation rate of 0.3 $l/(s \cdot m^2)$ while the absence indicates that there was no base ventilation. Results from the reference CAV scenario are shown in row #1.

Table 5.6 – Selected results from simulations showing scores and relative energy demands

#	Control variables				B03	Scores				Energy demand	
	θ	CO_2	RH	HCHO		θ	CO_2	RH	HCHO	conSFP [%]	varSFP [%]
1	-	-	-	-	CAV	B	C	C	A	0	0
2	X	-	-	-	X	A	C	C	A	[0.6,2.4]	[-0.1,-2.0]
3	X	-	-	-	-	B	C	C	C	[-9.6,-10.9]	[-9.9,-11.1]
4	-	X	-	-	X	B	A	C	A	[0.8,2.5]	[-0.1,-1.8]
5	-	X	-	-	-	B-C	A	C	A-C	[-0.5,-1.7]	[-2.5,-3.8]
6	-	-	X	-	X	B	C	A	A	[0.7,2.5]	[-0.1,-1.9]
7	-	-	X	-	-	C	C	A-C	C	[-6.6,-7.9]	[-7.4,-8.9]
8	-	-	-	X	X	B-C	C	C	A	[0.1,2.0]	[-0.5,-2.3]
9	-	-	-	X	-	C	C	C	A	[-3.8,-10.2]	[-5.3,-10.8]
10	X	X	-	-	X	A	A	C	A	[1.2,2.9]	[0.2,-1.5]
11	X	X	-	-	-	A	A	C	A-C	[-0.1,-1.3]	[-2.1,-3.5]
12	X	-	X	-	X	A	C	A	A	[1.1,2.9]	[0.3,-1.6]
13	X	-	X	-	-	A	C	A-C	C	[-6.1,-7.4]	[-7.0,-8.4]
14	-	X	X	-	X	B	A	A	A	[1.3,3.0]	[0.3,-1.4]
15	-	X	X	-	-	B-C	A	A-C	B-C	[-0.1,-1.3]	[-2.1,-3.5]
16	-	-	X	X	X	B	C	A	A	[0.7,2.5]	[-0.1,-1.9]
17	-	-	X	X	-	C	C	A-C	A	[-3.0,-7.9]	[-4.5,-8.9]
18	X	X	X	-	X	A	A	A	A	[1.6,3.3]	[0.6,-1.2]
19	X	X	X	-	-	A	A	A-C	A-C	[0.3,-0.9]	[-1.8,-3.1]
20	X	X	X	X	X	A	A	A	A	[1.6,3.3]	[0.6,-1.1]
21	X	X	X	X	-	A	A	A-C	A	[1.1,-0.9]	[-1.1,-3.1]

The base ventilation rate of 0.3 l/(s·m^2) – used in the reference CAV scenario (row #1) – was found to keep HCHO concentrations for both normal and high level emissions below 0.1 mg/m^3 at all times.

Two ventilation strategies met all success criteria; one considered temperature, CO_2 and RH while employing a base ventilation rate of 0.3 l/(s·m^2) (#18) and the other considered all four control variables during all hours of the year (#21). The score of C for RH in #21 was for scenarios where the ventilation was off during unoccupied hours. Compared to the reference CAV scenario (#1) the first successful ventilation strategy (#18) had a higher energy demand at constant SFP ([1.6,3.3]) and a comparable energy demand at variable SFP ([0.6,-1.2]).

Compared to the reference CAV scenario (#1) the second successful ventilation strategy (#21) had a comparable energy demand at constant SFP ([1.1,-0.9]) and a lower energy demand at variable SFP ([-1.1,-3.1]). Scenarios without exhaust performed better than scenarios with exhaust in terms of energy demand. The scenario without exhaust and a normal level of HCHO emission had an energy demand that was 3.1 % lower than the reference CAV scenario. The scenario without exhaust and a high level of HCHO emission had an energy demand that was 2.5 % lower than the reference CAV scenario.

It has not been possible to estimate the effect that exhaust has on maximum HCHO concentration levels. The reason is that the emission models cannot handle RH levels above 80 % and that exhaust primarily influences the duration of high RH levels. Adding exhaust was found to lead to an average drop in total emitted mass of HCHO of about 2 %.

Table 5.7 – Selected results from simulations showing ACHs

¤	Control variables				B03	ACHs [h^{-1}] – Total time (incl. unoccupied hours)				
	θ	CO_2	RH	HCHO		Min	Max	Mean	Median	StdDev
1	X	-	-	-	-	[0.01,0.01]	[9.52,9.52]	[0.10,0.11]	[0.01,0.01]	[0.69,0.70]
2	-	X	-	-	-	[0.12,0.12]	[0.46,0.46]	[0.35,0.35]	[0.42,0.43]	[0.13,0.13]
3	-	-	X	-	-	[0.07,0.07]	[2.17,2.43]	[0.15,0.15]	[0.12,0.12]	[0.11,0.11]
4	-	-	-	X	-	[0.08,0.22]	[0.14,0.22]	[0.10,0.22]	[0.09,0.22]	[0.02,0.00]
						ACHs [h^{-1}] – During occupancy				
5	X	-	-	-	-	[0.01,0.01]	[9.52,9.52]	[0.12,0.12]	[0.01,0.01]	[0.77,0.78]
6	-	X	-	-	-	[0.13,0.13]	[0.46,0.46]	[0.40,0.40]	[0.45,0.45]	[0.10,0.10]
7	-	-	X	-	-	[0.07,0.07]	[2.17,2.43]	[0.15,0.15]	[0.12,0.12]	[0.11,0.11]
8	-	-	-	X	-	[0.08,0.22]	[0.14,0.22]	[0.10,0.22]	[0.09,0.22]	[0.02,0.00]

Table 5.7 shows ACHs for control of single variables. Results are from scenarios where ventilation control systems were always on. The values on the left-hand side of the intervals are for normal HCHO emission rates while the values on the right-hand side are for high HCHO emission rates.

An ACH of 0.22 h^{-1} was needed to keep HCHO concentration levels at the WHO guideline value of 0.1 g/m^3 for high HCHO emission levels (¤4 and ¤8). For this scenario, the resultant ACH was constant. The reason was that high level HCHO emissions rates were estimated from the ACH alone (see Eq. 28). Since the ACH controlled the HCHO concentration levels and no other variables were considered, the solution to the mass balance became the same at every time step.

In terms of ACH, the most demanding control variable was temperature (¤1 and ¤4). Results show that an ACH of 9.52 h^{-1} was needed to keep temperatures at the set-point of 25 °C while at peak load. The mean and median ACHs were both low and indicated that there for the simulated building design were relatively few instances of peak loads and that they were comparatively short.

5.3 Discussion

5.3.1 Indoor air quality

A significant proportion (> 50 %) of Scandinavian homes have ACHs below 0.5 h^{-1} [18,67,68]. A recent study comparing the methods used for determining these ventilation rates (real-time measurements of occupant generated CO_2 and passive tracer gas collected in tubes) concluded that the used methods may well overestimate ACHs by a factor of 2-3 [69]. This indicates that average ventilation rates in Scandinavia might be lower than what studies have shown. Considering that the simulations showed that ACHs of minimum 0.22 h^{-1} are required to effectively safeguard against HCHO, it is fair to conclude that building generated pollution also deserves future attention.

The study found two control strategies that could effectively prevent harmful levels of HCHO: A base level ventilation rate of 0.3 $l/(s \cdot m^2)$ and a DCV system that considers HCHO as a control variable. Considering current technology and prices, the former is probably the most viable option at present. As such, it must be recommended to continue current practice of prescribing base ventilation rates. However, current developments in sensor technology suggest that microscale gaseous HCHO detection systems will soon reach a mature level that will allow low-cost batch production [168]. When this happens, it might be worth considering changing the standards.

Meanwhile, it is worth asking if HCHO is the best indicator of building generated pollution. HCHO can come from a variety of sources (including combustion in car engines) and current developments might well mean that outdoor levels can increase [105]. Other pollutants might prove more useful as proxies for the general level of emissions from building materials [169,170], but presently there are hardly any VOCs that have been studied as much as HCHO.

5.3.2 Energy demand

Disregarding future usefulness, the prevalence of HCHO in building materials combined with the developed understanding of the processes governing emissions makes HCHO useful for studies such as the present. While the emission models implemented in the IDA ICE model cannot be used to predict concentration levels in homes, they can be used to run dynamic simulations allowing us to determine a first-order approximation of the impact that building generated pollution has on the IAQ and energy demand.

The results from the study show that, when compared to CAV systems with HR, DCV systems with HR can improve IAQ and that it is possible to obtain these improvements without a negative impact to the energy demand. With the advent of microscale sensors, it might be possible to obtain these improvements along with a reduction in the energy demand of up till 3 %. This reduction in the energy demand would not be insignificant on a societal scale.

It is worth noting that previous studies that have investigated how DCV impacts energy demand have reported possible reductions well in excess of 3 % [82]. However, most previous studies have not included HR as part of their ventilation designs. In this study, the reported reductions in energy demand are calculated relative to the performance of a CAV ventilation system with HR. Since HR on exhaust air itself is an efficient energy reduction measure [19,64–66], the potential impact of DCV is lower in a system using HR. Therefore, the relative improvements reported in this study are lower than the average of reported reductions in energy demand.

At the current price of energy, a reduction of the energy demand of approximately 3 % will not offset the costs of installation of such advanced ventilation systems. From the point of view of the end user, the selling point would be improvements to IAQ and TC. These benefits can be obtained from well near any balanced mechanical ventilation system with HR. Therefore, it might be necessary to change future legislation in order to harvest the energy saving potential of advanced ventilation systems.

5.4 Conclusion

The results from the dynamic simulation in IDA ICE, incorporating emission models for HCHO, show that it is necessary to have ACHs of minimum 0.22 h^{-1} to effectively safeguard against HCHO. Considering the level and price of current technology, it was recommended to continue the practice of prescribing base ventilation rates. Still, building generated pollution deserves future attention.

Compared to the performance of CAV ventilation systems, DCV systems can help improve both IAQ and TC. The study found two control strategies that could effectively prevent harmful levels of HCHO: A base level ventilation rate of 0.3 $l/(s{\cdot}m^2)$ and a DCV system that considers HCHO (as a proxy for building generated pollution) as a control variable.

Current developments in sensor technology suggest that microscale gaseous HCHO detection systems will soon reach a mature level that will allow low-cost batch production. With the advent of microscale sensors, DCV systems with HR might be able to deliver improvements in IAQ along with a reduction in the energy demand of up till 3 % seen relative to CAV ventilation systems with HR. Due to the low price of energy and the high price of DCV systems, it might be necessary to change legislation in order to harvest the energy saving potential of advanced ventilation systems.

6 Overall discussion and perspectives

There is a very real risk of climate change in the foreseeable future. If climate changes are to be avoided, we need to reduce our global demand for energy [5]. The official goal of the Danish government is to be independent of fossil fuels by 2050. In order to achieve independence, Denmark needs to reduce energy demand for heating by about 40 % relative to 2016 levels [17]. A common energy conservation measure is to increase the airtightness of a building envelope. With ventilation rates in Danish homes already low [18,67–69], increased airtightness can lead to poor IAQ and ultimately have a negative impact on occupants' health [11–14]. If means of ventilation are not considered as part of a low-energy design or renovation, there is a risk that efforts to avoid climate change end up harming people. This is the context of the thesis. The aim was to find the least energy demanding form of ventilation that keeps occupants healthy and comfortable.

6.1 Design features and control systems

As the project progressed, attention turned from general considerations on ventilation to specific design features (/technologies) and control systems. Comparing natural and mechanical ventilation, two design features stood out as particularly promising: supply air windows and HR. Estimates in published literature were that, when compared to natural ventilation, HR with an efficiency of 80 % and supply air windows would reduce energy demand by 22 % [64,65] and 11-24 % respectively [33,34,38]. With comparable estimates of achievable reduction in energy demand, existing literature did not allow for a definite conclusion as to which ventilation technology that is best in terms of energy efficiency in a temperate climate such as the Danish. The study presented in Chapter 3 found that estimates for ventilation with HR in literature were accurate, but that supply air windows only reduced energy demand by 8 %. The study went on to conclude that HR on the exhaust air is the most efficient energy conservation measure under Danish climatic conditions.

Having compared the relative performance of several representative CAV ventilation systems, attention was directed at more advanced control systems. Chapter 5 presents results from a study comparing an array of different DCV systems using HR to a reference scenario with CAV ventilation using HR. The results from the study show that, when compared to CAV ventilation systems with HR, DCV systems with HR can improve IAQ and TC without a negative impact on the energy demand. It was noted that where this study found little to no difference in energy demand, previous studies comparing CAV ventilation to DCV have estimated achievable reductions in energy demand on the order of 40-60 % [78–81]. Here, the key difference between the present and previous studies predicting large reductions in energy demand is that all ventilation was done using HR [81].

The work presented in this thesis has led to the conclusions that HR is the most efficient energy conservation measure and that DCV has the potential to increase IAQ and TC. Here, it is useful to differentiate between objectives. If the objective is to conserve energy, there is little to no difference in performance between DCV and CAV ventilation, as long as both use HR.

Current ventilation standards predominantly prescribe ventilation rates to address risks associated with discomfort. Recently published research has suggested a health-based guideline of 4 l/s of clean air per occupant [15]. The guideline is valid in the absence of pollution sources different from the occupants themselves. With a European average floor area of 34 m^2 per occupant [171], the health-based guideline translates to an average minimum ventilation rate of 0.12 l/(s·m^2). For the high level HCHO emission rate studied in Chapter 5, a ventilation rate of 0.16 l/(s·m^2) was needed to comply with WHO guidelines. BR18 prescribes a minimum ventilation rate of 0.3 l/(s·m^2). If the objective is to ensure occupants' health, in the majority of cases, CAV ventilation complying with prescribed minimum ventilation rates will do this.

Using HR, the prescribed minimum ventilation rate ensures energy efficiency and occupants' health. In Denmark, then, the real value of DCV is that it can be used to improve comfort. Meanwhile, there are barriers that must be overcome before it is possible to unlock the potential of DCV. In order for DCV to improve IAQ without having a negative impact on energy demand when compared to CAV ventilation, DCV must be allowed to lower ventilation rates below the prescribed minimum. At present, DCV is only allowed to operate at ventilation rates equal to or higher than the minimum prescribed ventilation rates.

6.1.1 Demand controlled ventilation and the future

There are good reasons why various national building codes prescribe minimum ventilation rates. At present, there is no consensus on what – if any – type of emission that can be used as a proxy for building generated pollution [82]. Also, sensor technology has still not matured to a level where the needs of the industry are met [168–170]. In short, we still do not have what we need in order to justify allowing DCV to ventilate at rates lower than the currently prescribed minimum level. However, research and development is ongoing and it may be a relatively short wait before sensor technology meets industry requirements.

As concluded in the previous section, the real value of DCV is its ability to improve comfort of occupants. In a relatively cool climate as the Danish, the demand for advanced DCV may not be that big. However, future climate changes may negatively impact indoor environments and increase the need for advanced ventilation systems [172,173]. Other external factors may also influence demand. A move towards smart homes, cities and grids may require flexible HVAC systems [174]. In any event, as DCV does have value in its own right, it may be worth preparing for a future where "true DCV" (here defined as DCV that is free to control ventilation rates according to given set points without observing minimum ventilation rates) is possible.

The principle barrier that must be overcome is the identification of which pollutants that can be used as reliable indicators of pollution from building materials and furniture. With reliable and quantifiable indicators for when the air is safe to breathe identified, building codes and national standards could be updated with performance based requirements in any number of ways. As it stands, there is no reason why work to this end could not start now.

6.2 Building physics and performance simulation

Building physics as a research field is unprepared for a future with true DCV. As the study in Chapter 4 concluded, existing emission models based on mass transfer theory are not suitable for estimating development in emissions under real world conditions. One immediate consequence is that at present, there is no general, reliable way to simulate IAQ or TC or calculate energy demand of a given building design using DCV controlled by pollutants. With true DCV soon being possible – maybe even necessary – this is unfortunate. Meanwhile, the issue has garnered international attention. Now, work to update BPS tools with the capability to estimate the impact that building generated pollution has on IAQ is ongoing [16].

The study presented in Chapter 4 identified three potential reasons as to why existing VOC emission models fail to predict emissions in practice: (i) In order to derive fully analytical solutions, researchers have assumed that material properties and testing conditions are constant. Therefore, models do not allow dynamic modelling, at least not from a strictly mathematical point the view. (ii) Surface conditions in test chambers are very different from what we observe in the real world. In practice, air velocities will be lower than they are in small test chambers and materials will usually be covered by upholstery or laminate. As a result, any lessons learned about the mechanics of mass transfer at the material surface during model testing and validation probably cannot be relied upon in practice [108,115]. (iii) Most emissions models assume that VOC generation is negligible. However, results of the comparison between predictions and observations presented in Chapter 4 indicated that significant amounts of HCHO were released or generated in particleboards over time. If such generation or release does happen in practice, this could explain why emission rates stay higher for longer in practice. Meanwhile, not much is known about VOC generation or release rates in materials [97,160,162,163].

6.2.1 Data-driven emission models

While the ideal standard for VOC emission modelling is physics-based models, it is unlikely that any new models will be published in the near future. Even if new models were published, and they addressed the weaknesses listed above, there would still be a shortage of knowledge of surface mass transfer mechanics and VOC generation and release rates in materials (i.e. unique material properties). Considering the number of challenges, it is sensible to look for alternatives to physics-based emission models. Historically, data-driven models have been used as an alternative to physics-based models. Current examples of data-driven models are the CO_2 [21] and moisture [93–95] emissions models used in BPS to estimate emissions produced by occupants. As studies that have used regression techniques to derive emission models have reported statistically significant correlations between independent and predictor variables, regression analysis is a reasonable alternative [118,165].

Chapter 4 presents results from a regression analysis. The analysis yielded two emission models for HCHO. One for 'normal' emission levels and one for 'high' emission levels. The models were based on data gathered in newer detached and semi-detached single-family homes in rural and suburban Denmark. The models, therefore, are limited to use for indoor climates and conditions present in such types of homes. As it turned out, data on HCHO emission in Danish homes were scarce. The scarcity of data influenced what could reasonably be inferred from the regression analysis and derived emission models. Though potential predictor variables were selected based on a documented ability to influence emission rates and all correlations between dependent and predictor variables were statistically significant, the models suffer from being overfitted and predict behaviour that is inconsistent with laboratory observations. Meanwhile, predicted emission rates are in good agreement with the underlying observations and the emission models do appear to capture at least part of the dynamic behaviour exhibited by HCHO emissions in real world settings. Ultimately, in spite of their flaws, the emission models were concluded to have value in the context of BPS and the present research project.

Obtaining useful data can present a challenge. This may also be a problem outside of Denmark. Observations of VOC concentrations in indoor air need to be accompanied by data on the ambient environment. Dependent on the type of VOC, information is needed on variables such as temperature, ACH, RH, room volume, area of the emitting surface area and concentration in supply air. If regression analysis is to able to capture dynamic behaviour, data on emission rates or concentrations in air has to correlate to data on the ambient environment in time. This may make it impossible to use some existing time-averaged data.

Therefore, as it is unlikely that a physics-based solution will be published anytime soon, it is possible that the shortest path to accurate VOC emission models is to start a programme of dedicated measurements.

Besides providing the data necessary to develop emission models, a dedicated measurement programme could also help identify dominant pollutants species. This way, a dedicated measurement programme could help identify useful, reliable proxies for building generated pollution.

Since the summer of 2017, commissioning has been an industry standard for all new ventilation systems in Denmark. One efficient way to collect data could be to include measurements of concentrations of selected pollutants and ambient conditions in a randomly selected subset of all homes when ventilation systems are commissioned. Another similar way could be to conduct measurements in connection with maintenance of ventilation systems. Combining the two approaches could help give insight into pollutant composition in indoor air in both new and old homes, albeit measurements might be biased in that only homes with mechanical ventilation are included. A separate programme could determine whether homes with mechanical ventilation are representative for the total building stock or not.

7 Conclusions

At the end of the day, ventilation is all about people. We use ventilation to ensure that people are healthy and comfortable in their homes, in transportation, and their workplaces. Meanwhile, ventilation comes at a cost. In terms of energy, indoor environments are expensive to condition. In a time where the production of energy still has a negative impact on the environment and the global demand is growing, it is in everybody's best interest that ventilation is done correctly. Whether in connection with new developments or energy renovations, when designing ventilation systems the focus – in prioritised order – has to be on health, comfort and energy efficiency.

The two main issues that need to be addressed when designing a ventilation system are dependency and price. Here dependency is synonymous with control of airflows and ACHs, and price refers to costs in terms of money (i.e. cost of acquisition, installation and maintenance) and energy. In a climate such as the Danish, the best way to ensure control and energy efficiency is by using a mechanical ventilation system with HR. As such, this should be the go-to solution and standard recommendation of all designers. However, in connection with energy renovations, there will be cases where it will not be possible to find space for a ventilation unit, ducting or both. In such instances it is important that options for single-room ventilation and natural ventilation are thoroughly researched.

At present, many Scandinavian homes have ACHs that are lower than the currently recommended 0.5 h^{-1} (0.3 $l/(s \cdot m^2)$ in Denmark). This means that many Scandinavians risk long term exposure to hazardous chemicals. Raising ventilation rates to the currently recommended level will help protect occupants from poor IAQ negatively impacting their health. CAV ventilation can do this. Both using HR, CAV ventilation is about as energy efficient as DCV. DCV does hold advantage over CAV ventilation. Comparing CAV ventilation with HR to DCV with HR, DCV can improve IAQ and TC without a negative impact on the energy demand. In Denmark, then, the real value of DCV is that it can be used to improve comfort. In popular terms, it could be said that if HR is for the climate, then DCV is for the people.

There are barriers that must be overcome before it is possible to unlock the potential of DCV. In order for DCV to improve IAQ without having a negative impact on energy demand when compared to CAV ventilation, DCV must be allowed to lower ventilation rates below the prescribed minimum. At present, DCV is only allowed to operate at ventilation rates equal to or higher than the minimum prescribed ventilation rates. In order for DCV systems to be able to respond to changes in levels of building generated pollution, they need to make use of sensors. Presently, sensor technology has still not matured to a level where the needs of the industry are met. However, research and development is ongoing and it may be a relatively short wait before sensor technology meets industry requirements.

Research in recent decades have increased our understanding of the processes that influence indoor air chemistry and how the indoor air chemistry affects occupants' health and comfort. Still, there is a gap between what we know and how we act. Overall, ventilation standards still focus on comfort rather than health and BPS tools still do not consider indoor air chemistry. Work needs to be done to bridge the gap. There is no consensus on which if any chemical compounds that can be used as a proxy for the IAQ, current physics-based models that estimate emission rates are incomplete and there is no legislative framework to support implementation of health-based ventilation.

With this many unresolved issues, it is sensible to continue the current practice of prescribing base ventilation rates. When sensor technology is mature and reliable indicators of emissions from building materials and furniture have been found, the recommendation will be to change legislation in order to allow DCV to ventilate at rates lower than the current prescribed minimum.

While in no way exhaustive, the work presented in this thesis shows that it is possible to address some of the above issues with currently available tools and technology. It is possible to derive models for emission rates from regression analysis of measurements done in buildings and it is possible to implement such emission models in BPS tools.

In order for data-driven models to be accurate, they need exhaustive information on the distribution of emission rates and the variables influencing the emission rates of the respective chemical compounds. Since the summer of 2017, commissioning has been an industry standard for all new ventilation systems in Denmark. One way to collect data on pollutant concentrations and ambient conditions in homes could be to conduct measurements when new ventilation systems are commissioned. Similarly, measurements could be done in connection with maintenance of existing ventilation systems. Combining the approaches could help give insight into pollutant composition in indoor air in both new and old homes. A separate programme could address concerns as to whether homes with mechanical ventilation are representative for the total building stock or not. Such a dedicated measurement programme could also assist in the efforts to identify pollutants that can be used as reliable and quantifiable indicators for when indoor air is safe to breathe.

Due to the nature of the work presented in this thesis, all of the above results and conclusions are only valid in the context of the Danish weather and climate. Also, all considerations and conclusions on how DCV and CAV ventilation compare to each other are based on comparisons where both use HR to reduce the energy demand.

References

[1] European Commission on Energy Efficiency in Buildings [Internet]. [cited 2018 Mar 16]. Available from: https://ec.europa.eu/energy/en/topics/energy-efficiency/buildings

[2] U.S. Energy Information Administration - How much energy is consumed in U.S. residential and commercial buildings? [Internet]. [cited 2018 Mar 16]. Available from: https://www.eia.gov/tools/faqs/faq.php?id=86&t=1

[3] The Danish Construction Association. Byggeriets Energianalyse 2017. Copenhagen, Denmark; 2017.

[4] The International Energy Agency (IEA). Modernising Building Energy Codes to secure our Global Energy Future: Policy Pathway. Paris, France; 2013.

[5] IPCC. Global Warming of 1.5°C. An IPCC Special Report on the impacts of global warming of 1.5°C above pre-industrial levels and related global greenhouse gas emission pathways, in the context of strengthening the global response to the threat of climate change,. Masson-Delmotte V, Zhai P, Pörtner HO, Roberts D, Skea J, Shukla PR, et al., editors. 2018.

[6] Directive 2010/31/EU of the European Parliament and of the Council of 19 May 2010 on the energy performance of buildings. European Union; 2010.

[7] Klepeis NE, Nelson WC, Ott WR, Robinson JP, Tsang AM, Switzer P, et al. The National Human Activity Pattern Survey (NHAPS): a resource for assessing exposure to environmental pollutants. J Expo Anal Environ Epidemiol. 2001;11[3]:231–52.

[8] Brasche S, Bischof W. Daily time spent indoors in German homes - Baseline data for the assessment of indoor exposure of German occupants. Int J Hyg Environ Health. 2005;208[4]:247–53.

[9] Khajehzadeh I, Vale B. How New Zealanders distribute their daily time between home indoors, home outdoors and out of home. Kotuitui. 2017;12[1]:17–31.

[10] Stanaway JD, Afshin A, Gakidou E, Lim SS, Abate D, Abate KH, et al. Global, regional, and national comparative risk assessment of 84 behavioural, environmental and occupational, and metabolic risks or

clusters of risks for 195 countries and territories, 1990–2017: a systematic analysis for the Global Burden of Disease Stu. Lancet. 2018 Nov;392[10159]:1923–94.

[11] Sundell J, Levin H, Nazaroff WW, Cain WS, Fisk WJ, Grimsrud DT, et al. Ventilation rates and health: multidisciplinary review of the scientific literature. Indoor Air. 2011 Jun;21[3]:191–204.

[12] Carrer P, Wargocki P, Fanetti A, Bischof W, De Oliveira Fernandes E, Hartmann T, et al. What does the scientific literature tell us about the ventilation–health relationship in public and residential buildings? Build Environ. 2015 Dec;94[P1]:273–86.

[13] WHO Regional Office for Europe. WHO Guidelines for indoor air quality - Selected pollutants. Copenhagen, Denmark; 2010.

[14] WHO Regional Office for Europe. WHO Guidelines for indoor air quality - Dampness and mould. Heseltine E, Rosen J, editors. Copenhagen, Denmark; 2009.

[15] Carrer P, de Oliveira Fernandes E, Santos H, Hänninen O, Kephalopoulos S, Wargocki P. On the Development of Health-Based Ventilation Guidelines: Principles and Framework. Int J Environ Res Public Health. 2018 Jun 28;15[7]:1360.

[16] IEA-EBC Annex 68 - Indoor air quality design and control in low energy residential buildings [Internet]. [cited 2018 May 17]. Available from: http://www.iea-ebc-annex68.org/about_annex-68

[17] Mathiesen BV, Drysdale DW, Lund H, Paardekooper S, Skov IR, Connolly D, et al. Fremtidens byggeri - Nøglen til et omkostningseffektivt og bæredygtigt energisystem. Aalborg, Denmark; 2016.

[18] Bekö G, Lund T, Nors F, Toftum J, Clausen G. Ventilation rates in the bedrooms of 500 Danish children. Build Environ. Elsevier Ltd; 2010;45[10]:2289–95.

[19] Laverge J, Janssens A. Heat recovery ventilation operation traded off against natural and simple exhaust ventilation in Europe by primary energy factor, carbon dioxide emission, household consumer price and exergy. Energy Build. Elsevier B.V.; 2012 Jul;50:315–23.

[20] Danish Building Regulations 2018. Denmark: The Danish Transport, Construction and Housing Authority; 2018.

[21] ASHRAE. 2009 Ashrae Handbook: Fundamentals. SI ed. Atlanta, Georgia, USA; 2009.

[22] Chenari B, Dias Carrilho J, Gameiro Da Silva M. Towards sustainable, energy-efficient and healthy ventilation strategies in buildings: A review. Renew Sustain Energy Rev. 2016 Jun;59:1426–47.

[23] Laverge J, Janssens A. Optimization of design flow rates and component sizing for residential ventilation. Build Environ. Elsevier Ltd; 2013;65:81–9.

[24] Chen Y, Tong Z, Malkawi A. Investigating natural ventilation potentials across the globe: Regional and climatic variations. Build Environ. Elsevier Ltd; 2017;122:386–96.

[25] Oropeza-Perez I, Østergaard PA. Potential of natural ventilation in temperate countries – A case study of Denmark. Appl Energy. Elsevier Ltd; 2014 Feb;114:520–30.

[26] Danish Meteorological Institute. Decadal mean weather in Denmark [Internet]. [cited 2019 Jan 21]. Available from: http://www.dmi.dk/en/vejr/arkiver/decadal-mean-weather/decadal-mean-weather/

[27] Historical archive of Danish Building Regulations [Internet]. [cited 2018 Jun 22]. Available from: http://historisk.bygningsreglementet.dk/tidligerebygreg/0/40

[28] O'Connor D, Calautit JKS, Hughes BR. A review of heat recovery technology for passive ventilation applications. Renew Sustain Energy Rev. Elsevier; 2016 Feb;54:1481–93.

[29] Weschler CJ, Carslaw N. Indoor Chemistry. Environ Sci Technol. 2018 Mar 6;52[5]:2419–28.

[30] Kumar P, Morawska L. Energy-Pollution Nexus for Urban Buildings. Environ Sci Technol. 2013 Jul 16;47[14]:7591–2.

[31] Tong Z, Chen Y, Malkawi A, Liu Z, Freeman RB. Energy saving potential of natural ventilation in China: The impact of ambient air pollution. Appl Energy. Elsevier Ltd; 2016 Oct;179:660–8.

[32] Ellermann T, Nygaard J, Nøjgaard JK, Nordstrøm C, Brandt J, Christensen J, et al. The Danish Air Quality Monitoring Programme - Annual Summary for 2016. 2017.

[33] Heimonen I, Hemmilä K. Integration of Windows and Ventilation by

Smart Supply Air Windows. In: Glass Processing Days 2003: Conference Proceedings & Powerpoint Presentations. 2003. p. 287–90.

[34] McEvoy ME, Southall RG, Baker PH. Test cell evaluation of supply air windows to characterise their optimum performance and its verification by the use of modelling techniques. Energy Build. 2003 Nov;35[10]:1009–20.

[35] Tommerup H. Energibesparelse for ”Ventilationsvinduet”. 2005.

[36] Carlos JS, Corvacho H, Silva PD, Castro-Gomes JP. Real climate experimental study of two double window systems with preheating of ventilation air. Energy Build. Elsevier B.V.; 2010;42[6]:928–34.

[37] Appelfeld D, Svendsen S. Experimental analysis of energy performance of a ventilated window for heat recovery under controlled conditions. Energy Build. Elsevier B.V.; 2011 Nov;43[11]:3200–7.

[38] Heiselberg PK, Larsen OK, Liu M, Zhang C, Johra H, Herold L, et al. ClimaWin - Technical Summary Report. 2013.

[39] Laustsen JB, Johnston CJ, Raffnsøe LM. ProVent; Projekteringsviden om ventilationsvinduer. Allerød, Denmark; 2014.

[40] Raffnsøe LM. Thermal Performance of Air Flow Windows. The Technical University of Denmark; 2007.

[41] Ismail KAR, Henríquez JR. Two-dimensional model for the double glass naturally ventilated window. Int J Heat Mass Transf. 2005 Jan;48[3–4]:461–75.

[42] Ismail KAR, Henríquez JR. Simplified model for a ventilated glass window under forced air flow conditions. Appl Therm Eng. 2006 Feb;26[2–3]:295–302.

[43] Carlos JS, Corvacho H, Silva PD, Castro-Gomes JP. Modelling and simulation of a ventilated double window. Appl Therm Eng. Elsevier Ltd; 2011;31[1]:93–102.

[44] Bhamjee M, Nurick A, Madyira DM. An experimentally validated mathematical and CFD model of a supply air window: Forced and natural flow. Energy Build. Elsevier B.V.; 2013 Feb;57:289–301.

[45] Gloriant F, Tittelein P, Joulin A, Lassue S. Modeling a triple-glazed supply-air window. Build Environ. 2015;84:1–9.

[46] ASHRAE Terminology [Internet]. [cited 2018 Jul 16]. Available from:

https://xp20.ashrae.org/terminology/

[47] Statistics Denmark - Building stock [Internet]. [cited 2018 Jun 22]. Available from: https://www.dst.dk/en/Statistik/emner/erhvervslivets-sektorer/byggeri-og-anlaeg/bygningsbestanden

[48] Cao G, Awbi H, Yao R, Fan Y, Sirén K, Kosonen R, et al. A review of the performance of different ventilation and airflow distribution systems in buildings. Build Environ. 2014 Mar;73:171–86.

[49] Chung I-P, Dunn-Rankin D. Using numerical simulation to predict ventilation efficiency in a model room. Energy Build. 1998 Aug;28[1]:43–50.

[50] Chung K-C, Hsu S-P. Effect of ventilation pattern on room air and contaminant distribution. Build Environ. 2001 Nov;36[9]:989–98.

[51] Koufi L, Younsi Z, Cherif Y, Naji H, El Ganaoui M. A numerical study of indoor air quality in a ventilated room using different strategies of ventilation. Mech Ind. 2017;

[52] Bekö G, Clausen G, Weschler CJ. Is the use of particle air filtration justified? Costs and benefits of filtration with regard to health effects, building cleaning and occupant productivity. Build Environ. 2008;43[10]:1647–57.

[53] Aldred JR, Darling E, Morrison G, Siegel J, Corsi R. Benefit-Cost Analysis of Commercially Available Activated Carbon Filters for Indoor Ozone Removal in Single-Family Homes. Indoor Air. 2015;26:501–12.

[54] Jones P. The Rationale for Mechanical Ventilation [Editorial]. Indoor Built Environ. 2000 Mar 27;9[2]:63–4.

[55] Hanssen SO, Berner M. Indoor Environment in Smart Energy-Efficient Buildings A State-of-the-Art Report. Trondheim, Norway; 2002.

[56] Mathisen HM, Stang J, Novakovic V. Heating, Ventilation and Air Conditioning in Smart Energy-Efficient Buildings A State-of-the-Art. Trondheim, Norway; 2002.

[57] Mardiana-Idayu A, Riffat SB. Review on heat recovery technologies for building applications. Renew Sustain Energy Rev. Elsevier Ltd; 2012 Feb;16[2]:1241–55.

[58] Genvex - Manufacturer of ventilation units [Internet]. [cited 2018 Jul 13]. Available from: http://genvex.dk/

[59] Nilan - Manufacturer of ventilation units [Internet]. [cited 2018 Jul 13]. Available from: http://www.nilan.dk/

[60] InVentilate - Manufacturer of ventilation units [Internet]. [cited 2018 Jul 13]. Available from: https://www.inventilate.dk/

[61] Kamendere E, Zogla G, Kamenders A, Ikaunieks J, Rochas C. Analysis of Mechanical Ventilation System with Heat Recovery in Renovated Apartment Buildings. Energy Procedia. Elsevier B.V.; 2015 Jun;72:27–33.

[62] Roulet CA, Heidt FD, Foradini F, Pibiri MC. Real heat recovery with air handling units. Energy Build. 2001;33[5]:495–502.

[63] Choi Y, Song D, Seo D, Kim J. Analysis of the variable heat exchange efficiency of heat recovery ventilators and the associated heating energy demand. Energy Build. Elsevier B.V.; 2018 Aug;172:152–8.

[64] Mata É, Sasic Kalagasidis A, Johnsson F. Energy usage and technical potential for energy saving measures in the Swedish residential building stock. Energy Policy. 2013 Apr;55:404–14.

[65] Dodoo A, Gustavsson L, Sathre R. Primary energy implications of ventilation heat recovery in residential buildings. Energy Build. Elsevier B.V.; 2011 Jul;43[7]:1566–72.

[66] Tommerup H, Svendsen S. Energy savings in Danish residential building stock. Energy Build. 2006 Jun;38[6]:618–26.

[67] Dimitroulopoulou C. Ventilation in European dwellings: A review. Build Environ. 2012 Jan;47[1]:109–25.

[68] Stymne H, Axel Boman C, Kronvall J. Measuring ventilation rates in the Swedish housing stock. Build Environ. 1994;29[3]:373–9.

[69] Bekö G, Gustavsen S, Frederiksen M, Bergsøe NC, Kolarik B, Gunnarsen L, et al. Diurnal and seasonal variation in air exchange rates and interzonal airflows measured by active and passive tracer gas in homes. Build Environ. 2016;104:178–87.

[70] Bruce N, Adair-Rohani H, Puzzolo E, Dora C. WHO Guidelines for indoor air quality - Household fuel combustion. 2014.

[71] WHO. WHO Air quality guidelines for particulate matter, ozone, nitrogen dioxide and sulfur dioxide - Global update 2005 - Summary of risk assessment. 2005.

[72] EN 15251:2007 - Indoor environmental input parameters for design and assessment of energy per formance of buildings addressing indoor air quality, thermal environment, lighting and acoustics. 1st ed. Technical Committee CEN/TC 156 "Ventilation for buildings", BSI; 2007. 54 p.

[73] DS 474:1993 Code for indoor thermal climate. 1st ed. Denmark; p. 34.

[74] DS/CEN/CR 1752:2001 Ventilation for buildings - Design criteria for the indoor environment. 1st ed. Denmark; p. 147.

[75] Brandt E, Bunch-Nielsen T, Christensen G, Gudum C, Hansen MH, Møller EB. SBi-anvisning 224 - Fugt i bygninger. 2nd ed. Hørsholm, Denmark; 2013. 259 p.

[76] Rammer Nielsen T, Drivsholm C. Energy efficient demand controlled ventilation in single family houses. Energy Build. 2010;42[11]:1995–8.

[77] Merzkirch A, Maas S, Scholzen F, Waldmann D. A semi-centralized, valveless and demand controlled ventilation system in comparison to other concepts in field tests. Build Environ. Elsevier Ltd; 2015;93:21–6.

[78] Laverge J, Van Den Bossche N, Heijmans N, Janssens A. Energy saving potential and repercussions on indoor air quality of demand controlled residential ventilation strategies. Build Environ. Elsevier Ltd; 2011 Jul;46[7]:1497–503.

[79] Mysen M, Berntsen S, Nafstad P, Schild PG. Occupancy density and benefits of demand-controlled ventilation in Norwegian primary schools. Energy Build. 2005;37[12]:1234–40.

[80] Pavlovas V. Demand controlled ventilation: A case study for existing Swedish multifamily buildings. Energy Build. 2004;36:1029–34.

[81] Fisk WJ, De Almeida AT. Sensor-based demand-controlled ventilation: A review. Vol. 29, Energy and Buildings. 1998. p. 35–45.

[82] Guyot G, Sherman MH, Walker IS. Smart ventilation energy and indoor air quality performance in residential buildings: A review. Energy Build. 2018;165:416–30.

[83] Mortensen DK, Walker IS, Sherman MH. Optimization of occupancy based demand controlled ventilation in residences. Int J Vent. 2011;10[1]:49–60.

[84] Nabinger S, Persily AK. Impacts of airtightening retrofits on ventilation rates and energy consumption in a manufactured home. Energy Build. Elsevier B.V.; 2011;43[11]:3059–67.

[85] Bergsøe NC. Tæthed i eksisterende bygninger - Analyse af målte værdier. 2015.

[86] Bjørneboe MG, Svendsen S, Heller A. Evaluation of the renovation of a Danish single-family house based on measurements. Energy Build. 2017;1–24.

[87] Johansson D, Bagge H, Lindstrii L. Measurements of occupancy levels in multi-family dwellings - Application to demand controlled ventilation. Energy Build. Elsevier B.V.; 2011;43[9]:2449–55.

[88] Elshorbany Y, Barnes I, Becker KH, Kleffmann J, Wiesen P. Sources and Cycling of Tropospheric Hydroxyl Radicals – An Overview. Zeitschrift für Phys Chemie. 2010 Aug;224[7–8]:967–87.

[89] Anglada JM, Martins-Costa M, Ruiz-Lopez MF, Francisco JS. Spectroscopic signatures of ozone at the air-water interface and photochemistry implications. Proc Natl Acad Sci. 2014 Aug 12;111[32]:11618–23.

[90] Hopke PK. Air Pollution and Health Effects. Nadadur SS, Hollingsworth JW, editors. London: Springer London; 2015. 355-380 p. [Molecular and Integrative Toxicology].

[91] Fenske JD, Paulson SE. Human Breath Emissions of VOCs. J Air Waste Manage Assoc. 1999 May 27;49[5]:594–8.

[92] Wisthaler A, Weschler CJ. Reactions of ozone with human skin lipids: Sources of carbonyls, dicarbonyls, and hydroxycarbonyls in indoor air. Proc Natl Acad Sci. 2010 Apr 13;107[15]:6568–75.

[93] Tenwolde A, Pilon CL. The Effect of Indoor Humidity on Water Vapor Release in Homes. Therm Perform Exter Envel Whole Build X Int Conf. 2007;1–9.

[94] Straube JF. Moisture in buildings. ASHRAE J. 2002;44[1]:15–9.

[95] Christian JE. Moisture Sources. In: Moisture Control in Buildings: The Key Factor in Mold Prevention—2nd Edition. 100 Barr Harbor Drive, PO Box C700, West Conshohocken, PA 19428-2959: ASTM International; 1994. p. 103-103–7.

[96] Weschler CJ. Changes in indoor pollutants since the 1950s. Atmos Environ. Elsevier Ltd; 2009;43[1]:153–69.

[97] Zhang Y, Xiong J, Mo J, Gong M, Cao J. Understanding and controlling airborne organic compounds in the indoor environment: Mass transfer

analysis and applications. Indoor Air. 2016;26[1]:39–60.

[98] Weschler CJ. Chemistry in indoor environments: 20 years of research. Indoor Air. 2011 Jun;21[3]:205–18.

[99] Rim D, Gall ET, Maddalena RL, Nazaroff WW. Ozone reaction with interior building materials: Influence of diurnal ozone variation, temperature and humidity. Atmos Environ. Elsevier Ltd; 2016 Jan;125:15–23.

[100] Waring MS. Secondary organic aerosol in residences: predicting its fraction of fine particle mass and determinants of formation strength. Indoor Air. 2014 Aug;24[4]:376–89.

[101] Morrison G. Recent Advances in Indoor Chemistry. Curr Sustain Energy Reports. 2015 Jun 7;2[2]:33–40.

[102] Xu Y, Zhang J (Jensen). Understanding SVOCs. ASHRAE J. 2011;53[12]:121–5.

[103] Ye W, Won D, Zhang X. A Simple VOC Prioritization Method to Determine Ventilation Rate for Indoor Environment Based on Building Material Emissions. Procedia Eng. Elsevier B.V.; 2015;121:1697–704.

[104] Salthammer T, Mentese S, Marutsky R. Formaldehyde in the Indoor Environment, Chem. Rev. 110, 2536–2572. Chem Rev. 2010;110[4]:2536–72.

[105] Salthammer T. The formaldehyde dilemma. Int J Hyg Environ Health. Elsevier GmbH.; 2015;218[4]:433–6.

[106] Nielsen GD, Wolkoff P. Cancer effects of formaldehyde: a proposal for an indoor air guideline value. Arch Toxicol. 2010 Jun;84[6]:423–46.

[107] Andersen I, Lundqvist GR, Mølhave L. Indoor air pollution due to chipboard used as a construction material. Atmos Environ. 1975 Jan;9[12]:1121–7.

[108] Hoetjer JJ, Koerts F. A Model for Formaldehyde Release from Particleboard. In: ACS symposium series. 1986. p. 125–44.

[109] Huang S, Xiong J, Zhang Y. Impact of temperature on the ratio of initial emittable concentration to total concentration for formaldehyde in building materials: Theoretical correlation and validation. Environ Sci Technol. 2015;49[3]:1537–44.

[110] Liang W, Yang S, Yang X. Long-Term Formaldehyde Emissions from

Medium-Density Fiberboard in a Full-Scale Experimental Room: Emission Characteristics and the Effects of Temperature and Humidity. Environ Sci Technol. 2015;49[17]:10349–56.

[111] Liang W, Lv M, Yang X. The combined effects of temperature and humidity on initial emittable formaldehyde concentration of a medium-density fiberboard. Build Environ. Elsevier Ltd; 2016;98:80–8.

[112] Xiong J, Wei W, Huang S, Zhang Y. Association between the emission rate and temperature for chemical pollutants in building materials: General correlation and understanding. Environ Sci Technol. 2013;47[15]:8540–7.

[113] Huang S, Xiong J, Cai C, Xu W, Zhang Y. Influence of humidity on the initial emittable concentration of formaldehyde and hexaldehyde in building materials: experimental observation and correlation. Sci Rep. 2016;6[April]:23388.

[114] Xu J, Zhang J (Jensen), Liu X, Gao Z. Determination of partition and diffusion coefficients of formaldehyde in selected building materials and impact of relative humidity. J Air Waste Manag Assoc. 2012;62[6]:671–9.

[115] Myers GE, Nagaoka M. Emission of formaldehyde by particleboard: effect of ventilation rate and loading on air-contamination levels. For Prod J. 1981;31[7]:39–44.

[116] Lehmann WF. Effect of ventilation and loading rates in large chamber testing of formaldehyde emissions from composite panels. For Prod J. 1987;37[4]:31–7.

[117] Hult EL, Willem H, Price PN, Hotchi T, Russell ML, Singer BC. Formaldehyde and acetaldehyde exposure mitigation in US residences: In-home measurements of ventilation control and source control. Indoor Air. 2015;25[5]:523–35.

[118] Rackes A, Waring MS. Do time-averaged, whole-building, effective volatile organic compound (VOC) emissions depend on the air exchange rate? A statistical analysis of trends for 46 VOCs in U.S. offices. Indoor Air. 2016 Aug;26[4]:642–59.

[119] Logadóttir A, Gunnarsen L. Formaldehydkoncentrationen i nybyggede huse i Danmark. Statens Byggeforskningsinstitut. 2008.

[120] Little JC, Hodgson AT, Gadgil AJ. Modeling emissions of volatile organic compounds from new carpets. Atmos Environ. 1994;28[2]:227–

34.

[121] Xiong J, Yao Y, Zhang Y. C-history method: Rapid measurement of the initial emittable concentration, diffusion and partition coefficients for formaldehyde and VOCs in building materials. Environ Sci Technol. 2011;45[8]:3584–90.

[122] Huang S, Xiong J, Zhang Y. A rapid and accurate method, ventilated chamber C-history method, of measuring the emission characteristic parameters of formaldehyde/VOCs in building materials. J Hazard Mater. Elsevier B.V.; 2013;261:542–9.

[123] Zhang X, Cao J, Wei J, Zhang Y. Improved C-history method for rapidly and accurately measuring the characteristic parameters of formaldehyde / VOCs emitted from building materials. Build Environ. Elsevier; 2018;143[May]:570–8.

[124] Guo Z. Review of indoor emission source models—part 1. Overview. Environ Pollut. 2002;120:533–49.

[125] Qian K, Zhang Y, Little JC, Wang X. Dimensionless correlations to predict VOC emissions from dry building materials. Atmos Environ. 2007;41[2]:352–9.

[126] ASHRAE. ASHRAE Standard 90.1-2016 (SI) -- Energy Standard for Buildings Except Low-Rise Residential Buildings. Atlanta, Georgia, USA;

[127] Harish VSKV, Kumar A. A review on modeling and simulation of building energy systems. Renew Sustain Energy Rev. Elsevier Ltd; 2016;56:1272–92.

[128] Østergård T, Jensen RL, Maagaard SE. Building simulations supporting decision making in early design - A review. Renew Sustain Energy Rev. Elsevier; 2016;61:187–201.

[129] Coakley D, Raftery P, Keane M. A review of methods to match building energy simulation models to measured data. Renew Sustain Energy Rev. Elsevier; 2014;37:123–41.

[130] Karlsson F, Rohdin P, Persson M-L. Measured and predicted energy demand of a low energy building: important aspects when using Building Energy Simulation. Build Serv Eng Res Technol. 2007;28[3]:223–35.

[131] Turner C, Frankel M. Energy Performance of LEED ® for New Construction Buildings. New Build Inst. 2008;1–46.

[132] Li N, Yang Z, Becerik-Gerber B, Tang C, Chen N. Why is the reliability of building simulation limited as a tool for evaluating energy conservation measures? Appl Energy. Elsevier Ltd; 2015 Dec;159:196–205.

[133] de Wilde P. The gap between predicted and measured energy performance of buildings: A framework for investigation. Autom Constr. Elsevier B.V.; 2014 May;41:40–9.

[134] Imam S, Coley DA, Walker I. The building performance gap: Are modellers literate? Build Serv Eng Res Technol. 2017 May 18;38[3]:351–75.

[135] Dodoo A, Tettey UYA, Gustavsson L. Influence of simulation assumptions and input parameters on energy balance calculations of residential buildings. Energy. Elsevier Ltd; 2017 Feb;120:718–30.

[136] Attia S, De Herde A, Gratia E, Hensen JLM. Achieving informed decision-making for net zero energy buildings design using building performance simulation tools. Build Simul. 2013 Mar 8;6[1]:3–21.

[137] Attia S. Optimisation for zero energy building design: interviews with twenty eight international experts, international energy agency (IEA) task 40: towards net zero energy buildings subtask B. Louvain-la-Neuve, Belgium; 2012.

[138] IDA Indoor Climate and Energy (IDA ICE) [Internet]. [cited 2018 May 13]. Available from: https://www.equa.se/en/ida-ice

[139] Walker CE, Glicksman LR, Norford LK. Tale of two low-energy designs: Comparison of mechanically and naturally ventilated office buildings in temperate climates. In: ASHRAE Transactions. 2007. p. 36–50.

[140] McGill G, Oyedele LO, McAllister K. Case study investigation of indoor air quality in mechanically ventilated and naturally ventilated UK social housing. Int J Sustain Built Environ. 2015;4[1]:58–77.

[141] Ben-David T, Waring MS. Impact of natural versus mechanical ventilation on simulated indoor air quality and energy consumption in offices in fourteen U.S. cities. Build Environ. 2016;104:320–36.

[142] Swing Gustafsson M, Gustafsson M, Myhren JA, Dotzauer E. Primary energy use in buildings in a Swedish perspective. Energy Build. Elsevier B.V.; 2016 Oct;130:202–9.

[143] Wilby MR, Rodríguez González AB, Vinagre Díaz JJ. Empirical and

dynamic primary energy factors. Energy. 2014 Aug;73:771–9.

[144] Hitchin R, Thomsen KE, Wittchen KB. Primary Energy Factors and Members States Energy Regulations - Primary factors and the EPBD. Concerted Action EPBD; 2018. p. 4.

[145] Window Information System (WIS) [Internet]. [cited 2019 Jan 5]. Available from: http://www.windat.org/wis/html/index.html

[146] ISO 15099:2003 - Thermal performance of windows, doors and shading devices -- Detailed calculations. 1st ed. 2003. p. 71.

[147] Integrated Environmental Solutions Ltd - Virtual Environment (IESVE) [Internet]. [cited 2019 Jan 6]. Available from: https://www.iesve.com/

[148] Merzkirch A, Maas S, Scholzen F, Waldmann D. Primary energy used in centralised and decentralised ventilation systems measured in field tests in residential buildings. Int J Vent. Taylor & Francis; 2017 Mar 17;0[0]:1–9.

[149] Rasmussen B. Experiences with sound insulating open windows in traffic noise exposed housing. In: Inter-Noise 2015. 2015. p. 8.

[150] Søndergaard LS, Egedal R. Open windows with better sound insulation. In: Inter-Noise 2016. 2016. p. 1173–84.

[151] Haghighat F, Huang H, Lee C-S. Modeling approaches for indoor air VOC emissions from dry building materials - A review. ASHRAE Trans. 2005;111[Pt. 1]:635–45.

[152] Kleiber M, Joh R, Span R. D3 Properties of Pure Fluid Substances. In: VDI Heat Atlas. Berlin, Heidelberg: Springer Berlin Heidelberg; 2010. p. 301–418.

[153] Weschler CJ, Nazaroff WW. Semivolatile organic compounds in indoor environments. Atmos Environ. Elsevier Ltd; 2008;42[40]:9018–40.

[154] Huang H, Haghighat F. Modelling of volatile organic compounds emission from dry building materials. Build Environ. 2002;37[12]:1349–60.

[155] Xu Y, Zhang Y. An improved mass transfer based model for analyzing VOC emissions from building materials. Atmos Environ. 2003;37[18]:2497–505.

[156] Deng B, Kim CN. An analytical model for VOCs emission from dry building materials. Atmos Environ. 2004;38[8]:1173–80.

[157] Yang X, Chen Q, Zhang JS, Magee R, Zeng J, Shaw CY. Numerical simulation of VOC emissions from dry materials. Build Environ. 2001;36[10]:1099–107.

[158] Xiong J, Yang T, Tan J, Li L, Ge Y. Characterization of VOC emission from materials in vehicular environment at varied temperatures: Correlation development and validation. PLoS One. 2015;10[10]:1–21.

[159] Zinn TW, Cline D, Lehmann WF. Long-Term Study of Formaldehyde Emission Decay from Particleboard. Maloney, Thomas M.; Maloney TM, editor. Proceedings of the Washington State University International Particleboard/composite Materials Series Symposium. Washington State University; 1990. p. 95–103.

[160] Lee CS, Haghighat F, Ghaly WS. A study on VOC source and sink behavior in porous building materials - Analytical model development and assessment. Indoor Air. 2005;15[3]:183–96.

[161] Wang X, Zhang Y. General analytical mass transfer model for VOC emissions from multi-layer dry building materials with internal chemical reactions. Chinese Sci Bull. 2011;56[2]:222–8.

[162] Liu Z, Ye W, Little JC. Predicting emissions of volatile and semivolatile organic compounds from building materials: A review. Build Environ. Elsevier Ltd; 2013;64:7–25.

[163] Mao YF, Li Z, Zhang Y, He YL, Tao WQ. A review of mass-transfer models and mechanistic studies of semi-volatile organic compounds in indoor environments. Indoor Built Environ. 2017;0[28]:1–15.

[164] Kolarik B, Gunnarsen L, Funch LW. Afgivelse af formaldehyd fra byggevarer og forbrugerprodukter. Statens Byggeforskningsinstitut. 2010.

[165] Offermann FJ, Maddalena R, Offermann JC, Singer BC, Wilhelm H. The impact of ventilation on the emission rates of volatile organic compounds in residences. 10th Int Conf Heal Build 2012. 2012;1:2–7.

[166] Goel S, Rosenberg MI, Eley C. ANSI/ASHRAE/IES Standard 90.1-2016 Performance Rating Method Reference Manual. Richland, WA (United States); 2017 Sep.

[167] Danish Working Environment Authority - Indoor climate guideline [Internet]. [cited 2018 May 10]. Available from: https://arbejdstilsynet.dk/da/regler/at-vejledninger/i/a-1-2-indeklima

[168] Chung P-R, Tzeng C-T, Ke M-T, Lee C-Y. Formaldehyde Gas Sensors: A Review. Sensors. 2013 Apr 2;13[4]:4468–84.

[169] Kumar P, Skouloudis AN, Bell M, Viana M, Carotta MC, Biskos G, et al. Real-time sensors for indoor air monitoring and challenges ahead in deploying them to urban buildings. Sci Total Environ. Elsevier B.V.; 2016 Aug;560–561[April]:150–9.

[170] Schieweck A, Uhde E, Salthammer T, Salthammer LC, Morawska L, Mazaheri M, et al. Smart homes and the control of indoor air quality. Renew Sustain Energy Rev. Elsevier Ltd; 2018 Oct;94[July]:705–18.

[171] Wargocki P, Bischof W, Carrer P, Asimakopoulou M-N, Fernandes E de O, Hänninen O, et al. HealthVent - Final report - Health-based Ventilation Guidelines for Europe. Kgs. Lyngby, Denmark; 2013.

[172] Nazaroff WW. Exploring the consequences of climate change for indoor air quality. Environ Res Lett. 2013 Mar 1;8[1]:015022.

[173] Fisk WJ. Review of some effects of climate change on indoor environmental quality and health and associated no-regrets mitigation measures. Build Environ. Elsevier Ltd; 2015 Apr;86:70–80.

[174] Kohlhepp P, Harb H, Wolisz H, Waczowicz S, Müller D, Hagenmeyer V. Large-scale grid integration of residential thermal energy storages as demand-side flexibility resource: A review of international field studies. Renew Sustain Energy Rev. Elsevier Ltd; 2019 Mar;101[September 2018]:527–47.

List of figures

List of tables

Appendix

Table of results from parameter variation in IDA ICE

Appendix entry related to results given in Chapter 5. This table is an extension of results presented in Table 5.6 – Selected results from simulations showing scores and relative energy demands and Table 5.7 – Selected results from simulations showing ACHs. Table 5.6 and Table 5.7 can be found on pages 80 and 81 respectively.

Scenario	Control parameter				Exhaust	Base 03	@Occu	Succes criteria met - Total time				Succes criteria met - @Occu			
	T	CO_2	RH	HCHO				T	CO_2	RH	HCHO	T	CO_2	RH	HCHO
CAV, Deg-C								C	C	C	-	B	C	C	-
T-Always-03-ExN-EmisN, Deg-C	X					X		A	C	C	A	A	C	C	A
T-Always-03-ExN-EmisH, Deg-C	X					X		A	C	C	A	A	C	C	A
T-Always-03-ExY-EmisN, Deg-C	X				X	X		A	C	C	A	A	C	C	A
T-Always-03-ExY-EmisH, Deg-C	X				X	X		A	C	C	A	A	C	C	A
T-Occu-03-ExN-EmisN, Deg-C	X					X	X	A	C	C	A	A	C	C	A
T-Occu-03-ExN-EmisH, Deg-C	X					X	X	A	C	C	A	A	C	C	A
T-Occu-03-ExY-EmisN, Deg-C	X				X	X	X	A	C	C	A	A	C	C	A
T-Occu-03-ExY-EmisH, Deg-C	X				X	X	X	A	C	C	A	A	C	C	A
T-Always-00-ExN-EmisN, Deg-C	X							B	C	C	C	B	C	C	C
T-Always-00-ExN-EmisH, Deg-C	X							B	C	C	C	B	C	C	C
T-Always-00-ExY-EmisN, Deg-C	X				X			B	C	C	C	B	C	C	C
T-Always-00-ExY-EmisH, Deg-C	X				X			B	C	C	C	B	C	C	C
T-Occu-00-ExN-EmisN, Deg-C	X						X	B	C	C	C	B	C	C	C
T-Occu-00-ExN-EmisH, Deg-C	X						X	B	C	C	C	B	C	C	C
T-Occu-00-ExY-EmisN, Deg-C	X				X		X	B	C	C	C	B	C	C	C
T-Occu-00-ExY-EmisH, Deg-C	X				X		X	B	C	C	C	B	C	C	C
RH-Always-03-ExN-EmisN, Deg-C			X			X		C	C	A	A	B	C	A	A
RH-Always-03-ExN-EmisH, Deg-C			X			X		C	C	A	A	B	C	A	A
RH-Always-03-ExY-EmisN, Deg-C			X		X	X		C	C	A	A	B	C	A	A
RH-Always-03-ExY-EmisH, Deg-C			X		X	X		C	C	A	A	B	C	A	A
RH-Occu-03-ExN-EmisN, Deg-C			X			X	X	C	C	A	A	B	C	A	A
RH-Occu-03-ExN-EmisH, Deg-C			X			X	X	C	C	A	A	B	C	A	A
RH-Occu-03-ExY-EmisN, Deg-C			X		X	X	X	C	C	A	A	B	C	A	A
RH-Occu-03-ExY-EmisH, Deg-C			X		X	X	X	C	C	A	A	B	C	A	A
RH-Always-00-ExN-EmisN, Deg-C			X					C	C	A	C	C	C	A	C
RH-Always-00-ExN-EmisH, Deg-C			X					C	C	A	C	C	C	A	C
RH-Always-00-ExY-EmisN, Deg-C			X		X			C	C	A	C	C	C	A	C
RH-Always-00-ExY-EmisH, Deg-C			X		X			C	C	A	C	C	C	A	C
RH-Occu-00-ExN-EmisN, Deg-C			X				X	C	C	C	C	C	C	A	C
RH-Occu-00-ExN-EmisH, Deg-C			X				X	C	C	C	C	C	C	A	C
RH-Occu-00-ExY-EmisN, Deg-C			X		X		X	C	C	C	C	C	C	A	C
RH-Occu-00-ExY-EmisH, Deg-C			X		X		X	C	C	C	C	C	C	A	C
CO2-Always-03-ExN-EmisN, Deg-C		X				X		C	A	C	A	B	A	C	A
CO2-Always-03-ExN-EmisH, Deg-C		X				X		C	A	C	A	B	A	C	A
CO2-Always-03-ExY-EmisN, Deg-C		X			X	X		C	A	C	A	B	A	C	A
CO2-Always-03-ExY-EmisH, Deg-C		X			X	X		C	A	C	A	B	A	C	A
CO2-Occu-03-ExN-EmisN, Deg-C		X				X	X	C	A	C	A	B	A	C	A
CO2-Occu-03-ExN-EmisH, Deg-C		X				X	X	C	A	C	A	B	A	C	A
CO2-Occu-03-ExY-EmisN, Deg-C		X			X	X	X	C	A	C	A	B	A	C	A
CO2-Occu-03-ExY-EmisH, Deg-C		X			X	X	X	C	A	C	A	B	A	C	A
CO2-Always-00-ExN-EmisN, Deg-C		X						C	A	C	B	B	A	C	A
CO2-Always-00-ExN-EmisH, Deg-C		X						C	A	C	C	B	A	C	C
CO2-Always-00-ExY-EmisN, Deg-C		X			X			C	A	C	B	C	A	C	A
CO2-Always-00-ExY-EmisH, Deg-C		X			X			C	A	C	C	C	A	C	C
CO2-Occu-00-ExN-EmisN, Deg-C		X					X	C	C	C	B	B	A	C	A
CO2-Occu-00-ExN-EmisH, Deg-C		X					X	C	C	C	C	B	A	C	C
CO2-Occu-00-ExY-EmisN, Deg-C		X			X		X	C	C	C	B	C	A	C	A
CO2-Occu-00-ExY-EmisH, Deg-C		X			X		X	C	C	C	C	C	A	C	C

Scenario	Control parameter				Exhaust	Base 03	@Occu	Succes criteria met - Total time				Succes criteria met - @Occu			
	T	CO_2	RH	HCHO				T	CO_2	RH	HCHO	T	CO_2	RH	HCHO
CAV, Deg-C								C	C	C	-	B	C	C	-
HCHO-Always-03-ExN-EmisN, Deg-C				X		X		C	C	C	A	B	C	C	A
HCHO-Always-03-ExN-EmisH, Deg-C				X		X		C	C	C	A	C	C	C	A
HCHO-Always-03-ExY-EmisN, Deg-C				X	X	X		C	C	C	A	B	C	C	A
HCHO-Always-03-ExY-EmisH, Deg-C				X	X	X		C	C	C	A	B	C	C	A
HCHO-Occu-03-ExN-EmisN, Deg-C				X		X	X	C	C	C	A	B	C	C	A
HCHO-Occu-03-ExN-EmisH, Deg-C				X		X	X	C	C	C	A	C	C	C	A
HCHO-Occu-03-ExY-EmisN, Deg-C				X	X	X	X	C	C	C	A	B	C	C	A
HCHO-Occu-03-ExY-EmisH, Deg-C				X	X	X	X	C	C	C	A	B	C	C	A
HCHO-Always-00-ExN-EmisN, Deg-C				X				C	C	C	A	C	C	C	A
HCHO-Always-00-ExN-EmisH, Deg-C				X				C	C	C	A	C	C	C	A
HCHO-Always-00-ExY-EmisN, Deg-C				X	X			C	C	C	A	C	C	C	A
HCHO-Always-00-ExY-EmisH, Deg-C				X	X			C	C	C	A	C	C	C	A
HCHO-Occu-00-ExN-EmisN, Deg-C				X			X	C	C	C	C	C	C	C	A
HCHO-Occu-00-ExN-EmisH, Deg-C				X			X	C	C	C	C	C	C	C	A
HCHO-Occu-00-ExY-EmisN, Deg-C				X	X		X	C	C	C	C	C	C	C	A
HCHO-Occu-00-ExY-EmisH, Deg-C				X	X		X	C	C	C	C	C	C	C	A
T-CO2-Always-03-ExN-EmisN, Deg-C	X	X				X		A	A	C	A	A	A	C	A
T-CO2-Always-03-ExN-EmisH, Deg-C	X	X				X		A	A	C	A	A	A	C	A
T-CO2-Always-03-ExY-EmisN, Deg-C	X	X			X	X		A	A	C	A	A	A	C	A
T-CO2-Always-03-ExY-EmisH, Deg-C	X	X			X	X		A	A	C	A	A	A	C	A
T-CO2-Occu-03-ExN-EmisN, Deg-C	X	X				X	X	A	A	C	A	A	A	C	A
T-CO2-Occu-03-ExN-EmisH, Deg-C	X	X				X	X	A	A	C	A	A	A	C	A
T-CO2-Occu-03-ExY-EmisN, Deg-C	X	X			X	X	X	A	A	C	A	A	A	C	A
T-CO2-Occu-03-ExY-EmisH, Deg-C	X	X			X	X	X	A	A	C	A	A	A	C	A
T-CO2-Always-00-ExN-EmisN, Deg-C	X	X						A	A	C	B	A	A	C	A
T-CO2-Always-00-ExN-EmisH, Deg-C	X	X						A	A	C	C	A	A	C	C
T-CO2-Always-00-ExY-EmisN, Deg-C	X	X			X			A	A	C	B	A	A	C	A
T-CO2-Always-00-ExY-EmisH, Deg-C	X	X			X			A	A	C	C	A	A	C	C
T-CO2-Occu-00-ExN-EmisN, Deg-C	X	X					X	A	C	C	B	A	A	C	A
T-CO2-Occu-00-ExN-EmisH, Deg-C	X	X					X	A	C	C	C	A	A	C	C
T-CO2-Occu-00-ExY-EmisN, Deg-C	X	X			X		X	B	C	C	B	A	A	C	A
T-CO2-Occu-00-ExY-EmisH, Deg-C	X	X			X		X	A	C	C	C	A	A	C	C
T-RH-Always-03-ExN-EmisN, Deg-C	X		X			X		A	C	A	A	A	C	A	A
T-RH-Always-03-ExN-EmisH, Deg-C	X		X			X		A	C	A	A	A	C	A	A
T-RH-Always-03-ExY-EmisN, Deg-C	X		X		X	X		A	C	A	A	A	C	A	A
T-RH-Always-03-ExY-EmisH, Deg-C	X		X		X	X		A	C	A	A	A	C	A	A
T-RH-Occu-03-ExN-EmisN, Deg-C	X		X			X	X	A	C	A	A	A	C	A	A
T-RH-Occu-03-ExN-EmisH, Deg-C	X		X			X	X	A	C	A	A	A	C	A	A
T-RH-Occu-03-ExY-EmisN, Deg-C	X		X		X	X	X	A	C	A	A	A	C	A	A
T-RH-Occu-03-ExY-EmisH, Deg-C	X		X		X	X	X	A	C	A	A	A	C	A	A
T-RH-Always-00-ExN-EmisN, Deg-C	X		X					B	C	A	C	A	C	A	C
T-RH-Always-00-ExN-EmisH, Deg-C	X		X					B	C	A	C	A	C	A	C
T-RH-Always-00-ExY-EmisN, Deg-C	X		X		X			B	C	A	C	A	C	A	C
T-RH-Always-00-ExY-EmisH, Deg-C	X		X		X			B	C	A	C	A	C	A	C
T-RH-Occu-00-ExN-EmisN, Deg-C	X		X				X	B	C	C	C	A	C	A	C
T-RH-Occu-00-ExN-EmisH, Deg-C	X		X				X	B	C	C	C	A	C	A	C
T-RH-Occu-00-ExY-EmisN, Deg-C	X		X		X		X	B	C	C	C	A	C	A	C
T-RH-Occu-00-ExY-EmisH, Deg-C	X		X		X		X	B	C	C	C	A	C	A	C

Scenario	Control parameter				Exhaust	Base 03	@Occu	Succes criteria met - Total time				Succes criteria met - @Occu			
	T	CO_2	RH	HCHO				T	CO_2	RH	HCHO	T	CO_2	RH	HCHO
CAV, Deg-C								C	C	C	-	B	C	C	-
CO2-RH-Always-03-ExN-EmisN, Deg-C		X	X			X		C	A	A	A	B	A	A	A
CO2-RH-Always-03-ExN-EmisH, Deg-C		X	X			X		C	A	A	A	B	A	A	A
CO2-RH-Always-03-ExY-EmisN, Deg-C		X	X		X	X		C	A	A	A	B	A	A	A
CO2-RH-Always-03-ExY-EmisH, Deg-C		X	X		X	X		C	A	A	A	B	A	A	A
CO2-RH-Occu-03-ExN-EmisN, Deg-C		X	X			X	X	C	A	A	A	B	A	A	A
CO2-RH-Occu-03-ExN-EmisH, Deg-C		X	X			X	X	C	A	A	A	B	A	A	A
CO2-RH-Occu-03-ExY-EmisN, Deg-C		X	X		X	X	X	C	A	A	A	B	A	A	A
CO2-RH-Occu-03-ExY-EmisH, Deg-C		X	X		X	X	X	C	A	A	A	B	A	A	A
CO2-RH-Always-00-ExN-EmisN, Deg-C		X	X					C	A	A	B	B	A	A	B
CO2-RH-Always-00-ExN-EmisH, Deg-C		X	X					C	A	A	C	B	A	A	C
CO2-RH-Always-00-ExY-EmisN, Deg-C		X	X		X			C	A	A	B	C	A	A	B
CO2-RH-Always-00-ExY-EmisH, Deg-C		X	X		X			C	A	A	C	C	A	A	C
CO2-RH-Occu-00-ExN-EmisN, Deg-C		X	X				X	C	C	C	B	B	A	A	B
CO2-RH-Occu-00-ExN-EmisH, Deg-C		X	X				X	C	C	C	C	B	A	A	C
CO2-RH-Occu-00-ExY-EmisN, Deg-C		X	X		X		X	C	C	C	B	C	A	A	B
CO2-RH-Occu-00-ExY-EmisH, Deg-C		X	X		X		X	C	C	C	C	C	A	A	C
TCO2RH-Always-03-ExN-EmisN, Deg-C	X	X	X			X		A	A	A	A	A	A	A	A
TCO2RH-Always-03-ExN-EmisH, Deg-C	X	X	X			X		A	A	A	A	A	A	A	A
TCO2RH-Always-03-ExY-EmisN, Deg-C	X	X	X		X	X		A	A	A	A	A	A	A	A
TCO2RH-Always-03-ExY-EmisH, Deg-C	X	X	X		X	X		A	A	A	A	A	A	A	A
TCO2RH-Occu-03-ExN-EmisN, Deg-C	X	X	X			X	X	A	A	A	A	A	A	A	A
TCO2RH-Occu-03-ExN-EmisH, Deg-C	X	X	X			X	X	A	A	A	A	A	A	A	A
TCO2RH-Occu-03-ExY-EmisN, Deg-C	X	X	X		X	X	X	A	A	A	A	A	A	A	A
TCO2RH-Occu-03-ExY-EmisH, Deg-C	X	X	X		X	X	X	A	A	A	A	A	A	A	A
TCO2RH-Always-00-ExN-EmisN, Deg-C	X	X	X					A	A	A	B	A	A	A	A
TCO2RH-Always-00-ExN-EmisH, Deg-C	X	X	X					A	A	A	C	A	A	A	C
TCO2RH-Always-00-ExY-EmisN, Deg-C	X	X	X		X			A	A	A	B	A	A	A	B
TCO2RH-Always-00-ExY-EmisH, Deg-C	X	X	X		X			A	A	A	C	A	A	A	C
TCO2RH-Occu-00-ExN-EmisN, Deg-C	X	X	X				X	A	C	C	B	A	A	A	B
TCO2RH-Occu-00-ExN-EmisH, Deg-C	X	X	X				X	A	C	C	C	A	A	A	C
TCO2RH-Occu-00-ExY-EmisN, Deg-C	X	X	X		X		X	A	C	C	B	A	A	A	B
TCO2RH-Occu-00-ExY-EmisH, Deg-C	X	X	X		X		X	A	C	C	C	A	A	A	C
All4-Always-03-ExN-EmisN, Deg-C	X	X	X	X		X		A	A	A	A	A	A	A	A
All4-Always-03-ExN-EmisH, Deg-C	X	X	X	X		X		A	A	A	A	A	A	A	A
All4-Always-03-ExY-EmisN, Deg-C	X	X	X	X	X	X		A	A	A	A	A	A	A	A
All4-Always-03-ExY-EmisH, Deg-C	X	X	X	X	X	X		A	A	A	A	A	A	A	A
All4-Occu-03-ExN-EmisN, Deg-C	X	X	X	X		X	X	A	A	A	A	A	A	A	A
All4-Occu-03-ExN-EmisH, Deg-C	X	X	X	X		X	X	A	A	A	A	A	A	A	A
All4-Occu-03-ExY-EmisN, Deg-C	X	X	X	X	X	X	X	A	A	A	A	A	A	A	A
All4-Occu-03-ExY-EmisH, Deg-C	X	X	X	X	X	X	X	A	A	A	A	A	A	A	A
All4-Always-00-ExN-EmisN, Deg-C	X	X	X	X				A	A	A	A	A	A	A	A
All4-Always-00-ExN-EmisH, Deg-C	X	X	X	X				A	A	A	A	A	A	A	A
All4-Always-00-ExY-EmisN, Deg-C	X	X	X	X	X			A	A	A	A	A	A	A	A
All4-Always-00-ExY-EmisH, Deg-C	X	X	X	X	X			A	A	A	A	A	A	A	A
All4-Occu-00-ExN-EmisN, Deg-C	X	X	X	X			X	A	C	C	A	A	A	A	A
All4-Occu-00-ExN-EmisH, Deg-C	X	X	X	X			X	A	C	C	C	A	A	A	A
All4-Occu-00-ExY-EmisN, Deg-C	X	X	X	X	X		X	A	C	C	A	A	A	A	A
All4-Occu-00-ExY-EmisH, Deg-C	X	X	X	X	X		X	A	C	C	C	A	A	A	A

Scenario	Control parameter				Exhaust	Base 03	@Occu	Succes criteria met - Total time				Succes criteria met - @Occu			
	T	CO_2	RH	HCHO				T	CO_2	RH	HCHO	T	CO_2	RH	HCHO
CAV, Deg-C								C	C	C	-	B	C	C	-
RH-HCHO-Always-03-ExN-EmisN, Deg-C			X	X		X		C	C	A	A	B	C	A	A
RH-HCHO-Always-03-ExN-EmisH, Deg-C			X	X		X		C	C	A	A	B	C	A	A
RH-HCHO-Always-03-ExY-EmisN, Deg-C			X	X	X	X		C	C	A	A	B	C	A	A
RH-HCHO-Always-03-ExY-EmisH, Deg-C			X	X	X	X		C	C	A	A	B	C	A	A
RH-HCHO-Occu-03-ExN-EmisN, Deg-C			X	X		X	X	C	C	A	A	B	C	A	A
RH-HCHO-Occu-03-ExN-EmisH, Deg-C			X	X		X	X	C	C	A	A	B	C	A	A
RH-HCHO-Occu-03-ExY-EmisN, Deg-C			X	X	X	X	X	C	C	A	A	B	C	A	A
RH-HCHO-Occu-03-ExY-EmisH, Deg-C			X	X	X	X	X	C	C	A	A	B	C	A	A
RH-HCHO-Always-00-ExN-EmisN, Deg-C			X	X				C	C	A	A	C	C	A	A
RH-HCHO-Always-00-ExN-EmisH, Deg-C			X	X				C	C	A	A	C	C	A	A
RH-HCHO-Always-00-ExY-EmisN, Deg-C			X	X	X			C	C	A	A	C	C	A	A
RH-HCHO-Always-00-ExY-EmisH, Deg-C			X	X	X			C	C	A	A	C	C	A	A
RH-HCHO-Occu-00-ExN-EmisN, Deg-C			X	X			X	C	C	C	B	C	C	A	A
RH-HCHO-Occu-00-ExN-EmisH, Deg-C			X	X			X	C	C	C	C	C	C	A	A
RH-HCHO-Occu-00-ExY-EmisN, Deg-C			X	X	X		X	C	C	C	B	C	C	A	A
RH-HCHO-Occu-00-ExY-EmisH, Deg-C			X	X	X		X	C	C	C	C	C	C	A	A

Scenario	Energy demand - Constant SFP				Energy demand - Variable SFP				Air change rates - Total time					Air change rates - @Occu				
	HVAC aux	Heat	Total	Change	HVAC aux	Heat	Total	Change	Min	Max	Mean	Median	StdDev	Min	Max	Mean	Median	StdDev
CAV, Deg-C	4.7	148.9	153.6	0	4.7	148.9	153.6	0	0.40	0.43	0.42	0.42	0.00	0.40	0.43	0.42	0.42	0.00
T-Always-03-ExN-EmisN, Deg-C	5.3	149.2	154.5	0.6	1.3	149.2	150.5	-2.0	0.40	9.50	0.46	0.42	0.47	0.40	9.50	0.47	0.42	0.53
T-Always-03-ExN-EmisH, Deg-C	5.3	149.2	154.5	0.6	1.3	149.2	150.5	-2.0	0.40	9.51	0.46	0.42	0.47	0.40	9.51	0.47	0.42	0.54
T-Always-03-ExY-EmisN, Deg-C	5.5	151.8	157.3	2.4	1.6	151.8	153.4	-0.1	0.40	9.87	0.49	0.43	0.48	0.40	9.87	0.50	0.43	0.54
T-Always-03-ExY-EmisH, Deg-C	5.5	151.8	157.3	2.4	1.6	151.8	153.4	-0.1	0.40	9.86	0.49	0.43	0.48	0.40	9.86	0.50	0.43	0.54
T-Occu-03-ExN-EmisN, Deg-C	5.2	149.2	154.4	0.5	1.3	149.2	150.5	-2.0	0.40	9.51	0.46	0.42	0.46	0.40	9.51	0.47	0.42	0.53
T-Occu-03-ExN-EmisH, Deg-C	5.2	149.2	154.4	0.5	1.3	149.2	150.5	-2.0	0.40	9.51	0.46	0.42	0.46	0.40	9.51	0.47	0.42	0.53
T-Occu-03-ExY-EmisN, Deg-C	5.5	151.8	157.3	2.4	1.6	151.8	153.4	-0.1	0.40	9.87	0.48	0.43	0.47	0.40	9.87	0.50	0.43	0.54
T-Occu-03-ExY-EmisH, Deg-C	5.5	151.8	157.3	2.4	1.6	151.8	153.4	-0.1	0.40	9.87	0.48	0.43	0.47	0.40	9.87	0.50	0.43	0.54
T-Always-00-ExN-EmisN, Deg-C	1.3	135.6	136.9	-10.9	0.9	135.6	136.5	-11.1	0.01	9.52	0.10	0.01	0.69	0.01	9.52	0.12	0.01	0.77
T-Always-00-ExN-EmisH, Deg-C	1.4	135.6	137	-10.8	0.9	135.6	136.5	-11.1	0.01	9.52	0.11	0.01	0.70	0.01	9.52	0.12	0.01	0.78
T-Always-00-ExY-EmisN, Deg-C	1.6	137.3	138.9	-9.6	1.1	137.3	138.4	-9.9	0.03	9.79	0.13	0.04	0.69	0.03	9.79	0.15	0.04	0.76
T-Always-00-ExY-EmisH, Deg-C	1.6	137.3	138.9	-9.6	1.1	137.3	138.4	-9.9	0.03	9.94	0.13	0.04	0.70	0.03	9.94	0.15	0.04	0.78
T-Occu-00-ExN-EmisN, Deg-C	1.5	137.3	138.8	-9.6	1.1	137.3	138.4	-9.9	0.03	9.88	0.12	0.04	0.65	0.03	9.88	0.14	0.04	0.75
T-Occu-00-ExN-EmisH, Deg-C	1.5	137.3	138.8	-9.6	1.1	137.3	138.4	-9.9	0.03	9.85	0.12	0.04	0.66	0.03	9.85	0.14	0.04	0.76
T-Occu-00-ExY-EmisN, Deg-C	1.5	137.3	138.8	-9.6	1.1	137.3	138.4	-9.9	0.03	9.88	0.12	0.04	0.65	0.03	9.88	0.14	0.04	0.75
T-Occu-00-ExY-EmisH, Deg-C	1.5	137.3	138.8	-9.6	1.1	137.3	138.4	-9.9	0.03	9.85	0.12	0.04	0.66	0.03	9.85	0.14	0.04	0.76
RH-Always-03-ExN-EmisN, Deg-C	5	149.7	154.7	0.7	1	149.7	150.7	-1.9	0.40	2.51	0.44	0.42	0.08	0.40	2.51	0.43	0.42	0.09
RH-Always-03-ExN-EmisH, Deg-C	5	149.7	154.7	0.7	1	149.7	150.7	-1.9	0.40	2.47	0.44	0.42	0.08	0.40	2.47	0.43	0.42	0.09
RH-Always-03-ExY-EmisN, Deg-C	5.2	152.2	157.4	2.5	1.3	152.2	153.5	-0.1	0.41	2.62	0.46	0.43	0.09	0.41	2.62	0.46	0.43	0.10
RH-Always-03-ExY-EmisH, Deg-C	5.2	152.2	157.4	2.5	1.3	152.2	153.5	-0.1	0.41	2.62	0.46	0.43	0.09	0.41	2.62	0.46	0.43	0.10
RH-Occu-03-ExN-EmisN, Deg-C	5	149.7	154.7	0.7	1	149.7	150.7	-1.9	0.40	2.43	0.44	0.42	0.08	0.40	2.43	0.43	0.42	0.09
RH-Occu-03-ExN-EmisH, Deg-C	5	149.7	154.7	0.7	1	149.7	150.7	-1.9	0.40	2.48	0.44	0.42	0.08	0.40	2.48	0.43	0.42	0.09
RH-Occu-03-ExY-EmisN, Deg-C	5.2	152.2	157.4	2.5	1.3	152.2	153.5	-0.1	0.41	2.53	0.46	0.43	0.09	0.41	2.53	0.46	0.43	0.10
RH-Occu-03-ExY-EmisH, Deg-C	5.2	152.2	157.4	2.5	1.3	152.2	153.5	-0.1	0.41	2.53	0.46	0.43	0.09	0.41	2.53	0.46	0.43	0.10
RH-Always-00-ExN-EmisN, Deg-C	1.8	139.6	141.4	-7.9	0.4	139.6	140	-8.9	0.07	2.17	0.15	0.12	0.11	0.07	2.17	0.15	0.12	0.11
RH-Always-00-ExN-EmisH, Deg-C	1.8	139.6	141.4	-7.9	0.4	139.6	140	-8.9	0.07	2.43	0.15	0.12	0.11	0.07	2.43	0.15	0.12	0.11
RH-Always-00-ExY-EmisN, Deg-C	1.8	141.4	143.2	-6.8	0.6	141.4	142	-7.6	0.07	2.47	0.16	0.13	0.11	0.07	2.47	0.15	0.13	0.11
RH-Always-00-ExY-EmisH, Deg-C	1.8	141.5	143.3	-6.7	0.6	141.5	142.1	-7.5	0.07	2.51	0.16	0.13	0.11	0.07	2.51	0.15	0.13	0.11
RH-Occu-00-ExN-EmisN, Deg-C	1.8	139.7	141.5	-7.9	0.4	139.7	140.1	-8.8	0.07	2.45	0.15	0.12	0.10	0.07	2.45	0.15	0.12	0.11
RH-Occu-00-ExN-EmisH, Deg-C	1.8	139.8	141.6	-7.8	0.4	139.8	140.2	-8.7	0.07	2.29	0.15	0.12	0.11	0.07	2.29	0.15	0.12	0.11
RH-Occu-00-ExY-EmisN, Deg-C	1.8	141.6	143.4	-6.6	0.6	141.6	142.2	-7.4	0.07	2.46	0.16	0.13	0.11	0.07	2.46	0.15	0.13	0.11
RH-Occu-00-ExY-EmisH, Deg-C	1.8	141.6	143.4	-6.6	0.6	141.6	142.2	-7.4	0.07	2.46	0.16	0.13	0.11	0.07	2.46	0.15	0.13	0.11
CO2-Always-03-ExN-EmisN, Deg-C	5	149.8	154.8	0.8	1	149.8	150.8	-1.8	0.40	0.46	0.44	0.45	0.02	0.40	0.46	0.45	0.46	0.02
CO2-Always-03-ExN-EmisH, Deg-C	5	149.8	154.8	0.8	1	149.8	150.8	-1.8	0.40	0.46	0.44	0.45	0.02	0.40	0.46	0.45	0.46	0.02
CO2-Always-03-ExY-EmisN, Deg-C	5.2	152.3	157.5	2.5	1.2	152.3	153.5	-0.1	0.40	0.63	0.46	0.46	0.03	0.40	0.63	0.47	0.46	0.03
CO2-Always-03-ExY-EmisH, Deg-C	5.2	152.3	157.5	2.5	1.2	152.3	153.5	-0.1	0.40	0.63	0.46	0.46	0.03	0.40	0.63	0.47	0.46	0.03
CO2-Occu-03-ExN-EmisN, Deg-C	5	149.8	154.8	0.8	1	149.8	150.8	-1.8	0.40	0.46	0.44	0.45	0.02	0.40	0.46	0.45	0.46	0.02
CO2-Occu-03-ExN-EmisH, Deg-C	5	149.8	154.8	0.8	1	149.8	150.8	-1.8	0.40	0.46	0.44	0.45	0.02	0.40	0.46	0.45	0.46	0.02
CO2-Occu-03-ExY-EmisN, Deg-C	5.2	152.3	157.5	2.5	1.2	152.3	153.5	-0.1	0.40	0.63	0.46	0.46	0.03	0.40	0.63	0.47	0.46	0.03
CO2-Occu-03-ExY-EmisH, Deg-C	5.2	152.3	157.5	2.5	1.2	152.3	153.5	-0.1	0.40	0.63	0.46	0.46	0.03	0.40	0.63	0.47	0.46	0.03
CO2-Always-00-ExN-EmisN, Deg-C	4	147	151	-1.7	0.8	147	147.8	-3.8	0.12	0.46	0.35	0.42	0.13	0.13	0.46	0.40	0.45	0.10
CO2-Always-00-ExN-EmisH, Deg-C	4	147.1	151.1	-1.6	0.8	147.1	147.9	-3.7	0.12	0.46	0.35	0.43	0.13	0.13	0.46	0.40	0.45	0.10
CO2-Always-00-ExY-EmisN, Deg-C	4	148.8	152.8	-0.5	1	148.8	149.8	-2.5	0.12	0.50	0.35	0.43	0.13	0.13	0.50	0.40	0.45	0.10
CO2-Always-00-ExY-EmisH, Deg-C	4	148.8	152.8	-0.5	1	148.8	149.8	-2.5	0.12	0.50	0.35	0.43	0.13	0.13	0.50	0.40	0.45	0.10
CO2-Occu-00-ExN-EmisN, Deg-C	4	147	151	-1.7	0.8	147	147.8	-3.8	0.12	0.46	0.35	0.43	0.13	0.14	0.46	0.40	0.45	0.10
CO2-Occu-00-ExN-EmisH, Deg-C	4	147	151	-1.7	0.8	147	147.8	-3.8	0.12	0.46	0.35	0.43	0.13	0.14	0.46	0.40	0.45	0.10
CO2-Occu-00-ExY-EmisN, Deg-C	4	148.8	152.8	-0.5	1	148.8	149.8	-2.5	0.12	0.50	0.35	0.43	0.13	0.13	0.50	0.40	0.45	0.09
CO2-Occu-00-ExY-EmisH, Deg-C	4	148.8	152.8	-0.5	1	148.8	149.8	-2.5	0.12	0.50	0.35	0.43	0.13	0.13	0.50	0.40	0.45	0.09

Scenario	Energy demand - Constant SFP				Energy demand - Variable SFP				Air change rates - Total time					Air change rates - @Occu				
	HVAC aux	Heat	Total	Change	HVAC aux	Heat	Total	Change	Min	Max	Mean	Median	StdDev	Min	Max	Mean	Median	StdDev
CAV, Deg-C	4.7	148.9	153.6	0	4.7	148.9	153.6	0	0.40	0.43	0.42	0.42	0.00	0.40	0.43	0.42	0.42	0.00
HCHO-Always-03-ExN-EmisN, Deg-C	4.7	149.1	153.8	0.1	0.9	149.1	150	-2.3	0.40	0.43	0.42	0.42	0.00	0.40	0.43	0.42	0.42	0.00
HCHO-Always-03-ExN-EmisH, Deg-C	4.7	149.1	153.8	0.1	0.9	149.1	150	-2.3	0.40	0.43	0.42	0.42	0.00					
HCHO-Always-03-ExY-EmisN, Deg-C	5	151.7	156.7	2.0	1.2	151.7	152.9	-0.5	0.40	0.60	0.44	0.43	0.04					
HCHO-Always-03-ExY-EmisH, Deg-C	5	151.7	156.7	2.0	1.2	151.7	152.9	-0.5	0.40	0.60	0.44	0.43	0.04					
HCHO-Occu-03-ExN-EmisN, Deg-C	4.7	149.1	153.8	0.1	0.9	149.1	150	-2.3	0.40	0.43	0.42	0.42	0.00					
HCHO-Occu-03-ExN-EmisH, Deg-C	4.7	149.1	153.8	0.1	0.9	149.1	150	-2.3	0.40	0.43	0.42	0.42	0.00					
HCHO-Occu-03-ExY-EmisN, Deg-C	5	151.7	156.7	2.0	1.2	151.7	152.9	-0.5	0.40	0.60	0.44	0.43	0.04					
HCHO-Occu-03-ExY-EmisH, Deg-C	5	151.7	156.7	2.0	1.2	151.7	152.9	-0.5	0.40	0.60	0.44	0.43	0.04	0.40	0.60	0.45	0.43	0.04
HCHO-Always-00-ExN-EmisN, Deg-C	1.2	137.1	138.3	-10.0	0.2	137.1	137.3	-10.6	0.08	0.14	0.10	0.09	0.02	0.08	0.14	0.10	0.09	0.02
HCHO-Always-00-ExN-EmisH, Deg-C	2.5	142.3	144.8	-5.7	0.4	142.3	142.7	-7.1	0.22	0.22	0.22	0.22	0.00	0.22	0.22	0.22	0.22	0.00
HCHO-Always-00-ExY-EmisN, Deg-C	1.4	139.9	141.3	-8.0	0.5	139.9	140.4	-8.6	0.09	0.22	0.12	0.12	0.02	0.09	0.22	0.13	0.12	0.02
HCHO-Always-00-ExY-EmisH, Deg-C	2.8	145	147.8	-3.8	0.7	145	145.7	-5.1	0.22	0.34	0.25	0.24	0.02	0.22	0.34	0.25	0.24	0.03
HCHO-Occu-00-ExN-EmisN, Deg-C	1.1	136.8	137.9	-10.2	0.2	136.8	137	-10.8	0.06	0.15	0.10	0.09	0.02	0.08	0.15	0.10	0.09	0.02
HCHO-Occu-00-ExN-EmisH, Deg-C	2.5	141.7	144.2	-6.1	0.6	141.7	142.3	-7.4	0.09	0.30	0.21	0.22	0.05	0.22	0.30	0.23	0.22	0.02
HCHO-Occu-00-ExY-EmisN, Deg-C	1.4	139.8	141.2	-8.1	0.5	139.8	140.3	-8.7	0.07	0.23	0.12	0.12	0.03	0.09	0.23	0.13	0.12	0.02
HCHO-Occu-00-ExY-EmisH, Deg-C	2.7	144.5	147.2	-4.2	0.9	144.5	145.4	-5.3	0.10	0.40	0.24	0.24	0.06	0.22	0.40	0.26	0.25	0.04
T-CO2-Always-03-ExN-EmisN, Deg-C	5.5	149.9	155.4	1.2	1.4	149.9	151.3	-1.5	0.40	9.51	0.48	0.45	0.46	0.40	9.51	0.50	0.46	0.52
T-CO2-Always-03-ExN-EmisH, Deg-C	5.5	149.9	155.4	1.2	1.4	149.9	151.3	-1.5	0.40	9.51	0.48	0.45	0.46	0.40	9.51	0.50	0.46	0.52
T-CO2-Always-03-ExY-EmisN, Deg-C	5.7	152.4	158.1	2.9	1.6	152.4	154	0.3	0.40	9.86	0.50	0.46	0.47	0.40	9.86	0.52	0.46	0.53
T-CO2-Always-03-ExY-EmisH, Deg-C	5.7	152.4	158.1	2.9	1.6	152.4	154	0.3	0.40	9.83	0.50	0.46	0.47	0.40	9.83	0.52	0.46	0.53
T-CO2-Occu-03-ExN-EmisN, Deg-C	5.5	149.9	155.4	1.2	1.4	149.9	151.3	-1.5	0.40	9.51	0.48	0.45	0.46	0.40	9.51	0.50	0.46	0.52
T-CO2-Occu-03-ExN-EmisH, Deg-C	5.5	149.9	155.4	1.2	1.4	149.9	151.3	-1.5	0.40	9.51	0.48	0.45	0.46	0.40	9.51	0.50	0.46	0.52
T-CO2-Occu-03-ExY-EmisN, Deg-C	5.7	152.3	158	2.9	1.6	152.3	153.9	0.2	0.40	9.82	0.50	0.46	0.46	0.40	9.82	0.52	0.46	0.53
T-CO2-Occu-03-ExY-EmisH, Deg-C	5.7	152.3	158	2.9	1.6	152.3	153.9	0.2	0.40	9.83	0.50	0.46	0.46	0.40	9.83	0.52	0.46	0.52
T-CO2-Always-00-ExN-EmisN, Deg-C	4.5	147.1	151.6	-1.3	1.2	147.1	148.3	-3.5	0.12	9.50	0.39	0.44	0.50	0.13	9.50	0.45	0.45	0.56
T-CO2-Always-00-ExN-EmisH, Deg-C	4.5	147.1	151.6	-1.3	1.2	147.1	148.3	-3.5	0.12	9.50	0.39	0.44	0.50	0.13	9.50	0.45	0.45	0.56
T-CO2-Always-00-ExY-EmisN, Deg-C	4.5	148.9	153.4	-0.1	1.5	148.9	150.4	-2.1	0.12	9.92	0.40	0.44	0.52	0.13	9.92	0.46	0.45	0.57
T-CO2-Always-00-ExY-EmisH, Deg-C	4.5	148.9	153.4	-0.1	1.5	148.9	150.4	-2.1	0.12	9.90	0.40	0.44	0.52	0.13	9.90	0.46	0.45	0.57
T-CO2-Occu-00-ExN-EmisN, Deg-C	4.5	147.1	151.6	-1.3	1.2	147.1	148.3	-3.5	0.12	9.51	0.39	0.44	0.49	0.13	9.51	0.45	0.45	0.54
T-CO2-Occu-00-ExN-EmisH, Deg-C	4.5	147.1	151.6	-1.3	1.2	147.1	148.3	-3.5	0.12	9.50	0.39	0.44	0.49	0.13	9.50	0.45	0.45	0.55
T-CO2-Occu-00-ExY-EmisN, Deg-C	4.5	148.8	153.3	-0.2	1.5	148.8	150.3	-2.1	0.12	9.92	0.39	0.44	0.51	0.13	9.92	0.46	0.45	0.56
T-CO2-Occu-00-ExY-EmisH, Deg-C	4.5	148.8	153.3	-0.2	1.5	148.8	150.3	-2.1	0.12	9.90	0.39	0.44	0.50	0.13	9.90	0.46	0.45	0.56
T-RH-Always-03-ExN-EmisN, Deg-C	5.5	149.8	155.3	1.1	1.4	149.8	151.2	-1.6	0.40	9.50	0.48	0.42	0.47	0.40	9.50	0.48	0.42	0.53
T-RH-Always-03-ExN-EmisH, Deg-C	5.5	149.8	155.3	1.1	1.4	149.8	151.2	-1.6	0.40	9.50	0.48	0.42	0.47	0.40	9.50	0.48	0.42	0.53
T-RH-Always-03-ExY-EmisN, Deg-C	5.7	152.3	158	2.9	1.7	152.3	154	0.3	0.41	9.83	0.50	0.44	0.47	0.41	9.83	0.51	0.44	0.54
T-RH-Always-03-ExY-EmisH, Deg-C	5.7	152.3	158	2.9	1.7	152.3	154	0.3	0.41	9.83	0.50	0.44	0.47	0.41	9.83	0.51	0.44	0.54
T-RH-Occu-03-ExN-EmisN, Deg-C	5.5	149.8	155.3	1.1	1.4	149.8	151.2	-1.6	0.40	9.51	0.48	0.42	0.46	0.40	9.51	0.48	0.42	0.52
T-RH-Occu-03-ExN-EmisH, Deg-C	5.5	149.8	155.3	1.1	1.4	149.8	151.2	-1.6	0.40	9.51	0.48	0.42	0.46	0.40	9.51	0.48	0.42	0.53
T-RH-Occu-03-ExY-EmisN, Deg-C	5.7	152.3	158	2.9	1.7	152.3	154	0.3	0.41	9.84	0.50	0.44	0.47	0.41	9.84	0.51	0.44	0.54
T-RH-Occu-03-ExY-EmisH, Deg-C	5.7	152.3	158	2.9	1.7	152.3	154	0.3	0.41	9.84	0.50	0.44	0.47	0.41	9.84	0.51	0.44	0.54
T-RH-Always-00-ExN-EmisN, Deg-C	2.6	139.7	142.3	-7.4	1	139.7	140.7	-8.4	0.07	9.52	0.22	0.13	0.60	0.07	9.52	0.23	0.13	0.67
T-RH-Always-00-ExN-EmisH, Deg-C	2.6	139.8	142.4	-7.3	1	139.8	140.8	-8.3	0.07	9.52	0.22	0.13	0.60	0.07	9.52	0.23	0.13	0.67
T-RH-Always-00-ExY-EmisN, Deg-C	2.6	141.6	144.2	-6.1	1.3	141.6	142.9	-7.0	0.07	9.92	0.22	0.13	0.61	0.07	9.92	0.24	0.13	0.68
T-RH-Always-00-ExY-EmisH, Deg-C	2.6	141.6	144.2	-6.1	1.3	141.6	142.9	-7.0	0.07	9.92	0.22	0.13	0.61	0.07	9.92	0.24	0.13	0.68
T-RH-Occu-00-ExN-EmisN, Deg-C	2.6	139.8	142.4	-7.3	1	139.8	140.8	-8.3	0.07	9.52	0.21	0.13	0.58	0.07	9.52	0.23	0.13	0.67
T-RH-Occu-00-ExN-EmisH, Deg-C	2.6	139.8	142.4	-7.3	1	139.8	140.8	-8.3	0.07	9.51	0.21	0.13	0.58	0.07	9.51	0.23	0.13	0.66
T-RH-Occu-00-ExY-EmisN, Deg-C	2.6	141.7	144.3	-6.1	1.2	141.7	142.9	-7.0	0.07	9.95	0.22	0.13	0.59	0.07	9.95	0.23	0.13	0.68
T-RH-Occu-00-ExY-EmisH, Deg-C	2.6	141.7	144.3	-6.1	1.2	141.7	142.9	-7.0	0.07	9.92	0.22	0.13	0.59	0.07	9.92	0.23	0.13	0.68

Since the high emission levels are a function of ACH alone, I shouldn't put too much trust in these figures. ... Or? Is it OK? Well, the figures correspond well with each other. The LEVEL is probably about

Scenario	Energy demand - Constant SFP				Energy demand - Variable SFP				Air change rates - Total time					Air change rates - @Occu				
	HVAC aux	Heat	Total	Change	HVAC aux	Heat	Total	Change	Min	Max	Mean	Median	StdDev	Min	Max	Mean	Median	StdDev
CAV, Deg-C	4.7	148.9	153.6	0	4.7	148.9	153.6	0	0.40	0.43	0.42	0.42	0.00	0.40	0.43	0.42	0.42	0.00
CO2-RH-Always-03-ExN-EmisN, Deg-C	5.3	150.4	155.7	1.4	1.1	150.4	151.5	-1.4	0.40	2.67	0.46	0.46	0.09	0.40	2.67	0.46	0.46	0.09
CO2-RH-Always-03-ExN-EmisH, Deg-C	5.3	150.4	155.7	1.4	1.1	150.4	151.5	-1.4	0.40	2.57	0.46	0.46	0.09	0.40	2.57	0.46	0.46	0.09
CO2-RH-Always-03-ExY-EmisN, Deg-C	5.4	152.8	158.2	3.0	1.3	152.8	154.1	0.3	0.41	2.62	0.48	0.46	0.09	0.41	2.62	0.48	0.46	0.09
CO2-RH-Always-03-ExY-EmisH, Deg-C	5.4	152.8	158.2	3.0	1.3	152.8	154.1	0.3	0.41	2.62	0.48	0.46	0.09	0.41	2.62	0.48	0.46	0.10
CO2-RH-Occu-03-ExN-EmisN, Deg-C	5.3	150.3	155.6	1.3	1.1	150.3	151.4	-1.4	0.40	2.47	0.46	0.46	0.08	0.40	2.47	0.46	0.46	0.09
CO2-RH-Occu-03-ExN-EmisH, Deg-C	5.3	150.3	155.6	1.3	1.1	150.3	151.4	-1.4	0.40	2.47	0.46	0.46	0.08	0.40	2.47	0.46	0.46	0.09
CO2-RH-Occu-03-ExY-EmisN, Deg-C	5.4	152.8	158.2	3.0	1.3	152.8	154.1	0.3	0.41	2.55	0.48	0.46	0.09	0.41	2.55	0.48	0.46	0.09
CO2-RH-Occu-03-ExY-EmisH, Deg-C	5.4	152.8	158.2	3.0	1.3	152.8	154.1	0.3	0.41	2.55	0.48	0.46	0.09	0.41	2.55	0.48	0.46	0.09
CO2-RH-Always-00-ExN-EmisN, Deg-C	4.2	147.4	151.6	-1.3	0.9	147.4	148.3	-3.5	0.11	2.47	0.36	0.43	0.16	0.11	2.47	0.41	0.45	0.14
CO2-RH-Always-00-ExN-EmisH, Deg-C	4.2	147.5	151.7	-1.2	0.9	147.5	148.4	-3.4	0.11	2.28	0.36	0.43	0.16	0.11	2.28	0.41	0.45	0.14
CO2-RH-Always-00-ExY-EmisN, Deg-C	4.2	149.3	153.5	-0.1	1.1	149.3	150.4	-2.1	0.11	2.47	0.36	0.43	0.16	0.11	2.47	0.41	0.45	0.14
CO2-RH-Always-00-ExY-EmisH, Deg-C	4.2	149.3	153.5	-0.1	1.1	149.3	150.4	-2.1	0.11	2.47	0.36	0.43	0.16	0.11	2.47	0.41	0.45	0.14
CO2-RH-Occu-00-ExN-EmisN, Deg-C	4.2	147.5	151.7	-1.2	0.9	147.5	148.4	-3.4	0.11	2.38	0.36	0.43	0.15	0.11	2.38	0.41	0.45	0.14
CO2-RH-Occu-00-ExN-EmisH, Deg-C	4.2	147.5	151.7	-1.2	0.9	147.5	148.4	-3.4	0.11	2.39	0.36	0.43	0.15	0.11	2.39	0.41	0.45	0.14
CO2-RH-Occu-00-ExY-EmisN, Deg-C	4.2	149.3	153.5	-0.1	1.1	149.3	150.4	-2.1	0.11	2.46	0.36	0.43	0.16	0.11	2.46	0.41	0.45	0.14
CO2-RH-Occu-00-ExY-EmisH, Deg-C	4.2	149.3	153.5	-0.1	1.1	149.3	150.4	-2.1	0.11	2.46	0.36	0.43	0.16	0.11	2.46	0.41	0.45	0.14
TCO2RH-Always-03-ExN-EmisN, Deg-C	5.7	150.4	156.1	1.6	1.5	150.4	151.9	-1.1	0.40	9.51	0.50	0.46	0.46	0.40	9.51	0.51	0.46	0.52
TCO2RH-Always-03-ExN-EmisH, Deg-C	5.7	150.4	156.1	1.6	1.4	150.4	151.8	-1.2	0.40	9.51	0.50	0.46	0.45	0.40	9.51	0.51	0.46	0.51
TCO2RH-Always-03-ExY-EmisN, Deg-C	5.9	152.8	158.7	3.3	1.7	152.8	154.5	0.6	0.41	9.79	0.52	0.46	0.46	0.41	9.79	0.53	0.46	0.53
TCO2RH-Always-03-ExY-EmisH, Deg-C	5.9	152.8	158.7	3.3	1.7	152.8	154.5	0.6	0.41	9.79	0.52	0.46	0.46	0.41	9.79	0.53	0.46	0.53
TCO2RH-Occu-03-ExN-EmisN, Deg-C	5.7	150.4	156.1	1.6	1.4	150.4	151.8	-1.2	0.40	9.50	0.50	0.46	0.45	0.40	9.50	0.51	0.46	0.52
TCO2RH-Occu-03-ExN-EmisH, Deg-C	5.7	150.4	156.1	1.6	1.4	150.4	151.8	-1.2	0.40	9.51	0.50	0.46	0.45	0.40	9.51	0.51	0.46	0.52
TCO2RH-Occu-03-ExY-EmisN, Deg-C	5.9	152.8	158.7	3.3	1.7	152.8	154.5	0.6	0.41	9.80	0.52	0.46	0.46	0.41	9.80	0.53	0.46	0.52
TCO2RH-Occu-03-ExY-EmisH, Deg-C	5.9	152.8	158.7	3.3	1.7	152.8	154.5	0.6	0.41	9.80	0.52	0.46	0.46	0.41	9.80	0.53	0.46	0.52
TCO2RH-Always-00-ExN-EmisN, Deg-C	4.7	147.5	152.2	-0.9	1.3	147.5	148.8	-3.1	0.11	9.51	0.40	0.44	0.50	0.11	9.51	0.46	0.45	0.55
TCO2RH-Always-00-ExN-EmisH, Deg-C	4.7	147.6	152.3	-0.8	1.3	147.6	148.9	-3.1	0.11	9.51	0.40	0.44	0.50	0.11	9.51	0.46	0.45	0.55
TCO2RH-Always-00-ExY-EmisN, Deg-C	4.7	149.3	154	0.3	1.5	149.3	150.8	-1.8	0.11	10.00	0.41	0.44	0.52	0.11	10.00	0.47	0.45	0.57
TCO2RH-Always-00-ExY-EmisH, Deg-C	4.7	149.3	154	0.3	1.5	149.3	150.8	-1.8	0.11	9.92	0.41	0.44	0.51	0.11	9.92	0.47	0.45	0.57
TCO2RH-Occu-00-ExN-EmisN, Deg-C	4.7	147.6	152.3	-0.8	1.3	147.6	148.9	-3.1	0.11	9.51	0.40	0.44	0.50	0.11	9.51	0.46	0.45	0.55
TCO2RH-Occu-00-ExN-EmisH, Deg-C	4.7	147.6	152.3	-0.8	1.3	147.6	148.9	-3.1	0.11	9.50	0.40	0.44	0.49	0.11	9.50	0.46	0.45	0.54
TCO2RH-Occu-00-ExY-EmisN, Deg-C	4.7	149.4	154.1	0.3	1.5	149.4	150.9	-1.8	0.11	9.88	0.40	0.44	0.50	0.11	9.88	0.46	0.45	0.56
TCO2RH-Occu-00-ExY-EmisH, Deg-C	4.7	149.3	154	0.3	1.5	149.3	150.8	-1.8	0.11	9.92	0.41	0.44	0.51	0.11	9.92	0.47	0.46	0.56
All4-Always-03-ExN-EmisN, Deg-C	5.7	150.4	156.1	1.6	1.5	150.4	151.9	-1.1	0.40	9.51	0.50	0.46	0.46	0.40	9.51	0.51	0.46	0.52
All4-Always-03-ExN-EmisH, Deg-C	5.7	150.4	156.1	1.6	1.5	150.4	151.9	-1.1	0.40	9.51	0.50	0.46	0.46	0.40	9.51	0.51	0.46	0.52
All4-Always-03-ExY-EmisN, Deg-C	5.9	152.8	158.7	3.3	1.7	152.8	154.5	0.6	0.41	9.78	0.52	0.46	0.46	0.41	9.78	0.53	0.46	0.53
All4-Always-03-ExY-EmisH, Deg-C	5.9	152.8	158.7	3.3	1.7	152.8	154.5	0.6	0.41	9.79	0.52	0.46	0.47	0.41	9.79	0.53	0.46	0.53
All4-Occu-03-ExN-EmisN, Deg-C	5.7	150.4	156.1	1.6	1.4	150.4	151.8	-1.2	0.40	9.50	0.50	0.46	0.45	0.40	9.50	0.51	0.46	0.52
All4-Occu-03-ExN-EmisH, Deg-C	5.7	150.4	156.1	1.6	1.4	150.4	151.8	-1.2	0.40	9.50	0.50	0.46	0.45	0.40	9.50	0.51	0.46	0.52
All4-Occu-03-ExY-EmisN, Deg-C	5.9	152.8	158.7	3.3	1.7	152.8	154.5	0.6	0.41	9.80	0.52	0.46	0.46	0.41	9.80	0.53	0.46	0.52
All4-Occu-03-ExY-EmisH, Deg-C	5.9	152.8	158.7	3.3	1.7	152.8	154.5	0.6	0.41	9.80	0.52	0.46	0.46	0.41	9.80	0.53	0.46	0.52
All4-Always-00-ExN-EmisN, Deg-C	4.7	147.5	152.2	-0.9	1.3	147.5	148.8	-3.1	0.11	9.50	0.40	0.44	0.50	0.11	9.50	0.46	0.45	0.55
All4-Always-00-ExN-EmisH, Deg-C	5	148.4	153.4	-0.1	1.3	148.4	149.7	-2.5	0.22	9.51	0.43	0.44	0.48	0.22	9.51	0.47	0.46	0.54
All4-Always-00-ExY-EmisN, Deg-C	4.7	149.3	154	0.3	1.5	149.3	150.8	-1.8	0.11	9.88	0.41	0.44	0.51	0.11	9.88	0.47	0.45	0.56
All4-Always-00-ExY-EmisH, Deg-C	5	150.3	155.3	1.1	1.6	150.3	151.9	-1.1	0.23	9.84	0.44	0.45	0.49	0.23	9.84	0.49	0.46	0.55
All4-Occu-00-ExN-EmisN, Deg-C	4.7	147.6	152.3	-0.8	1.3	147.6	148.9	-3.1	0.11	9.52	0.40	0.44	0.49	0.11	9.52	0.46	0.45	0.54
All4-Occu-00-ExN-EmisH, Deg-C	5	148.2	153.2	-0.3	1.4	148.2	149.6	-2.6	0.12	9.50	0.42	0.45	0.49	0.27	9.50	0.49	0.46	0.54
All4-Occu-00-ExY-EmisN, Deg-C	4.7	149.4	154.1	0.3	1.5	149.4	150.9	-1.8	0.11	9.91	0.40	0.44	0.50	0.11	9.91	0.47	0.46	0.56
All4-Occu-00-ExY-EmisH, Deg-C	5	150.2	155.2	1.0	1.7	150.2	151.9	-1.1	0.12	9.90	0.43	0.45	0.49	0.29	9.90	0.50	0.46	0.55

Scenario	Energy demand - Constant SFP				Energy demand - Variable SFP				Air change rates - Total time					Air change rates - @Occu				
	HVAC aux	Heat	Total	Change	HVAC aux	Heat	Total	Change	Min	Max	Mean	Median	StdDev	Min	Max	Mean	Median	StdDev
CAV, Deg-C	4.7	148.9	153.6	0	4.7	148.9	153.6	0	0.40	0.43	0.42	0.42	0.00	0.40	0.43	0.42	0.42	0.00
RH-HCHO-Always-03-ExN-EmisN, Deg-C	5	149.7	154.7	0.7	1	149.7	150.7	-1.9	0.40	2.55	0.44	0.42	0.08	0.40	2.55	0.43	0.42	0.09
RH-HCHO-Always-03-ExN-EmisH, Deg-C	5	149.7	154.7	0.7	1	149.7	150.7	-1.9	0.40	2.53	0.44	0.42	0.08	0.40	2.53	0.43	0.42	0.09
RH-HCHO-Always-03-ExY-EmisN, Deg-C	5.2	152.2	157.4	2.5	1.3	152.2	153.5	-0.1	0.41	2.62	0.46	0.43	0.09	0.41	2.62	0.46	0.43	0.10
RH-HCHO-Always-03-ExY-EmisH, Deg-C	5.2	152.2	157.4	2.5	1.3	152.2	153.5	-0.1	0.41	2.62	0.46	0.43	0.09	0.41	2.62	0.46	0.43	0.10
RH-HCHO-Occu-03-ExN-EmisN, Deg-C	5	149.7	154.7	0.7	1	149.7	150.7	-1.9	0.40	2.43	0.44	0.42	0.08	0.40	2.43	0.43	0.42	0.09
RH-HCHO-Occu-03-ExN-EmisH, Deg-C	5	149.7	154.7	0.7	1	149.7	150.7	-1.9	0.40	2.43	0.44	0.42	0.08	0.40	2.43	0.43	0.42	0.09
RH-HCHO-Occu-03-ExY-EmisN, Deg-C	5.2	152.2	157.4	2.5	1.3	152.2	153.5	-0.1	0.41	2.53	0.46	0.43	0.09	0.41	2.53	0.46	0.43	0.10
RH-HCHO-Occu-03-ExY-EmisH, Deg-C	5.2	152.2	157.4	2.5	1.3	152.2	153.5	-0.1	0.41	2.53	0.46	0.43	0.09	0.41	2.53	0.46	0.43	0.10
RH-HCHO-Always-00-ExN-EmisN, Deg-C	1.9	139.6	141.5	-7.9	0.4	139.6	140	-8.9	0.08	2.15	0.16	0.13	0.11	0.08	2.15	0.15	0.13	0.11
RH-HCHO-Always-00-ExN-EmisH, Deg-C	2.9	143.4	146.3	-4.8	0.6	143.4	144	-6.3	0.22	2.41	0.25	0.22	0.09	0.22	2.41	0.24	0.22	0.10
RH-HCHO-Always-00-ExY-EmisN, Deg-C	1.9	141.8	143.7	-6.4	0.7	141.8	142.5	-7.2	0.09	2.47	0.17	0.14	0.11	0.09	2.47	0.16	0.14	0.11
RH-HCHO-Always-00-ExY-EmisH, Deg-C	3.1	145.9	149	-3.0	0.8	145.9	146.7	-4.5	0.22	2.47	0.27	0.25	0.09	0.22	2.47	0.27	0.25	0.10
RH-HCHO-Occu-00-ExN-EmisN, Deg-C	1.9	139.8	141.7	-7.7	0.4	139.8	140.2	-8.7	0.08	2.48	0.16	0.13	0.10	0.08	2.48	0.15	0.13	0.11
RH-HCHO-Occu-00-ExN-EmisH, Deg-C	2.9	143.2	146.1	-4.9	0.7	143.2	143.9	-6.3	0.10	2.52	0.24	0.23	0.10	0.22	2.52	0.26	0.23	0.10
RH-HCHO-Occu-00-ExY-EmisN, Deg-C	2	141.9	143.9	-6.3	0.7	141.9	142.6	-7.2	0.09	2.46	0.17	0.14	0.11	0.09	2.46	0.17	0.14	0.11
RH-HCHO-Occu-00-ExY-EmisH, Deg-C	3.1	145.7	148.8	-3.1	1	145.7	146.7	-4.5	0.10	2.46	0.26	0.25	0.11	0.22	2.46	0.28	0.26	0.10

Paper 1. Comparing relative performance of supply air windows with conventional and heat recovery ventilation systems in a temperate climate

Submitted to Energy and Buildings on 9th February 2019.

Comparing relative performance of supply air windows with conventional and heat recovery ventilation systems in a temperate climate

Authors

Christopher Just Johnston* [a,b], Jacob Birck Laustsen [a], Jørn Toftum [b], Toke Rammer Nielsen [b].

[a] The NIRAS Group, Sortemosevej 19, 3450 Lillerød, Denmark

[b] Department of Civil Engineering, Technical University of Denmark, Brovej 118, 2800 Kgs. Lyngby, Denmark

* Corresponding author: cjj@niras.dk

Abstract

According to published literature, when compared to fresh air valves, supply air windows can reduce energy demand by 11-24 % in a temperate climate. Balanced mechanical ventilation has been estimated to lower energy demand by 22 %. To reach independence of fossil fuels, energy demand for heating must be reduced. It is vitally important to identify the most energy efficient form for ventilation.

This study compared relative performance of ventilation systems. Performance indicators were energy demand and supply air temperature. Performance estimates were based on results from simulation of eight scenarios in a validated building performance simulation tool, IESVE.

In terms of energy: Balanced ventilation with heat recovery outperformed natural ventilation in all scenarios but one. Supply air windows driven by natural ventilation performed on par with a balanced mechanical ventilation system with a heat recovery rate of 75 %, a specific fan power of 1800 J/m^3 and an infiltration rate of 0.13 l/(m^2·s).

In terms of supply air temperature: Balanced mechanical ventilation with heat recovery outperformed natural ventilation systems. On average, the supply air window raised the supply air temperature by 3.8 °C. In the cold months from December to February, the supply air temperature averaged 4.4 °C. In the same period, when outdoor temperatures averaged 0 °C, the ventilation system with a heat recovery rate of 75 % delivered supply air temperatures averaging 15 °C.

Keywords

- Supply air window
- Natural ventilation
- Mechanical ventilation
- Heat recovery
- Building performance simulation

Nomenclature

A_g	Glazed area of the supply air window	[m^2]
$c_{p,a}$	Specific heat capacity of air	[J/(kg·K)]
G_a	Volume flow rate of air	[m^3/s]

I_s	Solar irradiance (on the supply air window)	[W/m²]
$Q_{a,in}$	Energy entrained in the supply air	[W]
$Q_{a,out}$	Ventilation loss	[W]
Q_{diff}	Term correcting the energy balance in IESVE	[W]
$Q_{g,win}$	Heat loss from the glazed part of a basic window	[W]
Q_{heat}	Heating demand/heat loss	[W]
Q_{Ueff}	Effective heat loss through supply air windows	[W]
U_{eff}	Effective U-value	[W/(m²·K)]
U_g	(simulated) centre pane U-value of the window	[W/(m²·K)]

Greek symbols

θ_a	Supply(/inlet) air temperature	[°C]
θ_e	Outdoor temperature	[°C]
θ_i	Indoor temperature	[°C]
$\theta_{a,Is=0}$	Supply air temperature w/o solar radiation	[°C]
ρ_a	Density of air	[kg/m³]

Acronyms

ACH	Air change per hour
BPS	Building performance simulation
BR18	The Danish Building Regulations of 2018
SFP	Specific fan power
WIS	Windows Information System

1 Introduction

Compared to more conventional natural ventilation systems using fresh air valves to supply air, ventilation systems using supply air windows seem superior [1–7]. A common supply air window design will take outdoor air in trough a valve at the bottom. From here it will lead the air up through a cavity between window panes before directing it into the conditioned interior via a valve at the top of the window. For any temperature difference across a window, energy moves from high to low temperatures. In a supply air window, heat is entrained in the supply air as it passes up through the ventilated cavity between window panes. If not entrained in the supply air, this heat would otherwise have been be lost to the exterior. This way, supply air windows can both lower the heat loss through a window and preheat supply air.

Published literature (project reports and peer-reviewed journal articles) contains several studies of supply air windows [1–7]. The studies cover many different window designs and mathematical models – both white and grey box – have been created to examine the effects of design variations [8–13]. However, there have been few or no studies comparing performance of supply air windows with that of mechanical ventilation systems. As the supply air temperature and amount of energy exhausted to the exterior by a given ventilation system is dependent on the outdoor temperature, the relative performance of a ventilation system is related to the local climate. Therefore, any comparison – i.e. any attempt to identify the most energy efficient ventilation system for a given building – is only valid for local conditions (and comparable weather profiles). This study aimed to compare supply air temperatures and energy demand for ventilation systems using supply air windows with conventional natural and mechanical ventilation systems for Danish climatic conditions.

Denmark is not a big country and geographical variations in the climate are small. The Danish coast (which constitutes the majority of the land mass) has a temperate oceanic climate while the inland has a warm-summer humid continental climate (with Köppen climate classifications Cfb and Dfb, respectively). For 28 % of the full year and 90 % of summer, outdoor temperatures allow outdoor air to be used unconditioned [14,15]. With outdoor temperatures averaging a little above 1 °C, Denmark also has mild winters [16]. Consequently, Denmark has had a long tradition for natural ventilation in homes. This tradition continued up until 2010 when the Danish building regulations were updated to include requirements for preheated supply air and a minimum heat recovery rate on exhaust air of 80 % for multi-family housing [17].

Denmark has an official goal to be independent of fossil fuels by 2050. It has been estimated that, in order to reach this goal, Denmark must reduce energy demand for heating by 40 % [18]. With 91 % of the current Danish housing stock built prior to 2010 [19], there is a large potential for reducing the aggregate energy demand by retrofitting housing with energy efficient ventilation systems [20]. In order to be able to efficiently reduce the aggregate energy demand, it is vitally important that the most energy efficient form of ventilation for Danish homes is identified.

Previous studies comparing performance of ventilation designs in temperate climates fall into one of two groups: real world case studies [21,22] and simulated scenarios [20,23–27]. Meanwhile, these studies often do not compare the different ventilation systems on an equal basis [28]. In many ways, this is understandable: Regulations and traditions vary from country to country and use and design vary from scenario to scenario; drawing general conclusions from a comparison of a large centralised ventilation system supplying landscape offices with a de-centralised system in semi-detached housing may not be feasible or meaningful. This may explain why findings from existing literature appear contradictory at times. One UK case study that compared performance of ventilation systems in two office buildings found that, in terms of energy, a hybrid ventilation system without heat recovery performed better than a fully mechanical system with heat recovery [21]. Meanwhile, another UK case study comparing performance of ventilation systems in social housing found naturally ventilated homes to have a total energy demand that was nearly twice as high as mechanically ventilated homes using heat recovery [22]. With such inconsistent and diverging conclusions, results are not clear [26].

Conclusions presented in existing literature suggest that heat recovery ventilation may be the most energy efficient for Danish homes [20,23,24,26]. Two independent Swedish studies, both assuming that ventilation systems are upgraded with heat recovery with an efficiency of 80 %, estimate the potential to be a 22 % reduction of energy demand [23,24]. However, studies of supply air windows conducted in northern Europe estimate a comparable achievable reduction in energy demand. When upgrading ventilation systems to include supply air windows, studies estimate that for air change rates (ACH) between 0.4 h^{-1} and 0.64 h^{-1} reductions in energy demand can be on the order of 11-24 % [1,2,6]. With comparable estimates of achievable reduction in energy demand, existing literature does not allow for a definite conclusion as to which ventilation technology that is best in terms of energy efficiency in a temperate climate. Therefore, in order to conclusively determine the relative performances of supply air windows and mechanical ventilation with heat recovery, it is necessary to perform a dedicated analysis.

By comparing the performance of supply air windows to more conventional forms of ventilation, this study helps further the understanding of how supply air windows function as a technology and what types of scenario they are useful in. While performance was simulated under Danish climatic conditions, results and method can be of use to researchers that have to perform similar analysis to identify what ventilation systems are most efficient for other climatic conditions.

2 Method

This study was designed to allow for direct comparison of the performance of natural ventilation, ventilation using supply air windows and mechanical ventilation using heat recovery. The study used supply air temperature and energy demand as performance indicators. As primary energy factors have been found to be inaccurate predictors of actual primary energy demand and are subject change over time [29–31], they have been disregarded in this study. Instead, the total energy demand has been used. As the total energy demand under Danish climatic conditions is almost entirely dependent on the heat loss, the uncertainty this introduces was negligible. The respective performances were calculated relative to a reference scenario simulated with mechanical exhaust ventilation without heat recovery (scenario 1).

2.1 Supply air window

The supply air window used in this study consisted of three panes of 4 mm float glass. The two inner panes were separated by a 15 mm argon filled gap and the supply air was passed through an 84 mm gap between the middle and outermost panes. The innermost pane had a soft coating facing the argon filled gap and the middle plane a hard coating facing the ventilated air gap. The window measured 1.48 x 1.23 m and had a solid pine frame with a width of 82 mm, yielding a glazing fraction of 0.76. The glazing had a U-value of 0.80 W/(m^{2}K) and a g-value of 0.56. Estimates of performance of supply air window when unventilated was calculated in Windows Information System (WIS) [32], a programme based on ISO 15099:2003 [33]. The unventilated window had a U-value of 1.07 W/(m^{2}K) and a g-value of 0.43. Figure 1 shows the principle of the supply air window.

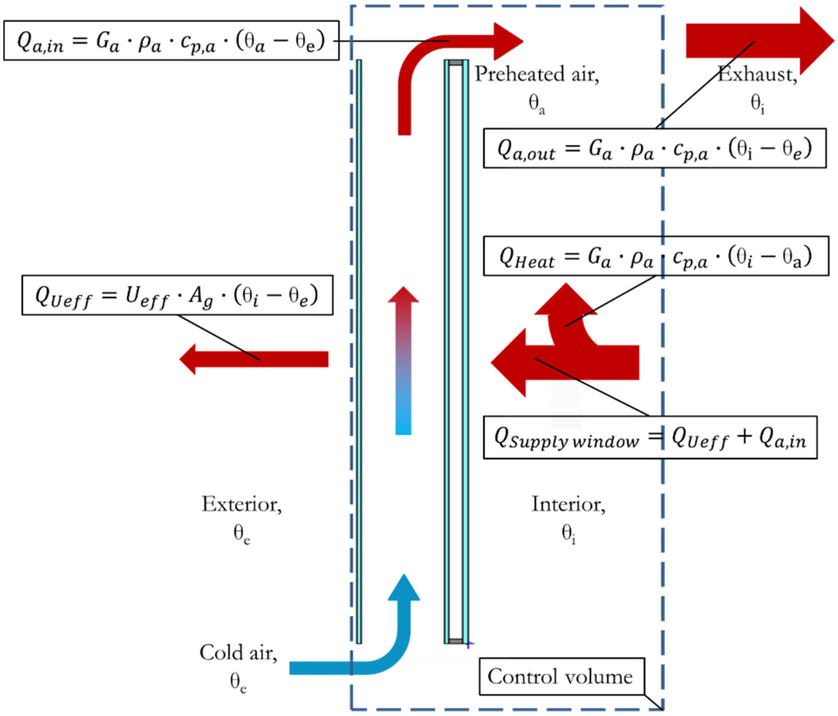

Figure 1 – Sketch showing the principles of the supply air window along with expressions for heat losses and gains

The heat balance for the system shown in Figure 1 can be written as seen below.

$$Q_{heat} = Q_{Ueff} + Q_{a,out} \qquad \text{Eq. 1}$$

Where	Q_{heat} is the heating demand/heat loss	[W]
	Q_{Ueff} is the effective heat loss through the supply air windows	[W]
	$Q_{a,out}$ is the ventilation loss	[W]

The different parts of the energy balance can be written as

$$\begin{aligned} Q_{Ueff} &= U_{eff} \cdot A_g \cdot (\theta_i - \theta_e) \\ Q_{a,out} &= G_a \cdot \rho_a \cdot c_{p,a} \cdot (\theta_i - \theta_e) \end{aligned} \qquad \text{Eq. 2}$$

Where	U_{eff} is the effective U-value	[W/(m²·K)]
	A_g is the glazed area of the supply air window	[m²]
	θ_i is the indoor temperature	[°C]
	θ_e is the outdoor temperature	[°C]
	G_a is the volume flow rate	[m³/s]
	ρ_a is the density of air	[kg/m³]
	$c_{p,a}$ is the specific heat capacity of air	[J/(kg·K)]

Supply air temperature and effective U-value (defined as heat leaving the system by the outermost pane normalised by area and the temperature difference between the interior and exterior) can be calculated by Eq. 3 and Eq. 4 respectively. The expressions were derived by regression analysis on 660 data sets derived from a parameter variation run in the WinVent algorithm (suggested by Raffnsøe [8] and validated by Laustsen et al. [7]). The parameter variation covered outdoor temperatures in the interval -10 to 16 °C, supply air flow rates in the interval 2 to 10 l/s and solar irradiance on the vertical plane in the interval 0 to 1000

W/m². As the chosen building performance simulation (BPS) tool (ISEVE, see section 2.2) could not handle expressions containing more than 156 characters [34], the regression analysis was designed to keep relationships within this range. The expressions can be used for extrapolation outside the given intervals for outdoor temperatures.

$$\begin{aligned}\theta_a &= 5.7431 + 0.775930\theta_e - 0.54042G_a + 3.3757 \cdot 10^{-2} I_s \\ &+1.5829 \cdot 10^{-2} G_a^2 - 1.5359 \cdot 10^{-6} I_s^2 \\ &+1.1067 \cdot 10^{-2} \theta_e \cdot G_a - 1.7066 \cdot 10^{-5} \theta_e \cdot I_s - 1.392 \cdot 10^{-3} G_a \cdot I_s\end{aligned} \qquad \textit{Eq. 3}$$

$$\begin{aligned}U_{eff} &= 0.84749 - 6.0054 \cdot 10^{-3} \theta_e - 0.1846G_a \\ &-6.4186 \cdot 10^{-5} \theta_e^2 + 1.8095 \cdot 10^{-2} G_a^2 - 6.553 \cdot 10^{-4} G_a^3 \\ &+9.6559 \cdot 10^{-4} \theta_e \cdot G_a + 1.6195 \cdot 10^{-5} \theta_e^2 \cdot G_a - 3.6015 \cdot 10^{-5} \theta_e \cdot G_a^2\end{aligned} \qquad \textit{Eq. 4}$$

Where	θ_a is the supply(/inlet) air temperature	[°C]
	I_s is the solar irradiance (on the supply air window)	[W/m²]

2.2 Building performance simulation

Physics-based BPS tools can predict the performance of a given building design under variable climatic conditions [35]. Using this ability to perform parametric analysis allows designers to estimate how changes in building design impact performance and to compare performances of different designs [36,37].

For this study, a BPS tool would have to allow a supply air window to impact both heat balance and supply air temperature. IESVE [34] is a validated and commercially available BPS tool. IESVE allows users to modify models by expressing variables (e.g. the supply air temperature) with customisable expressions (e.g. Eq. 3). As such, IESVE met the criteria for this study. A detailed description of how the supply air windows were implemented in the BPS model can be found in the appendix.

2.2.1 Building performance simulation model

The BPS model was kept simple with generic construction parts complying with criteria given in the Danish Building Regulations 2018 (BR18) [38]. Complex design features were avoided in order to ensure that identified trends were indeed generic and uninfluenced by specificities like overly intricate occupancy patterns or mass transport between zones in a complicated geometry. The model constituted a single unoccupied room that was representative of the general Danish contemporary building stock fulfilling current minimum requirements for new constructions.

The model had a floor area of 104 m² (nett) (16.0 x 6.5 m) and a ceiling height of 2.50 m (nett). The outer insulated cavity walls had a U-value of 0.30 W/(m²·K), the floor slab a value of 0.20 W/(m²·K), and the roofing construction a value of 0.20 W/(m²·K). The U-values equal the prescribed minimum requirement in BR18.

The ACH was kept constant at 0.5 h⁻¹. This ACH is a little higher than the prescribed minimum requirement in BR18 of 0.3 l/(m²·s) (ACH = 0,432 h⁻¹ for a room height of 2.5 m).

The temperature set point was kept constant at 20 °C. Heating was simulated using a traditional heating system with radiators. Besides the constant ventilation, the model did not use any form for cooling.

Operating hours were set to a full year (8760 hours) and the ventilation was simulated as active during all hours of the year. Values for specific fan power (SFP) for exhaust and balanced mechanical ventilation were

800 J/m^3 and 1800 J/m^3 respectively. These SFP values are the highest allowed by BR18 and so constituted a worst case scenario for energy demand for mechanical ventilation systems.

Scenarios with balanced mechanical ventilation were simulated with and without infiltration. In scenarios with infiltration, the rate was set to 0.13 l(m^2·s). The value for infiltration was the highest allowed by BR18 and so constituted a worst case scenario.

Eight windows were fitted into the 16 m long south-facing façade of the model. The windows measured 1.48 x 1.23 m^2 and had a solid pine frame with a width of 82 mm, yielding a glazing fraction of 0.76. The basic window had a U-value of 1.07 W/(m^{2}K) and a g-value of 0.43. The basic window was engineered to emulate the supply air window in the unventilated state.

With eight supply air windows ensuring an ACH of 0.5 h^{-1}, each supply air window had to supply air at a fixed rate of 4.57 l/s. For an outdoor temperature of 0 °C, an indoor temperature of 20 °C and no solar radiation, the supply air windows had an effective U-value of 0.33 W/(m^2·K) and delivered supply air at a temperature of 3.5 °C. Each supply air window supplied fresh air to a floor area of 13 m^2.

2.3 Examined scenarios

The BPS model was used to examine eight scenarios.

1. Basic windows (1+2 window panes) equivalent to the supply air window used in this investigation (without ventilation) with mechanical exhaust
2. Basic windows (1+2 window panes) equivalent to the supply air window used in this investigation (without ventilation) without mechanical exhaust
3. Supply air windows with mechanical exhaust
4. Supply air windows without mechanical exhaust
5. Basic windows (1+2 window panes) equivalent to the supply air window used in this investigation (without ventilation) and balanced mechanical ventilation with a heat recovery of 75 % without infiltration
6. Traditional new three-layer low-emission windows (U-value = 0.79 W/(m^2·K), g-value = 0.38) and balanced mechanical ventilation with a heat recovery of 80 % without infiltration
7. Basic windows (1+2 windows) equivalent to the supply air window used in this investigation (without ventilation) and balanced mechanical ventilation with a heat recovery rate of 75 % and an infiltration rate of 0.13 l/(m^2·s)
8. Traditional new three-layer low-emission windows (U-value = 0.79 W/(m^2·K), g-value = 0.38) and balanced mechanical ventilation with a heat recovery rate of 80 % and an infiltration rate of 0.13 l/(m^2·s)

Table 1 gives an overview of the input in the eight scenarios.

Table 1 – Overview of input in the eight simulated scenarios

Scenario	Short description	SFP [J/m3]	Inf. [l/(s·m2)]	HR [%]	U_{win} [W/(m²·K)]	g_{win} [-]
1	Basic windows w/ exhaust	800	-	-	U = 1.07	0.43
2	Basic windows w/o exhaust	-	-	-	U = 1.07	0.43
3	Supply air windows w/ exhaust	800	-	-	U_{eff}[1] = Var	0.43
4	Supply air windows w/o exhaust	-	-	-	U_{eff}[1] = Var	0.43
5	Basic windows w/ 75 % HR w/o infiltration	1800	-	75	U = 1.07	0.43
6	Efficient windows w/ 80 % HR w/o infiltration	1800	-	80	U = 0.79	0.38
7	Basic windows w/ 75 % HR w/ infiltration	1800	0.13	75	U = 1.07	0.43
8	Efficient windows w/ 80 % HR w/ infiltration	1800	0.13	80	U = 0.79	0.38

[1]Technically the window was implemented in the IESVE model as having a U-value of 1.07 and had the energy balance corrected by the variable Q_{diff} as defined by Eq. 5 (see appendix).

3 Results

3.1 Energy demand

Table 2 shows energy demand by different ventilation designs simulated in IESVE.

Table 2 – Energy demand by ventilation designs in IESVE model

Scenario	Short description	Heat loss [kWh/m²]	Fan power [kWh/m²]	Total [kWh/m²]	Savings [%]
1	Basic windows w/ exhaust	87.1	2.0	89.2	0
2	Basic windows w/o exhaust	87.1	-	87.1	2
3	Supply air windows w/ exhaust	79.9	2.0	82.0	8
4	Supply air windows w/o exhaust	79.9	-	79.9	10
5	Basic windows w/ 75 % HR w/o infiltration	60.5	4.6	65.0	27
6	Efficient windows w/ 80 % HR w/o infiltration	57.6	4.6	62.2	30
7	Basic windows w/ 75 % HR w/ infiltration	75.8	4.6	80.4	10
8	Efficient windows w/ 80 % HR w/ infiltration	73.1	4.6	77.7	13

Scenario 1 is the reference scenario with basic windows and mechanical exhaust ensuring the required ACH. Scenario 2 represents a home ventilated purely by natural ventilation. Comparing results from Scenarios 1 and 2 show that the relative cost of mechanical exhaust (SFP 800 J/m³) was negligible. In cases of exhaust ventilation with fresh air valves and supply air windows, fan power accounted for 2 % of the total yearly energy demand for heating and ventilation. For balanced mechanical ventilation (SFP 1800 J/m³) with basic windows, a heat recovery rate of 75 % and infiltration (scenario 7), fan power constituted 6 %. In the corresponding scenario without infiltration (scenario 5), fan power constituted 8 %.

Exchanging basic windows and fresh air valves for supply air windows resulted in savings of 8 % in terms of energy.

Infiltration significantly impacted the energy savings obtained by using balanced mechanical ventilation. The effect of keeping basic windows but exchanging natural ventilation for balanced mechanical with heat recovery of 75 % was savings of 27 % when disregarding the effects of infiltration. Using efficient triple glazed windows and a heat recovery rate of 80 % reduced the energy demand by 30 % when comparing to the reference case. Including the effect of infiltration, these savings were reduced to 10 % and 13 % respectively.

Comparing scenario 7 to scenario 4 showed equal levels of performance in terms of energy. That is, supply air windows driven by natural ventilation performed on par with a balanced mechanical ventilation system with a heat recovery rate of 75 % and SFP of 1800 J/m^3 when the model with mechanical ventilation included an infiltration rate of 0.13 l/(m^2·s). Balanced mechanical ventilation with heat recovery outperformed supply air windows in all remaining scenarios.

Implementing a system with efficient triple glazed windows and balanced mechanical ventilation with a heat recovery rate of 80 % instead of a system with basic windows and a heat recovery rate of 75 % resulted in savings of 3 % when including the effect of infiltration. When disregarding infiltration the savings were 4 %.

3.2 Supply air temperature

Figure 2 shows monthly averages of the supply air temperatures for a representative selection of simulated ventilation designs. The curve for fresh air valves shows the supply air temperatures for the scenarios with basic windows (scenarios 1-2). As air supplied by fresh air valves is unconditioned, the supply air temperature is equal to the outdoor temperature. The curve for supply air windows shows supply air temperatures for scenarios 3-4, the curve for a heat recovery rate of 75 % shows the inlet temperatures of the scenarios 5 and 7 and the curve for a heat recovery rate of 80 % shows the inlet temperatures of the scenarios 6 and 8.

On average, the supply air temperature was raised by 3.8 °C in the ventilated cavity between panes in the supply air window. The temperature increase was higher during the cold months of the year. The average supply air temperature was closely related to the outdoor temperature and averages 4.4 °C in the months from December to February.

The supply air temperatures from ventilation systems with heat recovery were higher than the ones delivered by the supply air windows. In the months from December to February systems with a heat recovery rate of 75 % averaged a supply air temperature of 15 °C. In the same period outdoor temperatures averaged 0 °C.

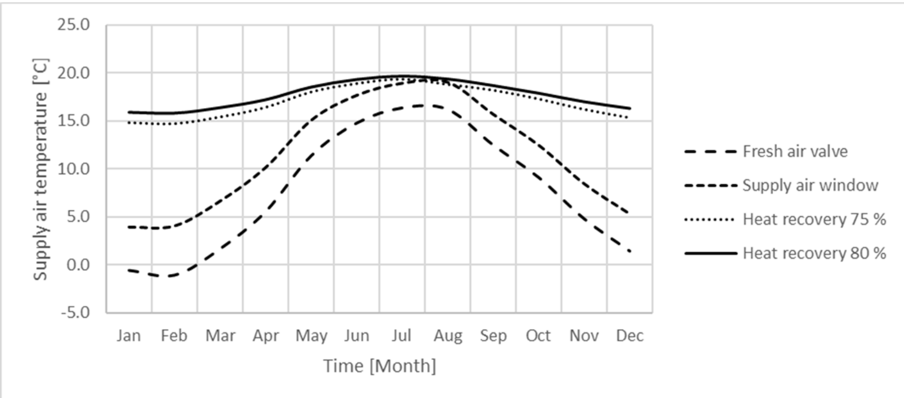

Figure 2 – Supply air temperatures of ventilation designs in IESVE model

4 Discussion and conclusions

4.1 Energy demand

Balanced mechanical ventilation with heat recovery outperformed natural ventilation in terms of energy in all instances but one. When comparing supply air windows driven by natural ventilation (scenario 4) with balanced mechanical ventilation with a heat recovery rate of 75 %, a SFP of 1800 J/m^3 and an infiltration rate of 0.13 l/(m^2·s) (scenario 7) their performance in terms of energy was about equal. That the two scenarios were equal was largely due to the relatively high level of infiltration included in the scenario with balanced mechanical ventilation.

Lowering the infiltration rate is known to improve performance of balanced mechanical ventilation systems with heat recovery [23,28,39]. When comparing the equivalent scenarios without infiltration (scenarios 4 and 5), the relative performance gap in terms of energy grew from about 0 % to 19 %. The reduction in energy demand is comparable with what is reported in the literature [39]. Dependent of type of housing, un-renovated Danish housing stock (prior to 2006) has average infiltration rates ranging from 0.22-0.28 l/(m^2·s) [40]. In order to ensure optimal performance, a home must be tightened to the exterior before employing a balanced mechanical ventilation system with heat recovery. Studies have found that it is possible to reduce infiltration rates by 70-80 % in single-family housing [39,41]. This level of reduction in infiltration is enough to make balanced mechanical ventilation with a heat recovery net profitable [20]. Alternatively, if tightening the building envelope is either not possible or not wanted, a balanced mechanical ventilation system can minimise harmful exfiltration by setting the exhaust rate higher than the inlet rate.

Results show that fan power is negligible when compared to the reduction in energy demand for heating. For exhaust ventilation, fan power accounts for only 2 % of the combined energy demand for heating and ventilation. For balanced mechanical ventilation with heat recovery, fan power constitutes between 6 % and 8 %. Choosing a ventilation system with energy efficient fans can lower the ratio further. Modern ventilation systems have nominal SFP values between 550 J/m^3 and 1450 J/m^3 [42]. Meanwhile, in practice, due to high pressure losses or malfunctions, actual SFP values can be higher than their nominal counterparts [43]. One study found that centralised ventilation systems in single- and multi-family housing, with nominal SFP values between 1050 J/m^3 and 1450 J/m^3, averaged a SFP value of 1730 J/m^3 [42]. Still, the potential for reduction in energy demand outweighs the possible consequences of implementing a ventilation system with higher than nominal SFP values.

The nominal heat recovery efficiency of a contemporary heat exchanger can be rated higher than 90 % at peak performance (e.g. Genvex [44], Nilan [45] and InVentilate [46]). Though it is possible for a carefully constructed ventilation system to meet the nominal heat recovery efficiency [47], there is a risk that systems will not perform as well as planned. Ventilation systems with heat recovery are vulnerable to leaks and studies have found that systems with nominal heat recovery rates between 70-80 % often do not recover more than 50-70 % [43,48]. In the above simulations, exchanging basic windows with efficient windows and improving the heat recovery rate from 75 % to 80 % in scenarios without infiltration (scenarios 5 and 6) improved relative performance in terms of energy by 4 %. Considering the extent of renovations, the return on investment in form of reduction in energy demand was marginal. Still, the results show that even relatively modest heat recovery rates can significantly reduce energy demand in Danish homes.

4.2 Supply air temperature

Balanced mechanical ventilation with heat recovery outperform natural ventilation systems in terms of supply air temperature. On average, the supply air window raised the supply air temperature by 3.8 °C. In the cold months from December to February the supply air temperature averaged 4.4 °C. In the same period, when outdoor temperatures averaged 0 °C, the ventilation system with a heat recovery rate of 75 % delivered supply air temperatures averaging 15 °C.

4.3 Supply air windows in system design

Supply air windows do not recover heat as such. The way supply air windows help reduce energy demand is by reducing the heat loss through the glazed part of the window. For a temperature difference of 20 °C and flow rate of 4.57 l/s, the effective U-value of the glazed part of the supply air window in this study was 0.33 W/(m²·K). In recent years, windows have become much better. Today, a tripled layered low-E window with krypton gas filling can have a centre of glass U-value of 0.5 W/(m²·K). In terms of energy, the difference is now marginal and supply air windows have lost some of their competitive edge.

Estimates in published literature were that, when compared to natural ventilation, heat recovery with an efficiency of 80 % and supply air windows would reduce energy demand by 22 % [23,24] and 11-24 % respectively [1,2,6]. Where estimates for ventilation with heat recovery were accurate, supply air windows only reduced energy demand by 8 %. Still, it is worth noting how close supply air windows and generic balanced mechanical ventilation with heat recovery ventilation are in performance in terms of energy. It is possible that the Danish climate constitutes a form of critical point: it is highly conceivable that supply air windows can outperform heat recovery ventilation in countries with warmer winters. Conversely, colder winters will probably exacerbate the performance gap that was observed in this study and favour heat recovery ventilation.

The above does not mean that natural ventilation does not have a place in modern buildings in Denmark. Certainly supply air windows can be successfully implemented in energy efficient hybrid designs. For example, supply air windows are good at reducing ambient noise and can be used to facilitate natural ventilation in areas with high outdoor sound pressure levels [49,50]. Also, there are supply air window designs that are different from the one used in this study. In terms of energy, various different designs will probably perform on par with each other (per unit area), but there are designs that are better at increasing the supply air temperature [6,13]. It is possible to increase the supply air temperature by increasing the time supply air spends in the ventilated cavity (larger area or longer pathway) and by reducing the number of panes separating the conditioned interior from the ventilated cavity. Such a supply air window would work well in a ventilation system where heat recovered from exhaust air is transferred to a reservoir, such as a domestic hot water storage tank, instead of the supply air.

Considering the above, it is concluded that the primary lesson learned from this study is that designers aspiring to design an energy efficient ventilation system in a climate like the Danish should consider some form of heat recovery on the exhaust air.

This work has not considered the carbon foot printing of a given ventilation system. Presumably a natural ventilation system will have lower production costs in terms of materials and energy. Also maintenance and reparations will play a role here. For example, supply air windows probably have a longer life span than a mechanical aggregate. It is wholly conceivable that a life cycle analysis of a building – or more specifically the ventilation systems in a building – can show that supply air windows are more cost effective in primary energy over the useful lifetime of the building than a mechanical ventilation system, despite the energy saving capability of air-to-air heat recovery. This, however, is a question to be answered by future research.

5 Acknowledgements

The article is based on work done as part of the research project ProVent (project number 340-035) [7] sponsored by ElForsk – a research and development programme under the Danish Energy Association. The aim of ProVent was to examine supply air windows in an attempt to determine the usefulness of the technology.

Funding: This work was supported by ElForsk – a research and development programme under the Danish Energy Association [project number 340-035].

6 Appendix – Implementation of supply air window in BPS model

This appendix explains how supply air windows were implemented. This appendix is based on content from the final report from ProVent [7].

IESVE could not handle supply air windows natively. Instead, the model used "basic" windows alongside a contribution, Q_{diff} (Eq. 5), that corrected the energy balance while considering that the supply air temperature was calculated separately using Eq. 3 (expression derived from regression analysis, see section 2.1 of main text).

In Eq. 5, $Q_{g,win}$ represents the heat loss from the glazed part of a basic window. Conversely, the sum of Q_{Ueff} and $Q_{a,in}$ represents the amount of heat entering a supply air window. This way, Q_{diff} represents the difference between energy entering a supply air window and leaving a basic window. When the exterior is colder than the interior, the amount of heat entering a supply air window is greater than the amount of heat leaving a basic window. Therefore Q_{diff} is usually negative. So, usually, Q_{diff} corrects the heat balance by increasing the total heat loss of the building. Meanwhile, this increase in heat loss is offset by the positive contribution of the increase in supply air temperature. Here, $Q_{a,in}$ represents the energy that is transferred to the supply air. This way the overall contribution of the supply air window ends up positive for outdoor temperatures colder than indoor temperatures.

$$Q_{diff} = Q_{g,win} - \left(Q_{Ueff} + Q_{a,in}\right) \Leftrightarrow$$
$$Q_{diff} = U_g \cdot A_g \cdot (\theta_i - \theta_e) - \left(U_{eff} \cdot A_g \cdot (\theta_i - \theta_e) + G_a \cdot \rho_a \cdot c_{p,a} \cdot \left(\theta_{a,I_s=0} - \theta_e\right)\right) \qquad \textit{Eq. 5}$$

Where	Q_{diff} is the term correcting the energy balance in IESVE	[W]
	$Q_{g,win}$ is the heat loss from the glazed part of a basic window	[W]
	Q_{Ueff} is the effective heat loss through the supply air windows (energy leaving the outer pane)	[W]
	$Q_{a,in}$ is the amount of energy entrained in the supply air	[W]
	U_g is the (simulated) centre pane U-value of the window	[W/(m²·K)]
	U_{eff} is the effective U-value of the supply air window (for Ag)	[W/(m²·K)]
	A_g is the glazed area of the supply air window	[m2]
	θ_i is the indoor temperature	[°C]
	θ_e is the outdoor temperature	[°C]
	θ_a is the supply(/inlet) air temperature	[°C]
	$\theta_{a,Is=0}$ is the supply air temperature w/o a contribution from solar radiation	[°C]
	G_a is the volume flow rate	[m³/s]
	ρ_a is the density of air	[kg/m³]
	$c_{p,a}$ is the specific heat capacity of air	[J/(kg·K)]

Expanding Eq. 5, it can be seen that there were only two unknown variables: the effective U-value of the supply air window, U_{eff}, and the supply air temperature calculated without contribution from solar radiation, $\theta_{a,Is=0}$. With the volume flow rate fixed at 4.57 l/s and the indoor temperature kept at a minimum of 20 °C, $\theta_{a,Is=0}$ is a function of the outdoor temperature (Eq. 6). Eq. 6 was determined by regression analysis. As IESVE did not allow expressions with more than 156 characters and Eq. 6 was to be substituted into Eq. 5, Eq. 6 was kept short. A short expression for U_{eff}, Eq. 7, was also determined by regression analysis.

$$\theta_{\mathrm{a,I_s=0}} = 3.5487 + 0.81724 \cdot \theta_e \qquad \textit{Eq. 6}$$

$$U_{eff} = 0.31958 - 0.0023482 \cdot \theta_e \qquad \textit{Eq. 7}$$

Substituting Eq. 6, Eq. 7, the given values for U_g, A_g and G_a and representative values for ρ_a and $c_{p,a}$ into Eq. 5 gave an expression for Q_{diff} (Eq. 8) that could be entered into IESVE. As Eq. 8 contains contributions from all of the eight supply air windows at a flow rate of 4.57 l/s, it is only valid for this specific BPS model.

$$\mathrm{Q_{diff}} = 5.3038 \cdot \theta_\mathrm{i} + 2.9615 \cdot \theta_\mathrm{e} - 160.49 + 0.0259 \cdot \theta_\mathrm{i} \cdot \theta_\mathrm{e} - 0.0259 \cdot \theta_\mathrm{e}^2 \qquad \textit{Eq. 8}$$

As solar energy is transferred to supply air, g-values (here defined as the fraction of incident solar radiation transmitted through the glazed part of the window) drop about 2 % when increasing solar irradiance on the supply window from 100 W/m2 to 1000 W/m2. By not adjusting g-values, this contribution is counted twice in the heat balance. Meanwhile, as cooling was not a concern of this study and periods with high solar irradiation are relatively uncommon, the effect on the overall heat balance of the BPS model was assumed negligible. As a consequence, g-values were assumed constant.

The temperature increase that happens in the frame of a supply air window has not been included. For a temperature difference of 20 °C and an airflow rate of 4.57 l/s, the temperature increase in the bottom frame of the used window is about 1 °C. In a similar fashion, infiltrating air is preheated when it passes through the building envelope. The effect of this preheating was not included either. The preheating in a supply air window frame and the preheating across a building envelope are approximately equivalent in size and therefore the omission of these effects should not affect the results or conclusions.

7 References

[1] Heimonen I, Hemmilä K. Integration of Windows and Ventilation by Smart Supply Air Windows. In: Glass Processing Days 2003: Conference Proceedings & Powerpoint Presentations. 2003. p. 287–90.

[2] McEvoy ME, Southall RG, Baker PH. Test cell evaluation of supply air windows to characterise their optimum performance and its verification by the use of modelling techniques. Energy Build. 2003 Nov;35[10]:1009–20.

[3] Tommerup H. Energibesparelse for "Ventilationsvinduet". 2005.

[4] Carlos JS, Corvacho H, Silva PD, Castro-Gomes JP. Real climate experimental study of two double window systems with preheating of ventilation air. Energy Build. Elsevier B.V.; 2010;42[6]:928–34.

[5] Appelfeld D, Svendsen S. Experimental analysis of energy performance of a ventilated window for heat recovery under controlled conditions. Energy Build. Elsevier B.V.; 2011 Nov;43[11]:3200–7.

[6] Heiselberg PK, Larsen OK, Liu M, Zhang C, Johra H, Herold L, et al. ClimaWin - Technical Summary Report. 2013.

[7] Laustsen JB, Johnston CJ, Raffnsøe LM. ProVent; Projekteringsviden om ventilationsvinduer. Allerød, Denmark; 2014.

[8] Raffnsøe LM. Thermal Performance of Air Flow Windows. The Technical University of Denmark; 2007.

[9] Ismail KAR, Henríquez JR. Two-dimensional model for the double glass naturally ventilated window. Int J Heat Mass Transf. 2005 Jan;48[3–4]:461–75.

[10] Ismail KAR, Henríquez JR. Simplified model for a ventilated glass window under forced air flow conditions. Appl Therm Eng. 2006 Feb;26[2–3]:295–302.

[11] Carlos JS, Corvacho H, Silva PD, Castro-Gomes JP. Modelling and simulation of a ventilated double window. Appl Therm Eng. Elsevier Ltd; 2011;31[1]:93–102.

[12] Bhamjee M, Nurick A, Madyira DM. An experimentally validated mathematical and CFD model of a supply air window: Forced and natural flow. Energy Build. Elsevier B.V.; 2013 Feb;57:289–301.

[13] Gloriant F, Tittelein P, Joulin A, Lassue S. Modeling a triple-glazed supply-air window. Build Environ. 2015;84:1–9.

[14] Chen Y, Tong Z, Malkawi A. Investigating natural ventilation potentials across the globe: Regional and climatic variations. Build Environ. Elsevier Ltd; 2017;122:386–96.

[15] Oropeza-Perez I, Østergaard PA. Potential of natural ventilation in temperate countries – A case study of Denmark. Appl Energy. Elsevier Ltd; 2014 Feb;114:520–30.

[16] Danish Meteorological Institute. Decadal mean weather in Denmark [Internet]. [cited 2019 Jan 21]. Available from: http://www.dmi.dk/en/vejr/arkiver/decadal-mean-weather/decadal-mean-weather/

[17] Historical archive of Danish Building Regulations [Internet]. [cited 2018 Jun 22]. Available from: http://historisk.bygningsreglementet.dk/tidligerebygreg/0/40

[18] Mathiesen BV, Drysdale DW, Lund H, Paardekooper S, Skov IR, Connolly D, et al. Fremtidens byggeri - Nøglen til et omkostningseffektivt og bæredygtigt energisystem. Aalborg, Denmark; 2016.

[19] Statistics Denmark - Building stock [Internet]. [cited 2018 Jun 22]. Available from: https://www.dst.dk/en/Statistik/emner/erhvervslivets-sektorer/byggeri-og-anlaeg/bygningsbestanden

[20] Tommerup H, Svendsen S. Energy savings in Danish residential building stock. Energy Build. 2006 Jun;38[6]:618–26.

[21] Walker CE, Glicksman LR, Norford LK. Tale of two low-energy designs: Comparison of mechanically and naturally ventilated office buildings in temperate climates. In: ASHRAE Transactions. 2007. p. 36–50.

[22] McGill G, Oyedele LO, McAllister K. Case study investigation of indoor air quality in mechanically ventilated and naturally ventilated UK social housing. Int J Sustain Built Environ. 2015;4[1]:58–77.

[23] Dodoo A, Gustavsson L, Sathre R. Primary energy implications of ventilation heat recovery in residential buildings. Energy Build. Elsevier B.V.; 2011 Jul;43[7]:1566–72.

[24] Mata É, Sasic Kalagasidis A, Johnsson F. Energy usage and technical potential for energy saving measures in the Swedish residential building stock. Energy Policy. 2013 Apr;55:404–14.

[25] Laverge J, Van Den Bossche N, Heijmans N, Janssens A. Energy saving potential and repercussions on indoor air quality of demand controlled residential ventilation strategies. Build Environ. Elsevier Ltd; 2011 Jul;46[7]:1497–503.

[26] Laverge J, Janssens A. Heat recovery ventilation operation traded off against natural and simple exhaust ventilation in Europe by primary energy factor, carbon dioxide emission, household consumer price and exergy. Energy Build. Elsevier B.V.; 2012 Jul;50:315–23.

[27] Ben-David T, Waring MS. Impact of natural versus mechanical ventilation on simulated indoor air quality and energy consumption in offices in fourteen U.S. cities. Build Environ. 2016;104:320–36.

[28] Laverge J, Janssens A. Optimization of design flow rates and component sizing for residential ventilation. Build Environ. Elsevier Ltd; 2013;65:81–9.

[29] Swing Gustafsson M, Gustafsson M, Myhren JA, Dotzauer E. Primary energy use in buildings in a Swedish perspective. Energy Build. Elsevier B.V.; 2016 Oct;130:202–9.

[30] Wilby MR, Rodríguez González AB, Vinagre Díaz JJ. Empirical and dynamic primary energy factors. Energy. 2014 Aug;73:771–9.

[31] Hitchin R, Thomsen KE, Wittchen KB. Primary Energy Factors and Members States Energy Regulations - Primary factors and the EPBD. Concerted Action EPBD; 2018. p. 4.

[32] Window Information System (WIS) [Internet]. [cited 2019 Jan 5]. Available from: http://www.windat.org/wis/html/index.html

[33] ISO 15099:2003 - Thermal performance of windows, doors and shading devices -- Detailed calculations. 1st ed. 2003. p. 71.

[34] Integrated Environmental Solutions Ltd - Virtual Environment (IESVE) [Internet]. [cited 2019 Jan 6].

Available from: https://www.iesve.com/

[35] Coakley D, Raftery P, Keane M. A review of methods to match building energy simulation models to measured data. Renew Sustain Energy Rev. Elsevier; 2014;37:123–41.

[36] Attia S, De Herde A, Gratia E, Hensen JLM. Achieving informed decision-making for net zero energy buildings design using building performance simulation tools. Build Simul. 2013 Mar 8;6[1]:3–21.

[37] Attia S. Optimisation for zero energy building design: interviews with twenty eight international experts, international energy agency (IEA) task 40: towards net zero energy buildings subtask B. Louvain-la-Neuve, Belgium; 2012.

[38] Danish Building Regulations 2018. Denmark: The Danish Transport, Construction and Housing Authority; 2018.

[39] Nabinger S, Persily AK. Impacts of airtightening retrofits on ventilation rates and energy consumption in a manufactured home. Energy Build. Elsevier B.V.; 2011;43[11]:3059–67.

[40] Bergsøe NC. Tæthed i eksisterende bygninger - Analyse af målte værdier. 2015.

[41] Bjørneboe MG, Svendsen S, Heller A. Evaluation of the renovation of a Danish single-family house based on measurements. Energy Build. 2017;1–24.

[42] Merzkirch A, Maas S, Scholzen F, Waldmann D. Primary energy used in centralised and decentralised ventilation systems measured in field tests in residential buildings. Int J Vent. Taylor & Francis; 2017 Mar 17;0[0]:1–9.

[43] Roulet CA, Heidt FD, Foradini F, Pibiri MC. Real heat recovery with air handling units. Energy Build. 2001;33[5]:495–502.

[44] Genvex - Manufacturer of ventilation units [Internet]. [cited 2018 Jul 13]. Available from: http://genvex.dk/

[45] Nilan - Manufacturer of ventilation units [Internet]. [cited 2018 Jul 13]. Available from: http://www.nilan.dk/

[46] InVentilate - Manufacturer of ventilation units [Internet]. [cited 2018 Jul 13]. Available from: https://www.inventilate.dk/

[47] Kamendere E, Zogla G, Kamenders A, Ikaunieks J, Rochas C. Analysis of Mechanical Ventilation System with Heat Recovery in Renovated Apartment Buildings. Energy Procedia. Elsevier B.V.; 2015 Jun;72:27–33.

[48] Choi Y, Song D, Seo D, Kim J. Analysis of the variable heat exchange efficiency of heat recovery ventilators and the associated heating energy demand. Energy Build. Elsevier B.V.; 2018 Aug;172:152–8.

[49] Rasmussen B. Experiences with sound insulating open windows in traffic noise exposed housing. In: Inter-Noise 2015. 2015. p. 8.

[50] Søndergaard LS, Egedal R. Open windows with better sound insulation. In: Inter-Noise 2016. 2016. p. 1173–84.

Paper 2. Comparing predictions by existing emission models to real world observations of formaldehyde emissions from solid materials

Submitted to Building Simulation on 10th February 2019.

Comparing predictions by existing emission models to real world observations of formaldehyde emissions from solid materials

Authors

Christopher Just Johnston* [a,b], Toke Rammer Nielsen [b], Jørn Toftum [b].

[a] The NIRAS Group, Sortemosevej 19, 3450 Allerød, Denmark

[b] Department of Civil Engineering, Technical University of Denmark, Brovej 118, 2800 Kgs. Lyngby, Denmark

* Corresponding author: cjj@niras.dk

Abstract

Existing general mass transfer models for volatile organic compound emissions have been validated against experimental results from small test chambers using fans to ensure ideal mixing. This study compared emission rates predicted by such models to observations from homes, large test chambers and full scale experiments. The comparison revealed that emission models overestimate emission rates and underestimate the time it takes to deplete the original content of un-bound formaldehyde. It is hypothesised that the reasons for the observed discrepancy are that:

1. The use of fans in small test chambers increase convective mass transfer rates to a level that is not observed in other settings.
2. The assumption that change in the concentration in an emitting material is determined by diffusion alone, implicitly implying that generation is negligible, may not be valid outside small test chambers.

It is concluded that models validated against experiments made in small test chambers using a fan for ideal mixing are not suitable for estimating development in emissions under real world conditions.

Keywords

- Volatile organic compound
- Formaldehyde
- Emissions
- Mass transfer
- Small test chambers
- Building material

Nomenclature

A_m	Emitting surface area of the sample material	[m^2]
AH	Absolute humidity	[g/m^3]
Bi_m	Biot number for mass transfer	[-]
C_0	Initial emittable concentration	[kg/m^3]
C_{1-3}	Coefficients determined in climate chambers	[-]
C_a	Concentration in the chamber or room air	[kg/m^3]
C_{as}	Concentration in air near the surface of material	[kg/m^3]
C_m	VOC concentration in the sample material	[kg/m^3]
D_{1-2}	Coefficients determined in climate chambers	[-]

D_m	Diffusion coefficient for mass transfer	[m^2/s]
Fo_m	Fourier number for mass transfer	[-]
G_a	Volume flow rate of air	[m^3/s]
h_m	Convective mass transfer coefficient	[m/s]
K_{1-2}	Coefficients determined by tests in climate chambers	[-]
K_{ma}	Material to air partition coefficient	[-]
n	Air exchange rate	[s^{-1}]
R	Emission rate	[$kg/(s\cdot m^2)$]
t	Time	[s]
T	Absolute temperature	[K]
V	Volume of the room	[m^3]
x	Distance (between surfaces of emitting material)	[m]

Greek symbols

α	Dimensionless air exchange rate	[-]
β	Ratio of building material volume to room volume	[-]
δ	Material thickness	[m]

Acronyms

ACH	Air change per hour
AH	Absolute humidity (total mass of water vapour in unit volume of air)
BPS	Building performance simulation
DK2004	VOC emission model by Deng and Kim, 2004
HCHO	Formaldehyde
HH2002	VOC emission model by Huang and Haghighat, 2002
Qa2007	VOC emission model by Qian et al., 2007
RH	Relative humidity
SVOC	Semi-volatile organic compound
VOC	Volatile organic compound
XZ2003	VOC emission model by Xu and Zhang, 2003

1 Introduction

Pollutant emission patterns are unique to given materials and products. Little et al. suggested that it might be possible to predict volatile organic compound (VOC) emissions based on knowledge of the physical properties of an emitting material [1]. Specifically, it was suggested that it might be possible to make predictions based on knowledge on the initial emittable concentration (C_0), the mass diffusion coefficient (D_m) and the material to air partition coefficient (K_{ma}). The proposed theory gained popularity and forms the theoretical foundation for a long line of emission models; a list including 20 of the most important models and model developments is given by Zhang et al. in their exhaustive review article from 2016 [2]. More recent efforts have resulted in the development of experimental procedures that allow rapid determination of the relevant physical properties of an emitting material [3–5]. Classically, emission models such as those developed by Andersen, Lundqvist and Mølhave [6] and Hoetjer and Koerts [7] have been semi-empirical. One important result of Little's work is that it has allowed researchers to develop fully analytical solutions for emissions.

Valid emission models are necessary for building performance simulation (BPS) tools to determine the effects of building generated pollution. At present, BPS tools do not include emission models for VOCs. One reason for this is that there is no consensus on which emitted compound can be used as a proxy for building generated pollution. Meanwhile, in the absence of a consensus, several researchers have suggested that VOCs can be used as a proxy for emissions from building materials and furniture [8].

Incentivised by the threat of climate change and continuously stricter energy requirements in national standards, the construction industry is working towards low-energy buildings [9]. One of the challenges of low energy status is developing methods that can ensure healthy and comfortable indoor environments at low costs in terms of energy. Currently there is an industry wide concerted effort to determine ventilation standards [10] and update BPS tools with the capability to determine the indoor environmental quality to a level that ensures that building designs deliver on both health and comfort at low energy demands [11].

A first step in the efforts to include building generated pollution in building simulations is to determine whether existing emission models for VOCs are accurate to a level that make them useful in this context. This article presents a comparison of predictions for formaldehyde (HCHO) emissions made by validated models based on mass transfer theory to practical observations from homes, large test chambers and full scale experiments.

2 Formaldehyde emission models

VOC emission models from dry building materials can be classified as being either multi-phase or one-phase models. Multi-phase models consider the effect pores have on mass transfer within a given material. As such, multi-phase models consider VOCs in both the solid and the gas phase. One-phase models lump the solid and gas phases into to one and assume that a given material acts as if homogenous. This assumption has been found to hold true for values for a material to air partition coefficient, K_{ma}, that are 10 times greater than the porosity, ε [12]. Since K_{ma} for VOCs are often in the thousands while ε is always smaller than one, it is rarely necessary to use a multi-phase model. Therefore this study focuses on one-phase models.

One-phase models have been developed for a large variety of scenarios: for VOCs and semi volatile organic compounds (SVOCs), for one or multiple layers and for combinations where some layers act as sources while others act as sinks. As HCHO has a saturation pressure of about 5 atm at 23.8 °C [13] and 10^{-3} atm is a common demarcation between VOCs and SVOCs (with SVOCs having saturation pressures equal to or lower than 10^{-4} atm) [14], HCHO is considered a VOC. Also considering that most building and furniture materials are single-layered (albeit often coated), the focus of this study is on one-phase models for VOC emissions from single-layered, solid materials with a single emitting surface.

The model Little et al. published in 1994 [1] was the first to allow researchers to simulate how VOCs diffuse from a homogenous, solid material into ambient air. Eq. 1 forms the basis of all one-phase models. The equation, also known as Fick's second law of diffusion, describes how a VOC – under the assumption of one-dimensional flow – diffuses through a homogenous solid.

$$\frac{\partial C_m(x,t)}{\partial t} = D_m \frac{\partial^2 C_m(x,t)}{\partial x^2} \qquad \text{Eq. 1}$$

Where	C_m is the VOC concentration in the sample material	[kg/m^3]
	D_m is the diffusion coefficient for mass transfer	[m^2/s]
	x is the distance (between surfaces of emitting material)	[m]
	t is time	[s]

In order to obtain an analytical solution, Little et al. simplified the problem. They made the following seven assumptions:

(1) That the concentration of the compound of interest was uniformly distributed throughout the sample material at the beginning of a test.

$$C_m(x,t)|_{t=0} = C_0 \; for \; 0 \leq x \leq \delta \qquad \textit{Eq. 2}$$

Where	C_0 is the initial emittable concentration	[kg/m^3]
	δ is the material thickness	[m]

(2) That only one surface emits the compound of interest (as with a carpet on a floor) (emission at surface where x = δ).

$$\left.\frac{\partial C_m(x,t)}{\partial t}\right|_{x=0} = 0 \; for \; t > 0 \qquad \textit{Eq. 3}$$

(3) That the convective mass transfer coefficient, h_m, is infinite (so that convective mass transfer from the emitting surface can be ignored) and (4) that the concentration of the compound of interest at the surface layer of the sample material is always in equilibrium with the concentration in the chamber or room air.

$$C_m(x,t)|_{x=\delta} = K_{ma} C_a \; for \; t > 0 \qquad \textit{Eq. 4}$$

Where	K_{ma} is the material to air partition coefficient	[-]
	C_a is the concentration in the chamber or room air	[kg/m^3]

(5) That the concentration in the inlet air and the initial concentration in the chamber or room air are both zero so that the mass balance reduces to Eq. 6.

$$C_a = 0 \; for \; t = 0, \qquad \textit{Eq. 5}$$

$$V \frac{\partial C_a(t)}{\partial t} = -D_m A_m \left.\frac{\partial C_m(x,t)}{\partial t}\right|_{x=\delta} - C_a G_a \; for \; t > 0 \qquad \textit{Eq. 6}$$

Where	V is the volume of the room	[m^3]
	A_m is the emitting surface area of the sample material	[m^2]
	G_a is the volume flowrate of air in and out the chamber or room	[m^3/s]

(6) That both the diffusion coefficient for mass transfer, D_m, and the material to air partition coefficient, K_{ma}, are constants and, finally, (7) that the chamber or room air is well mixed.

The series of assumptions allowed Little et al. to arrive at a fully analytical solution that enabled them to calculate the concentration distribution in the sample material over time, $C_m(x,t)$, and the concentration in the chamber or room air, $C_a(t)$. The model was validated against data from an experiment conducted in a 20 m^3 environmental chamber where the temperature (23 °C), relative humidity (RH) (50 %) and air exchange rate (1 h^{-1}) were kept constant and a fan was used to ensure that the chamber air was well mixed [1]. A weakness of this model was the assumption that the convective mass transfer, h_m, was infinite. The assumption leads the model to overestimate the emission rate [15]. This particular problem was fixed within a decade; Huang and Haghighat published a fully analytical solution in 2002 (HH2002) [15], Xu and Zhang published their solution in 2003 (XZ2003) [16] and Deng and Kim published their solution in 2004 (DK2004) [17].

The new solutions were found by exchanging Eq. 4 with Eq. 7.

$$C_m(x,t)|_{x=\delta} = K_{ma} C_{as}(t) \; for \; t > 0 \qquad \textit{Eq. 7}$$

Where	C_{as} is the concentration in the air near the surface (boundary layer) of the sample material	[kg/m^3]

And adding Eq. 8.

$$R(t) = -D_m \frac{\partial C_m(x,t)}{\partial t}\bigg|_{x=\delta} = h_m\big(C_{as}(t) - C_a(t)\big) \qquad \textit{Eq. 8}$$

Where	R is the emission rate	[kg/(s·m^2)]
	h_m is the convective mass transfer coefficient	[m/s]

Models HH2002, XZ2003 and DK2002 have all been validated against experimental data published by Yang et al. [18]. The data used for validation was obtained from a series of experiments conducted for different VOCs (TVOC, hexanal and α-pinene) performed in a small test chamber (0.05 m^3) at constant temperature (23 °C), RH (50 %) and air exchange rate (1 h^{-1}) using a fan to ensure that the chamber air was well mixed.

Despite constituting a fairly specific subset of emission models, these three models share the fundamental basics of all other one-phase models and, so, can in this context be considered representative of emission models that are based on the tradition founded by Little et al.

2.1 Emission model with regressed coefficients

While the focus of this study is on how the emission models by Huang and Haghighat [15], Xu and Zhang [16] and Deng and Kim [17] perform when compared to real world observations of HCHO emission rates, it is worth mentioning a fourth model published by Qian et al. in 2007 (Qa2007) [19]. The model is based on the same system of assumptions and equations as the other models and has been validated against the same experimental data [18] and model DK2002. However, the model is different in two ways that makes it useful as a case study: The model is constructed using dimensionless parameters such as the Biot number for mass transfer, Bi_m, and the Fourier number for mass transfer, Fo_m, and coefficients have been regressed to the included dimensionless parameters. This means that the model is readily interpretable. The dimensionless parameters each represent a physical quality or aspect of the model and the regressed coefficients are the weight that each respective dimensionless parameter has in the model. Being a statistical model with coefficients fitted to real, physical parameters, it is what is known as a grey-box model.

Besides the value as an easily accessible example, the model has other qualities that are desirable in the context of BPS. The model would be the easiest of the four representative models to implement into a BPS environment and may be the least expensive in terms of computational power (note that the model is not continuous – it has three discrete parts – and that this may make the model incompatible with a BPS tool that uses time steps of variable length).

Using the model fitted for Fourier numbers lower than or equal to 0.2 and higher than 0.01 (not at steady state), the grey-box model can be written as shown in Eq. 9.

$$R(t) = 0.469 \frac{D_m C_0}{\delta} \alpha^{0.022} (\beta K)^{-0.021} \left(\frac{Bi_m}{K}\right)^{0.021} Fo_m^{-0.48} \qquad \textit{Eq. 9}$$

Where	α is the dimensionless air exchange rate	[-]
	β is the ratio of building material volume to room volume	[-]
	Bi_m is the Biot number for mass transfer	[-]
	Fo_m is the Fourier number for mass transfer	[-]

The dimensionless parameters are defined as shown in Eq. 10.

$$\alpha = \frac{n\delta^2}{D_m}, 60 \leq \alpha \leq 36200$$
$$\beta = \frac{A\delta}{V}, 0.4 \leq \beta \cdot K \leq 150$$
$$Bi_m = \frac{h_m\delta}{D_m}, 20 \leq \frac{Bi_m}{K} \leq 700 \quad \textit{Eq. 10}$$
$$Fo_m = \frac{D_m t}{\delta^2}, Fo_m \geq 0$$

Where n is the air exchange rate [s^{-1}]

Qian et al. introduces two new dimensionless parameters in their model from 2007 [19]. The first is the dimensionless air exchange rate, α, which is the ratio between the actual air exchange rate and the mass diffusivity. According to model Qa2007, an increase in the actual air exchange rate seen relative to the mass diffusivity will result in an increase in the emission rate. The second dimensionless parameter is the ratio of the volume of building material to the volume of room or chamber air, β, which is directly related and proportional to the loading ratio (the ratio of the surface area of an emitting material to the volume of the surrounding air). According to model Qa2007, an increase in the material volume seen relative to the air volume ratio will result in a decrease in the emission rate.

The two other dimensionless parameters identified in the model are the Biot number for mass transfer, Bi_m, and the Fourier number for mass transfer, Fo_m. The Biot number for mass transfer describes the ratio between the mass transfer resistance at the surface of the material and the mass transfer resistance in the material itself. Here, decreasing the mass transfer resistance at the surface of the material – which, conceptually, is equivalent to increasing the convective mass transfer coefficient, h_m – will result in an increase in the emission rate and the Biot number for mass transfer.

Conceptually, the Fourier number for mass transport can be understood as the ratio of the rate of mass transport by diffusion to the rate of mass storage in a given material. Fo_m is dependent on time and increases as time passes. As such, Fo_m can be understood as dimensionless time and can under stable conditions be used as an indicator for proximity to steady state conditions. According to model Qa2007, an increase in the Fourier number for mass transport brought about by the progress of time will result in a decrease in the emission rate.

The patterns observed for model Qa2007 should all hold true for the other three models. That is, changes in α, β, Bi_m and Fo_m should affect emission rates estimated by models HH2002, XZ2003 and DK2002 in the same way as they affect the emission rate estimated by model Qa2007. This knowledge is useful to have when working with the other models as they are much less intuitive.

2.2 Expected pattern

The following is a description of the development of emission rates and concentration levels as expected in chamber tests [20].

1. Material emission rates in an environmental chamber decrease continuously.
2. In an environmental chamber, the highest emission rates usually occur at the beginning when materials are introduced.
3. When materials are tested in an environmental chamber, a "steady state" can be achieved with prolonged emission time.

Figure 1 shows how the four representative models predict the development of the VOC concentration in the air in small test chambers (e.g. 10-100 l [4]) over time. The input parameters were representative for fibreboards and the air change per hour (ACH) was 1 h^{-1}. All four models can be seen to follow the expected development and are in good agreement with one another. Despite some variation in the timing and level of peak concentration, all four models can be seen to converge to the same level and pattern.

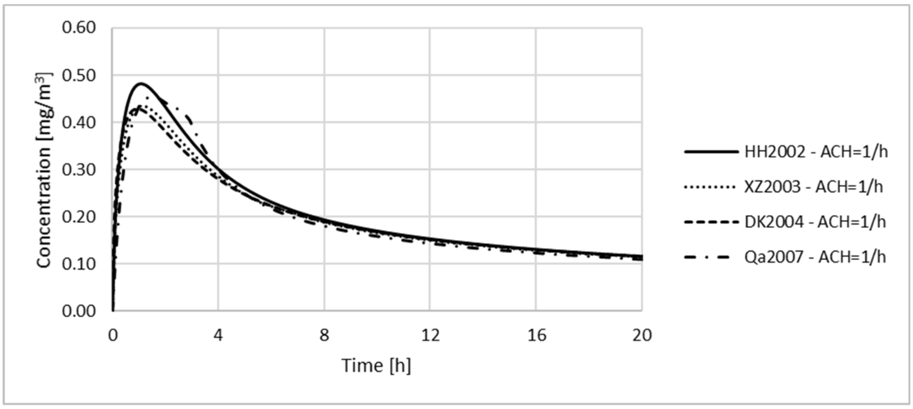

Figure 1 – Development in HCHO concentration level in small test chamber predicted by the four representative methods [15–17,19]

2.3 Influencing parameters

The initial emittable concentration, C_0, diffusion coefficient for mass transfer, D_m, and material to air partition coefficient, K_{ma}, are material properties and must be determined by tests in climate chambers using methods such as the C-History Method [3] or the Ventilated Chamber C-History Method [4]. The material properties are variable and influenced by the ambient environment. Eq. 11–Eq. 13 show how the material properties relate to the ambient environment [21–23].

$$C_0 = (1 + C_1 \cdot RH)C_2 T^{-0.5} \exp\left(-\frac{C_3}{T}\right) \quad \textit{Eq. 11}$$

$$D_m = D_1 T^{1.25} \exp\left(-\frac{D_2}{T}\right) \quad \textit{Eq. 12}$$

$$\ln(K_{ma}) = K_1 \cdot AH + K_2 \quad \textit{Eq. 13}$$

Where	$C_{1\text{-}3}$ are coefficients determined by tests in climate chambers	[-]
	$D_{1\text{-}2}$ are coefficients determined by tests in climate chambers	[-]
	$K_{1\text{-}2}$ are coefficients determined by tests in climate chambers	[-]
	T is the absolute temperature	[K]
	AH is the absolute humidity	[g/m^3]

Besides the properties of an emitting material itself, previous studies have established that HCHO concentration levels are influenced by the following parameters.

1. Loading ratio [6,7].
2. Temperature [20–22,24].
3. Humidity level [20,21,23,25].
4. Air change rate [26–29].

2.4 Mathematical limitations

The VOC emission models based on mass transfer theory are mathematical solutions to a mass balance equal or similar to Eq. 6. The mass balance can be recognised as an ordinary differential equation of the form shown in Eq. 14.

$$\frac{dO(t)}{dt} = -\lambda O(t), \lambda > 0, O(0) = O_0 \qquad \textit{Eq. 14}$$

For an initial condition (or quantity) O_0 and (decay) constant λ, Eq. 14 has the following solution:

$$O(t) = O_0 e^{-\lambda t} \qquad \textit{Eq. 15}$$

For the VOC emission models based on mass transfer theory, the initial condition and constant are, respectively, the initial emittable concentration, C_0, and the diffusion coefficient for mass transfer, D_m.

In order to derive fully analytical solutions, researchers have assumed that material properties (C_0, D_m and K_{ma}) and testing conditions (T, AH and ACH) are constant. This imposes technical limitations on how the VOC emission models can be used. For example, should C_0 be simulated as variable in time (e.g. by using Eq. 11), it will not be possible to adhere to the principle of conservation of mass (that is, the calculated total emitted mass at $t = \infty$ will not sum to the total mass of VOC at $t = 0$).

Therefore, it can be seen that VOC emission models do not allow dynamic modelling, at least not from a strictly mathematical point the view. However, since indoor environments are fairly stable over time, VOC emission models may work in practice.

3 Comparing predictions to observations

The VOC emission models HH2002 [15] and XZ2003 [16] (the dimensionless version) have both decoupled the VOC emission rate R from ACH; presumably this is an artefact stemming from the assumptions that the ACH is constant (Eq. 6) and decoupled from h_m. Meanwhile, the VOC emission models DK2004 [17] and Qa2007 [19] both include ACH in their modelling of R.

As studies have found indications that changes in ACH can impact HCHO emission rates [26–29], there may be a discrepancy between theory and practice. The remainder of this study focuses on this observed possible difference between theory and practice. As such, this study does not include analyses of whether changes in temperature or humidity influence predictions by VOC emission models differently than they do in practice.

3.1 Predictions by models based on results from small test chambers

Figure 2 shows how concentration levels in a small test chamber change over time. Figure 3 shows how the emission rate in a small test chamber changes over time (including the effect of ACH on R). The figures show the development for ACHs of 1 h^{-1} and 5 h^{-1}. The graphs have been calculated using model DK2004. The input parameters were representative for fibreboards and test conditions used to validate emission models: $C_0 = 10^7$ µg/m^3, $D_m = 1 \cdot 10^{-10}$ m^2/s, K = 3000, δ = 0.01 m, V = 30 l, A_m = 45 cm^2 and h_m = 0.0025 m/s. The figures show that while changes in the ACH significantly impact concentration levels, they only have little influence on the emission rates. In this instance the concentration in the chamber air drops by approximately 85 % within 80 hours. Based on this the half-life of the air concentration can be calculated to be 27 h.

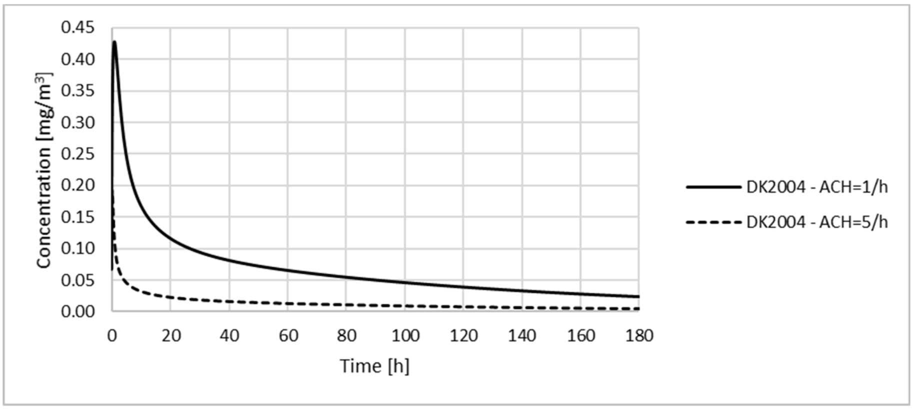

Figure 2 – Development in HCHO concentration level in small test chamber calculated using DK2004 [17]

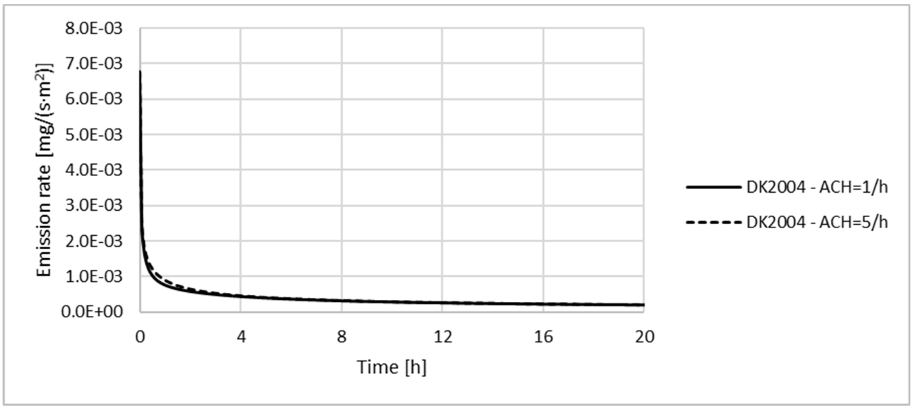

Figure 3 – Development in HCHO emission rate in small test chamber calculated using DK2004 [17]

Figure 4 shows how emission rates predicted by Qa2007 change with ACH ($0.01 \leq Fo_m \leq 0.2$). In this particular model the dimensionless air exchange rate, α, is the term considering the ACH. With α raised to the power of 0.022 (Eq. 9) any change to the ACH will have little effect on the predicted emission rate. A fivefold increase in the ACH from 0.25 to 1.25 increases the emission rate by 3.6 %.

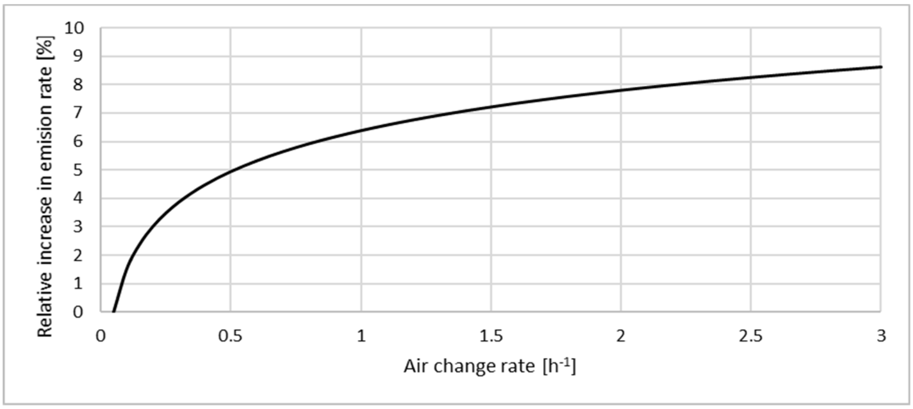

Figure 4 – Predicted relative increase in HCHO emission rates by model based on results from small test chamber using Qa2007 [19]

3.2 Observations from real world studies

Generally, studies that observe VOC emission rates in buildings do not include enough data on construction materials to allow for a simulation to be run for comparison. Instead, in order to compare predictions and observations, it is necessary to examine general trends. Existing literature contains information on how changes in ACH affect HCHO emission rates and how HCHO emission rates change over time. The four examined VOC emission models all predict that ACH has little or no influence on emission rates, that emission rates decrease continuously and that the half-life of the air concentration is of the order of days. If the emission models are to be used to simulate real world emission patterns, these patterns must be reflected in real world observations.

3.2.1 Influence of ACH on observed HCHO emission rates

Tests performed by Lehmann in a large-scale test chamber (55.4 m^3) found that a fivefold increase in the ACH (an ACH to loading ratio from 0.25 to 1.25 for an initial concentration of 0.6 ppm) would about halve the concentration of HCHO [27]. The fivefold increase in ACH resulted in a 170 % rise in the emission rate. An investigation of data gathered by Logadóttir and Gunnarsen, shown in Figure 5, shows a comparable trend [30]. Here a fivefold increase in ACH from 0.25 to 1.25 resulted in a roughly estimated 270 % rise in the emission rate. Similarly, a study of HCHO exposure in US residences conducted by Hult et al. found that, at a reference ACH of 0.35 h^{-1}, increasing ventilation was up to 60 % less effective than would be predicted if the HCHO emission rate was constant [28]. Hult et al. noted that this indicates that HCHO emission rates increase as air concentrations decrease.

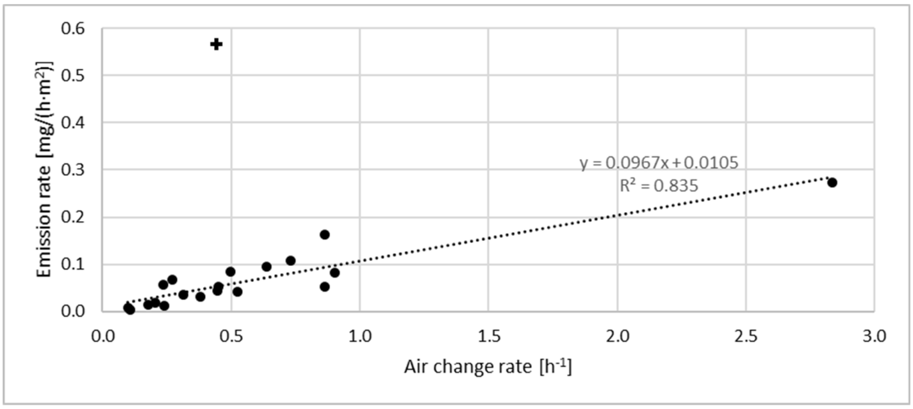

Figure 5 – HCHO emission rates derived from measured concentrations plotted over ACH [30] *– the cross marks an outlier*

Results from a study of VOC emissions from materials in vehicles by Xiong et al. suggest that change in the ACH might also influence emission rates for VOCs different from HCHO [31]. Xiong et al. reported a general relationship between the VOC concentration levels and the volume flow rate in the examined vehicles. Here a fivefold increase in ACH from 0.25 to 1.25 resulted in a 34 % drop in concentration levels and a 229 % increase in emission rates.

3.2.2 Influence of time on observed emission rates

Myers and Nagaoka tested emissions at low ACHs (an ACH to loading ratio of 0.060 m/h). They found that the amount of HCHO lost by some particleboard samples only amounted to a very small fraction of the potentially available amount. After 10 weeks of dynamic experiments, the loss was approximately 0.2 % of the total original content of HCHO [26]. Zinn et al. reported the findings of a long-term study of emissions from 16 particleboard products. They reported the half-life time of HCHO content in the particleboards to be 216 days [32]. Figure 6 shows excerpts from the results of a study by Liang et al. where a full-scale experiment followed a naturally ventilated building fitted with a loading of 0.5 m^2/m^3 raw MDF sheets for 29 months. The figure shows how the HCHO concentration varied over the seasons in relation to AH. The study found that the HCHO concentration decreased 20−65 % in corresponding months of the second year [20]. This corresponds well with the half-life time of 216 days as reported by Zinn et al. [32].

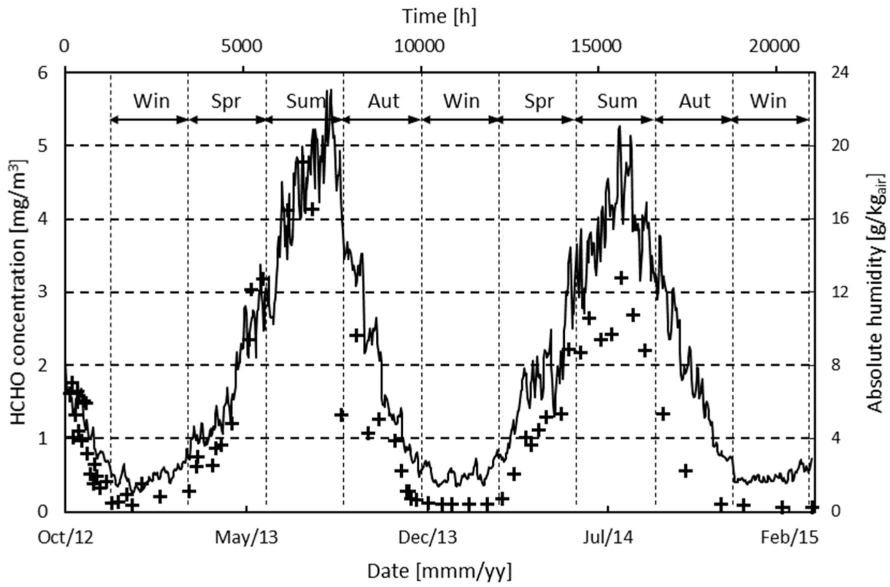

Figure 6 – Variation in HCHO concentration levels over the seasons in full-scale experiment seen in relation to AH [20] *– the line traces the humidity level and the crosses mark the HCHO concentration*

4 Discussion

The comparison found that emission rates predicted by the examined models based on mass transfer theory and validated against results from experiments performed in small test chambers do not correspond well with observations from homes, large test chambers and full scale experiments. Specifically, the emission models appear to underestimate the influence of changes in the ACH and forecasted drops in emission rates and concentration levels occur much later than predicted. Also, analysis of the mathematics behind the emission models found that such models have not been designed in a way that allows them to capture the dynamic behaviour of a system with varying temperature and RH.

The findings from the comparison and analysis show that the examined emission models are not suitable for use in connection with BPS. Moreover, the findings suggest that the examined models may lack or fail to properly appreciate aspects important to the emission process. This indicates that more research is needed in two areas: methods that will allow BPS to include considerations of building generated pollution and general mass transfer theory models for VOC emissions that can handle dynamic conditions. These two areas may well overlap. The latter of the two research areas include identification of why the examined models fail to emulate patterns observed in real world cases.

4.1 Influence of surface conditions on emission dynamics

It is possible that part of the reason for the observed discrepancy between predictions and observations is to be found in the physical test environment present in small test chambers using fans to ensure ideal mixing in the small test chambers. Myers and Nagaoka discuss the influence of air velocity on the emission pattern of HCHO [26]. They hypothesise that a high air velocity will lead to the depletion of the readily emittable (un-bound HCHO) concentration in a test specimen and that a low air velocity will not. They argue that, as a result, the problems are inherently different.

Hoetjer and Koerts describe several experiments to determine the emission characteristics of test specimens [7]. While Hoetjer and Koerts do not mention rate limitation as such, they do address the influence of ideal mixing. They state that experiments performed at low air velocities will not reach a steady state condition that allows for inference about HCHO levels in a test specimen. They also state that tests performed at low air velocities will yield results similar to those that would be found in a real world setting. They continue by stating that HCHO concentrations will be lower in tests with low air velocities and illustrate this by presenting results from their experiments. They explain the difference in concentrations by pointing out that still air presents a considerable resistance to mass transfer. This is directly analogous to the hypothesis presented by Myers and Nagaoka [26].

Surface conditions in test chambers are very different from what we observe in the real world. As mentioned, air velocities will be much higher at the emitting surface in small test chambers than in practice. Also, emitting materials such as particleboard are generally covered by upholstery or laminate. This positively affects the mass transfer resistance (lowers the effective mass transfer coefficient and Biot number for mass transfer) and may create a bottleneck that changes the emission dynamics.

4.2 Influence of HCHO generation in emitting material on emission dynamics

From the presented results it can be seen that while emissions in real world settings do decrease with time, the time it takes to deplete an original content of HCHO is on the order of years (with a half-life of 216 days it will take about 2.5 years for 95 % of the original content to diffuse out of the emitting material). Chamber tests reach steady state conditions – that is deplete the original content of HCHO – within a few weeks.

Figure 6 shows that emission rates change over time and that emission rates under the right conditions (higher temperature and humidity levels) can exceed those observed when test specimens are new. This departure from the behaviour predicted by models based on results from tests in small climate chambers (shown on Figure 3 and Figure 4) cannot be explained by a change in the surface mass transfer resistance alone.

Particleboards, fibreboards and plywood are all bonded by resins that contain urea-formaldehyde (UF) [33]. Unfortunately, UF resins have the undesirable trait that they react with water. The presence of free water results in hydrolysis that releases un-bound HCHO molecules from the building materials [20,33]. The strong correlation between AH and HCHO concentration levels shown on Figure 6 suggests that reactions between water and UF could be a significant source of HCHO. This implies that models may have to include considerations of the rate of generation of HCHO – e.g. as a result of hydrolysis – in order to accurately predict emission rates over time.

4.3 Perspectives

While there are a few mass transfer models that consider mass (e.g. HCHO) generation in emitting materials [34,35], not much is known about reaction rates (secondary sources) [34]. Judging from the conclusions of more recent reviews [2,36,37], it is apparent that more research into how environmental factors, such as temperature, RH and ventilation affect the emission dynamics is needed. Recent studies have shown and explained how temperature and humidity affect the initial emittable concentration, C_0, of HCHO [21–24]. However, dynamic effects, such as the reaction/generation rate and how the ambient environment affects this rate, still need to determined.

Liu, Ye and Little [36] describe Wang and Zhang's model [35] as the "most general" analytical solution. Like the models used for the above comparison, this model is also a one-phase exponential decay model that has been validated against the data published by Yang et al. [18]. As such, it shares some of the problems described in the discussion (i.e. unknown mass generation rate, unknown mass transfer resistance at emitting surface and material properties are assumed constant). As this is also one of the most – if not the most – recent of the VOC emission models, it can be concluded that more development is needed before models based on mass transfer theory can be used to estimate development in VOC emissions under real world conditions.

Since models based on mass transfer theory still cannot accurately predict VOC emissions under real world conditions, an alternative is needed. Recent work by Rackes and Waring [29] suggest that data driven (statistical) models may be such an alternative.

5 Conclusion

Comparing predictions from emission models for VOC based on mass transfer theory validated against results from small test chambers using fans to ensure ideal mixing to practical observations from homes, large test chambers and full scale experiments reveal that such emission models overestimate emission rates and underestimate the time it takes to deplete the original content of un-bound HCHO.

A part of the reason for the observed discrepancy might be that a test environment with high air velocity increases convective mass transfer rates to a level that is not observed outside such a test environment. Therefore scenarios in test chambers should be considered a subset of all emission scenarios and, as such, cannot be seen as representative of all emission scenarios.

The emission models included in this comparison were all based on the assumption that change in the concentration in an emitting material is determined by diffusion alone. It is implicit to this assumption that generation is negligible. Results of the comparison between predictions and observations indicate that models may have to include considerations of VOC generation in emitting materials in order to accurately predict emission rates over time.

It is concluded that models validated against experiments made in test chambers using a fan for ideal mixing are not suitable for estimating development in emissions under real world conditions.

6 Acknowledgments

We would like to thank Jianyin Xiong, Ph.D., Distinguished Research Fellow, Director of the Institute of Thermal Engineering, Beijing Institute of Technology for providing insight and expertise that greatly helped in our research.

We would also like to thank Weihui Liang, Ph.D., Research Assistant Professor, School of Architecture and Urban Planning, Nanjing University and Professor Xudong Yang, PhD, Deputy Director of the Department of Building Science, School of Architecture, Tsinghua University for sharing their data on long term HCHO emissions (Figure 6).

Finally we want to thank Ásta Logadóttir, PhD, Senior Researcher, Danish Building Research Institute, Aalborg University and Professor Lars Gunnarsen, PhD, Danish Building Research Institute, Aalborg University for collecting and sharing the data on HCHO concentration levels in newer Danish homes (Figure 5).

References

[1] J.C. Little, A.T. Hodgson, A.J. Gadgil, Modeling emissions of volatile organic compounds from new carpets, Atmos. Environ. 28 (1994) 227–234. doi:10.1016/1352-2310(94)90097-3.

[2] Y. Zhang, J. Xiong, J. Mo, M. Gong, J. Cao, Understanding and controlling airborne organic compounds in the indoor environment: Mass transfer analysis and applications, Indoor Air. 26 (2016) 39–60. doi:10.1111/ina.12198.

[3] J. Xiong, Y. Yao, Y. Zhang, C-history method: Rapid measurement of the initial emittable concentration, diffusion and partition coefficients for formaldehyde and VOCs in building materials, Environ. Sci. Technol. 45 (2011) 3584–3590. doi:10.1021/es200277p.

[4] S. Huang, J. Xiong, Y. Zhang, A rapid and accurate method, ventilated chamber C-history method, of measuring the emission characteristic parameters of formaldehyde/VOCs in building materials, J. Hazard. Mater. 261 (2013) 542–549. doi:10.1016/j.jhazmat.2013.08.001.

[5] X. Zhang, J. Cao, J. Wei, Y. Zhang, Improved C-history method for rapidly and accurately measuring the characteristic parameters of formaldehyde / VOCs emitted from building materials, Build. Environ. 143 (2018) 570–578. doi:10.1016/j.buildenv.2018.07.030.

[6] I. Andersen, G.R. Lundqvist, L. Mølhave, Indoor air pollution due to chipboard used as a construction material, Atmos. Environ. 9 (1975) 1121–1127. doi:10.1016/0004-6981(75)90188-2.

[7] J.J. Hoetjer, F. Koerts, A Model for Formaldehyde Release from Particleboard, in: ACS Symp. Ser., 1986: pp. 125–144. doi:10.1021/bk-1986-0316.ch011.

[8] G. Guyot, M.H. Sherman, I.S. Walker, Smart ventilation energy and indoor air quality performance in residential buildings: A review, Energy Build. 165 (2018) 416–430. doi:10.1016/j.enbuild.2017.12.051.

[9] Directive 2010/31/EU of the European Parliament and of the Council of 19 May 2010 on the energy performance of buildings, European Union, 2010.

[10] P. Wargocki, W. Bischof, P. Carrer, M.-N. Asimakopoulou, E. de O. Fernandes, O. Hänninen, F. Allard, B. Malvik, O. Seppänen, T. Popov, S. Palkonen, S. Kephalopoulos, M. Braubach, M.-E. Héroux, HealthVent - Final report - Health-based Ventilation Guidelines for Europe, Kgs. Lyngby, Denmark, 2013.

[11] IEA-EBC Annex 68 - Indoor air quality design and control in low energy residential buildings, (n.d.). http://www.iea-ebc-annex68.org/about_annex-68 (accessed May 17, 2018).

[12] F. Haghighat, H. Huang, C.-S. Lee, Modeling approaches for indoor air VOC emissions from dry building materials - A review, ASHRAE Trans. 111 (2005) 635–645.

[13] M. Kleiber, R. Joh, R. Span, D3 Properties of Pure Fluid Substances, in: VDI Heat Atlas, Springer Berlin Heidelberg, Berlin, Heidelberg, 2010: pp. 301–418. doi:10.1007/978-3-540-77877-6_18.

[14] C.J. Weschler, W.W. Nazaroff, Semivolatile organic compounds in indoor environments, Atmos. Environ. 42 (2008) 9018–9040. doi:10.1016/j.atmosenv.2008.09.052.

[15] H. Huang, F. Haghighat, Modelling of volatile organic compounds emission from dry building materials, Build. Environ. 37 (2002) 1349–1360. doi:10.1016/S0360-1323(01)00116-0.

[16] Y. Xu, Y. Zhang, An improved mass transfer based model for analyzing VOC emissions from building materials, Atmos. Environ. 37 (2003) 2497–2505. doi:10.1016/S1352-2310(03)00160-2.

[17] B. Deng, C.N. Kim, An analytical model for VOCs emission from dry building materials, Atmos. Environ. 38 (2004) 1173–1180. doi:10.1016/j.atmosenv.2003.11.009.

[18] X. Yang, Q. Chen, J.S. Zhang, R. Magee, J. Zeng, C.Y. Shaw, Numerical simulation of VOC emissions from dry materials, Build. Environ. 36 (2001) 1099–1107. doi:10.1016/S0360-1323(00)00078-0.

[19] K. Qian, Y. Zhang, J.C. Little, X. Wang, Dimensionless correlations to predict VOC emissions from dry building materials, Atmos. Environ. 41 (2007) 352–359. doi:10.1016/j.atmosenv.2006.07.042.

[20] W. Liang, S. Yang, X. Yang, Long-Term Formaldehyde Emissions from Medium-Density Fiberboard in a Full-Scale Experimental Room: Emission Characteristics and the Effects of Temperature and Humidity, Environ. Sci. Technol. 49 (2015) 10349–10356. doi:10.1021/acs.est.5b02217.

[21] W. Liang, M. Lv, X. Yang, The combined effects of temperature and humidity on initial emittable formaldehyde concentration of a medium-density fiberboard, Build. Environ. 98 (2016) 80–88. doi:10.1016/j.buildenv.2015.12.024.

[22] J. Xiong, W. Wei, S. Huang, Y. Zhang, Association between the emission rate and temperature for chemical pollutants in building materials: General correlation and understanding, Environ. Sci. Technol. 47 (2013) 8540–8547. doi:10.1021/es401173d.

[23] S. Huang, J. Xiong, C. Cai, W. Xu, Y. Zhang, Influence of humidity on the initial emittable concentration of formaldehyde and hexaldehyde in building materials: experimental observation and correlation, Sci. Rep. 6 (2016) 23388. doi:10.1038/srep23388.

[24] S. Huang, J. Xiong, Y. Zhang, Impact of temperature on the ratio of initial emittable concentration to total concentration for formaldehyde in building materials: Theoretical correlation and validation, Environ. Sci. Technol. 49 (2015) 1537–1544. doi:10.1021/es5051875.

[25] J. Xu, J. (Jensen) Zhang, X. Liu, Z. Gao, Determination of partition and diffusion coefficients of formaldehyde in selected building materials and impact of relative humidity, J. Air Waste Manag. Assoc. 62 (2012) 671–679. doi:10.1080/10962247.2012.665812.

[26] G.E. Myers, M. Nagaoka, Emission of formaldehyde by particleboard: effect of ventilation rate and loading on air-contamination levels, For. Prod. J. 31 (1981) 39–44.

[27] W.F. Lehmann, Effect of ventilation and loading rates in large chamber testing of formaldehyde emissions from composite panels, For. Prod. J. 37 (1987) 31–37.

[28] E.L. Hult, H. Willem, P.N. Price, T. Hotchi, M.L. Russell, B.C. Singer, Formaldehyde and acetaldehyde exposure mitigation in US residences: In-home measurements of ventilation control and source control, Indoor Air. 25 (2015) 523–535. doi:10.1111/ina.12160.

[29] A. Rackes, M.S. Waring, Do time-averaged, whole-building, effective volatile organic compound (VOC) emissions depend on the air exchange rate? A statistical analysis of trends for 46 VOCs in U.S. offices, Indoor Air. 26 (2016) 642–659. doi:10.1111/ina.12224.

[30] A. Logadóttir, L. Gunnarsen, Formaldehydkoncentrationen i nybyggede huse i Danmark, 2008.

[31] J. Xiong, T. Yang, J. Tan, L. Li, Y. Ge, Characterization of VOC emission from materials in vehicular environment at varied temperatures: Correlation development and validation, PLoS One. 10 (2015) 1–21. doi:10.1371/journal.pone.0140081.

[32] T.W. Zinn, D. Cline, W.F. Lehmann, Long-Term Study of Formaldehyde Emission Decay from Particleboard, Proc. Washingt. State Univ. Int. Part. Mater. Ser. Symp. (1990) 95–103.

[33] T. Salthammer, S. Mentese, R. Marutsky, Formaldehyde in the Indoor Environment, Chem. Rev. 110, 2536–2572., Chem. Rev. 110 (2010) 2536–2572.

[34] C.S. Lee, F. Haghighat, W.S. Ghaly, A study on VOC source and sink behavior in porous building materials - Analytical model development and assessment, Indoor Air. 15 (2005) 183–196. doi:10.1111/j.1600-0668.2005.00335.x.

[35] X. Wang, Y. Zhang, General analytical mass transfer model for VOC emissions from multi-layer dry building materials with internal chemical reactions, Chinese Sci. Bull. 56 (2011) 222–228.

doi:10.1007/s11434-010-4254-5.

[36] Z. Liu, W. Ye, J.C. Little, Predicting emissions of volatile and semivolatile organic compounds from building materials: A review, Build. Environ. 64 (2013) 7–25. doi:10.1016/j.buildenv.2013.02.012.

[37] Y.F. Mao, Z. Li, Y. Zhang, Y.L. He, W.Q. Tao, A review of mass-transfer models and mechanistic studies of semi-volatile organic compounds in indoor environments, Indoor Built Environ. 0 (2017) 1–15. doi:10.1177/1420326X17704275.

Paper 3. Effect of formaldehyde on ventilation rate and energy demand in Danish homes: Development of emission models and building performance simulation

Submitted to Building Simulation on 10th February 2019.

Effect of formaldehyde on ventilation rate and energy demand in Danish homes: Development of emission models and building performance simulation

Authors

Christopher Just Johnston* [a,b], Rune Korsholm Andersen [b], Jørn Toftum [b], Toke Rammer Nielsen [b].

[a] The NIRAS Group, Sortemosevej 19, 3450 Allerød, Denmark

[b] Department of Civil Engineering, Technical University of Denmark, Brovej 118, 2800 Kgs. Lyngby, Denmark

* Corresponding author: cjj@niras.dk

Abstract

Building performance simulation (BPS) tools need valid emission models to quantify the effects building generated pollution has on indoor air quality (IAQ) and energy demand. Predictions from existing emission models for volatile organic compounds have been shown not to correspond well with real world observations.

This study aimed to approximate the impact building generated pollution has on the energy demand of Danish homes fitted with balanced mechanical ventilation systems using heat recovery. Two emission models were developed by regression analysis: One for normal level and one for high level formaldehyde (HCHO) emission rates. Data came from measurements done in detached and semi-detached homes in rural or sub-urban Denmark. Analysis included temperature, humidity and air changes per hour (ACH) as possible predictor variables. ACH was found to be the most important predictor.

The emission models were implemented into a validated BPS tool, IDA ICE. Simulations showed it was necessary to have an ACH of minimum 0.22 h^{-1} to safeguard against HCHO. Two control strategies could prevent harmful levels of HCHO: A base level ventilation rate of 0.3 $l/(s \cdot m^2)$ and a demand controlled ventilation (DCV) system using HCHO as a control variable. The DCV systems with heat recovery improved IAQ and reduced energy demand up till 3 % seen relative to constant air volume ventilation systems with heat recovery.

Based on considerations of the current level of technology and pricing, it was recommended to continue the current practice of prescribing base ventilation rates. Still, building generated pollution deserves continued attention.

Keywords

- Building generated pollution
- Emission models
- Regression analysis
- Building performance simulations
- Demand controlled ventilation

Nomenclature

A	Floor area of the room	[m^2]
AH	Absolute humidity	[g/m^3]
C_a	Concentration in the chamber or room air	[kg/m^3]
C_s	Concentration in the supply air	[kg/m^3]
E	Emission rate estimated by models derived from regression analysis	[$mg/(s \cdot m^2)$]
G_a	Volume flow rate of air	[m^3/s]
$G_{a,max}$	Maximum volume flow rate for the DCV system	[m^3/s]
n	Air exchange rate	[s^{-1}]
N	Air change rate per hour	[h^{-1}]
PLR	Part load of the flow [0,1]	[-]
R	Emission rate	[$kg/(s \cdot m^2)$]
SFP_{Frac}	Fraction of the SFP a DCV is running [0,1]	[-]
t	Time	[s]
T	Absolute temperature	[K]
V	Volume of the room	[m^3]

Greek symbols

θ	Temperature	[°C]

Acronyms

ACH	Air change per hour
AH	Absolute humidity (total mass of water vapour in unit volume of air)
BPS	Building performance simulation
BR18	The Danish Building Regulations of 2018
CAV	Constant air volume
CO_2	Carbon dioxide
DCV	Demand controlled ventilation
HCHO	Formaldehyde
IAQ	Indoor air quality
IDA ICE	Building performance simulation tool
NMF	Neutral model format
RH	Relative humidity
SVOC	Semi-volatile organic compound
SFP	Specific fan power
SI	Supplementary Information
TC	Thermal comfort
VAV	Variable air volume
VOC	Volatile organic compound
WHO	World Health Organization

1 Introduction

While many chemical processes in the indoor air are known, there is no consensus on what type of emission – if any – that can be used as a proxy for building generated pollution [1]. The reason is that the chemistry of the indoor air is complex and driven by many processes in the air and on interior surfaces [2–4]. There are daily cycles driven by factors such as the presence of daylight and ambient pollution (e.g. ozone and nitrogen dioxide) [5]. Here volatile organic compounds (VOCs) can react with ozone and form potentially harmful reactive oxygen species [6]. Adding to the complexity is that chemical components in our cleaning products, personal care products, furniture and building materials change over time [7]. Also, legislation regulating the use of chemicals in our indoor environment varies from country to country. Despite the complex nature of indoor air chemistry, researchers have suggested that a carefully selected proxy will allow a building performance simulation (BPS) tool to estimate the energy demand and overall indoor air quality (IAQ) without a detailed chemical model [1].

A suitable proxy for building generated pollution may consider two main categories of pollutants: VOCs and semi-volatile organic compounds (SVOCs). SVOCs are different from VOCs in that they readily condense on surfaces in the indoor environment [8]. Once introduced, SVOCs may migrate throughout the indoor environment sticking to surfaces and dust. This has two immediate consequences. The first is that modelling SVOC behaviour is a lot more complex. The other is that SVOCs cannot be handled by ventilation alone. In addition to ventilation, SVOCs have to be managed by source control, cleaning and potentially also by sealing or removal. Since the overall aim of the project was to study the impact that building generated pollution has on the energy demand in homes, it was chosen to disregard the impact SVOCs have on the IAQ. This allowed for a simpler model only considering the impact of pollutants that primarily stay in the gas phase.

As several researchers before us, we chose to use formaldehyde (HCHO) as a proxy [1,9]. There were several reasons for this choice. Since HCHO is used in resins to bond fibreboards and plywood, it is prevalent in both construction materials and furniture [10]. Being ubiquitous in our environment and a known carcinogen [11], HCHO has been the subject of investigation for decades and has been used as the foundation for several VOC emission models [12]. As a result, the behaviour and prevalence of HCHO is well documented. HCHO emission rates have been found to be dependent on the loading ratio (the ratio of the surface area of the emitting material to the room/chamber volume) [13,14] and changes in temperature [15–18], humidity level [16,17,19,20] and air change per hour (ACH) [21–25]. Also, although well understood and heavily regulated, HCHO still poses a problem in indoor environments. An example of this is a Danish study that documented indoor levels in excess of the World Health Organization (WHO) guidelines of 0.1 mg/m^3 in 2 out of 20 homes [11,26].

In order for BPS tools to determine the effects of building generated pollution on IAQ and energy demand, they need valid emission models. Our recent study of emission models found that predictions from existing emission models for VOCs did not correspond well with real world observations [27–30]. The conclusion was that the examined existing models underestimated the influence of the ACH on VOC emission rates. Since the attempts at identifying a suitable emission model in the existing literature failed, it was decided to develop VOC emission models by regression analysis of data collected in buildings in practice. The first part of this article presents work done to develop HCHO emission models based on regression analysis performed on data collected in 20 newer Danish homes [26]. It is worth noting that these emission models have not been created as a substitute for chemical or mass transfer models. Rather, the models are examples of how applied science can make use of assumptions and mathematics to create a temporary solution to an immediate problem such as missing valid emission models.

The second part of this article presents work done to approximate the impact that building generated pollution has on the energy demand of a building fitted with a balanced mechanical ventilation system using heat recovery. The method was to implement the developed emission models into an already existing building performance simulation (BPS) tool, IDA ICE [31].

This study assumed that demand controlled ventilation (DCV) can help lower the energy demand of homes while at the same time delivering high IAQ. Results from our recent study comparing the performance of natural ventilation with that of balanced mechanical ventilation showed that fan power accounted for less than 5 % of the combined energy demand for heating and ventilation [32]. One of the conclusions of the study was that heat recovery from exhaust air is one of the most efficient ways to reduce the energy demand in Danish homes. Consequently, heat recovery from exhaust air was implemented as a standard feature in all ventilation systems examined in this study.

This study was different from previous studies examining the performance of DCV systems [1] in that it included multiple concurrent control variables, namely temperature (θ), relative humidity (RH), carbon dioxide (CO_2) and HCHO. While it would be possible to use the method presented in this article to estimate the impact that building generated pollution has on a specific building in terms of energy demand, the simulation model was designed with a different purpose. The simulation model has been used to gain insight into when which control variable was dominant, what volume flow rate was needed to satisfactorily meet set criteria for selected control variables and asses the value of prescribed minimum ventilation rates. The simulation model was also used to examine the relative performances of different control systems in terms of energy demand and IAQ. In order to ensure that results were representative of overall trends rather solutions optimised to a given design, the simulation model was kept simple consisting of a single room with generic occupancy and equipment.

2 Method

2.1 Development of formaldehyde emission models

2.1.1 Data sample

HCHO emissions were estimated based on data on concentration levels gathered by Logadóttir and Gunnarsen [26]. The data set included observations from 20 newer Danish homes. The measurements were conducted in 2008 and the average age of the homes was 2.75 years.

Logadóttir and Gunnarsen measured HCHO concentration levels, ACH, temperature, RH and room geometry. Their study included notes on whether occupants smoked indoors and the type of ventilation system. Where the study did not include information on background HCHO levels or mention the type of outdoor environment (urban, suburban or rural) it did report that homes were either detached or semi-detached. This allowed the assumption that measurements were done in a suburban or rural environment which, in turn, allowed the assumption that HCHO background levels were 0.001 mg/m^3 [33].

HCHO emission rates were calculated using Eq. 2. The relationship was derived from Eq. 1 under the assumption that the ACH, supply air concentration and indoor air concentration were constant during measurements.

$$\frac{dC_a(t)}{dt} = \frac{R(t)A}{V} + C_s(t)n(t) - C_a(t)n(t) \qquad \textit{Eq. 1}$$

Where	C_a is the concentration in the room air	[kg/m^3]
	C_s is the concentration in the supply air	[kg/m^3]
	R is the emission rate	[kg/(s·m^2)]
	n is the air exchange rate	[s^{-1}]
	t is the time	[s]
	V is the room volume	[m^3]
	A is the floor area of the room	[m^2]

$$R = \frac{V(C_a n - C_s n)}{A} \quad \textit{Eq. 2}$$

Logadóttir and Gunnarsen did not include estimations of the loading ratio in their report. Assuming a constant room height, the floor area was used as a proxy for the loading ratio. To allow comparison between different room sizes, the derived emission rates were normalised by the floor area. After also normalising the derived emission rates by ACH it became possible to describe the distribution with a log-normal distribution function. The test for log-normality identified a single outlier. Figure 1 shows the distribution of the emission rates normalised by area and ACH as it is without the outlier. Table 1 shows the descriptive statistics of the log-normal distribution.

Table 1 – Descriptive statistics of the log-normal distribution of the normalised emission rates

Statistic	[mg·h/(h·m^2)]
Mean	0.181
Mode	0.0825
Median	0.105
StdDev	0.0615

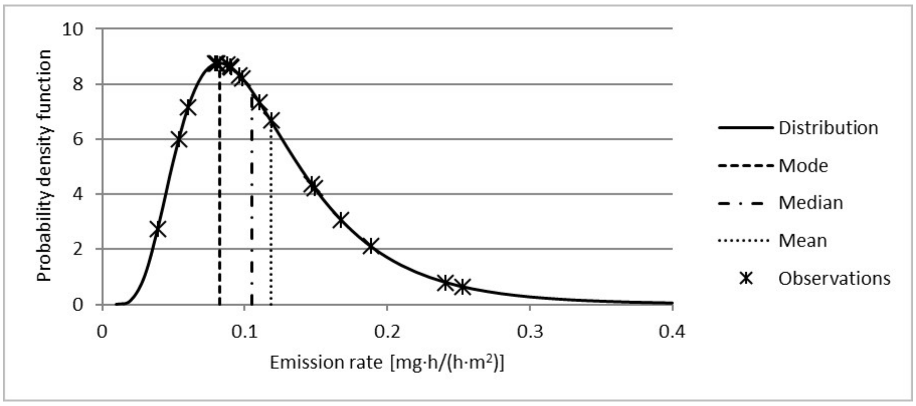

Figure 1 – Log-normal distribution describing normalised emission rates and observations

The emission rates normalised by area and ACH were divided into three groups; low, normal and high. Low emissions were found in the first quartile (up till 25 %) (≤ 0.0753 mg·h/(h·m^2)), normal in the second quartile (from 25 % to 75 %) (0.0753 mg·h/(h·m^2) < R < 0.146 mg·h/(h·m^2)) and high in the third quartile (from 75 % and up) (≥ 0.146 mg·h/(h·m^2)). Three observations were classified as being low emission rates, 10 as normal and 7 as high. The outlier (ID F15 in Table 2) was found among the high emission rates.

Figure 2 shows the emission rates normalised by area only plotted over ACH. The cross on Figure 2 marks the outlier. Table 2 contains a selection of the data collected by Logadóttir and Gunnarsen [26]. The second to last column contains HCHO emission rates normalised by area only. The last column contains HCHO emission rates normalised by both area and ACH.

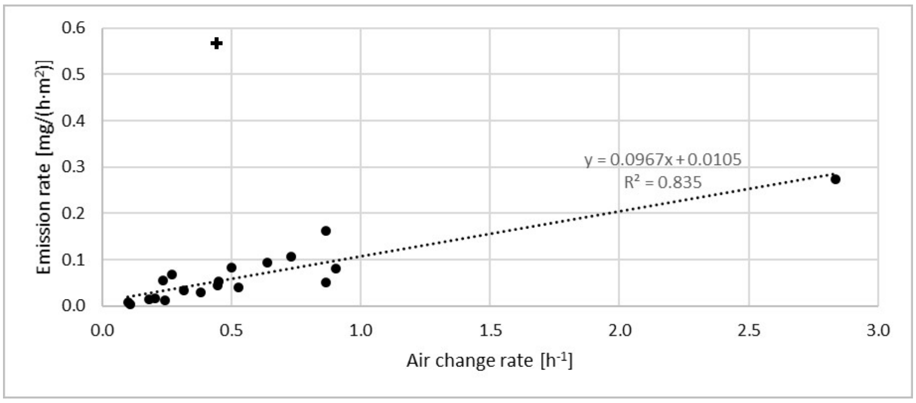

Figure 2 – HCHO emission rates derived from measured concentrations plotted over ACH – outlier marked with a cross

Table 2 – Data collected by Logadóttir and Gunnarsen [26] and derived normalised HCHO emission rates – outlier marked in bold

Level	ID	ACH	Temp.	RH	Conc.	Emission rate	
		[h^{-1}]	[°C]	[%]	[mg/m^3]	[$mg/(h \cdot m^2)$]	[$mg \cdot h/(h \cdot m^2)$]
Low	F16	0.11	21.0	51	0.018	4.26E-03	3.91E-02
	F12	0.24	22.3	66	0.024	1.30E-02	5.39E-02
	F5	0.86	18.8	53	0.029	5.23E-02	6.05E-02
Normal	F8	0.52	20.0	58	0.034	4.15E-02	7.91E-02
	F4	0.38	20.6	54	0.035	3.06E-02	8.03E-02
	F17	0.18	22.8	43	0.033	1.45E-02	8.06E-02
	F20	0.20	22.0	49	0.030	1.78E-02	8.74E-02
	F6	0.90	22.0	37	0.031	8.13E-02	9.00E-02
	F9	0.10	27.0	51	0.036	8.99E-03	9.08E-02
	F10	2.84	24.2	59	0.042	2.73E-01	9.64E-02
	F18	0.45	24.0	55	0.040	4.40E-02	9.86E-02
	F14	0.31	23.4	58	0.050	3.46E-02	1.10E-01
	F11	0.45	22.4	53	0.050	5.32E-02	1.18E-01
High	F1	0.73	23.7	41	0.050	1.07E-01	1.47E-01
	F19	0.64	26.4	44	0.064	9.50E-02	1.49E-01
	F2	0.50	17.6	56	0.069	8.35E-02	1.67E-01
	F3	0.86	19.6	51	0.081	1.63E-01	1.89E-01
	F13	0.23	26.2	43	0.104	5.65E-02	2.41E-01
	F7	0.27	22.0	44	0.110	6.82E-02	2.53E-01
	F15	**0.44**	**22.4**	**55**	**0.550**	**5.67E-01**	**1.28E+00**

2.1.2 Regression analysis

2.1.2.1 Independent variables

Temperature, RH, absolute humidity (AH) and ACH were included in the analysis as possible predictor variables. While both humidity and temperature are associated with ACH, this association was assumed negligible. Each possible predictor may affect emission in its own way [10]. ACH may work as a proxy for the driving potential for mass transport from material to air; increasing the ACH increases the concentration difference and therefore may increase the emission rate. Temperature may work as a proxy for kinetic energy in the HCHO molecules; increasing the temperature increases kinetic energy which helps molecules break their chemical bonds and therefore may increase the emission rate. Humidity may work as a proxy for production rate of HCHO; increasing the humidity level may increase the rate with which HCHO is being released from resin by hydrolysis and thereby increase the emission rate.

2.1.2.2 Zero-emission assumptions

Acknowledging the significance of the low number of observations in the respective bins and the narrow bands of the predictor variables, analyses in some instances also included assumptions for scenarios with zero-emission. It was assumed that emissions would go towards zero-as temperatures neared -19 °C, which is the boiling point of HCHO. Crossing this temperature, un-bound formaldehyde will undergo a phase change from a gaseous to a liquid state. While emissions can still continue by evaporation, it was assumed that this effect was negligible.

It was assumed that net emissions would go towards zero as the ACH neared zero. With no influx of clean air to dilute concentration levels, an equilibrium will be reached. At this equilibrium the flux of desorbed HCHO will be equal to the adsorbed totalling a net emission of zero. Of course, net positive emissions will continue in the time before a steady state is reached. However, it was judged that the assumption of zero-emissions at zero ACH was reasonable in the context of the regression analysis.

It was assumed that net emissions would go towards zero as the humidity levels neared zero. In the absence of un-bound HCHO molecules the rate of HCHO emission depends on urea−formaldehyde depolymerisation and hydrolysis, which needs water [16]. In the absence of water, HCHO emissions would continue until the time that stores of un-bound HCHO are depleted. However, it was judged that the assumption of zero-emissions at zero RH and AH was reasonable in the context of the regression analysis.

The assumptions were included in the regression analysis by adding fabricated "observations" to the pool of data. Since assumptions for zero-emission were included in the pool of data they did not constitute actual boundary conditions. Emission models were trained on the expanded data pool but were not forced to zero-emissions. A total of 12 fabricated data sets were added to the pool; 4 data sets per assumption. The fabricated data sets each contained a unique combination of values for the predictor variables. Table 3 shows the combinations of predictor variables used to train the regression model using the assumption of zero-emission.

Table 3 – Fabricated "observations" added to data pool to train model with assumptions of zero-emission

Predictor		Temperature				Humidity				ACH			
Θ	[°C]	-19	-19	-19	-19	10	30	10	30	10	30	10	30
RH	[%]	40	80	40	80	0.1	0.1	0.1	0.1	40	40	80	80
ACH	[h^{-1}]	0.2	0.2	0.4	0.4	0.2	0.2	0.4	0.4	0.01	0.01	0.01	0.01

2.1.2.3 Regression technique

The regression analysis was performed in Matlab. Emission models were developed in two steps. The first step was to identify potential models. This was done using the Matlab function for stepwise linear regression to construct models and the Akaike information criterion to estimate the relative quality of the constructed models. The next step was to test potential models by leave-one-out cross-validation. The models with the lowest cross-validation root-mean-square error were chosen. Using cross-validation allowed models to be trained on the complete data set (for each given bin) and ensured that the selected models were among the best to predict values in the held-out test sets. All included terms were statistically significant ($p < 0.05$).

2.2 Dynamic simulation of performance

The purpose of the BPS was to study the impact that building generated pollution has on the energy demand and ventilation rates in a building fitted with a balanced mechanical ventilation system using heat recovery.

In order to do so, it was necessary to perform a parameter variation. Therefore, both BPS tool and model design needed to allow this. Furthermore, the chosen BPS tool also had to allow ventilation to react in response to the dynamic emissions of the HCHO emission models developed by regression analysis.

IDA ICE [31] is a validated open source BPS tool that has a built-in function that facilitates a parameter variation. Users can extend IDA ICE's functionality by importing blocks coded in either neutral model format (NMF) or Modelica. As such, IDA ICE was a well suited tool. The HCHO emission models were coded in NMF.

The BPS model was kept simple with generic construction parts and occupancy profile. Complex design features were avoided in order to ensure that identified trends were indeed generic and uninfluenced by specificities like overly intricate occupancy patterns or mass transport between zones in a complicated geometry. The model constituted a single room occupied by a single person that showered in the morning, left during office hours and cooked in the evening. In this way, the model could be said to be reminiscent of a small studio apartment.

The focus of the study was on energy demand and ventilation control. In order to ensure that ventilation rates were determined by need and not capacity, the main ventilation system had a larger than standard capacity. The pseudo-random influence of wind and stack driven infiltration can make trends harder to identify. Therefore, infiltration was disabled in the model. Also, the model ignored transient moisture effects; the only moisture that was considered was that which was present in the included air volumes.

2.2.1 Building performance simulation model

The model was subjected to Danish weather conditions (with Köppen climate classifications Cfb and Dfb, respectively corresponding to a temperate oceanic climate and a warm-summer humid continental climate).

The model consisted of a single rectangular room with a floor area of 20 m^2 (4 m x 5 m) and a room height of 2.6 m. The outer walls had a U-value of 0.30 $W/(m^2 \cdot K)$, the floor slab a value of 0.20 $W/(m^2 \cdot K)$, and the roofing construction a value of 0.20 $W/(m^2 \cdot K)$. The U-values are consistent with the minimum requirements given in the Danish Building Regulations 2018 (BR18) [34].

The building had two windows on the 4 m long north-facing façade of the model. The dimensions of the windows were 1.23 x 1.48 m. The windows had a U-value of 1.67 $W/(m^2K)$ and a g-value of 0.68. The windows were placed in the northern façade to minimise the impact of solar radiation on the indoor temperatures.

Thermal bridges along the perimeter of the windows and the ground slab were included. Thermal bridges around the windows were simulated as 0.6 $W/(m \cdot K)$ and the thermal bridge around the ground slab was simulated as 0.4 $W/(m \cdot K)$. The values given for the thermal bridges are consistent with the minimum requirements given in BR18.

Operating hours were set to a full year (8760 hours) with occupancy following the profile shown in Table 4. Occupancy was simulated as a single person with an activity level of 1 Met. Simulations included moisture production from showers and cooking. Showers lasted 15 minutes from 6:45-7:00 and emitted water at a rate of $7.22 \cdot 10^{-4}$ kg/s [35]. Cooking lasted 30 minutes from 17:30-18:00 and emitted water at a rate of $1.33 \cdot 10^{-4}$ kg/s [35].

Table 4 – Occupancy profile

Weekday	Time interval	Occupancy
Mon-Fri:	08:00-15:00	0.0
	15:00-17:00	0.5
	17:00-08:00	1.0
Sat-Sun:	00:00-24:00	1.0

Heating was simulated using an ideal heater with a set-point temperature of 21 °C. Heating was simulated as being active all year round. The model did not include mechanical cooling. All cooling was done by ventilation with air at outdoor temperatures.

2.2.1.1 Ventilation control

The ventilation rate was controlled based on temperature, RH, CO_2 and HCHO. The control included a scheduling function that was used to select which of the control variables that would be included in a given simulation. Separate PI controllers were used to determine the ventilation volume flow rate based on the levels of the control variables. In scenarios including multiple control variables, the ventilation rate was determined by the variable requiring the highest ventilation rate. A schematic of the ventilation control system is shown in Figure 3. Set-points for ventilation control are shown in Table 5.

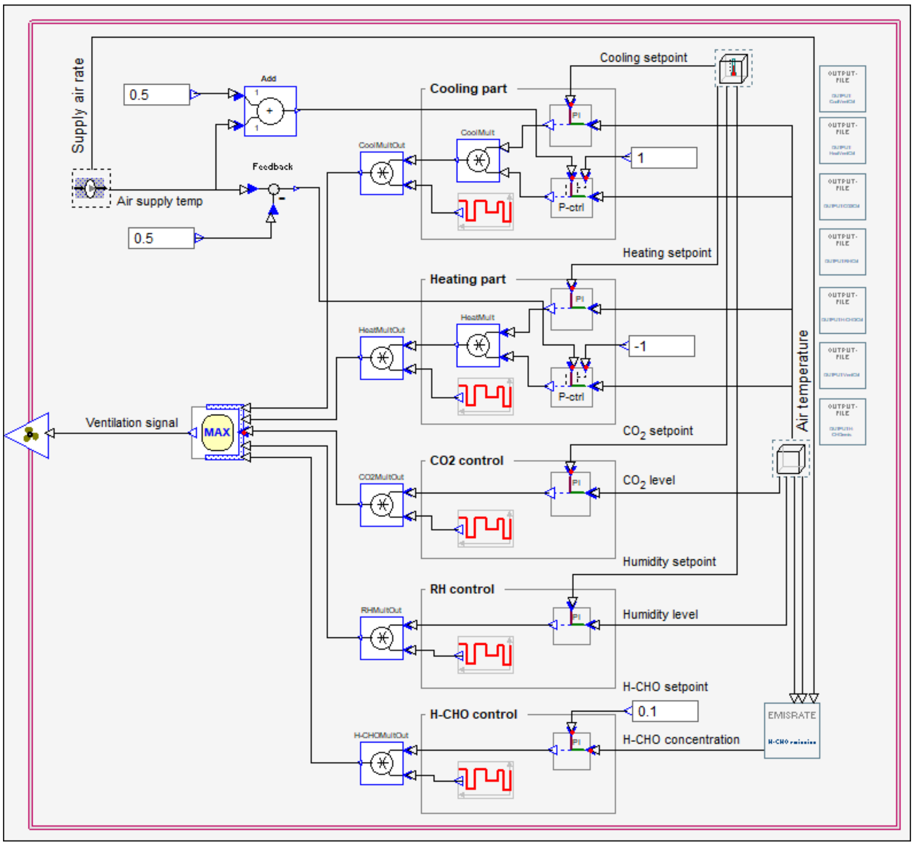

Figure 3 – Schematic of the ventilation control system in IDA ICE

Table 5 – Set-points for ventilation control

Variable	θ	RH	CO_2	HCHO
Unit	[°C]	[%]	[ppm]	[mg/m^3]
Min	21	20	700	0.0
Max	25	80	1100	0.1

Background levels for CO_2 and HCHO were 400 ppm and 0.001 mg/m^3, respectively [33]. Minimum and maximum ventilation rates depended on the examined scenario.

Five different ventilation systems were simulated (ventilation rates are normalised by unit floor area):

A. Constant air volume (CAV) at 0.3 l/(s·m^2)
B. DCV with a base ventilation rate of 0.3 l/(s·m^2)
C. DCV without a base ventilation rate (allowing a ventilation rate of 0 l/(s·m^2))
D. DCV with exhaust and a base ventilation rate of 0.3 l/(s·m^2)
E. DCV with exhaust without a base ventilation rate (allowing a ventilation rate of 0 l/(s·m^2))

Table 6 – Volume flow rates for the five different ventilation systems

ID	Ventilation [l/(s·m2)]		Exhaust [l/s]	
	Min	Max	Cooking	Shower
A	0.3	0.3	0	0
B	0.3	7	0	0
C	0	7	0	0
D	0.3	7	20	15
E	0	7	20	15

Table 6 shows the volume flow rates associated with the different ventilation systems listed above. The ventilation rate for CAV and base ventilation rate for the DCV systems correspond to the minimum rate stated in BR18. The maximum rate of 7 l/(s·m^2) was chosen to enable DCV to meet set-points for all control variables (disregarding problems that could arise from draught). When included, exhaust was simulated as 0.45 l/(s·m^2) during showers and 0.7 l/(s·m^2) during cooking. Added to the base ventilation rate, the total ventilation rate was 15 l/s and 20 l/s during showers and cooking respectively. These ventilation rates correspond to the minimum criteria for exhaust as stated in BR18. Infiltration was not included in the calculations.

While designing the ventilation control system (Figure 3) it became apparent that it was not possible to solve the mass balance for HCHO (Eq. 1) using the total ACH; it was only possible to link the mass balance to one air flow (as opposed to the sum of all air flows). The mass balance was connected to the supply airflow of the main ventilation system. Therefore, the extra exhaust in systems D and E did not affect HCHO levels in the model. With infiltration set to zero, the only source of error was the extra exhaust. As the extra exhaust was only activated for a total of 45 minutes a day, it was assumed that the long term influence on the HCHO concentration was negligible. The extra exhaust did influence RH and CO_2 levels.

Specific fan power (SFP) values for the CAV and DCV system were both set to 1800 J/m^3 which is the highest allowed by BR18 for CAV (the allowed value for variable air volume (VAV) and DCV is 2100 J/m^3). Fans had an efficiency of 60 %.

The ventilation systems all used heat recovery with an effectiveness of 80 %. Exhaust ventilation did not use heat recovery and the make-up air volumes were therefore all delivered at outdoor temperatures.

2.2.1.2 Parameter variation/scenarios

The model built in IDA ICE was used to simulate scenarios for different ventilation systems with varying control settings.

Simulations were run for normal and high levels of HCHO emission. The column labelled Emis shows which scenarios have normal (N) and high (H) emission levels. Also, simulations were run with controls set to be active during all hours and with controls set to be active during the occupied hours only. The base ventilation rate was active throughout all hours even if other controls were not active. The column labelled Occu shows which scenarios have controls active during all hours (A) and which scenarios only have controls active during the occupied hours (O). The combinations of control variables are shown on the right-hand side of Table 7. Here, an X marks an included control variable. In total, 161 scenarios were simulated.

Table 7 – Combinations of control variables used in simulations for the four DCV systems

Emis	Occu
N	O
N	A
H	O
H	A

→

θ	CO_2	RH	HCHO
X	-	-	-
-	X	-	-
-	-	X	-
-	-	-	X
X	X	-	-
X	-	X	-
-	X	X	-
-	-	X	X
X	X	X	-
X	X	X	X

The energy demand for every scenario was calculated for two different levels of SFP; constant and variable. Comparing energy demands calculated with a constant SFP is the equivalent of comparing the summed ventilation volumes for the full year. Comparing the variable SFP of the DCV to the constant of the CAV allows incorporating an estimate of the energy savings that comes from using DCV. IDA ICE uses the method described in ASHRAE's standard 90.1:2007 [36] Appendix G to estimate a generic performance curve for a VAV aggregate. The method uses a polynomial to estimate the fraction of the max SFP a DCV system is running under given conditions. Eq. 3 shows the polynomial used by IDA ICE.

$$SFP_{Frac} = 0.0013 + (0.147 \cdot (0.9506 - 0.0998 \cdot \mathrm{PLR}) \cdot \mathrm{PLR}) \cdot \frac{G_a}{\mathrm{G_{a,max}}},$$
$$PLR = \min\left(\frac{G_a}{\mathrm{G_{a,max}}}, 1\right) \qquad \textit{Eq. 3}$$

Where	SFP_{Frac} is the fraction of the SFP a DCV is running [0,1]	[-]
	PLR is the part load of the flow [0,1]	[-]
	G_a is the volume flow rate at a given time	[m^3/s]
	$G_{a,max}$ is the maximum volume flow rate for the DCV system	[m^3/s]

3 Results

3.1 Emission models

Regression analyses were done for normal level and high level emission rates. There were not enough observations to perform the analysis for low level emission rates. The regression analyses resulted in the development of three separate models for HCHO emissions normalised by area.

$$E_{extended} = -1.123 \cdot 10^{-5}N + 3.425 \cdot 10^{-6}N \cdot AH + 2.985 \cdot 10^{-5}N^2 - 2.478 \cdot 10^{-5}N^2 \cdot AH \quad \text{Eq. 4}$$

$$E_{normal} = -1.340 \cdot 10^{-2} + 2.627 \cdot 10^{-5}N + 9.019 \cdot 10^{-5}T + 3.498 \cdot 10^{-7}AH - 1.518 \cdot 10^{-7}T^2 \quad \text{Eq. 5}$$

$$E_{high} = 1.377 \cdot 10^{-5} + 3.723 \cdot 10^{-5}N^2 \quad \text{Eq. 6}$$

Where	E is the emission rate estimated by models derived from regression analysis	[mg/(s·m^2)]
	N is the ACH	[h^{-1}]
	AH is the absolute humidity	[g/m^3]
	T is the absolute temperature	[K]

The first model is a general model for normal level emission rates (Eq. 4). The data pool consisted of 22 observations including 12 sets of data from the added assumptions for zero-emission. The model uses ACH and AH as predictor variables. The regression analysis found that neither temperature nor RH added to the predictive power of the model. The model has an adjusted R^2 of 1 and a root-mean-square error of $1.08 \cdot 10^{-6}$ mg/(s·m^2).

The second model (Eq. 5) is also for normal level emission rates but is based on data not including assumptions for zero-emission. As a possible outlier (F14) was excluded from the data, the model was based on 9 observations. The model uses ACH, AH and temperature as predictor variables. The regression analysis found that RH did not add to the predictive power of the model. The model has an adjusted R^2 of 1 and a root-mean-square error of $4.2 \cdot 10^{-7}$ mg/(s·m^2).

The high adjusted R^2 values for the two models for normal emission rates are not reliable measures of the goodness of fit. Rather, the high adjusted R^2 values are due to the high ratio of predictor variables to observations. As such, the adjusted R^2 values overestimate the variance that is explained by the independent variables. Here, the emission models for normal emission rate are overfitted.

The third model (Eq. 6) is for high level emission rates and is based on data not including assumptions for zero-emission. As a possible outlier (F21) was excluded from the data, the model was based on 6 observations. The model only uses ACH as a predictor variable. The regression analysis found that AH, RH and temperature did not add to the predictive power of the model. The model has an adjusted R^2 of 0.9 and a root-mean-square error of $3.31 \cdot 10^{-6}$ mg/(s·m^2).

3.1.1 Residual analysis

Analyses of normal probability plots found that residuals, on the whole, appear to follow a normal distribution. Still, there were indications of deviation from normality on the plots for the first and second model. On the plot for the first model (Eq. 4) (Figure 4), there was one data set at the end of the right hand tail did not follow the normal distribution. The value was identified as the highest measured emission rate in the bin for normal level HCHO emissions (ID F11 in Table 2). The residuals from the second model (Eq. 5) (Figure 5) follow a gentle s-shaped curve. Such a curve can indicate that a distribution may be short-tailed, meaning that it displays less variance than expected. This could be due to the low number of observations included in the analysis.

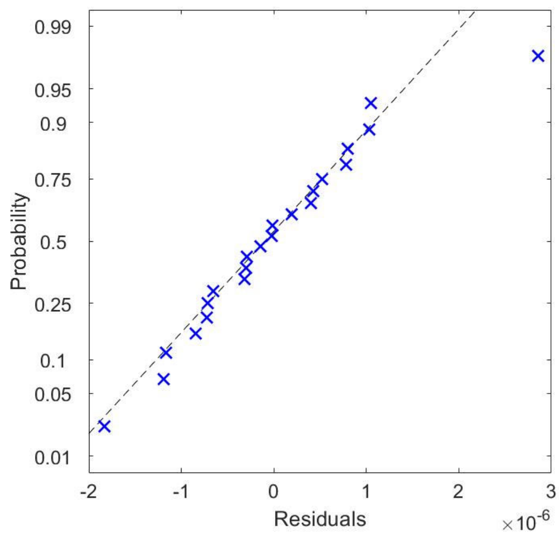

Figure 4 – Normal probability plot of residuals for normal level emission model from data including zero-emission assumptions

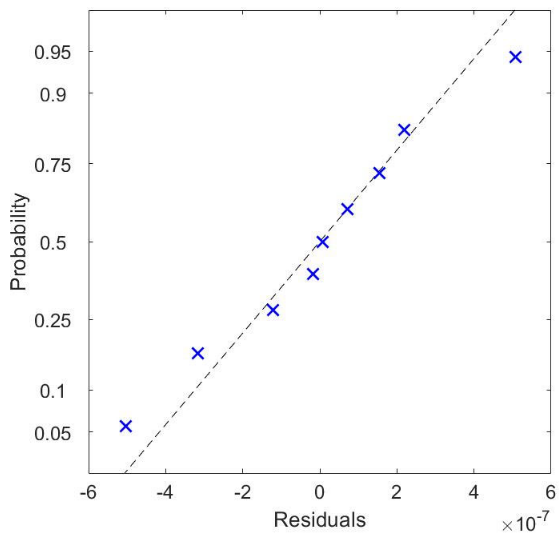

Figure 5 – Normal probability plot of residuals for normal level emission model from data without zero-emission assumptions

Analysis of standardised residuals identified two possible outliers (standardised residual > 1.96) for the first model (Eq. 4) (Figure 6). This is a little higher than what would be expected as 95 % of standardised residuals were expected to be within a band of ±1.96 ($\alpha = 0.05$). The possible outliers were identified as F11 and F6. No outliers were identified for either of the second or third models. Analysis of standardised residuals found no indication of heteroscedasticity in either of the three models. However, the low number of observations and the limited variation in the ranges of the predictor variables make it impossible to come to a definite conclusion as to whether the data is heteroscedastic or not.

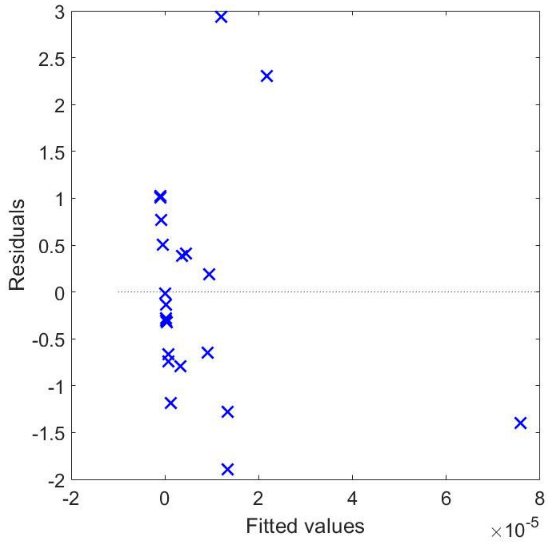

Figure 6 – Plot of standardised residuals for normal level emission model from data including zero-emission assumptions

3.1.2 Evaluation of models

The above analysis found that the normal level HCHO emission model trained on data including zero-emission assumptions (Eq. 4) provide inaccurate predictions for emission rates higher than the median. Dividing the normal level emission rate group into bins for emissions below and above the median of the distribution (0.105 mg·h/(h·m^2)) shows that the lower bin contains 8 observations while the higher bin contains 2. The inability to accurately predict higher emission rates may be explained by the low number of observations of emission rates higher than the median.

Figure 7 shows how temperature affects the predicted normal level HCHO emission rate (Eq. 5). The effect is inconsistent with findings from earlier studies that suggest a continuous increase in emission rates with increasing temperatures. This limits the use of the model; the model cannot be used to estimate emission rates at temperatures higher than those included in the observations (F9 was measured at 27 °C). Possible explanations for the observed inconsistency are that the model may describe random error or noise instead of the underlying relationship and that the model is trained on a data set that does not contain observations above 27 °C. However, the effects are statistically significant (for both terms including temperature $p < 0.009$).

While it was found that the elements of the second model (Eq. 5) do not have a direct physical interpretation (and misinterprets the effect of temperature on emission), the predictive power for conditions found in the indoor environment is higher than that of the first model (Eq. 4). So, despite its flaws, it was found that the model for normal emission rates based on data without including assumptions of zero-emission (Eq. 5) has value in the framework of the study.

Besides being based on a very small sample of observations, no issues were identified during analysis of the residuals from the emission model for high level emission rates (Eq. 6).

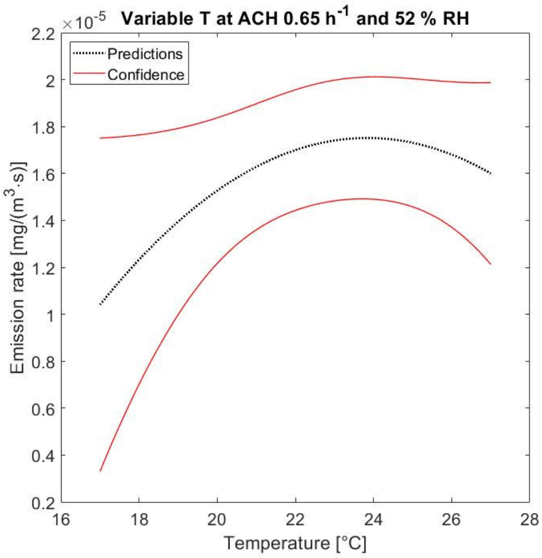

Figure 7 – Influence of temperature on model for normal level emission from data without zero-emission assumptions

3.1.3 Limitations on use of models

While the quality of the data used for the regression analysis was good, the number of observations was low. Also, due to the nature of conditioned indoor environments, all measurements were done within a narrow band of temperature, RH and ACH. Therefore, the use of the expressions for normal emission rates based on data not including assumptions for zero-emission (Eq. 5) is limited to temperatures ranging from 17 °C to 27 °C, RHs ranging from 30 % to 80 % and ACHs ranging from 0.05 h^{-1} to 3 h^{-1}. The use of the expression for high emission rates based on data not including assumptions for zero-emission (Eq. 6) is limited to ACHs ranging from 0.1 h^{-1} to 1.5 h^{-1}.

The measurements used to develop the models were made in detached and semi-detached Danish homes. Presumably in a sub-urban and/or rural environment. The models can be used to estimate emission rates only in such homes.

3.2 Simulation output

Results focused on IAQ, thermal comfort (TC) and energy demand. TC refers to temperature levels only. IAQ refers to the levels of HCHO, CO_2 and RH. Here HCHO was a proxy for building generated pollution while CO_2 was a proxy for pollution from occupants. RH levels were a result of occupancy, activities (cooking and showering) and outdoor conditions and were primarily considered as a pollutant that could harm the building itself (e.g. cause mould infestation and rot in wood).

The results were scored for TC and IAQ as either A, B or C. The scenarios received an A if they had less than 25 hours above the values in Table 8, a B if they had between 25 and 100 hours and a C if they had above 100 hours. The value used to evaluate temperature corresponded to the upper limit for summer of category 1 in EN 15251 [37]. The value used to evaluate CO_2 (700 ppm above outdoor levels) was in compliance with the guidelines given by the Danish Working Environment Authority [38] (< 1500 ppm) and corresponded to category 3 in EN 15251. The value used to evaluate RH corresponded to category 4 in EN 15251. The value used to evaluate HCHO corresponded to the guidelines set by WHO [11] and BR18.

Table 8 – Evaluation criteria for simulated scenarios

	Limit
θ	25.5 °C
CO_2	1100 ppm
RH	80 %
HCHO	0.1 mg/m^3

The energy demand was simulated in part as a heating demand and in part as the auxiliary energy used for driving the ventilation systems. Due to the simplicity of the model, the calculated energy demands were not expected to relate to any real world energy demand. Therefore, the energy demand calculated in the simulations only had value when seen relative to each other. The energy demands are presented relative to the CAV reference scenario. To allow for easy interpretation, the energy demand for the reference scenario was defined as zero. This means that positive values for energy demand indicated a higher energy demand than the CAV scenario.

The below text contains an interpretation of the obtained results. For a full view of all obtained results readers are referred to the spread sheet in the Supplementary Information (SI). Table 9 contains a suite of selected results that are representative of the trends found in the simulation results. The scores for temperature, CO_2 and HCHO are for the fully occupied hours (Mon-Fri 17:00-08:00 and Sat-Sun 00:00-24:00, see Table 4). The presented scores for RH are for all hours of the year.

The energy demands for constant and variable SFPs are for the full year and are given in relative terms. Energy demands calculated for a constant SFP are in the column labelled conSFP. Energy demands calculated for a variable SFP are in the column labelled varSFP. Columns conSFP and varSFP contain intervals for energy demand. The intervals comprise of results from simulations with varying HCHO emission levels and with ventilation controls turned on and off outside the occupied hours (see left-hand side of Table 7) (8 results per interval). The intervals show the lowest and highest calculated changes in energy demand relative to the reference CAV scenario.

An X in the column labelled B03 indicates that the scenarios have a base ventilation rate of 0.3 l/(s·m^2) while the absence indicates that there was no base ventilation. Results from the reference CAV scenario are shown in row #1.

Table 9 – Selected results from simulations showing scores and relative energy demands

#	Control variables				B03	Scores				Energy demand	
	θ	CO_2	RH	HCHO		θ	CO_2	RH	HCHO	conSFP [%]	varSFP [%]
1	-	-	-	-	CAV	B	C	C	A	0	0
2	X	-	-	-	X	A	C	C	A	[0.6,2.4]	[-0.1,-2.0]
3	X	-	-	-	-	B	C	C	C	[-9.6,-10.9]	[-9.9,-11.1]
4	-	X	-	-	X	B	A	C	A	[0.8,2.5]	[-0.1,-1.8]
5	-	X	-	-	-	B-C	A	C	A-C	[-0.5,-1.7]	[-2.5,-3.8]
6	-	-	X	-	X	B	C	A	A	[0.7,2.5]	[-0.1,-1.9]
7	-	-	X	-	-	C	C	A-C	C	[-6.6,-7.9]	[-7.4,-8.9]
8	-	-	-	X	X	B-C	C	C	A	[0.1,2.0]	[-0.5,-2.3]
9	-	-	-	X	-	C	C	C	A	[-3.8,-10.2]	[-5.3,-10.8]
10	X	X	-	-	X	A	A	C	A	[1.2,2.9]	[0.2,-1.5]
11	X	X	-	-	-	A	A	C	A-C	[-0.1,-1.3]	[-2.1,-3.5]
12	X	-	X	-	X	A	C	A	A	[1.1,2.9]	[0.3,-1.6]
13	X	-	X	-	-	A	C	A-C	C	[-6.1,-7.4]	[-7.0,-8.4]
14	-	X	X	-	X	B	A	A	A	[1.3,3.0]	[0.3,-1.4]
15	-	X	X	-	-	B-C	A	A-C	B-C	[-0.1,-1.3]	[-2.1,-3.5]
16	-	-	X	X	X	B	C	A	A	[0.7,2.5]	[-0.1,-1.9]
17	-	-	X	X	-	C	C	A-C	A	[-3.0,-7.9]	[-4.5,-8.9]
18	X	X	X	-	X	A	A	A	A	[1.6,3.3]	[0.6,-1.2]
19	X	X	X	-	-	A	A	A-C	A-C	[0.3,-0.9]	[-1.8,-3.1]
20	X	X	X	X	X	A	A	A	A	[1.6,3.3]	[0.6,-1.1]
21	X	X	X	X	-	A	A	A-C	A	[1.1,-0.9]	[-1.1,-3.1]

The base ventilation rate of 0.3 $l/(s \cdot m^2)$ – used in the reference CAV scenario (row #1) – was found to keep HCHO concentrations for both normal and high level emissions below 0.1 mg/m^3 at all times.

Two ventilation strategies met all success criteria; one considered temperature, CO_2 and RH while employing a base ventilation rate of 0.3 $l/(s \cdot m^2)$ (#18) and the other considered all four control variables during all hours of the year (#21). The score of C for RH in #21 was for scenarios where the ventilation was off during unoccupied hours. Compared to the reference CAV scenario (#1) the first successful ventilation strategy (#18) had a higher energy demand at constant SFP ([1.6,3.3]) and a comparable energy demand at variable SFP ([0.6,-1.2]).

Compared to the reference CAV scenario (#1) the second successful ventilation strategy (#21) had a comparable energy demand at constant SFP ([1.1,-0.9]) and a lower energy demand at variable SFP ([-1.1,-3.1]). Scenarios without exhaust performed better than scenarios with exhaust in terms of energy demand. The scenario without exhaust and a normal level of HCHO emission had an energy demand that was 3.1 % lower than the reference CAV scenario. The scenario without exhaust and a high level of HCHO emission had an energy demand that was 2.5 % lower than the reference CAV scenario.

It has not been possible to estimate the effect that exhaust has on maximum HCHO concentration levels. The reason is that the emission models cannot handle RH levels above 80 % and that exhaust primarily influences the duration of high RH levels. Adding exhaust was found to lead to an average drop in total emitted mass of HCHO of about 2 %.

Table 10 – Selected results from simulations showing ACHs

¤	Control variables				B03	ACHs [h^{-1}] – Total time (incl. unoccupied hours)				
	θ	CO_2	RH	HCHO		Min	Max	Mean	Median	StdDev
1	X	-	-	-	-	[0.01,0.01]	[9.52,9.52]	[0.10,0.11]	[0.01,0.01]	[0.69,0.70]
2	-	X	-	-	-	[0.12,0.12]	[0.46,0.46]	[0.35,0.35]	[0.42,0.43]	[0.13,0.13]
3	-	-	X	-	-	[0.07,0.07]	[2.17,2.43]	[0.15,0.15]	[0.12,0.12]	[0.11,0.11]
4	-	-	-	X	-	[0.08,0.22]	[0.14,0.22]	[0.10,0.22]	[0.09,0.22]	[0.02,0.00]
						ACHs [h^{-1}] – During occupancy				
5	X	-	-	-	-	[0.01,0.01]	[9.52,9.52]	[0.12,0.12]	[0.01,0.01]	[0.77,0.78]
6	-	X	-	-	-	[0.13,0.13]	[0.46,0.46]	[0.40,0.40]	[0.45,0.45]	[0.10,0.10]
7	-	-	X	-	-	[0.07,0.07]	[2.17,2.43]	[0.15,0.15]	[0.12,0.12]	[0.11,0.11]
8	-	-	-	X	-	[0.08,0.22]	[0.14,0.22]	[0.10,0.22]	[0.09,0.22]	[0.02,0.00]

Table 10 shows ACHs for control of single variables. Results are from scenarios where ventilation control systems were always on. The values on the left-hand side of the intervals are for normal HCHO emission rates while the values on the right-hand side are for high HCHO emission rates.

An ACH of 0.22 h^{-1} was needed to keep HCHO concentration levels at the WHO guideline value of 0.1 g/m^3 for high HCHO emission levels (¤4 and ¤8). For this scenario, the resultant ACH was constant. The reason was that high level HCHO emissions rates were estimated from the ACH alone (see Eq. 6). Since the ACH controlled the HCHO concentration levels and no other variables were considered, the solution to the mass balance became the same at every time step.

In terms of ACH, the most demanding control variable was temperature (¤1 and ¤4). Results show that an ACH of 9.52 h^{-1} was needed to keep temperatures at the set-point of 25 °C while at peak load. The mean and median ACHs were both low and indicated that there for the simulated building design were relatively few instances of peak loads and that they were comparatively short.

4 Discussion

4.1 Indoor air quality

A significant proportion (> 50 %) of Scandinavian homes have ACHs below 0.5 h^{-1} [39–41]. A recent study comparing the methods used for determining these ventilation rates (real-time measurements of occupant generated CO_2 and passive tracer gas collected in tubes) concluded that the used methods may well overestimate ACHs by a factor of 2-3 [42]. This indicates that average ventilation rates in Scandinavia might be lower than what studies have shown. Considering that the simulations showed that ACHs of minimum 0.22 h^{-1} are required to effectively safeguard against HCHO, it is fair to conclude that building generated pollution also deserves future attention.

The study found two control strategies that could effectively prevent harmful levels of HCHO: A base level ventilation rate of 0.3 $l/(s{\cdot}m^2)$ and a DCV system that considers HCHO as a control variable. Considering current technology and prices, the former is probably the most viable option at present. As such, it must be recommended to continue current practice of prescribing base ventilation rates. However, current developments in sensor technology suggest that microscale gaseous HCHO detection systems will soon reach a mature level that will allow low-cost batch production [43]. When this happens, it might be worth considering changing the standards.

Meanwhile, it is worth asking if HCHO is the best indicator of building generated pollution. HCHO can come from a variety of sources (including combustion in car engines) and current developments might well mean that outdoor levels can increase [44]. Other pollutants might prove more useful as proxies for the general level of emissions from building materials [45,46], but presently there are hardly any VOCs that have been studied as much as HCHO.

4.2 Emission models

The regression analysis was performed on the basis of a very small data set. Still, correlations between predictor variables and the dependent variable were all statistically significant. It was possible to identify two trends: ACH was a predictor in all models, RH in none. Temperature and AH were significantly correlated with the dependent variable in some models.

It is clear that the findings of this study support the findings of previous studies that have identified ACH as a powerful predictor variable [24,25]. The roles of the other possible predictor variables are less clear. To the best of our knowledge, there are no studies that have shown a statistically significant correlation between HCHO emission rates and temperature and humidity. Based solely on the presented regression analysis, it is not possible to conclude whether changes in temperature or humidity influence dynamics in HCHO emissions. However, there is still reason to believe that at least one of these may.

As explained, each possible predictor variable may influence the chemistry in a given material. Though inconclusive, the regression analysis may indicate that humidity does influence the rate of emission: Seen relative to RH, AH appears to be a much better predictor. If humidity did not influence the emission rate, the stepwise linear regression algorithm should be as likely to pick RH as it should AH. There may also be a physical explanation as to why AH would be a better predictor than RH. AH is a direct measure of the amount of water present in the air. RH is dependent on both temperature and AH. So, if the humidity level does influence the rate of production (or release by hydrolysis), it stands to reason that the AH would be the better indicator of the potential.

Temperature was only significantly correlated to the dependent variable in one model. In laboratory tests [15,17], changes in temperature have been shown to increase the initial emittable concentration. It has been hypothesised that increasing the temperature increases the rate of emission because the increase in kinetic energy helps HCHO molecules break the bonds that keep them adsorbed to the surfaces in porous materials. This then may have no effect on the rate of production. Since the initial emittable concentration has been seen to be depleted within weeks in laboratory experiments, it is possible that subsequent HCHO emissions are limited by the rate of production – and therefore not significantly influenced by changes in temperature. Either way, more research is needed before it can be concluded whether temperature influences the dynamics of emission rates in the long term.

The performed regression analysis is comparatively simple. Qian et al. have published an emission model where coefficients have been regressed to the (dimensionless) parameters [47]. As their model is non-linear (with power terms that are non-integers), it is wholly conceivable that stepwise linear regression does not allow the identification of the correct expression for an emission model. Nevertheless, the derived models for normal and high level emissions (Eq. 5 and Eq. 6) both give good predictions for HCHO emission rates within the stated boundaries and – being simple and easily implementable – therefore has value in the context of BPS.

4.3 Energy demand

Disregarding future usefulness, the prevalence of HCHO in building materials combined with the developed understanding of the processes governing emissions makes HCHO useful for studies such as the present. While the emission models implemented in the IDA ICE model cannot be used to predict concentration levels in homes, they can be used to run dynamic simulations allowing us to determine a first-order approximation of the impact that building generated pollution has on the IAQ and energy demand.

To this day, buildings take up 40 % of the energy demand in both the EU and the US [48,49]. Despite efforts to upgrade the building stock in Denmark, the energy demand for buildings has remained constant during the last 25 years [50]. The results from the study show that, when compared to CAV systems with heat recovery, DCV systems with heat recovery can improve IAQ and that it is possible to obtain these improvements without a negative impact to the energy demand. With the advent of microscale sensors, it might be possible to obtain these improvements along with a reduction in the energy demand of up till 3 %. This reduction in the energy demand would not be insignificant on a societal scale.

It is worth noting that previous studies that have investigated how DCV impacts energy demand have reported possible reductions well in excess of 3 % [1]. However, most previous studies have not included heat recovery as part of their ventilation designs. In this study, the reported reductions in energy demand are calculated relative to the performance of a CAV ventilation system with heat recovery. Since heat recovery on exhaust air itself is an efficient energy reduction measure [27–30], the potential impact of DCV is lower in a system using heat recovery. Therefore, the relative improvements reported in this study are lower than the average of reported reductions in energy demand.

At the current price of energy, a reduction of the energy demand of approximately 3 % will not offset the costs of installation of such advanced ventilation systems. From the point of view of the end user, the selling point would be improvements to IAQ and TC. These benefits can be obtained from well near any balanced mechanical ventilation system with heat recovery. Therefore, it might be necessary to change future legislation in order to harvest the energy saving potential of advanced ventilation systems.

5 Conclusion

Emission models developed by regression analysis represent an alternative to emission modelling based on mass transfer theory. With information on the baseline level of emission in a given indoor environment, this type of model can estimate emission rates for indoor environments under varying conditions. Since it is possible to express this type of emission model by simple equations, they can easily be implemented in BPS tools. Based on this, it is concluded that emission models developed by regression analysis can be used in BPS to estimate the effect building generated pollution has on IAQ and energy demand.

The findings of the regression analysis support the findings of previous studies that have identified ACH as a powerful predictor variable for HCHO emissions. The roles of temperature and humidity as possible predictor variables are less clear. Based solely on the presented regression analysis, it is not possible to conclude whether changes in temperature or humidity influence dynamics in HCHO emissions.

The results from the dynamic simulation in IDA ICE, incorporating emission models for HCHO, show that it is necessary to have ACHs of minimum 0.22 h^{-1} to effectively safeguard against HCHO. Considering the level and price of current technology, it was recommended to continue the practice of prescribing base ventilation rates. Still, building generated pollution deserves future attention.

Compared to the performance of CAV ventilation systems, DCV systems can help improve both IAQ and TC. The study found two control strategies that could effectively prevent harmful levels of HCHO: A base level ventilation rate of 0.3 $l/(s \cdot m^2)$ and a DCV system that considers HCHO (as a proxy for building generated pollution) as a control variable.

Current developments in sensor technology suggest that microscale gaseous HCHO detection systems will soon reach a mature level that will allow low-cost batch production. With the advent of microscale sensors, DCV systems with heat recovery might be able to deliver improvements in IAQ along with a reduction in the energy demand of up till 3 % seen relative to CAV ventilation systems with heat recovery. Due to the low price of energy and the high price of DCV systems, it might be necessary to change legislation in order to harvest the energy saving potential of advanced ventilation systems.

6 Acknowledgments

We would like to thank Ásta Logadóttir, PhD, Senior Researcher, Danish Building Research Institute, Aalborg University and Professor Lars Gunnarsen, PhD, Danish Building Research Institute, Aalborg University for collecting and sharing the data on HCHO concentration levels in newer Danish homes [26].

References

[1] Guyot G, Sherman MH, Walker IS. Smart ventilation energy and indoor air quality performance in residential buildings: A review. Energy Build. 2018;165:416–30.

[2] Weschler CJ. Chemistry in indoor environments: 20 years of research. Indoor Air. 2011 Jun;21[3]:205–18.

[3] Rim D, Gall ET, Maddalena RL, Nazaroff WW. Ozone reaction with interior building materials: Influence of diurnal ozone variation, temperature and humidity. Atmos Environ. Elsevier Ltd; 2016 Jan;125:15–23.

[4] Waring MS. Secondary organic aerosol in residences: predicting its fraction of fine particle mass and determinants of formation strength. Indoor Air. 2014 Aug;24[4]:376–89.

[5] Morrison G. Recent Advances in Indoor Chemistry. Curr Sustain Energy Reports. 2015 Jun 7;2[2]:33–40.

[6] Hopke PK. Air Pollution and Health Effects. Nadadur SS, Hollingsworth JW, editors. London: Springer London; 2015. 355-380 p. [Molecular and Integrative Toxicology].

[7] Weschler CJ. Changes in indoor pollutants since the 1950s. Atmos Environ. Elsevier Ltd; 2009;43[1]:153–69.

[8] Xu Y, Zhang J (Jensen). Understanding SVOCs. ASHRAE J. 2011;53[12]:121–5.

[9] Ye W, Won D, Zhang X. A Simple VOC Prioritization Method to Determine Ventilation Rate for Indoor Environment Based on Building Material Emissions. Procedia Eng. Elsevier B.V.; 2015;121:1697–704.

[10] Salthammer T, Mentese S, Marutsky R. Formaldehyde in the Indoor Environment, Chem. Rev. 110, 2536–2572. Chem Rev. 2010;110[4]:2536–72.

[11] WHO Regional Office for Europe. WHO Guidelines for indoor air quality - Selected pollutants. Copenhagen, Denmark; 2010.

[12] Zhang Y, Xiong J, Mo J, Gong M, Cao J. Understanding and controlling airborne organic compounds in the indoor environment: Mass transfer analysis and applications. Indoor Air. 2016;26[1]:39–60.

[13] Andersen I, Lundqvist GR, Mølhave L. Indoor air pollution due to chipboard used as a construction material. Atmos Environ. 1975 Jan;9[12]:1121–7.

[14] Hoetjer JJ, Koerts F. A Model for Formaldehyde Release from Particleboard. In: ACS symposium series.

1986. p. 125–44.

[15] Huang S, Xiong J, Zhang Y. Impact of temperature on the ratio of initial emittable concentration to total concentration for formaldehyde in building materials: Theoretical correlation and validation. Environ Sci Technol. 2015;49[3]:1537–44.

[16] Liang W, Yang S, Yang X. Long-Term Formaldehyde Emissions from Medium-Density Fiberboard in a Full-Scale Experimental Room: Emission Characteristics and the Effects of Temperature and Humidity. Environ Sci Technol. 2015;49[17]:10349–56.

[17] Liang W, Lv M, Yang X. The combined effects of temperature and humidity on initial emittable formaldehyde concentration of a medium-density fiberboard. Build Environ. Elsevier Ltd; 2016;98:80–8.

[18] Xiong J, Wei W, Huang S, Zhang Y. Association between the emission rate and temperature for chemical pollutants in building materials: General correlation and understanding. Environ Sci Technol. 2013;47[15]:8540–7.

[19] Huang S, Xiong J, Cai C, Xu W, Zhang Y. Influence of humidity on the initial emittable concentration of formaldehyde and hexaldehyde in building materials: experimental observation and correlation. Sci Rep. 2016;6[April]:23388.

[20] Xu J, Zhang J (Jensen), Liu X, Gao Z. Determination of partition and diffusion coefficients of formaldehyde in selected building materials and impact of relative humidity. J Air Waste Manag Assoc. 2012;62[6]:671–9.

[21] Myers GE, Nagaoka M. Emission of formaldehyde by particleboard: effect of ventilation rate and loading on air-contamination levels. For Prod J. 1981;31[7]:39–44.

[22] Lehmann WF. Effect of ventilation and loading rates in large chamber testing of formaldehyde emissions from composite panels. For Prod J. 1987;37[4]:31–7.

[23] Hult EL, Willem H, Price PN, Hotchi T, Russell ML, Singer BC. Formaldehyde and acetaldehyde exposure mitigation in US residences: In-home measurements of ventilation control and source control. Indoor Air. 2015;25[5]:523–35.

[24] Offermann FJ, Maddalena R, Offermann JC, Singer BC, Wilhelm H. The impact of ventilation on the emission rates of volatile organic compounds in residences. 10th Int Conf Heal Build 2012. 2012;1:2–7.

[25] Rackes A, Waring MS. Do time-averaged, whole-building, effective volatile organic compound (VOC) emissions depend on the air exchange rate? A statistical analysis of trends for 46 VOCs in U.S. offices. Indoor Air. 2016 Aug;26[4]:642–59.

[26] Logadóttir A, Gunnarsen L. Formaldehydkoncentrationen i nybyggede huse i Danmark. Statens Byggeforskningsinstitut. 2008.

[27] Tommerup H, Svendsen S. Energy savings in Danish residential building stock. Energy Build. 2006 Jun;38[6]:618–26.

[28] Dodoo A, Gustavsson L, Sathre R. Primary energy implications of ventilation heat recovery in residential buildings. Energy Build. Elsevier B.V.; 2011 Jul;43[7]:1566–72.

[29] Mata É, Sasic Kalagasidis A, Johnsson F. Energy usage and technical potential for energy saving measures in the Swedish residential building stock. Energy Policy. 2013 Apr;55:404–14.

[30] Laverge J, Janssens A. Heat recovery ventilation operation traded off against natural and simple exhaust ventilation in Europe by primary energy factor, carbon dioxide emission, household consumer price and exergy. Energy Build. Elsevier B.V.; 2012 Jul;50:315–23.

[31] IDA Indoor Climate and Energy (IDA ICE) [Internet]. [cited 2018 May 13]. Available from: https://www.equa.se/en/ida-ice

[32] Johnston CJ, Birck Laustsen J, Toftum J, Rammer Nielsen T. Comparing relative performance of supply air windows with conventional and heat recovery ventilation systems in a temperate climate. Manuscript submitted for publication. 2019;

[33] Kolarik B, Gunnarsen L, Funch LW. Afgivelse af formaldehyd fra byggevarer og forbrugerprodukter. Statens Byggeforskningsinstitut. 2010.

[34] Danish Building Regulations 2018. Denmark: The Danish Transport, Construction and Housing Authority; 2018.

[35] Tenwolde A, Pilon CL. The Effect of Indoor Humidity on Water Vapor Release in Homes. Therm Perform Exter Envel Whole Build X Int Conf. 2007;1–9.

[36] Goel S, Rosenberg MI, Eley C. ANSI/ASHRAE/IES Standard 90.1-2016 Performance Rating Method Reference Manual. Richland, WA (United States); 2017 Sep.

[37] EN 15251:2007 - Indoor environmental input parameters for design and assessment of energy per formance of buildings addressing indoor air quality, thermal environment, lighting and acoustics. 1st ed. Technical Committee CEN/TC 156 "Ventilation for buildings", BSI; 2007. 54 p.

[38] Danish Working Environment Authority - Indoor climate guideline [Internet]. [cited 2018 May 10]. Available from: https://arbejdstilsynet.dk/da/regler/at-vejledninger/i/a-1-2-indeklima

[39] Bekö G, Lund T, Nors F, Toftum J, Clausen G. Ventilation rates in the bedrooms of 500 Danish children. Build Environ. Elsevier Ltd; 2010;45[10]:2289–95.

[40] Stymne H, Axel Boman C, Kronvall J. Measuring ventilation rates in the Swedish housing stock. Build Environ. 1994;29[3]:373–9.

[41] Dimitroulopoulou C. Ventilation in European dwellings: A review. Build Environ. 2012 Jan;47[1]:109–25.

[42] Bekö G, Gustavsen S, Frederiksen M, Bergsøe NC, Kolarik B, Gunnarsen L, et al. Diurnal and seasonal variation in air exchange rates and interzonal airflows measured by active and passive tracer gas in homes. Build Environ. 2016;104:178–87.

[43] Chung P-R, Tzeng C-T, Ke M-T, Lee C-Y. Formaldehyde Gas Sensors: A Review. Sensors. 2013 Apr 2;13[4]:4468–84.

[44] Salthammer T. The formaldehyde dilemma. Int J Hyg Environ Health. Elsevier GmbH.; 2015;218[4]:433–6.

[45] Kumar P, Skouloudis AN, Bell M, Viana M, Carotta MC, Biskos G, et al. Real-time sensors for indoor air monitoring and challenges ahead in deploying them to urban buildings. Sci Total Environ. Elsevier B.V.; 2016 Aug;560–561[April]:150–9.

[46] Schieweck A, Uhde E, Salthammer T, Salthammer LC, Morawska L, Mazaheri M, et al. Smart homes and the control of indoor air quality. Renew Sustain Energy Rev. Elsevier Ltd; 2018 Oct;94[July]:705–18.

[47] Qian K, Zhang Y, Little JC, Wang X. Dimensionless correlations to predict VOC emissions from dry building materials. Atmos Environ. 2007;41[2]:352–9.

[48] European Commission on Energy Efficiency in Buildings [Internet]. [cited 2018 Mar 16]. Available from: https://ec.europa.eu/energy/en/topics/energy-efficiency/buildings

[49] U.S. Energy Information Administration - How much energy is consumed in U.S. residential and commercial buildings? [Internet]. [cited 2018 Mar 16]. Available from: https://www.eia.gov/tools/faqs/faq.php?id=86&t=1

[50] The Danish Construction Association. Byggeriets Energianalyse 2017. Copenhagen, Denmark; 2017.

Report 1. ProVent – Projekteringsviden om ventilationsvinduer

The final report from the research project ProVent (project number 340-035) sponsored by ElForsk – a research and development programme under the Danish Energy Association. The aim of ProVent was to examine supply air windows in an attempt to determine the usefulness of the technology.

Report published May 2014.

Note:

There is an error in the heat balance on page 19 of the report. The term $Q_{a,in}$ should not have been subtracted. The heat balance have been corrected for use in this thesis.

With the additional term in place, based on considerations of the energy balance, it appeared possible to identify an ideal ventilation rate. This was incorrect. The error does not affect results or conclusions in the report. These are all still correct.

NIRAS

Elforsk

Maj 2014

PROVENT

PROJEKTERINGSVIDEN OM VENTILATIONSVINDUER

PROJEKT

ProVent
Elforsk

Projekt nr. 13.749.00
Version 1
Udarbejdet af CJJ og JBI
Kontrolleret af KGE

Forord

Denne rapport er resultatet af PSO projektet 340-035 ”ProVent, Projekteringsviden om ventilationsvinduer” udført med støtte fra Dansk Energi.

Projektet er gennemført af følgende projektgruppe med NIRAS som projektleder:

NIRAS A/S (projektleder):	Jacob Birck Laustsen Christopher Just Johnston Lau Markussen Raffnsøe
SBi	Rob Marsh
DTU BYG	Svend Svendsen David Appelfeld
HORN vinduer	Poul Christensen
HansenProfile A/S	Søren Haubjerg Sørensen

Juni 2014

NIRAS A/S
Sortemosevej 19
3450 Allerød

CVR-nr. 37295728
Tilsluttet FRI
www.niras.dk

T: +45 4810 4200
F: +45 4810 4300
E: niras@niras.dk

D: +45 2556 8040
M: +45 2556 8040
E: cjj@niras.dk

INDHOLD

1 RESUME

Der er stor interesse for såkaldte Ventilationsvinduer, som fungerer ved, at der føres ventilationsluft fra udeklimaet ind via en åbning i bunden af vinduet, op gennem et stort hulrum mellem glaslagene, og videre ind i bygningen via en åbning i toppen af vinduet. På vej op gennem det ventilerede hulrum sker der en vis forvarmning af den kolde udeluft, idet en del af varmetabet gennem ruden overføres til ventilationsluften som en form for varmegenvinding. Samtidig forventes det, at der kan opnås en forbedret udnyttelse af solindfaldet, idet en del af den absorberede solstråling i glaslagene transporteres med ventilationsluften ind i bygningen.

Der er forventninger om, at ventilationsvinduer kan reducere energibehovet i bygninger og eventuelt øge komforten, men der er stadig uklarhed om besparelsespotentialet, og hvordan de påvirker indeklimaet i bygninger. Idet ventilationsvinduer har dynamiske egenskaber, kan de ikke håndteres på traditionel vis i gængse bygningssimuleringsprogrammer.

I dette projekt er der udviklet en metode til at bestemme ventilationsvinduers energimæssige egenskaber og deres effekt på energibehovet i bygninger på en retvisende måde. Metoden er baseret på simuleringer i en CFD-model af ventilationsvinduet, målinger i Guarded Hot Box (GHB), samt beregningsalgoritmen WinVent. Ved at sammenholde WinVent-beregninger med CFD-simuleringer og Hot Box målingerne er det fundet, at WinVent kan bestemme ventilationsvinduers energimæssige egenskaber tilfredsstillende ved varierende fysiske rammebetingelser.

Vha. en lang række parametervariationer i WinVent er der udviklet generelle formeludtryk, som beskriver indblæsningstemperaturen og den effektive U-værdi (varmetabet fra det yderste glas til omgivelserne) som funktion af udetemperatur, volumenstrøm og solstråling. Med de udviklede formeludtryk kombineret med bl.a. g-værdien og den ”almindelige” U-værdi uden ventilation kan ventilationsvinduets energimæssige egenskaber bestemmes for vilkårlige rammebetingelser. De udviklede formeludtryk gør det således muligt, at foretage bygningssimuleringer på årsbasis med ventilationsvinduer, og på den måde bestemme deres effekt på energiforbruget og indeklima i bygninger.

Ved hjælp af den udviklede metode er der foretaget beregninger i programmet IES-VE på en simplificeret bygningsmodel med ventilationsvinduer monteret i den sydvendte facade. Beregningerne viser, at der for den konkrete model med mekanisk udsugning på en halv gang i timen, kan opnås en årlig energibesparelse på 7% ved anvendelse af ventilationsvinduer sammenlignet med tilsvarende traditionelle vinduer. Til sammenligning viser beregningerne med traditionelle men energioptimerede lavenergivinduer med tre-lags ruder og mekanisk ventilation med effektiv varmegenvinding og det samme luftskifte en

årlig energibesparelse på op til 22%. Der er i projektet ikke taget højde for effekten på eventuelt kølebehov.

Således kan anvendelse af ventilationsvinduer give en ikke ubetydelig energibesparelse, men der kan stadig opnås væsentlig større energibesparelse med traditionelle lavenergivinduer kombineret med mekanisk ventilation med varmegenvinding.

2 INTRODUKTION

2.1 Baggrund

Der har i de senere år været en stigende interesse for ventilationsvinduer, hvor den kolde udeluft forvarmes af transmissionstabet og solindfaldet i et lodret luftfyldt hulrum mellem to af vinduets glaslag. Princippet og fordelen ved vinduet er, at en del af varmetabet fra vinduet varmegenvindes til ventilationsluften som strømmer ind gennem hulrummet i vinduet. Samtidig reducerer den øgede indblæsningstemperatur generne ved kold indblæsningsluft til en vis grad sammenlignet med traditionelle vinduer med friskluftsventiler.

Der er de seneste år gennemført forskellige analyser samt forsknings- og udviklingsprojekter vedrørende ventilationsvinduers energimæssige egenskaber og deres effekt på energiforbruget i bygninger. De opnåede resultater er dog ikke enslydende og den reelle effekt er endnu ikke endeligt kortlagt på en retvisende måde. Mange analyser er kun baseret på et teoretisk grundlag og mangler at blive verificeret af empiriske målinger og tests, som kan dokumentere egenskaberne.

Samtidig er der sket betydelige stramninger af energibestemmelserne i bygningsreglementet, som stiller højere krav til ventilation og det samlede energibehov i bygninger. Det er endnu uvist om ventilationsvinduer kan leve op til disse høje krav til energiforbrug, samtidig med at der opretholdes et behageligt indeklima, som bl.a. kræver et luftskifte af en vis størrelse.

På grund af ventilationsvinduers dynamiske egenskaber kan de ikke håndteres som traditionelle vinduer i gængse bygningssimuleringsprogrammer, hvor de normalt beskrives ved bl.a. angivelse af faste U- og g-værdier.

Der er derfor et behov for at analysere og dokumentere ventilationsvinduers energimæssige egenskaber og virkemåde samt udvikle metoder til at vurdere deres reelle effekt på energiforbruget og indeklimaet i bygninger.

2.2 Formål

Formålet med projektet er at analysere ventilationsvinduers energimæssige egenskaber og bestemme deres effekt på energiforbrug og indeklima i bygninger. For at kunne regne på ventilationsvinduer og sammenligne med andre løsninger, skal der udvikles en CFD-model, som kan beskrive vinduets egenskaber. Resultaterne fra CFD-modellen sammenholdt med målinger på ventilationsvinduet i Guarded Hot Box for givne fysiske rammebetingelser, skal verificere rigtigheden af en udviklet numerisk beregningsalgoritme, som kan bestemme vinduets egenskaber for en vilkårlig kombination af rammebetingelserne. På baggrund af parametervariationer er det målet at udvikle regressionsudtryk, der kan implementeres i et bygningssimuleringsprogram, som herved kan bestemme ventilationsvinduers effekt på energiforbrug og indeklima i bygninger.

3 METODE

Formålet med den nedenfor beskrevne metode er at udarbejde en metode, der til praktisk anvendelig præcision kan kvantificere energibidraget fra det undersøgte ventilationsvindue til konditionerede indeklimaer ved givne vejrforhold. Det undersøgte ventilationsvindue antages at repræsentere et typisk gennemsnitligt ventilationsvindue i forhold til udformning og funktionalitet og er derfor egnet til generel analyse af anvendeligheden af teknologien.

Til at udarbejde den matematiske metode benyttes beregningsprogrammet WinVent (WV), måleresultater fra Guarded Hot Box (GHB) forsøg udført ved DTU BYG og Fraunhofer – Institut für Bauphysik (FH IBP) (uden solstråling) samt CFD-simuleringer af det ventilerede hulrum (ligeledes uden solstråling). Det har inden for projektets rammer ikke været muligt at foretage målinger af vinduets energimæssige egenskaber under påvirkning af solstråling.

Måleresultater fra GHB forsøg og beregnede resultater fra CFD bruges til at vurdere kvaliteten af WV's metode til at bestemme U- og g-værdier for ventilationsvinduet samt temperatur af den leverede friske luft. Idet der er vurderet tilstrækkeligt sammenfald mellem resultaterne fra beregningerne og målingerne, er det konkluderet, at de af WV bestemte resultater er anvendelige til videre analyse af ventilationsvinduet.

WV benyttes til at foretage serier af beregninger for varierende fysiske rammebetingelser (udetemperatur, volumenstrøm og strålingsintensitet). Resultaterne bruges i en multipel lineær regressionsanalyse. Regressionsanalysen har til formål at levere beregningsudtryk for energitab gennem ventilationsvinduet til omgivelserne (effektive U-værdier) og leveret friskluftstemperatur.

Beregningsudtrykkene benyttes i en dynamisk analyse af ventilationsvinduets performance over tid under danske klimaforhold. Den dynamiske analyse udføres i beregningsprogrammet IES-Virtual Environment (IESVE). I analysen bliver ventilationsvinduet testet under designmæssigt optimale forhold. Ventilationsvinduerne installeres kun i en enkelt facade, orienteres mod syd og simuleres med den volumenstrøm, der yder de bedste energitekniske resultater. Bygningen, hvori ventilationsvinduerne testes, designes således, at grundarealet sikrer, at der ved den mest effektive volumenstrøm altid er et luftskifte på en halv gang i timen, som det foreskrives af Bygningsreglementet. Det konstante luftskifte sikres ved mekanisk udsugning.

Energiforbruget for den designede bygning bliver ligeledes beregnet for situationer hvor bygningen er udstyret med almindelige 1+2 vinduer (identiske med ventilationsvinduet uden ventilation) med henholdsvis mekanisk udsugning, og balanceret mekanisk ventilation med varmegenvinding, samt nye 3-lags lavenergivinduer med mekanisk ventilation med varmegenvinding.

Energiforbrugene for de forskellige scenarier bliver sammenholdt. Udover energiforbruget bliver ventilationsvinduets indflydelse på det termiske indeklima også vurderet kort.

3.1 Fremgangsmåde

I dette afsnit bliver den anvendte metodes trin kort listet og begrundet. For detaljer om de enkelte trin henvises til de følgende relevante sektioner i metodeafsnittet.

Metoden kan groft opdeles i tre trin

1. Identifikation og validering af matematisk metode til analyse af ventilationsvinduesteknologi

2. Udformning af matematiske udtryk til beskrivelse af ventilationsvinduesteknologi

3. Anvendelse af matematiske udtryk i dynamisk analyse for kvantitativt at kunne vurdere ventilationsvinduers indflydelse på bygningers energibalance og indeklima

3.1.1 Første trin

I metodens første trin benyttes GHB måledata til at vise, at WV ved varierende volumenstrømme gennem det ventilerede hulrum præcist kan beregne både den leverede frisklufttemperatur og den mængde af energi, der går ind i systemet.

De udførte CFD simuleringer er ikke direkte sammenlignelige med GHB målingerne, fordi CFD simuleringerne ikke er foretaget med varmetransmissionbidrag fra stråling. Derfor er CFD simuleringernes evne til præcist at kunne beregne lufttemperatur og energistrøm ind i systemet ved varierende volumenstrømme blevet bestemt ved at sammenholde med resultater fra WV, som i denne sammenhæng er kørt uden bidrag fra stråling. I og med at WV er valideret på baggrund af GHB, bliver CFD simuleringerne også valideret på baggrund af GHB, hvor WV er benyttet som stedfortræder for GHB.

WV's evne til at beregne lufttemperatur og energistrøm ind i systemet ved varierende udetemperaturer bestemmes ved at sammenholde med CFD simuleringer, hvor udetemperaturen er variabel men volumenstrømmen fast. Disse sammenligninger er foretaget med resultater, der er opnået ved simuleringer uden strålingsbidrag.

Det har ikke været muligt at finde målinger, der tilstrækkeligt detaljeret dokumenterer ventilationsvinders ydelse under påvirkning af solstråling til sammenligningsgrundlag med WV's beregninger. I kraft af at WV benytter sig af den anerkendte og i ISO 15099 [1] beskrevne teori om solstråling på rudesystemer antages det, at WV korrekt kan bestemme indflydelsen af solstråling.

På bagrund af ovenstående del-trin fastslås det, at WV er egnet til projektet ProVents formål.

3.1.2 Andet trin

Der udformes to matematiske udtryk: Ét til bestemmelse af den leverede frisklufttemperatur og ét til bestemmelse af det effektive varmetab, altså det som forlader systemet til omgivelserne. De to udtryk bestemmes ved hjælp af trinvis lineær regression foretaget på baggrund af et datasæt, der er produceret ved parametervariationer udført i WV.

3.1.3 Tredje trin

I IESVE designes en forsimplet bygning med det formål, at sikre at ventilationsvinduerne bliver simuleret under de mest gunstige forhold. Til dette formål identificeres bl.a. den volumenstrøm gennem ventilationsvinduet, der minimerer systemets tab til omgivelserne. De i det andet trin udformede matematiske udtryk simplificeres og omformes til et format, som passer til IESVE og implementeres i modellen. På denne baggrund køres en dynamisk simulering.

Den konstruerede model modificeres til at kunne simulere scenarier med alternativer til ventilationsvinduer. Alternativer er eksempelvis et scenarie med almindelige lavenergiruder og balanceret mekanisk ventilation med varmegenvinding og et scenarie med almindelige lavenergiruder og udsugningsventilation.

På baggrund af de udførte dynamiske simuleringer bliver den relative effektivitet af ventilationsvinduesteknologien vurderet.

3.2 Vindueskonstruktion

Princippet i et ventilationsvindue er, at ruden er opbygget med et stort ventileret hulrum mellem de yderste og inderste glaslag. I bunden udvendigt findes en ventilationsåbning, hvor udeluften føres ind i hulrummet og op og videre ind i bygningen via en åbning i toppen på den indvendige side. På vej op gennem hulrummet overføres en del af varmetabet fra den indvendige rude til ventilationsluften, som herved forvarmes inden den sendes ind i bygningen. Således sker der en vis varmegenvinding af transmissionstabet. Ligeledes kan der ske en vis opvarmning af ventilationsluften, når der er solstråling på ruden, idet en del af den solenergi, der absorberes i glaslagene, som vender mod hulrummet, afgives som varme til luften i hulrummet. Det er dog kun en lille del af solstrålingen, som kan udnyttes til forvarmning af luften, da størstedelen transmitteres direkte igennem ruden. Princippet i ventilationsvinduet er vist på Figur 3.1.

Figur 3.1

Princip for ventilationsvindue

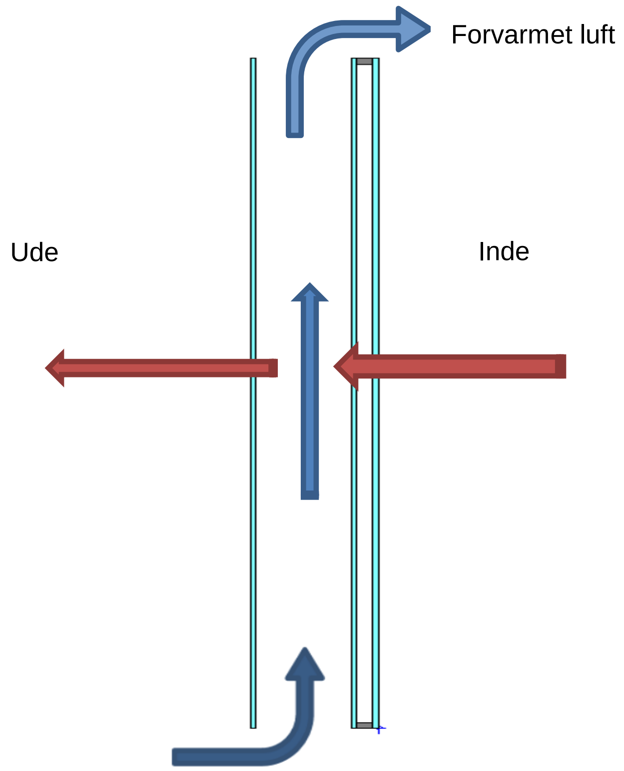

Det undersøgte ventilationsvindue er opbygget som en 1+2 vinduesløsning, dvs. et enkelt 4 mm lag glas yderst, et tykt luftfyldt ventileret hulrum i midten og en to-lags energirude med blød lavemissionsbelægning og argon inderst.

En konstruktion med et enkelt lag glas kunne alt andet lige give en større forvarmning af ventilationsluften pga. større varmetab gennem det inderste glas. Men idet det er forudsat, at der altid vil være en fast volumenstrøm gennem vinduet, for at sikre et ønsket luftskifte på en halv gang i timen, vil der, når det er koldt udenfor, være meget stor risiko for kondensdannelse på indersiden af ruden i den nederste del nær karmen. Dette er hovedårsagen til, at der er valgt en opbygning med 2-lags energirude inderst.

3.3 Guarded Hot Box (GHB)

For at undersøge om den udviklede CFD model og WinVent (WV) giver retvisende resultater af ventilationsvinduers virkemåde og energimæssige egenskaber er der som en del af projektet udført målinger af vinduets U-værdi og temperaturforhold i Guarded Hot Box (GHB) på DTU. Ligeledes er der gjort brug af GHB målinger udført på Fraunhofer-Institut für Bauphysik (IBP) [2]. GHB målingerne er udført i henhold til ISO 12567-1 [3].

3.3.1 *Forsøgsopstilling*

Måleprincippet i GHB er som følger: Forsøgsopstillingen består af en kold kasse, hvor temperaturen holdes konstant ved ca. 0 °C og en varm kasse, hvor temperaturen holdes konstant ved ca. 20 °C. I skillevæggen mellem de to kasser placeres vinduet, der skal måles på. På vinduets varme side monteres en målekasse på selve vinduet. Målekassen er forsynet med et elektrisk varmelegeme, som afgiver en kendt varmemængde. Ved at holde temperaturen konstant ved 20 °C i både den varme kasse og i målekassen og 0 °C i den kolde kasse sikres det, at alt den afgivne varme fra varmelegemet transmitteres ud gennem vinduet. Den afgivne varme fra varmelegemet i målekassen er således et direkte mål for vinduets U-værdi. Der korrigeres for eventuelle linjetab i samlingen mellem vindue og skillevæg. Forsøgsopstillingen er vist på Figur 3.2

For at kunne tage højde for ventilationsluften i ventilationsvinduet er forsøgsopstillingen modificeret ved at tilslutte en variabel udsugningsventilator til vinduets øverste ventil. Ved målingerne udført på DTU suges ventilationsluften ud på den varme side via en fleksibel kanal, som er ført gennem målekassens væg. Efter ventilatoren sendes ventilationsluften tilbage til den kolde kasse. Ventilatoren og mikromanometret sørger for, at der suges en kontrolleret mængde luft gennem vinduet. Ved at måle temperaturen af indblæsningsluften, som forlader vinduet, kan den overførte varmemængde til ventilationsluften således bestemmes. Yderligere detaljer om GHB målingerne fremgår af Appelfeld og Svendsen 2011 [4].

Forsøgsopstillingen ved målingerne udført på Fraunhofer IBP er identisk med den fra DTU, bortset fra at ventilationsluften på Fraunhofer suges direkte ud på den kolde side af vinduet via en fleksibel kanal, som er monteret udvendigt på den øverste ventil. Således udføres målingen af vinduets U-værdi korrekt efter ISO 12567-1, idet ventilationsluften gennem vinduet holdes adskilt fra målekassen og varmelegemet på den varme side. Effekten af ventilationsluften gennem vinduet kommer til udtryk i form af, at U-værdien varierer for forskellige volumenstrømme. Yderligere detaljer om GHB målingerne fra Fraunhofer IPB fremgår af rapporten fra Fraunhofer IBP [2].

Den samlede varmestrøm gennem det målte vindue inkluderer varmetabet gennem ruden og ramme/karm samt energiforbruget til at forvarme luften som transporteres fra ude til inde via det ventilerede hulrum.

Figur 3.2

Guarded Hot Box forsøgsopinstilling. Anordninger til måling af ventilation gennem vinduet er ikke vist.

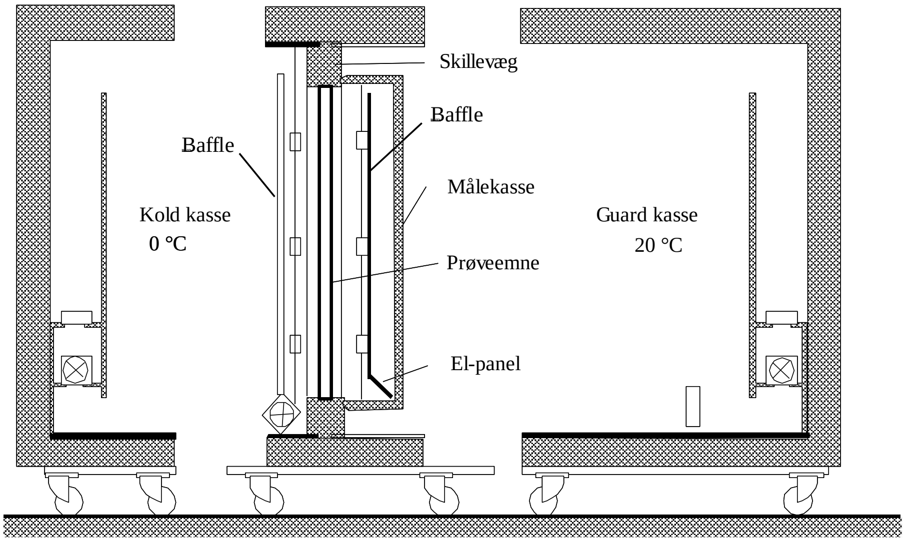

Figur 3.3

Ventilationsvinduet som blev testet i GHB ved DTU BYG.

Testvindue 1, DTU BYG.

De to vinduer der er testet er ikke 100 % identiske i opbygningen. De to testede vinduer har følgende rudeopbygning:

3.3.2 Testvindue 1, DTU BYG

Vinduet testet ved DTU BYG er opbygget af

- 4 mm float gals
- 84 mm ventileret hulrum
- 24 mm energirude, 4-16-4, med argon

Med en blød lavemissionsbelægning på overfladen i position 5 og en hård lavemissionsbelægning i position 3, talt udefra.

3.3.3 Testvindue 2, FH IBP

Vinduet testet ved FH IBP er opbygget af

- 4 mm float gals
- 100 mm ventileret hulrum
- 24 mm energirude, 4-16-4, med argon

Med en blød lavemissionsbelægning på overfladen i position 5, talt udefra.

3.3.4 Ramme/karmkonstruktion

Ramme/karmkonstruktionen er identisk for de to vinduer, bortset fra tykkelsen. På Figur 3.4 ramme/karmprofilet i Testvindue 1, fra DTU BYG vist.

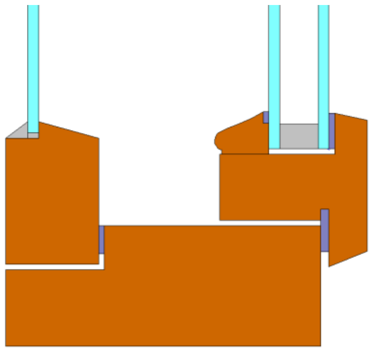

Figur 3.4

Skitse af ramme/karm i vinduet som blev testet i GHB på DTU BYG.

Testvindue 1, DTU BYG.

I de efterfølgende sammenligninger af måleresultaterne for de to vinduer og beregninger i CFD og WV er der taget højde for forskellene i de to vinduers opbygning.

3.4 Computational Fluid Dynamics (CFD)

I nedenstående tekst vil der blive givet et overordnet indblik i fremgangsmåden og de numeriske modeller, der er benyttet i forbindelse med udarbejdelsen af CFD analyserne af de undersøgte scenarier.

De udførte CFD simuleringer blev foretaget i open source programmet OpenFOAM. OpenFOAM kommer med en stribe eksempler på beregninger for forskellige typer af problemer. Udover at illustrere brugen af OpenFOAM er et af formålene med eksemplerne, at disse kan bruges som skabeloner og omformes og tilpasses til de aktuelle problemer som brugerne søger løsninger til. En styrke i denne tilgangsmåde er, at beregningseksemplerne støtter sig op af måleresultater. Det betyder, at de i eksemplerne anvendte metoder har en høj grad af troværdighed, der ellers kan være svær at skabe, når en metode designes fra bunden. Et eksempel fra OpenFOAMs katalog er benyttet som basis for undersøgelserne, der er foretaget i forbindelse med nærværende projekt.

Metoden der er udviklet til at simulere de fysiske forhold i de undersøgte ventilationsvinduer er inddelt i to trin. Det første trin er en steady state beregningsrunde på et groft mesh, der har til formål at skabe udgangspunktet for den anden beregningsrunde. Det andet trin er en pseudo-transient beregningsrunde på et forfinet mesh, der har til formål at opnå en konvergeret løsning. Opbygningen i to trin er lavet således for at nedbringe den overordnede beregningstid.

3.4.1 *Første beregningstrin: SIMPLE & groft mesh*

Første beregningstrin benytter sig af en steady state algoritme ved navn SIMPLE (Semi-Implicit Method for Pressure Linked Equations) til at løse Navier-Stokes ligningerne og en turbulens model der kendes som SST k-ω. Turbulens modellen beskrives kort i det følgende.

Det fysiske problem der arbejdes med, kan ikke løses som et steady state problem og skal i stedet løses som et pseudo-transient problem, altså ét der reelt ikke bevæger sig i tid men heller ikke har en endelig løsning. Tilfælde som dette kan opstå i sager, hvor der forekommer turbulens. I forhold til computerkraft og tid er SIMPLE metoden billigere end den følgende PISO (Pressure implicit with splitting of operator) metode og SIMPLE benyttes derfor til at skabe grundlaget for det følgende beregningstrin. Det første beregningstrin er sat til at udføre 1000 iterationer, før den opnåede løsning eksporteres til det andet beregningstrin. De 1000 iterationer er valgt på baggrund af en simpel analyse af residualer. Fra disse kan det ses, at SIMPLE efter 1000 iterationer ikke længere nærmer sig en konvergeret løsning, men at residualerne antager tilnærmelsesvist konstante værdier.

De diskretiserede dele af Navier-Stokes ligningerne og de yderligere ligninger, der er tilføjet systemet af den valgte turbulensmodel, løses med de i OpenFOAMs eksempler foreslåede diskretiseringsmetoder, solvere og under-relaxation faktorer. De valgte diskretiseringsmetoder er præcise til den første eller anden orden.

3.4.2 *Andet beregningstrin: PISO & fint mesh*

Andet beregningstrin benytter sig af en transient algoritme ved navn PISO (Pressure Implicit with Splitting of Operator) til at løse Navier-Stokes ligningerne og en turbulens model der kendes som SST k-ω. Turbulens modellen beskrives kort i det følgende.

PISO metoden er i OpenFOAM implementeret i en lettere modereret udgave under navnet PIMPLE. PISO er i ProVent benyttet i OpenFOAMs PIMPLE version. Forkortelsen PIMPLE hentyder til oprindelsen af algoritmen, der stammer fra PISO som igen oprindeligt stammer fra SIMPLE. Navnet er en sammensmeltning af navnene på de to oprindelige algoritmer. PIMPLE reduceres i sin mest simple form til PISO, men er blevet tilføjet yderligere muligheder for kontrol. Ideen bag PIMPLE er, at metoden kan indstilles til at køre flere PISO beregningsrunder per tidsskridt, hvor resultater fra én beregningsrunde/iteration benyttes som grundlaget for den følgende. Dette giver mulighed for at benytte sig af under-relaxation faktorer som det ses i SIMPLE og generelt bedre kontrol over størrelsen af tidsskridt (og Courant numre).

Ved at udnytte mulighederne for at raffinere løsningerne i hvert enkelt tidsskridt bliver det muligt at opnå konvergens for simuleringer af forholdene i ventilationsspalten. For at sikre, at CFD simuleringerne går mod konvergens, er de kørt med variable tidsskridt med en maksimal værdi for Courant nummeret på 0.4. Beregningstrinnet er sat til at køre indtil algoritmen har bestemt løsninger for i alt 1 sekund. I og med at løsningen reelt er uafhængig af tid (kun pseudo-transient), skal tidsskridtene i stedet ses som iterationer, hvor ændringer i variable mellem iterationer gøres i en størrelse, der er forsøgt optimeret, set i forhold til ønsker om stabilitet af beregning og lav beregningstid. Længden af det "tidsrum" der simuleres, er valgt på baggrund af en simpel analyse af residualer. Fra disse kan det ses, at PIMPLE efter 1 sekund har nået en konvergeret løsning for det undersøgte problem.

De diskretiserede dele af Navier-Stokes ligningerne og de yderligere ligninger, der er tilføjet systemet af den valgte turbulensmodel, løses med de i OpenFOAMs eksempler foreslåede diskretiseringsmetoder, solvere og under-relaxation faktorer. De valgte diskretiseringsmetoder er præcise til den første eller anden orden.

3.4.3 *Turbulens model: SST k-ω*

Turbulens modellen SST k-ω er en variant af standard k-ω modellen. k-ω modellen er en model, der beskriver turbulensen ved turbulent kinetisk energi, k, og en specifik dissipation, ω ,med enheden tid^{-1}. SST k-ω modellen tilhører gruppen af RANS (Reynolds-averaged Navier-Stokes) sammen med de mere klassiske k-ε modeller. SST k-ω kombinerer de fordelagtige nær-væg egenskaber fra standard k-ω modellen med standard k-ε modellen, der benyttes i resten af det simulerede volumen. Metoden har vist at opnå gode resultater og er blevet populær på baggrund af sin blanding af styrkerne fra henholdsvis k-ε og k-ω modellerne. Metoden er også den, der blev benyttet i OpenFOAMs eksempel.

For at benytte turbulens modellen anbefales det i teorien, at det yderste lag af meshet (viscous sub-layer) skal designes således, at de har en y+-værdi i en størrelsesorden af 1, hvor y+ er en dimensionsløs distance, der bruges til at beskrive hvor grov eller fin et mesh skal være. Der er nogen usikkerhed og forskellige kilder angiver forskellige størrelser, men det nævnes flere steder, at $0 < y+ < 1$ men at $0 < y+ < 5$ også kan bruges. For at holde antallet af celler lavt, er der for det grove og fine mesh henholdsvis benyttet y+-værdier på ca. 5 og 3.

3.4.4 *Geometri og rammebetingelser*

CFD simuleringerne er kun blevet lavet for de ventilerede hulrum, der at finde mellem vinduernes ruder. Der er ikke taget højde for opvarmning af luften i vinduernes rammer. Der er set bort fra rammernes bidrag, fordi det er vurderet, at kernen af teknologien i ventilationsvinduet er det ventilerede hulrum. På denne vis bliver konklusioner draget fra indeværende analyse uafhængige af design af fremtidige rammer og deres indflydelse på energitab og opvarmning af luft. Simuleringerne er lavet på forsimplede modeller af ventilationsspalterne. Spalterne er simuleret som værende 1316 mm høje og 1066 mm brede. Disse dimensioner er beregnet ud fra størrelsen af standard vinduer fratrukket en karmbredde på 82 mm. Dybden af det simulerede hulrum er afhængig af vinduets design. Ind- og aftag i det ventilerede hulrum er simuleret som værende 1066 mm lange (den fulde længde af ventilationsspaltens bund) og 24 mm brede. Hvor udformning af indtag vil have en indflydelse på flowmønstre, er det antaget, at denne effekt kun vil være synlig i bunden af ventilationsspalten og uden betydning for de overordnede flowmønstre, det samlede energitab og opvarmningen af ventilationsluften. Meshets endelige udformning er for hvert trin bygget på betragtninger af y+-værdier, cellers vækstrate og cellers resulterende størrelse i midten af det diskretiserede volumen.

Simuleringerne er foretaget i de tre rumlige dimensioner, grænsefladerne mod rammerne er behandlet som adiabatiske og rudernes overflader er simuleret med U-værdier beregnet i WIS og fratrukket de relevante overgangskoefficienter som de er opgivet i DS 418 [5].

De simulerede resultaters uafhængighed af meshets udformning er testet, ved at sammenligne resultaterne fra de to beregningstrin. I og med at resultaterne, på trods af manglende konvergens i første trin, er sammenlignelige bekræftes det, at resultaterne er uafhængige af meshets udformning. Det er også på baggrund af resultatet af denne betragtning, at der i simuleringerne kun foretages to trin og ikke et tredje på et endnu finere mesh.

3.4.5 Begrænsninger

OpenFOAMs funktionalitet er begrænset når det kommer til at håndtere varmeoverførsel ved stråling. Hvor det er forholdsvis nemt at simulere den afsatte effekt i et medie (fluid) fra stråling, er det mere besværligt at simulere den afsatte effekt fra stråling i grænseflader. Denne ønskede funktionalitet er, hvis ikke umulig, stort set udokumenteret og usikkerhed om kvaliteten af resultatet af implementering af stråling fra overflade til overflade har gjort, at forsøget blev forkastet. I teorien betyder denne manglende implementering af stråling, at CFD simuleringernes resultater ikke er direkte sammenlignelige med GHB testenes måleresultater. Dette har en indvirkning på hvorledes resultater fra de forskellige metoder benyttet i analysen kan sammenholdes. At der ikke tages højde for stråling kan medføre at simuleringerne undervurderer varmetabet gennem ruderne til omgivelserne, have en dæmpende effekt på de sete trends i flowmønstrene og mindske præcisionen af den beregnede temperaturforøgelse i ventilationsspalten. Det vurderes, at det er overvejende sandsynligt, at en effekt på varmetabet vil kunne findes ved implementering af varmeoverførsel ved stråling, men at påvirkningen af flowmønstre og lufttemperaturer vil være begrænset.

3.5 Numerisk algoritme WinVent (WV)

I nedenstående tekst vil der blive givet et overordnet indblik i hvilke metoder og antagelser, der ligger til grund for metoden, der anvendes i algoritmen WinVent (WV). En mere detaljeret beskrivelse af hvordan WV fungerer, kan findes i Raffnsøe 2007 [6].

3.5.1 Varmeledning og konvektion

WV er en algoritme der kan bestemme ventilationsvinduers energimæssige egenskaber som funktion af udetemperatur, solstråling, volumenstrøm. WV blev udviklet i forbindelse med et tidligere projekt [6] der havde til formål at vurdere ventilationsvinduers potentiale som energibesparende teknologi. Historisk set var motivationen for udviklingen af WV, at det i projektet blev fastslået, at den i ISO 15099 [1] beskrevne teori for beregning af temperaturstigninger i ventilerede hulrum (i vinduesruder) ikke var tilstrækkelig præcis til projektets formål.

Metoden der står beskrevet i ISO 15099 antager en uniform temperaturfordeling i ventilationsvinduers ventilerede hulrum. Denne antagelse har vist sig at være for upræcis og at have den effekt, at metoden undervurderer opvarmningen af den leverede friskluft. En uniform temperaturfordeling kræver en total opblanding af luften i hulrummet. For at en antagelse om uniform temperaturfordeling kan anvendes, kræves det, at luften i hulrummet overordnet set kan betragtes som fuldstændigt opblandet. CFD undersøgelser foretaget i forbindelse med Raffnsøe 2007 [6] og ProVent har vist, at det konvektive flowmønster, der normalt optræder i ikke-ventilerede hulrum, kortsluttes af den gennemgående volumenstrøm. Det reelle flowmønster er et, hvor luften i hulrummet fra indtag til afkast stort set udelukkende bevæger sig op ad hulrummets varme flade. Det konvektive varmetab til hulrummets kolde flade er derfor mindre, end antagelsen i ISO 15099 giver anledning til at tro. Af samme årsag er luftens opvarmning og vinduets varmetab også i højere grad domineret af luftens varmeledningsevne og kan derfor med god præcision beskrives som tidsafhængige funktioner af varmeledningsevne og opvarmningspotentiale.

Konkret kvantificerer WV den konvektive opvarmning af luften i hulrummet ved en numerisk Finite Control Volume (FCV) algoritme under antagelse af, at opvarmningen kan beskrives som en endimensionel, transient varmeledning i et semi-uendeligt element. Potentialet for opvarmning er temperaturforskellen over den kolde og varme flade i hulrummet.

Ved brug af denne tilnærmelse bliver det oprindelige flerdimensionelle, analytiske problem reduceret til at være et relativt simpelt problem, som i øvrigt er væsentligt billigere at løse rent beregningsmæssigt. Det tidligere udførte projekt Raffnsøe 2007 [6] dokumenterer, at denne antagelse er anvendelig. Analyser af metoden udført i forbindelse med ProVent konkluderer ligeledes, at metoden er anvendelig med en præcision, der er egent til projektets formål.

3.5.2 *Stråling og solstråling*

Med henblik på beskrivelse af indflydelse af stråling og solstråling på friskluftens temperaturudvikling benytter WV sig af den i ISO 15099 [1] beskrevne teori om varmeoverførsel ved stråling og energibidrag fra solstråling. Præcisionen af denne teori er anerkendt og veldokumenteret og er ikke yderligere undersøgt i forbindelse med ProVent. Teorien beskriver hvorledes overflader udveksler energi med hinanden og hvorledes disse overflader opvarmes af stråling. I og med at WV's antagelse om opvarmning af luften i hulrummet kun arbejder med hulrummets overfladetemperaturer over tid, er der ingen problemer i at benytte ISO 15099's teori om varmeoverførsel via stråling sammen med WV's antagelse.

3.5.3 *Kontrol af kvalitet*

Kvaliteten af beregningsmetoden som benyttes i WV er undersøgt ved at sammenholde resultater fra GHB målinger og CFD beregninger med resultater beregnet af WV. Direkte sammenligning mellem de tre metoder har ikke været mulig.

GHB målingerne er blevet foretaget på prototyper af ventilationsvinduet med vinduesrammer og uden solstråling. Der sker en forvarmning af friskluften i den nederste ramme af vinduet med det resultat, at den luft, der kommer ind i det ventilerede hulrum, ikke har samme temperatur som udeklimaet. Det er ikke umiddelbart muligt at ændre temperaturerne i WV således, at der er forskel på temperaturen af luften i bunden af hulrummet og udeluften. Derfor vil potentialet for opvarmning reelt være større i WV, end det er i selve hulrummet mellem ruderne i vinduerne i GHB målingerne. For at sammenholde GHB med WV har det derfor været nødvendigt at korrigere for opvarmning i rammen.

CFD beregningerne er som nævnt udført uden at tage højde for effekten af varmeoverførsel ved stråling. Det valgte open source CFD program, OpenFOAM (OF), har endnu ingen veldokumenteret eller lettilgængelig funktionalitet, der muliggør inklusion af stråling i simuleringerne af det ventilerede hulrum. For at sammenholde CFD simuleringer med WV har det derfor været nødvendigt at fjerne for strålingsbidrag i WV.

Ydermere har det ikke været muligt at sammenholde CFD simuleringerne med GHB målingerne, fordi det ikke er muligt at korrigere GHB målingerne for stråling. Herudover har hverken GHB målinger eller CFD simuleringer inkluderet solstråling. Derfor har det heller ikke været muligt at teste WV's evne til at beregne solstrålingens effekt på opvarmningen af luften eller varmetabet gennem vinduet til omgivelserne.

For at teste WV's evne til at beregne U- og g-værdier samt opvarmning af friskluft er følgende fremgangsmåde anvendt.

1. GHB målinger er blevet korrigeret for opvarmning i nederste ramme og sammenholdt med standardberegninger fra WV. Dette har givet indblik i

om hvorvidt WV er i stand til at beregne korrekte værdier og har evalueret WV's evne til at håndtere varierende volumenstrømme gennem det ventilerede hulrum.

2. Strålingsbidrag er blevet fjernet fra WV's beregningsmodel og er blevet sammenholdt med CFD simuleringer. Dette har ligeledes givet indblik i, om hvorvidt WV er i stand til at beregne korrekte værdier og har evalueret WV's evne til at håndtere varierende udetemperaturer. Samtidig har sammenligningen, via WV's dobbelte bekræftelse, givet styrke til både GHB målinger og CFD simuleringer.

3. WV's evne til at beregne effekt af solstråling på systemet har ikke været mulig at teste mod hverken GHB målinger eller CFD simuleringer. I og med, at ISO 15099's teori om solstråling (og stråling) er (relativt) simpel, generelt accepteret og direkte implementerbar i WV's programmel, er det vurderet, at det er rimeligt at antage, at WV med tilstrækkelig præcision kan beregne solstrålings effekt på systemet af ruder og hulrum.

Efter at have fulgt ovenstående fremgangsmåde, er det endeligt konkluderet, at WV kan estimere teknologiens formåen til en rimelig præcision og til et niveau der gør WV anvendelig til projektets formål.

3.5.4 Anvendelighed og brug

Ved brug af WV's tidbesparende fremgangsmåde og algoritmens opsætning er det muligt at lave serier af parametervariationer, der tydeligt kan illustrere teknologiens anvendelighed. Formatet af algoritmens output tillader nem databehandling.

Algoritmen kræver en serie af input, der beskriver de fysiske rammer omkring vinduet og leverer en stribe outputdata, der inkluderer, men ikke er begrænset til, mørke U- og g-værdier, energimængder der går ind og ud af systemet og leveret frisklufttemperatur.

3.5.5 Begrænsninger

Algoritmen er skrevet i programsproget MATLAB og brug er derfor begrænset til interessenter, der holder MATLAB licenser.

Selve algoritmen har på grund af dens udformning problemer med at håndtere lave flow hastigheder. Ifølge Raffnsøe 2007 [6] bliver algoritmen upræcis ved volumenstrømme under 2 l/s. Denne størrelse er dog kun vejledende, eftersom flowhastighederne er afhængige af hulrummets geometri.

Ligeledes er algoritmen udformet således, at den, i dens nuværende form, kun kan håndtere vindueskonstruktioner, hvor der er et enkelt lag glas på ydersiden af hulrummet og en dobbeltrude på indersiden.

Hertil kommer at algoritmen ikke har mulighed for at tage højde for rammers indflydelse på systemet.

3.6 Parametervariation og multipel lineær regression

Ventilationsvinduer har dynamiske egenskaber som bl.a. afhænger af volumenstrømmen af ventilationsluften gennem vinduet, udetemperaturen og solstrålingen. Det er derfor ikke muligt at udføre årsberegninger i bygningssimuleringsprogrammer på traditionel vis, hvor vinduernes egenskaber beskrives ved en fast U-værdi og g-værdi. Der er derfor, på baggrund af beregninger i WV med en række parametervariationer, udviklet matematiske udtryk for temperaturstigningen af ventilationsluften og den effektive U-værdi, U_{eff}.

Parametervariationer og efterfølgende multiple lineære regressionsanalyser er baseret på samme design af ventilationsvindue som blev undersøgt ved GHB tests udført ved DTU BYG. Analysen bliver kun fortaget på rudesystemet og ser bort fra vinduesrammens bidrag fra opvarmning af leveret friskluft og energibalance.

3.6.1 Parametervariation

Parametervariationerne tager udgangspunkt i variationer af tre variable: Volumenstrøm gennem vinduet, udetemperatur og solstråling. Der er til formålet udviklet en version af WV, der kan tage vektorer med inputvariable.

Følgende vektorer er indtastet i WV

T_e	[°C]	-10	-6	-4	-2	0	2	4	6	8	10	12	16
I_s	[W/m^2]	0	100	200	300	400	500	600	700	800	900	1000	
G_a	[l/s]	2	4	6	8	10							

Hvor	T_e	er udetemperaturen	[°C]
	I_s	er solbestrålingsstyrken	[W/m^2]
	G_a	er volumenstrømmen	[l/s]

En parametervariation gøres for hver mulig kombination af variable. I alt bliver der således foretaget 660 parametervariationer.

3.6.2 Multipel lineær regression

På baggrund af resultaterne fra paratmetervariationerne bliver der lavet to lineære regressionsanalyser, der hver resulterer i et matematisk udtryk. Der laves en lineær regression for at bestemme et udtryk for den leverede frisklufttemperatur og en for at bestemme den effektive U-værdi. Der gøres brug af trinvis lineær regression til at bestemme de matematiske udtryk.

Den leverede frisklufttemperatur er afhængig af alle de tre variable, der er indtastet i parametervariationen og det matematiske udtryk bliver udarbejdet på det fulde grundlag af 660 parametervariationer. Den effektive U-værdi bliver i WV beregnet som mørk, altså uden solstråling, og er derfor kun afhængig af udetemperaturer og volumenstrømme. I og med at den effektive U-værdi kun er afhængig af to variable, bliver det matematiske udtryk udført på bagrund af de tilbageværende 60 mulige parametervariationer.

3.6.3 *Matematiske modeller til dynamisk simulering*

For at kunne simulere hvorledes ventilationsvinduerne fungerer i praksis over tid og under varierende danske klimaforhold og for at kunne vurdere, hvilken indflydelse ventilationsvinduerne har på bygningers energibalance og indeklima, er der brug for matematiske udtryk i et format, der lader sig implementere i det valgte dynamiske simuleringsprogram. Simuleringsprogrammet IESVE er valgt til simuleringen, da dets brugerflade tillader integration af sådanne matematiske udtryk. Der er dog begrænsninger på, hvor lange de matematiske udtryk må være, og hvor de kan implementeres i beregningssystemet. I nedenstående afsnit gennemgås, hvorledes disse matematiske udtryk udformes.

3.6.3.1 *Bestemmelse af optimal volumenstrøm gennem ventilationsvindue*

Bygningsreglementet foreskriver, at boliger skal et have konstant luftskifte på mindst en halv gang i timen. For at kunne optimere ventilationsvinduers bidrag til bygningers energibalance er det nødvendigt at bestemme ved hvilken volumenstrøm gennem ventilationsvinduet, energiforbruget til opvarmning af ventilationsluften er mindst. Dette gøres i to trin. Første trim er at opskrive energibalancen for rummet, hvori ventilationsvinduerne placeres og omforme den til et udtryk for opvarmningsbehovet som en funktion af luftskiftet i rummet.

Det andet trin er at udføre en søgning, der skal bestemmes funktionens minimum

Den optimale volumenstrøm bliver bestemt for en situation uden solstråling, og hvor ude- og indetemperaturerne er henholdsvis 0 og 20 °C.

Energibalancen

Hvor	Q_{heat}	er opvarmningsbehovet	[W]
	Q_{Ueff}	er det effektive varmetab gennem vinduerne	[W]
	$Q_{a,out}$	er varmetabet til omgivelserne (her ved ventilation)	[W]
	$Q_{a,in}$	er energitilførslen med den leverede friskluft	[W]

Som det ses er der set bort fra bidrag til varmebalancen for rummets konstruktioner. Dette er gjort, fordi formålet med undersøgelsen er at bestemme bidragene fra ventilationsvinduerne. De øvrige konstruktionsdele har ingen indflydelse på dette bidrag.

De forskellige bestanddele af energibalancen skrevet ud

$$(20 \qquad)$$
$$(T \qquad C)$$

Hvor	U_{eff}	er den effektive U-værdi	$[W/(m^2 \cdot K)]$
	A_g	er ventilationsvinduets glasareal	$[m^2]$
	ΔT_{i-e}	er temperaturforskellen mellem inde og ude	[°C]
	G_a	er volumenstrømmen gennem ventilationsvinduet	$[m^3/s]$
	ρ_a	er luftens densitet	$[kg/m^3]$
	$c_{p,a}$	er luftens specifikke varmekapacitet	$[J/(kg \cdot K)]$
	$Q_{a,in}$	er energitilførslen med den leverede friskluft	[W]
	T_{v2}	er den leverede frisklufttemperatur	[°C]

Både den effektive U-værdi og den leverede frisklufttemperatur er under undersøgelsens rammebetingelser kun afhængige af volumenstrømmen. De følgende udtryk er bestemt ved lineær regression

Ved at gøre volumenstrømmen afhængig af antallet af vinduer i rummet fås følgende funktion

$$\frac{\qquad}{-}$$

Hvor	H_r	er rummets højde	[m]
	A_r	er rummets gulvareal	$[m^2]$
	n	er luftskiftet (sat til en halv gang i timen)	$[h^{-1}]$
	x	er antallet af ventilationsvinduer	$[m^3/s]$

Løses ovenstående ligningssystem for en mindsteværdi af varmetabet Q_{heat}, kan det optimale antal af vinduer for det givne rum bestemmes. I og med at volumenstrømmen er defineret som en funktion af det ukendte antal ventilationsvinduer, vil en sådan løsning af ligningssystemet også betyde, at den optimale volumenstrøm for ventilationsvinduet er bestemt. Ligningssystemet skal løses iterativt med en matematisk metode, der kan bestemme netop mindsteværdien af varmetabet Q_{heat}.

Den optimale volumenstrøm gennem det givne ventilationsvinduesdesign er under de givne forhold (20 °C temperaturforskel) konstant og ved ovenstående metode bestemt til at være 4,57 l/s.

3.6.3.2 *Model til bestemmelse af temperaturstigning i dynamisk simulering*

Som beskrevet ovenfor kan der i et begrænset omfang implementeres matematisk udtryk i IESVE. Bl.a. har IESVE en begrænsning på hvor lange matematiske udtryk kan være. Derfor er det nødvendigt at forsimple det udledte udtryk for beregning af den leverede frisklufttemperatur. Udtrykket beskriver den leverede frisklufttemperatur og er det udtryk, der benyttes til at bestemme den positive energitilvækst, der tilkommer til energibalancen i form af varmegenvinding i ventilationsvinduerne.

Udtrykket udledes ved hjælp at samme tidligere omtalte trinvise lineære regressionsmetode. Udtrykket er

Hvor	T_{v2}	er den leverede frisklufttemperatur	[°C]
	T_e	er udetemperaturen	[°C]
	I_s	er solbestrålingsstyrken	[W/m^2]

Solbestrålingsstyrken på ruden er ikke en parameter der findes direkte i IESVE. Derfor laves følgende omregning:

Hvor	I_r	er solvarmetilskuddet i rummet	[W]
	g_g	er den totale solenergitransmittans for ruden	
	n	er antallet af ruder/vinduer	
	A_g	Er arealet af ruden	m^2

Årsagen til at volumenstrømmen ikke optræder i ovenstående udtryk skal findes i, at IESVE simuleringerne kører med en fast volumenstrøm, der sikrer et konstant luftskifte på en halv gang i timen.

3.6.3.3 *Model til bestemmelse af energitab i dynamisk simulering*

IESVE tillader ikke ændringer i måden hvorpå vinduer behandles. Derfor er det ikke praktisk at benytte den effektive U-værdi i den form, den oprindeligt er blevet udtrykt. I stedet omformes et forsimplet udtryk (grundet pladskrav stillet af IESVE) produceret ved lineær regression til at være et udtryk for en ændring af varmetabet gennem de traditionelle vinduer, der bliver simuleret i IESVE. Det omformede udtryk, der beskriver mertabet der skal suppleres til varmetabet fra vinduerne, Q_{diff}, har følgende form

$$(Q \qquad)$$
$$(G \qquad\qquad\qquad)$$

Hvor	Q_{diff}	er udtrykket for mertab af energi gennem vinduerne	[W]
	$Q_{g,win}$	er varmetabet gennem vinduets glasareal	[W]
	$Q_{a,in}$	er energitilførslen med den leverede friskluft	[W]
	Q_{Ueff}	er det effektive varmetab gennem vinduerne	[W]
	U_g	er den simulerede rudes center U-værdi	[W/(m²·K)]
	U_{eff}	er ventilationsvinduets effektive U-værdi (for A_g)	[W/(m²·K)]
	A_g	er ventilationsvinduets glasareal	[m²]
	ΔT_{i-e}	er temperaturforskellen mellem inde og ude	[°C]
	ΔT_{Tv2-i}	er temp.diff. mellem leveret friskluft og inde	[°C]
	G_a	er volumenstrømmen gennem ventilationsvinduet	[m³/s]
	ρ_a	er luftens densitet	[kg/m³]
	$c_{p,a}$	er luftens specifikke varmekapacitet	[J/(kg·K)]

Ved at indsætte standardværdier for densitet og specifik varmekapacitet for luft og at gøre brug af følgende forsimplede udtryk for opvarmningen af friskluften og den effektive U-værdi kan udtrykket reduceres.

Hvor	T_e	er udetemperaturen	[°C]

Årsagen til at volumenstrømmen ikke optræder i ovenstående udtryk skal findes i, at IESVE simuleringerne kører med en fast volumenstrøm, der sikrer et konstant luftskifte på en halv gang i timen. Udtrykkene er udledt ved en lineær regressionsanalyse. Det endelige reducerede udtryk for Q_{diff} er

Hvor	T_i	er indetemperaturen	[°C]

Det kan her tilføjes at Q_{diff} er udformet således, at det giver et negativt bidrag til energibalancen i de tilfælde, hvor udetemperaturerne er lavere end de indvendige.

3.6.4 *Begrænsninger*

De udførte matematiske udtryk er udført på bagrund af måle- og simuleringsresultater opnået i forbindelse med analysen af ventilationsvinduet som blev undersøgt ved DTU BYG. De matematiske udtryk er således kun gyldige for netop dette design. Til gengæld vurderes det, at det undersøgte design er repræsentativt for design af ventilationsvinduer og at de matematiske udtryk også kan benyttes til at give overslag på leverede frisklufttemperaturer og effektive U-værdier for lignende design. Med lignende design menes en opbygning, hvor der er et enkelt lag glas yderst, en dobbeltrude inderst og vinduets størrelse ikke afviger markant fra standarddimensionerne.

3.7 Dynamisk simulering i simpel bygning (IESVE)

For at vurdere ventilationsvinduers indflydelse på energibehov og indeklima i bygninger er beregningsudtrykkene fra de linerære regressionsanalyser brugt i en dynamisk analyse af ventilationsvinduets performance over tid under danske klimaforhold. Disse bygningssimuleringer er udført i programmet IESVE, som giver mulighed for at anvende variable parametre beskrevet ved funktionsudtryk.

3.7.1 Implementering i IESVE

Ventilationsvinduets dynamiske egenskaber er implementeret i IESVE ved anvendelse af de udviklede regressionsudtryk, beskrevet i foregående afsnit, på følgende måde.

Vinduerne beskrives som udgangspunkt i IESVE ved faste U- og g-værdier gældende for basisvinduet uden hensyntagen til ventilation. Korrektion for effekten af ventilationen gennem vinduet sker ved for hvert tidsskridt at bestemme indblæsningstemperaturen, T_{v2}, og forskellen i varmetabet, Q_{diff}, mellem basisvinduet og det virkelige vindue med ventilation. Effekten på eventuelt kølebehov er ikke behandlet i projektet.

Vha. indblæsningstemperaturen tages der højde for den genvundne varmemængde i ventilationsluften, hvilket også inkluderer evt. ændring i g-værdien, når der er solstråling på vinduet. Når indblæsningstemperaturen hæves over udetemperaturen, reduceres ventilationstabet til udsugning tilsvarende.

Q_{diff} udtrykker som nævnt forskellen mellem varmetabet baseret på den faste U-værdi for basisvinduet og varmetabet for det virkelige vindue baseret på den effektive U-værdi, U_{eff}, for det aktuelle tidskridt under hensyntagen til ventilation gennem vinduet. Den effektive U-værdi udtrykker det effektive varmetab som sker gennem vinduets udvendige overflade til omgivelserne. Det håndteres i IESVE ved at tilføre den fiktive varmemængde Q_{diff} til rummet som korrigerer for, at U-værdien afviger fra basis U-værdien. Varmen, som bliver genvundet via ventilation gennem vinduet, tilføres som en del af den temperaturstigning, der udtrykkes i indblæsningstemperaturen. Q_{diff} er derfor et negativt bidrag (varmetab) som udtrykker forøgelsen af varmetab, netop fordi der trækkes (ofte kold) luft ind igennem vinduet.

3.7.2 Model geometri

Ved hjælp af IESVE er ventilationsvinduet analyseret under designmæssigt optimale forhold i en simplificeret bygning: Ventilationsvinduerne installeres kun i en enkelt facade orienteret mod syd, hvor deres fordele er størst, og simuleres med den volumenstrøm gennem vinduerne, der yder de bedste energitekniske resultater. Således er bygningen designet, så etagearealet svarer til, at der ved den mest effektive volumenstrøm gennem vinduerne altid er et luftskifte på en halv gang i timen, som det foreskrives af Bygningsreglementet. Da bygningens udformning sammen med ventilationsvinduerne i sig selv ikke er tilstrækkeligt til at sikre et konstant luftskifte på en halv gang i timen, er dette sikret ved mekanisk udsugning.

3.7.2.1 *Rum*

For at simplificere analysen og rette fokus på ventilationsvinduernes effekt på energibehovet, er der regnet på et enkelt rektangulært rum med et gulvareal på 104 m^2 (netto) (16,0 x 6,5 m) og en rumhøjde på 2,50 m (netto). Der er monteret 8 vinduer i den sydvendte facade på 16 m. Dette er valgt, så det passer med, at der opnås et på luftskifte 0,5 h^{-1} med en ventilationsmængde på 4,5 l/s per vindue. Som den forudgående analyse har vist, giver denne volumenstrøm den bedste energitekniske performance af vinduerne. En skitse af rummet er vist i Figur 3.5.

Figur 3.5

Udformning af bygningen der regnes på i IESVE

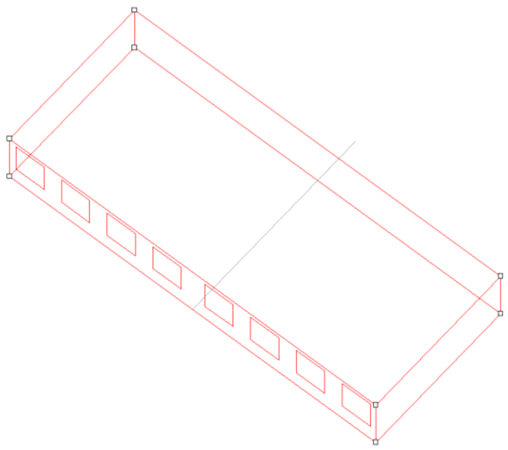

3.7.2.2 *Vinduer*

Der er som nævn monteret 8 vinduer i den sydvendte facade med en indbyrdes afstand på 750 mm (1000 mm mellem de midterste)

Alle vinduerne har standardstørrelsen (b x h) 1230 x 1480 mm og glasandelen, F_f, udgør 77 % af vindues arealet.

3.7.2.3 *Konstruktioner*

Da ventilationsvinduer kan være relevante at benytte i både nybyggeri eller eksisterende bygninger, er det valgt at designe bygningen, så den blot overholder bygningsreglementets (BR10) krav til mindste varmeisolering af bygningsdele, jf. BR10 kap. 7.6.

Konstruktionsopbygningerne og U-værdier for ydervægge, terrændæk og tag er vist i Tabel 1 til Tabel 3.

Tabel 1. Egenskaber for ydervægge

Ydervæg	Tykkelse [mm]	Varmeledning [W/(m·K)]	Densitet [kg/m^3]	U-værdi [W/(m^2·K)]
tegl	100	0,84	1700	
Isolering	110	0,039	200	
Beton	100	0,51	1400	
Puds	4	0,42	1200	
I alt	314			0,30

Tabel 2. Egenskaber for terrændæk

Terrændæk	Tykkelse [mm]	Varmeledning [W/(m·K)]	Densitet [kg/m^3]	U-værdi [W/(m^2·K)]
Kapillarbrydende lag	650	0,36	1840	
Isolering	100	0,039	200	
Beton (støbt)	300	1,13	2000	
Trægulv	20	0,14	650	
I alt	1070			0,20

Tabel 3. Egenskaber for tag

Tag	Tykkelse [mm]	Varmeledning [W/(m·K)]	Densitet [kg/m^3]	U-værdi [W/(m^2·K)]
Tagpap	6	0,19	960	
Undertag	5	0,50	1700	
Beton	100	0,51	1400	
Isolering	170	0,039	200	
Luftspalte	100	–	–	
Gips	13	0,16	950	0,20
I alt	394			0,20

3.7.2.4 Opvarmning og ventilationssystem

Brugstiden er 8760 timer pr. år, svarende til boliger.

Infiltrationen er sat til 0,13 l/(s·m^2)

Der er foretaget beregninger for fire forskellige scenarier: 2 med udsugning og 2 med mekanisk ventilation med varmegenvinding

I henhold til BR10 kapitel 8.3 Ventilationssystemer stk. 9, er SEL-værdierne for hhv. udsugningsanlæg og ventilationsanlæg med varmegenvinding 800 og 1800 J/m^3. Yderligere detaljer om ventilationsanlæg fremgår af afsnit 4.3.

Udsugning/mekanisk ventilation er aktiv for alle årets 8760 timer.

Der er anvendt et traditionelt varmeanlæg med radiatorer med en sætpunktstemperatur på 20 °C.

Ved beregning af bygningens energibehov indgår energibehovet til opvarmning med en faktor 1 og elforbruget til ventilation med en faktor 2,5.

4 RESULTATER

Der er to hovedformål med den tekniske analyse af ventilationsvinduet som teknologi. Det første er at bestemme en matematisk metode, der nemt og hurtigt kan give en forståelse af teknologiens performance under givne forhold. Det andet formål er at anvende denne metode i en dynamisk analyse til at bestemme, hvordan ventilationsvinduet som teknologi påvirker bygningers energiforbrug og indeklima over tid under danske klimaforhold. For at nå disse mål er der blevet opstillet eksperimenter og arbejdet med matematiske analyser af de opnåede måleresultater. Nedenfor bliver relevante resultater fra de forskellige delprojekter præsenteret i den rækkefølge, projektet er blevet bygget op.

4.1 Eksperimentelt- og beregningsteknisk grundlag for metode

4.1.1 Sammenhold af resultater fra GHB og WV – Volumenstrømme

Figur 4.1 viser temperaturer som de er blevet målt ved GHB forsøg ved DTU BYG og beregnet af WV ved varierende volumenstrømme gennem det ventilerede hulrum. De præsenterede temperaturer er opvarmningen af luften i det ventilerede hulrum og altså eksklusiv bidrag til opvarmning fra vinduets ramme.

Det ses, at WV med stor præcision kan regne sig frem til opvarmningen af luften mellem ruderne i ventilationsvinduet. Den gennemsnitlige afvigelse fra de målte resultater i det analyserede interval er 0,1 °C. En hypotesetest angiver, at der under antagelse af normalfordelte forskelle, er en 32 % sandsynlighed ($p = 0,32$) for, at de to temperaturserier er ens. En hypotese test med $\alpha = 0,05$ kan således ikke afvise, at de to temperaturserier er ens. Det betyder altså, at de af WV beregnede resultater for temperatur er statistisk signifikante.

Figur 4.1

Opvarmningen af luften mellem ruderne i ventilationsvinduet som målt ved GHB ved DTU og beregnet af WV ved varierende volumenstrømme

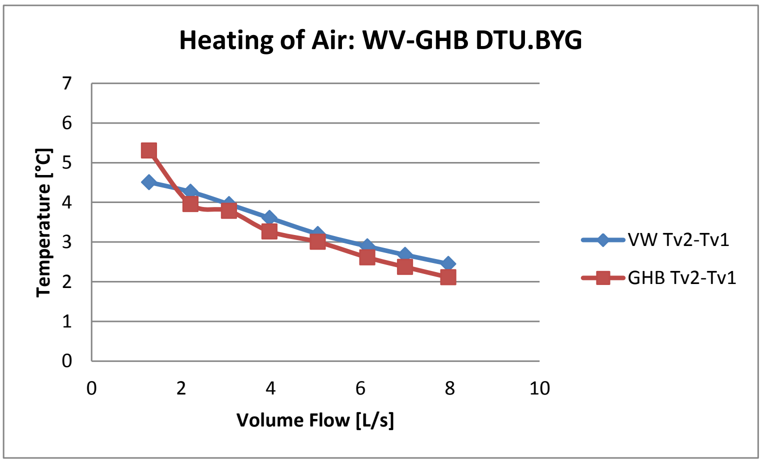

Figur 4.2 viser de energimængder, der går ind systemet (dvs. varmeoverførslen fra rummet til indersiden af det indvendige glas) målt ved GHB forsøg ved Fraunhofer-Institut für Bauphysik IBP (FH IBP) og beregnet af WV ved varierende volumenstrømme gennem det ventilerede hulrum. Systemet, der

henvises til her, er den specifikke sammensætning af ruder, der blev testet af FH IBP. De præsenterede måleresultater er justeret fra de oprindelige målinger ved at fratrække overslag på vinduesrammens bidrag til energibalancen. Der er således indført en mindre usikkerhed i forhold til størrelsen af energimængden.

Ikke desto mindre kan det ses, at WV med god præcision kan regne sig frem til energimængden, der går ind i systemet. Den gennemsnitlige afvigelse fra de justerede målte resultater i det analyserede interval er 1,1 W. En hypotesetest angiver, at der under antagelse af normalfordelte forskelle er en 7 % sandsynlighed (p = 0,07) for at de to energiserier er ens. En hypotese test med α = 0,05 kan således ikke afvise, at de to energiserier er ens. Det betyder altså, at de af WV beregnede resultater for mængder af energi, der går ind i systemet er statistisk signifikante.

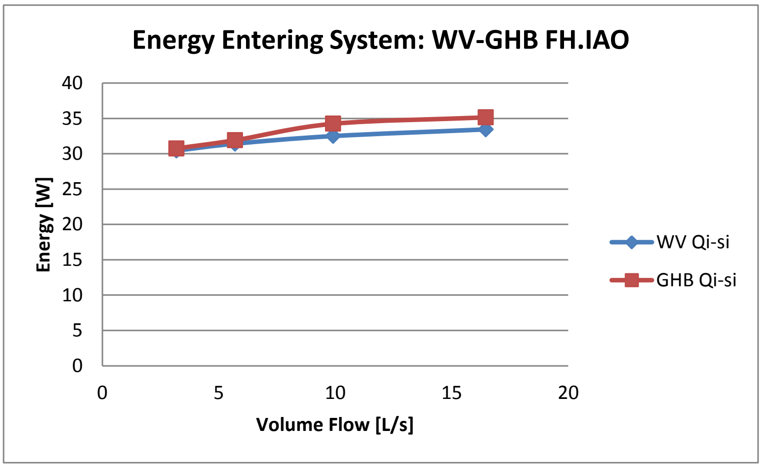

Figur 4.2

Mængder af energi der går ind systemet som de er blevet målt ved GHB ved FH IBP og beregnet af WV ved varierende volumenstrømme

Ved sammenligning af måleresultater fra GHB med beregnede resultater fra WV kan det konkluderes, at WV regner præcist til et niveau der møder projektet ProVents behov.

4.1.2 Sammenhold af resultater uden strålingsbidrag fra WV og CFD – Volumenstrømme

Figur 4.3 viser temperaturer som de er blevet beregnet af henholdsvis WV og CFD ved varierende volumenstrømme gennem det ventilerede hulrum og uden bidrag til varmetransmission fra stråling. Årsagen til den manglende stråling skal findes i, at det benyttede CFD program OpenFOAM endnu ikke understøtter stråling i en form der har gjort anvendelse mulig i projektet. De præsenterede temperaturer er opvarmningen af luften i det ventilerede hulrum og altså eksklusiv bidrag til opvarmning fra vinduets ramme.

Figur 4.4 viser de energimængder, der går ind systemet som de er blevet beregnet af henholdsvis WV og CFD ved varierende volumenstrømme gennem det ventilerede hulrum og uden bidrag til varmetransmission via stråling.

Figur 4.3

Opvarmningen af luften mellem ruderne i ventilationsvinduet beregnet af WV og CFD uden bidrag fra stråling ved varierende volumenstrømme

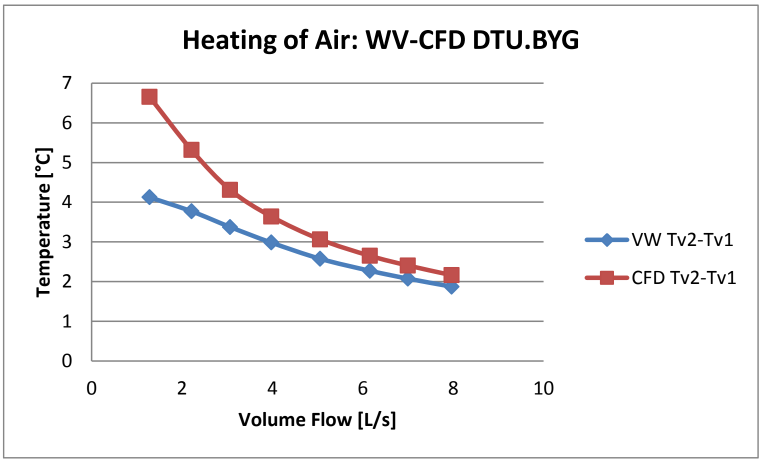

Figur 4.4

Mængder af energi der går ind systemet som de er beregnet af WV og CFD uden bidrag fra stråling ved varierende volumenstrømme

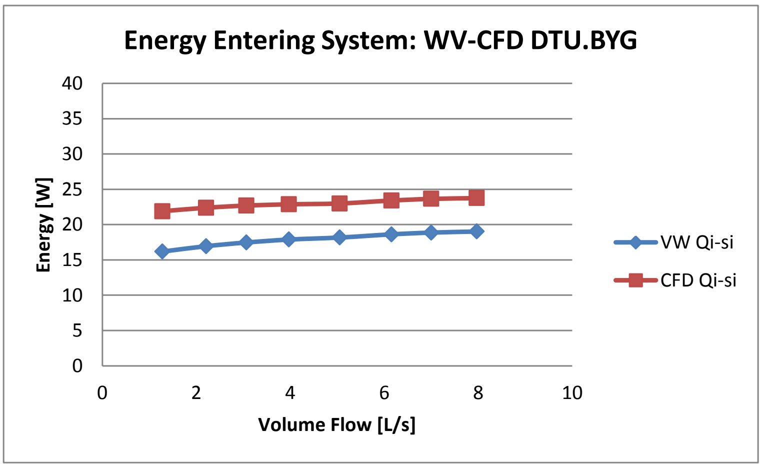

Det kan af henholdsvis Figur 4.3 og Figur 4.4 ses, at CFD beregner højere leverede friskluftemperaturer end WV og at CFD ligeledes beregner energi mængder, der går ind systemet som værende højere. Forklaringen på dette forventes at skulle findes i, at de to beregningsformer benytter sig af forskellige U-værdier (overgangstal). Hvor WV selv beregner vinduessystemets energimæssige egenskaber, skal der i CFD indtastes overslag på systemets forskellige bestanddeles varmetransportegenskaber. Disse overslag er behæftet med usikkerheder og er angiveligt blevet designeret for høje værdier.

Denne teori støttes af resultaterne præsenteret på både Figur 4.3 og Figur 4.4. På Figur 4.3 kan det ses, at forskellene i de beregnede temperaturer mindskes ved større volumenstrømme. Overgangstal beskriver potentialet for overførsel af energi som en funktion af temperaturforskellen. Eftersom temperaturforskellen mindskes over tid i takt med at luften opvarmes, bliver forskelle i varmeovergangstal relativt mere indflydelsesrige over tid. Højere volumenstrømme vil betyde, at et givent luftvolumen vil tilbringe kortere tid i det ventilerede hulrum. Altså er relativt små forskelle i overgangstal mindre betydningsfulde ved høje volumenstrømme, fordi der er mindre tid til at reducere temperaturforskellene. Det forventelige resultat af at have værdisat for høje varmetransmissionsegenskaber i rammebetingelserne i CFD analysen, vil altså være, at der beregnes for høje temperaturer og at betydningen af fejlen vil mindskes ved højere volumenstrømme, ganske som det ses i Figur 4.3

Ses der herefter på Figur 4.4 kan det ses, at forskellen mellem de beregnede mængder af energi der går ind i systemet er stort set er konstant over variationerne i volumenstrømmene. Forskellen er gennemsnitlig 5,1 W og standard deviationen er lav på 0,4. De konstante forskelle understøtter ligeledes teorien om at overgangstallene er blevet sat for højt i CFD simuleringerne.

På trods af den beskrevne usikkerhed kan det ses, at der er god overensstemmelse mellem WV og CFD målingerne for volumenstrømme større end 3 l/s. Ved sammenligning af beregnede resultater for volumenstrømme fra 3 l/s og op og med den beskrevne usikkerhed i mente konkluderes det, at CFD simuleringerne regner præcist til et niveau, der møder projektet ProVents behov.

4.1.3 Sammenhold af resultater uden strålingsbidrag fra CFD og WV – Udetemperaturer

Figur 4.5 viser temperaturer som de er blevet beregnet af henholdsvis CFD og WV ved varierende udetemperaturer ved volumenstrømme på 3,06 og 6,16 l/s og uden bidrag til energitransport og -balance fra stråling. Årsagen til den manglende energitransportform skal findes i, at det benyttede CFD program OpenFOAM endnu ikke understøtter stråling i en form, der har gjort anvendelse mulig i projektet. De præsenterede temperaturer er opvarmningen af luften i det ventilerede hulrum og altså eksklusiv bidrag til opvarmning fra vinduets ramme.

Figur 4.6 viser de mængder af energi, der går ind systemet som de er blevet beregnet af henholdsvis CFD og WV ved varierende udetemperaturer ved volumenstrømme på 3,06 og 6,16 l/s og uden bidrag til energitransport og -balance fra stråling.

Figur 4.5

Opvarmningen af luften mellem ruderne i ventilationsvinduet beregnet af CFD og WV uden bidrag fra stråling ved varierende udetemperaturer

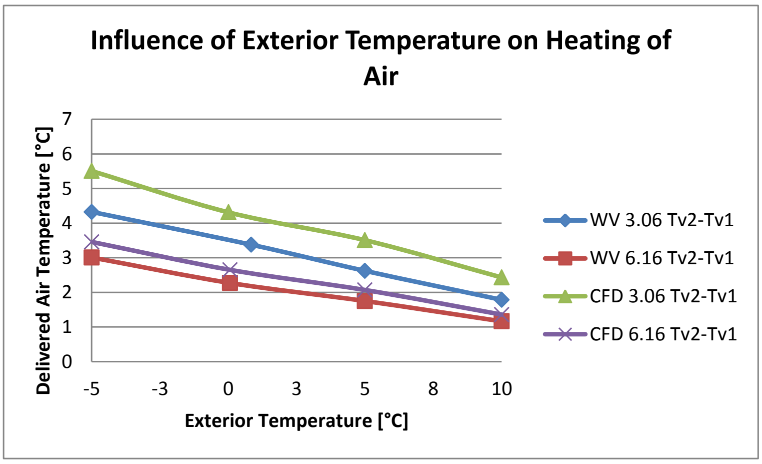

Figur 4.6

Mængder af energi der går ind systemet som de er beregnet af CFD og WV uden bidrag fra stråling ved varierende udetemperaturer

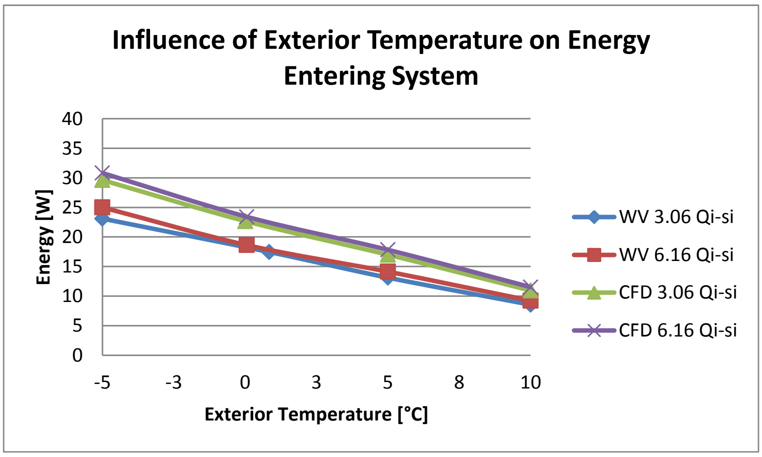

Det kan af henholdsvis Figur 4.5 og Figur 4.6 ses, at CFD beregner højere leverede friskluftttemperaturer end WV og, at CFD ligeledes beregner energimængder, der går ind systemet, som værende højere. Forklaringen på og de umiddelbare implikationer af dette kan findes i det foregående afsnit 4.1.2.

De sete uoverensstemmelser mellem resultaterne på CFD og WV er direkte sammenlignelige med dem, der er beskrevet i afsnit 4.1.2 og betragtes, under antagelsen af, at problemet er forstået, ikke som værende problematiske set i forhold til projektet ProVents behov. Med udgangspunkt i denne forståelse og efter at have sammenholdt de beregnede data, konkluderes det, at WV kan håndtere udetemperaturvariationer præcist til et niveau, der møder projektet ProVents behov.

4.1.4 Solstråling

Det har ikke været muligt at teste WV's evne til at beregne solstrålings effekt på opvarmning af luft og varmebalance i systemet. Det er i afsnit 3.5.2 kort beskrevet hvorfra WV's benyttede teori er hentet. Det er en begrundet antagelse, at WV kan beregne effekten af solstråling.

4.1.5 Delkonklusion

På baggrund af de ovenstående fremlagte målinger, beregninger og analyser konkluderes det, at WV regner præcist på de undersøgte ventilationsvindues designs til en præcision, der er anvendelig for projektet ProVent.

4.2 Multipel lineær regression – Matematiske modeller

Baseret på designet af det testvindue 1, DTU, er der foretaget to trinvise lineære regressionsanalyser med det formål at bestemme matematiske udtryk, der kan beregne værdier for henholdsvis opvarmningen af luften i ventilationsspalten og den effektive U-værdi. De lineære regressionsanalyser indeholder krydsprodukter og led op til anden orden.

4.2.1 *Matematisk model til beregning af leveret frisklufttemperatur*

Det matematiske udtryk der beregner opvarmningen af luften i ventilationsspalten er bestemt til

Hvor	T_{v2}	er den leverede frisklufttemperatur	[°C]
	T_e	er udetemperaturen	[°C]
	I_s	er solbestrålingsstyrken	[W/m^2]
	G_a	er volumenstrømmen	[L/s]

Til den lineære regression er benyttet WVs beregningsresultater fra 660 parametervariationer. Modellens R^2 og Justerede R^2 har begge værdien 1. Modellens Root Mean Squared Error, der er en analog til standard deviationen, har en værdi på 0,178 °C. Disse statistikker indikerer, at modellen er af høj kvalitet og præcist kan bestemme ventilationsvinduets rudesystems leverede frisklufttemperaturer.

Figur 4.7 viser et punktdiagram hvor regressionsmodellen for leverede frisklufttemperaturer beskrives ved den røde linje og WV's beregnede temperaturer er markeret ved blå punkter. Figurforklaringen indikerer, at der et konfidensinterval omkring den røde modellinje. Grundet det høje antal af datapunkter og regressionsmodellens præcision er konfidensintervallet meget tyndt og det kan derfor ikke ses på grafen. Alle datapunkter er samlet omkring modellens linje. Grafen viser, at regressionsmodellen forudser værdierne beregnet ved parametervariationerne med stor præcision.

Figur 4.7

Punktdiagram af regressionsmodellens forudsete temperaturer overfor WVs beregnede temperaturer

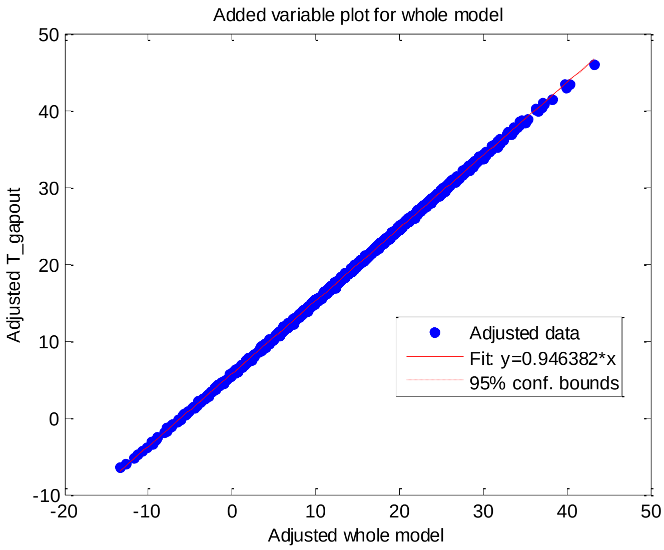

Figur 4.8 viser et punktdiagram hvor de af regressionsmodellen forudsete leverede frisklufttemperaturer er placeret ud af x-aksen og afvigelserne (residualerne) fra WV's beregnede temperaturer fra parametervariationerne er fordelt op af y-aksen.

Residualernes afstand og placering i forhold til den horisontale linje, der går fra y-aksens nulpunkt kan hjælpe til at analysere på kvaliteten af den beregnede regressionsmodel. Det ses, at residualerne ligger uniformt fordelt om y-aksens nulpunkt ud langs x-aksen. Dette viser, at residualernes varians er af samme størrelsesorden. Det kan ligeledes ses, at der ikke er markante outliers, altså residualer, der ligger uforholdsmæssigt langt fra y-aksens nulpunktlinje. Disse er gode tegn og indikerer, at den valgte regressionsmetode er egent til den udførte analyse. Tilbage er at vurdere hvorvidt residualerne er tilfældigt fordelt omkring nulpunktlinjen. Det ses, at de ikke er tilfældigt fordelt. Men en tilfældig fordeling kan ikke rimeligt forventes, da de fittede data ikke er tilfældigt genereret. Dataene er beregnet af WV og tilfældighed kan derfor ikke forventes.

Figur 4.8

Punktdiagram af regressionsmodellens forudsete temperaturer overfor afvigelserne (residualerne) fra WVs beregnede temperaturer

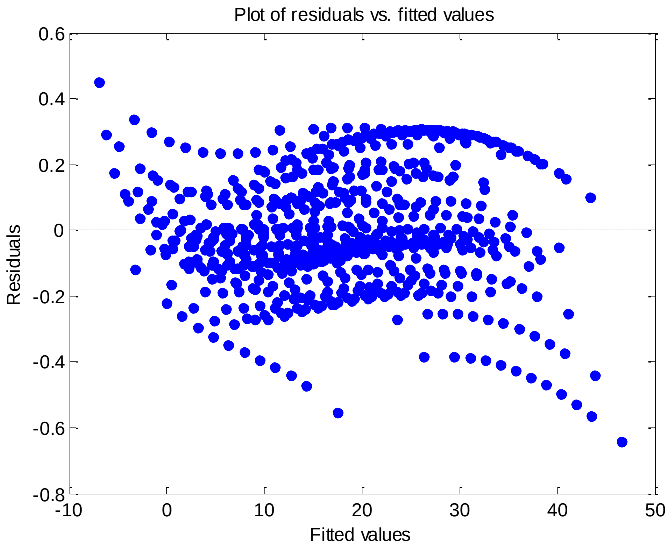

Figur 4.9 viser et punktdiagram hvor regressionsmodellens afvigelser fra WV's beregnede leverede frisklufttemperaturer er placeret ud af x-aksen og deres sandsynligheder under normalfordelingen er fordelt op af y-aksen.

Grafens repræsentation kan give et indblik i om hvorvidt residualernes fordeling lever op til kravet om normalfordeling. Gør de ikke det, kan det betyde, at den valgte metode til regressionsanalysen ikke er gyldig for den form de analyserede data har. På grafen kan det ses, at størstedelen af residualerne følger normalfordelingen. Det er kun de største residualer, dem der henholdsvis ligger under 5 % og over 95 %, der ikke helt følger normalfordelingen. Disse afvigelser vurderes at være acceptable.

Figur 4.9

Punktdiagram af regressionsmodellens afvigelser (residualer) fra WVs beregnede temperaturer overfor deres sandsynlighed under normalfordelingen

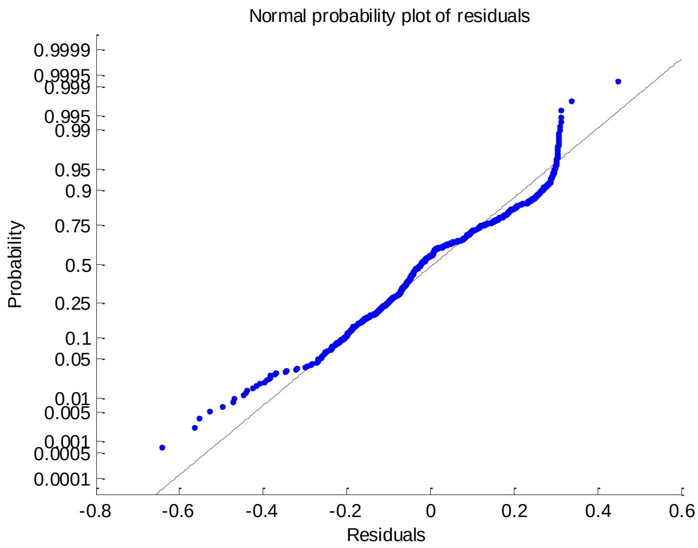

4.2.2 *Matematisk model til beregning af effektiv U-værdi*

Det matematiske udtryk der beregner den effektive U-værdi for ventilationsvinduets rudesystem er bestemt til

Hvor	U_{eff}	er den effektive U-værdi	[W/(m^2·K)]
	T_e	er udetemperaturen	[°C]
	I_s	er solbestrålingsstyrken	[W/m^2]
	G_a	er volumenstrømmen	[l/s]

Til den lineære regression er benyttet WV's beregningsresultater fra 60 parametervariationer. Modellens R2 og Justerede R2 har begge værdien 1. Modellens Root Mean Squared Error, der er en analog til standard deviationen, har en værdi på 0,00224 W/(m^2·K). Disse statistikker indikerer, at modellen er af høj kvalitet og præcist kan bestemme ventilationsvinduets rudesystems effektive U-værdi.

Figur 4.10 viser et punktdiagram hvor regressionsmodellen for effektive U-værdier beskrives ved den røde linje og WV's beregnede effektive U-værdier er markeret ved blå punkter. Figurforklaringen indikerer, at der et konfidensinterval omkring den røde modellinje. Grundet det høje antal af datapunkter og regressionsmodellens præcision er konfidensintervallet meget tyndt og det kan derfor ikke ses på grafen. Alle datapunkter er samlet omkring modellens linje. Grafen viser, at regressionsmodellen forudser værdierne beregnet ved parametervariationerne med god præcision.

Figur 4.10

Punktdiagram af regressionsmodellens forudsete effektive U-værdier overfor WVs beregnede effektive U-værdier

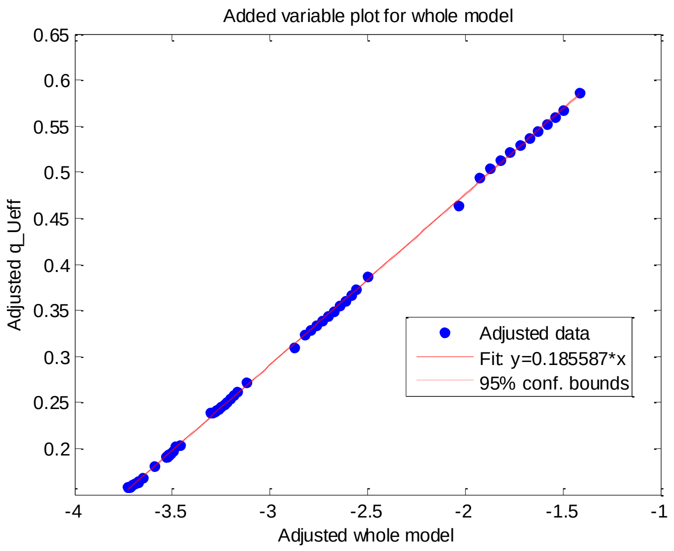

Figur 4.11 viser et punktdiagram hvor de af regressionsmodellen forudsete effektive U-værdier er placeret ud af x-aksen og afvigelserne (residualerne) fra WV's beregnede effektive U-værdier fra parametervariationerne er fordelt op af y-aksen.

Det ses, at residualerne ligger uniformt fordelt om y-aksens nulpunkt ud langs x-aksen. Dette viser, at residualernes varians er af samme størrelsesorden. Det kan ligeledes ses, at der ikke er markante outliers, altså residualer der ligger uforholdsmæssigt langt fra y-aksens nulpunktlinje. Disse er gode tegn og indikerer, at den valgte regressionsmetode er egent til den udførte analyse. Med henblik på fordelingen af residualer kan det ses, at den ikke er aldeles tilfældig. Som før nævnt kan sand tilfældig fordeling ikke forventes, når dataene beregnet af programmer som WV.

Figur 4.11

Punktdiagram af regressionsmodellens forudsete effektive U-værdier overfor afvigelserne (residualerne) fra WVs beregnede effektive U-værdier

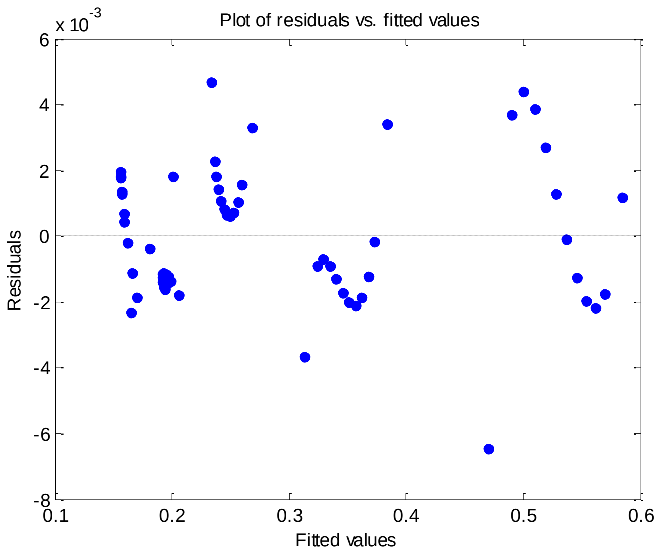

Figur 4.12 viser et punktdiagram, hvor regressionsmodellens afvigelser fra WV's beregnede effektive U-værdier er placeret ud af x-aksen, og deres sandsynligheder under normalfordelingen er fordelt op af y-aksen.

På grafen kan det ses, at størstedelen af residualerne følger normalfordelingen. Afvigelserne fra normalitet er mindre og vurderes at være acceptable.

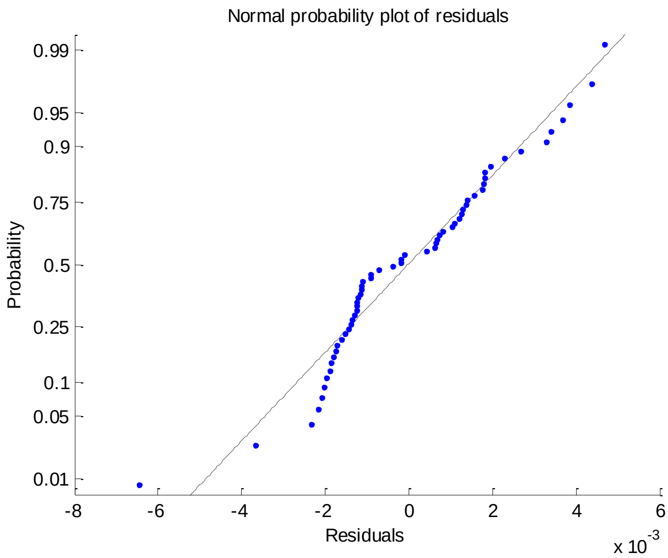

Figur 4.12

Punktdiagram af regressionsmodellens afvigelser (residualer) fra WVs beregnede effektive U-værdier overfor deres sandsynlighed under normalfordelingen

4.2.3 *Delkonklusion*

Det konkluderes på baggrund af de præsenterede statistikker og den gennemgåede analyse af residualer, at de producerede matematiske modeller til bestemmelse af størrelsen af opvarmningen af luft i ventilationsvinduernes rudesystem og den effektive U-værdi for samme rudesystem er præcis til et niveau, der er acceptabelt for projektet ProVent.

4.3 Dynamisk simulering i simpel bygning (IESVE)

For at sammenligne ventilationsvinduet med "almindelige vinduer" og mekanisk ventilation med varmegenvinding, er energiforbruget for den designede bygning beregnet for følgende fire scenarier:

1. Basisvinduer (1+2 vinduer) svarende til ventilationsvinduet (uden ventilation) og mekanisk udsugning
2. Ventilationsvinduet og mekanisk udsugning.
3. Basisvinduer (1+2 vinduer) svarende til ventilationsvinduet (uden ventilation) og balanceret mekanisk ventilation med varmegenvinding på 75 %
4. Traditionelle nye tre-lags lavenergivinduer og effektiv balanceret mekanisk ventilation med varmegenvinding på 80 %.

Scenarie 4 er medtaget for at vise besparelsespotentialet ved anvendelse af nogle af de bedste teknologier på markedet. Data for de fire scenarier er vist i Tabel 4.

Som tidligere nævnt, er der af hensyn til opnåelse af et godt indeklima i henhold til bygningsreglementets krav i alle beregningerne regnet med et fast luftskifte på 0,5 h^{-1}. Dimensionerne er ens for alle vinduerne i de fire scenarier, dvs. vinduerne har standardstørrelse (1480 x 1230 mm) og en ramme/karm-bredde på 82 mm, hvilket giver en glasandel, F_f, på 76 %.

Tabel 4. Energimæssige egenskaber for vinduer og ventilationstype for de fire scenarier.

	Rude		Ramme-karm	Vindue		Ventilation
	U_g [W/(m^2·K)]	g_g [-]	U [W/(m^2·K)]	U_w [W/(m^2·K)]	g_w [-]	
Scenarie 1. Basisvindue	0,80	0,56	1,9	1,07	0,43	Udsugning
Scenarie 2. Ventilationsvindue	0,80	0,56	1,9	1,07	0,43	Udsugning
Scenarie 3. Basisvindue	0,80	0,56	1,9	1,07	0,43	Balanceret med VGV
Scenarie 4. 3-lags energivindue	0,59	0,50	1,4	0,80	0,38	Balanceret med VGV

4.3.1 *Resultater*

I Tabel 5 og Figur 4.13 kan hovedresultaterne for det beregnede årlige energiforbrug ses. Af tabellen og figuren fremgår det, at der for den aktuelle bygning opnås en årlig energibesparelse på 7 % ved at anvende ventilationsvinduer med mekanisk udsugning fremfor basisvinduer med udsugning. Således har det altså en gavnlig effekt på energiforbruget at trække den friske luft til rummet ind gennem hulrummet i ventilationsvinduet fremfor, at trække den ind gennem traditionelle friskluftventiler eller lignende ventilationsåbninger.

I scenarie 3, hvor der etableres mekanisk ventilation med varmegenvinding kombineret med basisvinduer, opnås der til gengæld en energibesparelse på 19 %. Den større besparelse skyldes hovedsagligt, at ventilationsanlægget har en væsentlig mere effektiv varmegenvinding (temperaturvirkningsgrad på 75) sammenlignet med den varmebesparelse, der kan opnås ved forvarmningen af ventilationsluften i ventilationsvinduerne, hvor afkastluften sendes direkte ud i det fri. For ventilationsvinduerne er det kun varmetabet ud gennem vinduerne samt en del af solindfaldet, der potentielt kan udnyttes til forvarmning af indblæsningsluften og dermed opvarmning af bygningen. Omvendt er det ved ventilation med varmegenvinding hele luftskiftet, der potentielt kan varmegenvindes på, og ved det aktuelle luftskifte på 0,5 h^{-1} er energiindholdet i den ventilerede luftmængde væsentlig større end varmetabet fra vinduerne.

For scenarie 4 ses en endnu større energibesparelse på 22 %, hvilket skyldes, at der anvendes nogle af markedets energimæssigt bedste 3-lags vinduer med U-værdi på 0,8 $W/(m^2 \cdot K)$ og en varmegenvinding på ventilationsanlægget på 80 %.

Det skal bemærkes, at der ikke er taget højde for behovet for køling pga. overtemperaturer.

Tabel 5. Bygningens årlige energibehov for de fire scenarier. Besparelse angiver den opnåede energibesparelse i procent i forhold til scenarie 1.

	Energibehov [kWh/m^2]	Besparelse [%]
Scenarie 1 Basisvinduer + udsugning	108	0 %
Scenarie 2. Ventilationsvinduer + udsugning	101	7 %
Scenarie 3. Basisvinduer + ventilation med VGV 75 %	87	19 %
Scenarie 4. 3-lags energivinduer + ventilation med VGV 80 %	85	22 %

Figur 4.13

Bygningens årlige energibehov for de fire scenarier

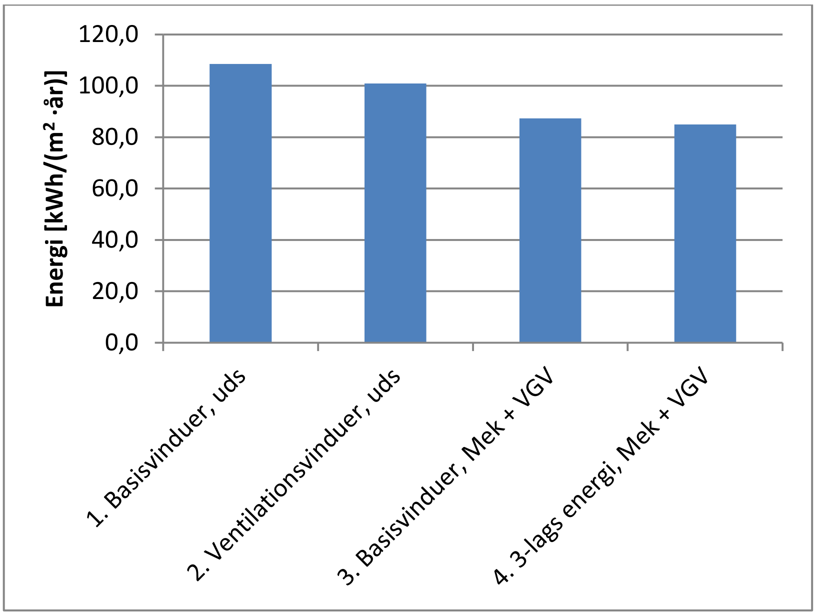

5 DISKUSSION

I dette afsnit behandles eventuelle forbehold og begrænsninger i de udførte analyser og der diskuteres fordele, ulemper og problemstillinger ved anvendelse af ventilationsvinduer.

5.1 Luftskifte

Det er gennem hele projektet forudsat, at der tilvejebringes et luftskifte på 0,5 h^{-1} ved mekanisk udsugning eller mekanisk balanceret ventilationsanlæg med varmegenvinding. Dette for at sikre, at der er et tilfredsstillende indeklima i bygningen og for at opfylde bygningsreglementets krav. Selvom ventilationsvinduer i sig selv og/eller i samspil med aftræk over husets tag kan skabe en skorstenseffekt og dermed et naturligt luftskifte, vurderes det ikke at være tilstrækkeligt til på alle tidspunkter, at sikre et tilstrækkeligt luftskifte til det termiske og atmosfæriske indeklima, som kræves i moderne bygninger. Den naturlige ventilation afhænger i høj grad af udeklimaet, f.eks. spiller vindforhold en meget stor rolle. Indendørs kan simple brugsforhold som åbnede eller lukkede døre også have en indflydelse på den dominerende trykfordeling og dermed også det resulterende luftskifte. Således vurderes det, at det kan være svært at sikre at luftstrømmen altid bevæger sig indad gennem vinduet, med mindre ventilationsåbningerne er forsynet med kontraventiler.

5.2 Indeklima

Målingerne og beregningerne viser, at forvarmningen af ventilationsluften gennem ventilationsvinduet er forholdsvis begrænset, når der ikke er solskin på vinduet. F.eks. vil indblæsningstemperaturen en mørk vinteraften med en udetemperatur på 0 °C, med den givne volumenstrøm på 4,5 l/s, medføre en opvarmning på ca. 3,5 °C. Dog vil den yderligere forvarmning i ramme og karm forventeligt forøge indblæsningstemperatur til 5-6 °C. Det er en ikke uvæsentlig forbedring i forhold til traditionelle friskluftsventiler, men det er dog stadig så koldt, at det kan give anledning til oplevelsen af træk og kuldenedfald tæt ved vinduet. Indblæsningstemperaturen kan øges betydeligt hvis volumenstrømmen reduceres, men i givet fald er det på bekostning af luftskiftet og dermed indeklimaet. Selvom den kolde og ofte tørre udeluft om vinteren giver mulighed for, at reducere frisklufttilførslen i forhold til at opnå en passende lav relativ luftfugtighed i bygningen, er der stadig ofte behov for et luftskifte af en vis størrelse, for at sikre et godt atmosfærisk indeklima ved opblanding og fortynding og bortskaffelse af forurening fra byggematerialer, inventar og personer mv.

5.3 Køling

Det skal bemærkes, at der i projektet ikke er taget højde for eventuel behov for køling pga. overtemperaturer. Her kan ventilationsvinduer også have en gavnlig effekt hvis de er forsynet med ventiler eller åbninger, som gør det muligt at sende den solopvarmede luft i hulrummet ud igen til omgivelserne i toppen af vinduet. Det vurderes dog, at ventilation af hulrummet i ruden kun vil kunne reducere solenergitilskuddet i begrænset omfang da størstedelen af solenergitilskuddet sker ved direkte transmission gennem glassene til rummet, hvor det afsættes som varme. Samtidig vil en returnering af luften i hulrummet direkte til udeklimaet betyde, at den nødvendige friske luft til rummet skal komme andre steder fra.

5.4 Arkitektur og pladsforhold.

Som det fremgår af afsnit 4.3 viser beregningerne at ventilationsvinduerne giver en besparelse i energibehovet på 7 % under de givne forudsætninger sammenlignet med tilsvarende basisvinduer, mens mekanisk ventilation med varmegenvinding og basisvinduer giver en besparelse på 19 %. Dette skal holdes op imod, at der ofte kan være store omkostninger forbundet med etablering af mekanisk ventilation. Særligt hvis der er tale om eksisterende ejendomme, hvor der skal etableres nye ventilationskanaler mv. I mange ældre ejendomme er det problematisk, at få plads til de nødvendige ventilationskanaler og ventilationsaggregatet, og det er ikke altid foreneligt med bygningens indretning og arkitektur.

5.5 Vinduesopbygning

De undersøgte ventilationsvindue er opbygget som en 1+2 vinduesløsning, dvs. et enkelt lag glas yderst, et tykt luftfyldt ventileret hulrum i midten og en to-lags energirude inderst. En konstruktion med et enkelt lag glas kunne alt andet lige give en større forvarmning af ventilationsluften pga. større varmetab gennem det inderste glas. Men idet det er forudsat, at der altid vil være en fast volumenstrøm gennem vinduet, for at sikre et ønsket luftskifte på en halv gang i timen, vil der, når det er koldt udenfor, være meget stor risiko for kondensdannelse på indersiden af ruden i den nederste del nær karmen. Samtidig vurderes det, at en øget forvarmning af ventilationsluften, ved en opbygning med et-lags rude inderst, direkte kommer fra et tilsvarende øget varmetab, hvilket samlet set ikke medfører en yderligere varmebesparelse. Dette er hovedårsagerne til, at der er valgt opbygningen med 2-lags energirude inderst, for at sikre at der undgås problemer med kondensdannelse.

5.6 Solstråling

Som nævnt giver ventilationsvinduer mulighed for at udnytte solstrålingen til forvarmning af ventilationsluften, inden den sendes ind i rummet. Muligheden for dette vurderes dog at være begrænset, da antallet af solskinstimer i fyringssæsonen er ganske få. For at få den bedste udnyttelse af solstrålingen i form af en ”behagelig” indblæsningstemperatur skal vinduerne placeres mod syd og til dels øst/vest vendt i bygninger, som anvendes i dagtimerne, hvor der er solskin. For boliger er dette ofte et problem, da solskinstimerne i fyringssæsonen som regel falder på tidspunkter i dagtimerne, hvor mange beboere er ude af huset. Dvs. fordelen ved solopvarmningen af indblæsningsluften som skulle reducere eventuelle problemer med kuldenedfald og træk, ikke kommer til gavn en stor del af tiden.

5.7 g-værdi

Ifølge WV er der kun en 1,66 % stigning i g-værdien når det kun er effekten af udetemperatur og solstråling der undersøges. Størstedelen af "variationen" i g-værdien skal findes i opvarmningen af luften. Den er der taget højde i den leverede frisklufttemperatur. Andelen af solstråling der går gennem vinduet er kun ændret fordi mere varme vil blive afsat i glasset.

5.8 Støjdæmpning

Ventilationsvinduers indflydelse på støjforhold er ikke behandlet i nærværende projekt. Der findes dog en række studier, der omhandler ventilationsvinduers støjdæmpende egenskaber. Disse peger på, at rudekonstruktionen med tre lag glas og et stort luftfyldt hulrum i sig selv giver en effektiv støjdæmpning. Selv med ventilationsspalterne åbne i vinduet er støjdæmpningen betydelig. Pga. den lange vej gennem ventilationsvinduet fra den udvendige åbning nederst til de indvendige åbning øverst i vinduet giver ventilationsvinduer en betydelig bedre støjdæmpning end et tilsvarende traditionelt vindue, som er åbnet så meget, at det leverer den samme ventilationsmængde. Ventilationsvinduer kan derfor være attraktive i støjplagede områder, hvor man ønsker mulighed for frisk luft gennem vinduerne, men samtidig ønsker støjdæmpning.

5.9 Forvarmning i ramme/karm

I forbindelse med målingerne i GHB blev det observeret, at der sker en forvarmning af ventilationsluften på op til 2,5 grader (afhængig af volumenstrømmen) i passagen gennem rammen og karmen allerede før luften når hulrummet i ruden. Det må formodes, at der sker en lignende forvarmning i samme størrelsesorden af udeluft, som trænger ind via friskluftsventiler i traditionelle vinduer eller sprækker og andre utætheder i klimaskærmen. Der er ikke taget højde for dette i bygningssimuleringerne hvor der sammenlignes med traditionelle vinduer. Det vurderes dog at effekt kun har ganske lille betydning og primært er relevant i forbindelse med udsugning.

Det skal her nævnes, at der ved infiltration generelt vil forekomme en form for varmegenvinding men, at det er et koncept der ses bort fra i standardberegninger af bygningers energiforbrug. Ved ikke at regne på den genvundne varme ved infiltration i standardsituationer giver man ventilationsvinduet en regneteknisk fordel. For resultaterne betyder det at den beregnede forskel på 7 % givetvis vil være mindre i den virkelige verden. Hvor stor en indflydelse denne udeladte effekt har, er ikke bestemt i projektet.

6 REFERENCER

[1] ISO 15099. Thermal performance of windows, doors and shading devices -- Detailed calculations. International Organization for Standardization, 2003.

[2] Zegowitz A, Heusler I. Fraunhofer IBP report name [An intelligent window for optimal ventilation and minimum thermal loss, Final test report]. Stuttgart, Germany: Fraunhofer Institute for Building Physics; 2012.

[3] ISO 12567-1. Thermal performance of windows and doors -- Determination of thermal transmittance by the hot-box method -- Part 1: Complete windows and doors. International Organization for Standardization, 2010.

[4] Appelfeld D, Svendsen S. Experimental analysis of energy performance of a ventilated window for heat recovery under controlled conditions. Energy and Buildings 2011;43:3200-7.

[5] DS 418. Beregning af bygningers varmetab. Dansk Standard, 2011.

[6] Raffnsøe LM. Thermal Performance of Air Flow Windows [master thesis]. Lyngby, Denmark: Technical University of Denmark; 2007.

We use ventilation to ensure that people are healthy and comfortable in their homes and workplaces. When designing ventilation systems, focus – in prioritised order – must be on health, comfort and energy efficiency.

At present, many Scandinavian homes have air change rates lower than the current recommendations. This means that many Scandinavians risk long term exposure to hazardous chemicals present in the indoor environment. This thesis documents that it is possible to design ventilation systems that can ensure healthy and comfortable indoor environments at no extra cost in terms of energy.

DTU Civil Engineering
Technical University of Denmark

Brovej, Bygning 118
2800 Kongens Lyngby

www.byg.dtu.dk

ISBN 9788778774927
ISSN 1601-2917